CONTRIBUTION OF THE VOLTAGE-GATED SODIUM CHANNEL NAV1.6 AND TOLL LIKE RECEPTOR 2 IN THE PATHOPHYSIOLOGY OF EAE

By

BARAKAT M. ALRASHDI

Submitted in partial fulfillment of the requirements
for the degree of Doctor of Philosophy

At

Dalhousie University
Halifax, Nova Scotia
February 2020

DEDICATION

I dedicate this thesis to beloved people who have meant and continue to mean so much to me, my Mom, my wife Maryam, my kids, Saad, Abdulmalik, Alin, and Eyad, my brother Saad and my Dad, who passed away and no longer of this world, his memories continue to regulate my life.

TABLE OF CONTENTS

LIST OF TABLES

LIST OF FIGURES

ABSTRACT

Multiple sclerosis (MS) is a chronic, inflammatory, demyelinating, and neurodegenerative disorder of the central nervous system (CNS) with the highest worldwide prevalence existing in Canada and affecting over 3000 Nova Scotians. MS is characterized by the autoimmune-mediated destruction of myelin and axons in the CNS and has been linked to inflammatory processes that activate the immune system. The most recent understanding of the mechanisms associated with the development of MS suggests that the inflammatory processes in the early stages of the disease trigger a cascade of events including microglial activation, the release of reactive mediators, and mitochondria damage, which subsequently leads to axonal damage. Axonal degeneration, one of the hallmarks of the disease and a non-reversible process, leads to several neurological disabilities including visual impairment and vision loss. However, the mechanisms underlying axonal degeneration remain unclear. This thesis sought to characterize the impact of two key regulatory molecules: the voltage-gated sodium channel Nav1.6 and the Toll-like receptor 2, a component of the innate immune system, in the pathogenesis of EAE. To this end, I used experimental autoimmune encephalomyelitis (EAE), a rodent model that recapitulates key aspects of the human disease. I investigated the role of voltage-gated sodium channels (especially Nav1.6), which have previously been linked to axonal degeneration and loss (**Chapter 2**) by gene targeting in the retina and optic nerve. We extended these studies to determine the impact of the reduction of Nav1.6 in mice heterozygous for a null-allele of *Scn8a*. (**Chapter 3**). This *in vivo* study is the first to link a reduction of Nav1.6 in EAE to immune profile changes, such as a reduction of inflammation marked by decreased IL-6 in the plasma and myeloid cell infiltration in the optic nerve. Analysis of murine bone-marrow-derived mast cell (BMMCs) cultured *in vitro*, suggest a potential role of Nav1.6 in regulating the inflammatory process during EAE and LPS challenge. Additionally, I investigated the impact of TLR2 in brain inflammation and optic nerve axonal damage (**Chapter 4**). I found that the absence of TLR2 was associated with reduced inflammation in the periphery and within the CNS, including in blood, spleen, and brain, which is marked by decreased myeloid cells, such as Gr-1^{+}/$CD11b^{+}$ cells, chemokines in the plasma, and pro-inflammatory cytokines in the brain. The present study provides novel information by highlighting the role of TLR2 and Nav1.6 in EAE. This knowledge expands our understanding and ultimately promotes further investigation to target these molecules and unmask the mystery of their roles in MS.

LIST OF ABBREVIATIONS USED

AAV2	Adeno-associated virus, serotype 2
ACK	Ammonium-chloride-potassium buffer
APC	Antigen Presenting Cell
APP	Amyloid-beta precursor protein
BBB	Blood-Brain Barrier
BSA	Bovine serum albumin
CD	Cluster of differentiation
cDNA	Complementary DNA
CFA	Complete Freund's adjuvant
CNS	Central nervous system
CSF	Cerebrospinal fluid
CSLO	Confocal scanning laser ophthalmology
dmu	degenerating muscle mouse
EAE	Experimental autoimmune encephalomyelitis
ELISA	Enzyme-linked immunosorbent assay
FITC	Fluorescein isothiocyanate
GFP	Green fluorescent protein
GM-CSF	granulocyte-macrophage colony-stimulating factor
H&E	Hematoxylin and eosin
Iba-1	Ionized Calcium Binding Adaptor Molecule 1
IHC	Immunohistochemistry
IL-	Interleukin
LPC	Lysophosphatidylcholine
LPS	Lipopolysaccharide
MBP	Myelin Basic Protein
MOG_{35-55}	Myelin Oligodendrocyte Glycoprotein Fragment 35-55
Nav	Voltage-gated sodium channel
NCX	$Na^{+}/Ca2^{+}$ exchanger
NO	Nitric Oxide
OPC	Oligodendrocyte Precursor Cell
Pam_3CSK_4	Palmitoyl3-Cys-Ser-Lys-Lys-Lys-Lys-Lys
PAMP	Pathogen-associated molecular patterns
PCC	Peritoneal Cavity Cells
PFA	Paraformaldehyde
PNS	Peripheral nervous system
PPMS	Primary-Progressive Multiple Sclerosis
PRMS	Progressive-Relapsing Multiple Sclerosis
ROS	Reactive Oxygen Species
qRT-PCR	Quantitative reverse-transcription polymerase chain reaction

RBPMS	RNA binding protein with multiple splicing
RGC	Retinal ganglion cell
RRMS	Relapsing-Remitting Multiple Sclerosis
Scn2a	Gene that encodes the Nav1.2 α subunit
Scn2b	sodium channel subunit β-subunit
Scn8a	Gene that encodes the Nav1.6 α subunit
SPMS	Secondary-Progressive Multiple Sclerosis
TCR	T-cell receptor
TGF-β	Tumor-growth factor beta
Th	T-helper cell
TIL	Tumor-infiltrating leukocytes
TLR	Toll-like receptor
TMB	3,3',5,5'-Tetramethylbenzidine
TNF	Tumor necrosis factor
Tregs	T regulatory cells
TTX	tetrodotoxin

ACKNOWLEDGEMENTS

I would like to express my sincere appreciation to my supervisors Dr. Patrice Côté and Dr. Jean Marshall, for their patience while continually mentoring me through this project and offering their supportive guidance, especially during challenging times. My scientific accomplishments would not have been possible without their ongoing respect and encouragement that motivated me to achieve my goals. They have been extremely knowledgeable and have provided many new insights that have developed my ideas. This thesis would not have become what it is without their involvement and mentorship. Their passion and dedication to my work have been valuable, and I do not have the words to describe my sincere appreciation toward them.

In addition to my supervisors, a special thanks must go to my supervisory committee, Dr. Francois Tremblay and Dr. William Baldridge, for their guidance, valuable feedback, and critical suggestions through my journey.

I would like to express my gratitude to my external examiner Dr. Shalina Ousman, for agreeing to serve in my examination committee.

My extended thanks to Dr. Ian Haidl for all his advice and discussions that assisted my progress through my research and facilitated the development of my experimental designs. He provided great feedback and suggestions on my manuscripts and offered critical comments on my thesis.

Sincere thanks to our collaboration Dr. Stefanie Kuerten, Sabine Tacke, and Dr. Andrea Schampel.

Furthermore, I would like to extend a warm thanks to the Chair of the Graduate Students in the Biology Department, Dr. Sophia Stone, for her continuous support and always taking time to assist me during my project. Her humanity is unforgettable.

I would also like to pass my thanks to my scholarship organization, the Ministry of High Education in Saudi Arabia Jouf university and the Saudi Arabian Culture Bureau in Canada for giving me the opportunity to complete my postgraduate study.

Additionally, my lab mates brought joy to the experience and made stressful times more bearable. Thanks to Bassel Dawod, Maria Vaci, Dr. Liliana Portales Cervantes, Edwin Leong, Mark Hanes, Dr. Dihia Meghnem, Stephanie Legère, Owen Crump and Christopher Liwski. Bassel, thank you for your hard work and collaboration on our grant proposal and for taking time out of your busy schedule to assist me with my experiments. Thank you to Maria Vaci, Alexander Edgar, and Nong Xu for teaching me several lab techniques and with assistance with several experiments. Also, I would like to thank Dr. Corey Smith, Michele Hooper and Janette Nason for technical support.

Thanks to my lovely family, my Mom, my wife, and my kids. To my beloved wife, Maryam, you have lived with this work from the beginning and have supported me through this challenging life. You have sacrificed a lot during these times and to help me complete my education. Through all the stress, you have been there to offer your love and kindness. Thank you is not enough to express my deep respect and love. I owe a big thanks to my Mom, whose dreams for me have resulted in this achievement and for raising me and

shaping me into the person I am today. Thanks for each prayer you made for me. You have guided me through life while offering your unconditional love. I love you so much! Huge thanks to my kids Saad, Abdulmalik, Alin, and busy little boy Eyad for their patience, understanding, made my life meaningful and I will face every challenge just for you.

I am especially grateful to my brother Dr. Saad Al Rashidi, though you are far away thanks for your frequent calls asking about my progress and your supportive conversations every step from the beginning of my project to this moment. You have believed in me and have helped make this possible. I could not have accomplished this without you. Special also thanks to my brother, Abdulaziz, you have stood beside me and provide me kind of support and motivation through every step of my study. My sincere appreciation also goes to my brothers, Abdulkareem, Abdullah, and Mabruak. Thank you for being there every time. Whenever I felt down, you were always there to make me stand. Thanks also to my sisters for their support, kindness, support, and generosity.

I want to extend my thanks to my colleagues for their support Dr. Musa Garmoushi, Dr. Kamal Alsihk, Dr. Daifallah Almarwani, Dr. Monief Alrashidi, Dr. Mohammed Abu-gamer, Mohammed Alrashidi, Abdulaziz Alaufi, Fahad Alrashidi, Fahad Alseedi.

Finally, thank you, Allah (God), for all the opportunities that you gave me to complete this thesis and to reach my goal.

الحمد لله سبحانه وتعالى الذي تتم بنعمته الصالحات وتدوم النعمة بشكره

Chapter 1 Introduction

1.1 Overview of Multiple Sclerosis

Multiple sclerosis (MS) is an inflammatory demyelinating disease that affects the central nervous system (CNS). It impacts the lives of over 2.5 million people worldwide with high prevalence in Canada, and particularly in Nova Scotia (Marrie et al., 2013). Over 75% of MS patients are women, and it is projected that the risk for MS will increase from 4051 in 2011 to 4794 per 100,000 people by 2031 (Amankwah et al., 2017; Cotsapas and Mitrovic, 2018; Mohr, 2011). This poses a significant financial burden to those individuals and society, as 80% of MS patients remain unemployed, which highlights the necessity for further investigation of the causes of MS (Amankwah et al., 2017; Piwko et al., 2007). MS patients can exhibit a wide range and different symptoms, including difficulty in walking, poor coordination of voluntary muscle movement, fatigue, tremor, abnormal skin sensations, loss of sight, cognitive deficits, depression, and bladder dysfunction (Coles, 2009; Noseworthy et al., 2000). Moreover, MS patients could suffer from positive (gain of sensation) symptoms and negative (loss of function) symptoms during the progression of the disease (Sakurai and Kanazawa, 1999). Positive symptoms are caused by ectopic impulses generated at sites of demyelination, whereas the negative symptoms occur due to loss of conduction (Sakurai and Kanazawa, 1999).

The etiology of MS is still unknown; however, environmental and genetic factors are believed to be the main trigger for developing MS (Ascherio, 2013; Constantinescu et al., 2011; Mohr, 2011). The studies of genome-wide association have identified over 230 loci related to MS susceptibility with specific HLA alleles, that is located in polygenic regions on chromosome 6, include *DRB1*1501, DRB5*0101* haplotypes representing the

most significant association with MS (Beecham et al., 2013; Hafler et al., 2007). MS is common in Europe, North America, Australia, and New Zealand, and the distribution is altered by where at-risk individuals live early in life. Several studies show that people who move in early childhood from high-risk to low-risk regions have less risk for developing the disease (Beck et al., 2005; Dean and Elian, 1997; Wade, 2014). Several reports have proposed that environmental factors such as vitamin D deficiency, cigarette smoking, increased body mass index, and exposure to Epstein-Barr virus (EBV) are risk factors for MS (Amato et al., 2017; Ascherio, 2013). Therefore, understanding the link between neuroinflammation progression and neurodegeneration might be critical in the development of effective therapeutic strategies for MS

1.1.1 Pathology of MS

It is believed that the main trigger of the disease is an inflammatory autoimmune response within the CNS that causes tissue damage, including demyelination and axonal loss (Burda and Sofroniew, 2014; Constantinescu et al., 2011). The axon is the projection of the neuron that carries the information from the cell body to the nerve terminals and acts as a transmitter of the action potential (Debanne, 2004). Axons exist in two types, myelinated and unmyelinated. Myelinated axons are encapsulated within a layer of fatty substance, called myelin, that arises from glial cells, oligodendrocytes, and helps to insulate the axon and increase the conducting speed of the action potential (Giuliodori and DiCarlo, 2004; Trapp and Kidd, 2003). Oligodendrocytes are specialized glial cells that are highly involved not only in the deposition of myelin but also in the clustering of Nav channels in the nodes of Ranvier, which are the unmyelinated gaps between the myelinated segments of the axon (Freeman et al., 2016). The nodes of Ranvier are

flanked by the paranodal and the juxtaparanodal regions, and these regions are defined by myelin-producing glial cells such as oligodendrocytes in the CNS and by Schwann cells in the peripheral nervous system (PNS) (Marcus et al., 2002; Zawadzka et al., 2010; Zonta et al., 2008). Another type of glia, astrocytes, respond to CNS inflammation through the process of reactive astrogliosis (Burda and Sofroniew, 2014). However, in the condition of severe inflammation, the gliosis can lead to the formation of a glial scar, which can result in the attenuation of neuronal regeneration in damaged areas (Burda and Sofroniew, 2014; Frohman et al., 2008; Trapp et al., 1998a). The main pathological features of MS include inflammation, demyelination, gliosis, perivascular infiltration by inflammatory cells, and, ultimately axonal and neuronal loss (Friese et al., 2014; Frohman et al., 2008; Trapp et al., 1998a). In the early stages of the disease, axonal demyelination, with the axon remaining viable, is associated with variable degrees of inflammation and astrogliosis (Mancardi et al., 2001). However, permanent neurological deficits become increasingly prominent as the neuroaxonal degeneration progresses (Friese et al., 2014).

Axonal damage occurs during the acute phase of inflammation and before demyelination, as confirmed by histopathological studies (de Leeuw et al., 2014; Trapp et al., 1998a). The progression of the disease correlates with the level of axonal damage, which can be latent in the beginning before progressing into relapsing-remitting MS (RRMS) (Bjartmar et al., 2003). Nevertheless, irreversible neurological disability develops at advanced stages of the disease when the axonal loss exceeds a threshold and upon exhaustion of the CNS compensatory mechanisms (Bjartmar et al., 2003; Friese et al., 2014). Lesions, also known as plaques, which form in the brain, spinal cord, and optic

nerve, combined with inflammation, produce the primary symptoms of MS (Noseworthy et al., 2000).

MS is a complex disease that involves interactions between immune cells, glial cells, and neurons, which together contribute to the progression of the disease (Goldenberg, 2012). Autoimmune responses within the nervous system cause tissue damage, including demyelination and axonal damage, and give rise to the activation and infiltration of myelin-autoreactive T cells and macrophages (Frohman et al., 2006; Stys et al., 2012). As yet, there is no precise test for diagnosis; magnetic resonance imaging (MRI) is the primary diagnostic test, which has the capacity to detect changes such as atrophy and lesions in the brain. Cerebrospinal fluid can be analyzed for indicators of brain-related atrophy linked to MS (Romme Christensen et al., 2013; Tumani et al., 2009).

Several studies including Duffy et al., (2014) and Kuhlmann et al., (2017) have reported that T cells may play a potential role in the immune pathogenesis of MS by crossing the blood-brain barrier (BBB) and subsequently triggering autoimmune inflammation resulting in the destruction of myelin autoreactive T cells. Then T cells differentiate and produce cytokines such as TNF, IL-6, and IL-1β, which activate other immune cells and attract inflammatory cells into the CNS, including B cells, natural killer (NK) cells, and monocytes/macrophages (Raddassi et al., 2011). These cells can cross the BBB and increase the degree of inflammation, which is the primary attribute of MS. Inflammation, in turn, leads to disruption of the BBB, which is associated with increased infiltration of various immune cells, such as $CD4^+$ T cells and macrophages, into the CNS and activation of antigen-presenting cells (APCs), such as microglia. Finally, activated

macrophages phagocytose the myelin sheath and are toxic to oligodendrocytes (Barnett et al., 2006; Kigerl et al., 2009).

1.1.2 Clinical subtypes of MS

There are four different types of MS, related to the clinical presentation and course of the disease: relapsing-remitting MS (RRMS), secondary-progressive MS (SPMS), primary-progressive MS (PPMS), and progressive-relapsing MS (PRMS). Around 85% of patients initially present with RRMS, which is the most common form for MS. RRMS involves periods of attacks affecting different regions of CNS, and increased disease severity, which is known as relapse, followed by remission, characterized by the absence of symptoms (Weiner, 2008). Approximately 80% of patients with RRMS will ultimately develop into SPMS, which is characterized by a continuous worsening of symptoms and the absence of remission (Scalfari et al., 2014). About 10% of patients are diagnosed with PPMS, which is characterized by a steady increase in disability without attacks and is resistant to drugs (Prineas, 2001). The least common form of MS, PRMS, affects around 5% of patients and is characterized by a steady increase in functional disability with sporadic relapses and absence of remission. Currently, Health Canada has approved 14 drug treatments that commonly reduce disease progression or are used as disease-modifying therapies (DMTs). These drugs are only successful in decreasing the frequency and number of new attacks, but they have limited value in reducing , completely halting ,or slowing disease progression (Cohen et al., 2010; Walker et al., 2011). Furthermore, these drugs are not effective in enhancing remyelination in MS (Ransohoff, 2012).

1.2 Animal models of MS

Animal models enable researchers to study the pathology of MS and overcome the various economic and ethical issues regarding human studies. Though the models are not fully identical to the human disease, they share similar aspects such as the immune response, demyelination, and inflammation (’t Hart et al., 2011; Lassmann and Bradl, 2017). There are several animal models used in MS research, including experimental autoimmune encephalomyelitis (EAE), which is the main focus of this study, Theiler's’ murine encephalomyelitis virus, Cuprizone and Lysolecithin (Procaccini et al., 2015) and T cell receptor (TCR) transgenic mice (Bell et al., 2013; Bettelli et al., 2003) (Table 1).

1.2.1 Experimental autoimmune encephalomyelitis (EAE)

EAE was first discovered by Rivers et al. (1933) when the team was exploring a rabies vaccine’s neurological complications in monkeys. These complications, relating to the post-vaccinal perivascular-related paralysis, included many of MS’s clinical and pathological characteristics. The development of EAE by Rivers et al. not only helped to better understand the pathogenesis of this post-vaccinal encephalomyelitis (Rivers et al., 1933) but also of demyelinating diseases. While limitations certainly exist as far as representing the full clinical course of MS in humans, EAE mimics the interaction between complex neuropathological and immunopathological features and has greatly helped to study MS immunology and brain inflammation necessary to develop drugs to reduce disease progression (Bettelli, 2007a; Constantinescu et al., 2011; Friese et al., 2006; Lassmann and Bradl, 2017). In mice, EAE was initially generated using active immunization in spinal cord homogenates (OLITSKY and YAGER, 1949; Robinson et al., 2014).

The EAE model is considered a $CD4^+$ mediated disease characterized by immune cells, such as T cells and monocytes, that infiltrate the CNS and, combined with local inflammation, produce a highly stereotyped symptom progression (Friese et al., 2014; Owens and Sriram, 1995; Sriram et al., 1982). EAE shares many features of MS, including optic neuritis and CNS histopathological symptoms (Bettelli, 2007b; Mix et al., 2010). EAE can be induced in many mammalian species, including mice, guinea pigs, rabbits, sheep, pigs, and primates. To date, mice are considered by researchers to be the most attractive species for lab research involving encephalitogenic peptides, due in large part to the ease of genetically manipulating these animals for use in targeted mechanistic studies. C56BL/6 is the most commonly used strain and multiple antigens can be used for the induction of EAE such as myelin oligodendrocyte (MOG) amino acids 35 to 55 (MOG_{35-55}), myelin basic protein (MBP)on, and proteolipid protein (LPL) (Constantinescu et al., 2011; Linnington et al., 1984; Marcus et al., 2002; Stromnes and Goverman, 2006a).

In more than half of the MS patients studied, MOG peptides showed autoimmune reactivity (Kerlero De Rosbo et al., 1997; Zhong et al., 2002). Based on this observation Mendel and colleagues generated the mouse MOG EAE model during experiments on the immunization of female C57BL/6 mice using synthetic peptides corresponding to amino acids 1–21, 35–55, and 104–117 of MOG (Mendel et al., 1995). The researchers observed that a T-cell response was initiated in all MOG peptide-immunized mice, whereas extreme neurological impairment occurred in $MOG_{35–55}$-immunized animals. $MOG_{35–55}$ displayed CNS inflammation, gliosis, axonal loss, persistent neuropathy, and increasing degrees of paralysis (Mendel et al., 1995; Stromnes and Goverman, 2006a). Such

pathological and clinical traits are not unlike the ones exhibited by MS patients, which led to the wide adoption of $MOG_{35–55}$ EAE as a model for MS studies (Mangiardi et al., 2011; Rangachari and Kuchroo, 2013). Indeed, the $MOG_{35–55}$ EAE model recapitulates aspects of the three MS subtypes that have a relapsing-remitting or progressive and secondary progressive phase (Lassmann et al., 2007). $MOG_{35–55}$ EAE can be applied as a model for early relapses as well as for monitoring potential effectors of MS disease progression. The model is used for testing interventions that may prevent varying degrees of CNS damage (Barthelmes et al., 2016; Procaccini et al., 2015). In addition to the 'active' method of inducing EAE with $MOG_{35–55}$, with complete Freund's adjuvant (CFA) and with pertussis toxin (PTX), induction can also be passive, and "humanized" (Stromnes and Goverman, 2006 b). In the active model, symptoms appear approximately 9 days post-induction and typically peak at day 13, followed by a short remission phase – which is often marginal – and the chronic phase established by day 24. MOG_{35-55} facilitates the invasion of immune cells into the CNS leading to the development of lesions in the spinal cord and brain as well as optic neuritis (Rangachari and Kuchroo, 2013). The passive model also causes CNS inflammation and demyelination in naïve mice which is achieved through the transfer of myelin-specific $CD4^+$ T cells from EAE mice, whereas the "humanized" transgenic mouse model expresses human TCR receptors that interact with major histocompatibility complex (MHC) class II molecules presenting myelin epitopes (Bell et al., 2013; Bettelli, 2007a; Madsen et al., 1999).

1.2.2 EAE disease phases

The clinical signs for EAE develop across three distinct phases, namely the induction, effector and recovery phases (Lassmann et al., 2007). In the disease's

induction phase, there is the priming of myelin-specific $CD4^+$ T cells as a result of active immunization using myelin antigens, PTX, and CFA. In the effector (second) phase, the myelin-specific $CD4^+$ T cells migrate to the CNS through the disrupted BBB. This process causes peripheral immune cells to enter the CNS parenchyma (Barthelmes et al., 2016; Lassmann et al., 2007). It has been reported that monocytes become elevated with tissue damage in EAE mice (Ajami et al., 2011). In MS, many immune cells, especially $CD4^+$ T cells, damage healthy tissue leading to widespread demyelination, axon damage, and neurological deficits (Murray et al., 1998; Noseworthy et al., 2000).

The EAE model has many advantages for studying the interactions between the immune system and the nervous system and the chronic phase of the disease (’t Hart et al., 2011). However, it is important to note that despite many similarities, the EAE disease progression is unlike that of MS, such as the facilitated development of MS in mice through injection of antigen, whereas the antigen is unknown in humans and spontaneously develops. Additionally, in the EAE model, $CD4^+$ T cells are responsible for the development of the disease, while $CD8^+$ T cells occupy this role in humans (Brown and Sawchenko, 2007; Friese and Fugger, 2009; Hafler et al., 1985; Lassmann and Bradl, 2017; Marta, 2009). EAE is by far not the only applied animal model for MS but it is the model that most closely represents the pathogenesis of MS (Baxter, 2007; Mangiardi et al., 2011). Therefore, despite certain limitations, the EAE model is an appropriate choice for studying the chronic phase of MS and to develop therapeutic regimens to slow disease progression.

Table 1 Rodent models for MS

Animal Model	Induction and Pathology	Advantage	References
Experimental autoimmune encephalomyelitis (EAE)	EAE is a $CD4^+$ mediated disease characterized by immune cells, such as T cells and monocytes, that infiltrate the CNS	This model reflects the autoimmune pathogenesis of MS. It is useful for studying the chronic phase of MS and for developing treatments to slow disease progression.	(Mix et al., 2010; Procaccini et al., 2015; Ransohoff, 2012)
Theiler's murine encephalomyelitis virus	Viruses directly injected into the CNS to induce demyelination in the brain.	This model is valuable for the presence of demyelination. The disease only manifests if the virus is injected directly into the CNS.	(McCarthy et al., 2012; Murray et al., 1998)
Cuprizone	Chemically induce demyelination.	This model is suitable to study demyelination and remyelination.	(Gudi et al., 2014; Matsushima and Morell, 2006; Praet et al., 2014)
Lysolecithin	This chemical is toxic to oligodendrocytes and induces demyelination in the corpus callosum, brain, and spinal cord. Involves injection with 1% lysolecithin directly into the white matter, lumbar region of the spinal cord, and corpus callosum of mice.	This model is suitable for studying demyelination and remyelination during disease progression	(Ousman and David, 2000)
TCR transgenic	2D2 transgenic mice or MOG-specific TCR transgenic mice immunized with a sub-optimal immunization regimen (only MOG_{35-55} with CFA without PTX) leads to infiltration of myelin-specific T cells mainly to the optic nerves compared to the rest of the CNS.	This model was designed to study spontaneous autoimmunity in mice following immunization with myelin protein or PTX alone.	(Bell et al., 2013; Bettelli et al., 2003)
Non-obese diabetic.	Type 1 diabetes is an autoimmune disease characterized by immune cell infiltration, mainly T cells, into the pancreas leading to the destruction of β insulin cells.	Induction of EAE in the NOD mouse strain with MOG_{35-55} leads to a relapsing-remitting disease that advances to secondary progressive disease	(Jacobsen et al., 2018; Mayo and Quinn, 2007)

1.3 Immunology of MS

The immune system can be considered in two parts, the innate and adaptive immune systems. The innate immune response is the first line of defense against infections in healthy organisms (Akira, 2003; Kennedy, 2010). The process of protection involves the complex use of a network of cells, tissues, and factors that work together to form a line of defense against diseases (Kumar et al., 2011). In MS, immune cells such as macrophages, neutrophils, and dendritic cells, are recruited during the early inflammation to the site of the injured area and produce pro-inflammatory cytokines and reactive oxygen species that destroy the myelin sheath in the CNS (King et al., 2009). Indeed, the involvement of the innate immune system is becoming increasingly appreciated in MS, which is thought to be the main trigger of the disease through its effect on APC that modulates the T-cell response (Hossain et al., 2017). However, uncertainty exists regarding the link between the innate and adaptive immune response with the pathogenesis of MS. In this section, the role of macrophages, neutrophils, T and B cells in the pathophysiology of MS and EAE will be described.

1.3.1 The role of innate and adaptive immune systems in MS and EAE

1.3.1.1 Pattern recognition receptors, cytokines, and innate immune cells

Pattern recognition receptors (PRRs) are a set of proteins that are part of the innate immune system and able to recognize molecules that are typically derived from microorganisms or endogenous sources (Walsh et al., 2013). The ligands of these receptors can be categorized into pathogen-associated molecular patterns (PAMPs) or damage-associated molecular patterns (DAMPs) (Kawai and Akira, 2009). Signaling through PRRs can induce the production of immune mediators that can impact the

adaptive immune response (Jang et al., 2015). Several PRRs have been recognized, including toll-like receptors (TLRs), nucleotide-binding oligomerization domain (NOD)-like receptors, retinoic acid-inducible gene 1-like receptors, and C-type lectin receptors (Amarante-Mendes et al., 2018; Walsh et al., 2013). These receptors can be expressed extracellularly, intracellularly, or in soluble forms within body fluids.

TLRs are a family of PRRs (Prinz et al., 2006) that play a crucial role in the innate immune system through their recognition of several ligands, such as endogenous DAMPs or exogenous PAMPs (Janeway and Medzhitov, 2002; Kawai and Akira, 2011; Qureshi and Medzhitov, 2003). Eleven types of TLRs have been identified in humans (TLR1 to TLR11) and twelve in mice (TLR1 to TLR 9 and TLR 11 to TLR 13) (Akira et al., 2006; Kawai and Akira, 2010). TLRs typically consist of one ectodomain, type-1 transmembrane glycoprotein containing an α-helix, and an intracellular Toll/interleukin-1 receptor domain (Brennan and Anderson, 2004; Jin and Lee, 2008; Li et al., 2002). Upon recognition of a corresponding ligand, TLRs dimerize to form hetero- or homodimers, which leads to downstream signaling and induction of immune mediators (Botos et al., 2011). The elicited immune response occurs through activation of transcription factors, such as transcription factors nuclear factor κB (NF-κB), translocation of these factors into the nucleus, and the production of either pro- or anti-inflammatory cytokines (Botos et al., 2011; Sasai and Yamamoto, 2013). The secretion of such cytokines can impact the several immune cells such as APCs and T-cells; therefore, establish a link between the innate and the adaptive immune responses (Akira and Takeda, 2004). It is known that myeloid differentiation primary response gene 88 (MyD88) is a crucial adaptor for the major TLR singling pathway (Werling and Jungi, 2003). MyD88 adaptor is necessary for

the induction phase of EAE through activation of peripheral myeloid dendritic cells (mDCs) and differentiation of autoimmune Th17 cells (Marta, 2009). The TLRs that are most studied in the context of EAE are TLR2, TLR4, and TLR9 (Marta, 2009; Miranda-Hernandez and Baxter, 2013; Prinz et al., 2006).

TLR2 recognizes microbial ligands including lipoteichoic acid, zymosan, lipoproteins, and peptidoglycan (Medzhitov, 2001), as well as endogenous ligands such as hyaluronan, heat shock protein, and High Mobility Group Box 1 Protein (HMGB1) that can be found in the CNS (Tsan and Gao, 2004). Activation of TLR2 impacts the development of several neurological conditions, including MS (Bsibsi et al., 2002). More specifically, TLR2 triggers the inflammatory process by activating glial cells, which can ultimately lead to tissue injury and neuronal death (Figure 1.1) (Tang et al., 2007). Furthermore, the activation of TLR2 suppresses the differentiation of oligodendrocytes progenitor cells (OPC) and inhibit remyelination (Sloane et al., 2010). However, the mechanisms that regulate TLR2 signaling have not been well defined in the context of MS and EAE.

TLR4 recognizes a broad range of exogenous ligands, such as lipopolysaccharides (LPS) from gram-negative bacteria, PTX, and *Mycobacterium tuberculosis toxin*. In addition, endogenous proteins can be recognized by TLR4 including heat shock proteins (HSP70), HMGB1, fibrinogen, heparan sulfate, and hyaluronic acid, which have been shown to induce inflammation to the CNS and EAE progression (Harris and Raucci, 2006; Uzawa et al., 2013). TLR4 is present in a variety of immune cells, including monocytes, macrophages, microglia in the CNS, myeloid DC, T and B lymphocytes, and tissues such as the intestinal and cerebral epithelium (Bsibsi et al., 2002; Reynolds et al.,

2012). The mechanisms that regulate TLR4 signaling in EAE have not been studied in-depth in the context of MS. One study demonstrated that TLR4 knockout mice exhibited a decreased disease severity, while another study showed a worsened disease state of EAE in the mice lacking TLR4. These results highlight the potential role of TLR4 in EAE. Moreover, the presence of TLR4 in microglial cells enhances brain injury in cerebral ischemia models and $CD4^+$ T-cell transgenic models following the administration of LPS enhanced EAE (Reynolds et al., 2012).

Endosomes in plasmacytoid DCs and lysosomes in myeloid DCs express TLR9, which has the ability to induce EAE through recognizing unmethylated CpG DNA motifs present in mycobacterial DNA (Krieg, 2002). Upon activation of TLR9, proinflammatory cytokines such as type I IFN, which leads to the inhibition of Th17 activity, and IL-6 or IL-23, are produced by plasmacytoid DCs or macrophages and myeloid DCs, respectively (Harrington et al., 2005). The studies published so far regarding the role of TLR9 in the regulation or progression of EAE are inconsistent. A study by Marta et al. (2008) identified a regulatory role in inducing EAE rather than enhancing EAE, by showing that TLR9 knockout mice exhibited a worsened clinical score compared to WT mice that were immunized with MOG protein. In contrast, (Prinz et al., 2006) showed a delay in the severity of the disease after immunizing TLR9 knockout and WT mice with MOG_{35-55} peptide. The explanation for these conflicting results may be due to the pathogenic B-cell response and production of antibodies to MOG protein rather than MOG peptide (Iglesias et al., 2001; Lyons et al., 1999).

Cytokines are another aspect of the innate immune inflammatory response involved in many inflammatory diseases, including MS, such as TNF, IL-1β, and IL-6

(Centonze et al., 2010). These cytokines contribute to damage of oligodendrocytes, axons, and neurons to promote the progression of the disease, and inhibition of these cytokines may be a potential target to protect oligodendrocytes and prevent neuronal death (Centonze et al., 2010; Imitola et al., 2005). Activated mononuclear phagocytic cells, macrophages, T cells, microglia, and astrocytes express TNF, which promotes the inflammatory process through controlling cellular differentiation and apoptosis as well as cell recruitment processes. In EAE, Th1 activation linked to the production of TNF enhances the release of other cytokines, chemokines, adhesion molecules, and may be involved in remyelination (Arnett et al., 2001). Inhibition of TNF by neutralizing antibodies reduces EAE disease severity in mice by decreasing infiltration and demyelination (Williams et al., 2014). In contrast, human MS patients treated with TNF neutralizing antibodies exhibited a worsened disease progression, which suggests that TNF has important roles in the early stages of the disease (Probert et al., 1995).

IL-1β mediates an innate immune response involving adhesion molecules to enhance inflammatory cell recruitment and stimulates astrocytes to release vascular endothelial growth factor-A (VEGF-A) that together disrupt the integrity of the BBB, which allows T cells to enter the CNS and subsequently degrade the myelin sheath and causes CNS damage (Marui et al., 1993). Furthermore, it has been observed that IL-1β is elevated in the CSF of MS patients and IL-1 knockout mice, resulting in reduced severity of EAE, suggesting that this cytokine plays a crucial role in the early phase of the disease (Matsuki et al., 2006).

Another cytokine, IL-6, expressed in mononuclear phagocytes, T cells, microglia, astrocytes, and vascular endothelial cells is elevated in MS patients and is crucial for the

activation of autoimmunity by promoting $CD4^+$ T cell activation and the acute phase of the inflammatory response (Imitola et al., 2005). IL-6 is also required for the development of antibody-producing plasma cells. IL-6 knockout mice failed to develop EAE, suggesting that this cytokine is required for the initiation of the disease progression (Samoilova et al., 1998). Furthermore, IL-6 may be implicated in the remission phase of EAE through the clearance of myelin debris that hinders remyelination (Heinrich et al., 2003).

Neutrophils are granulocytes that represent the first line of defense in the innate immune system and have a vital role in the inflammatory process by responding to infection or injury and can be marked as Gr-1^{high}/$CD11b^+$ in mice (Kennedy, 2010; Mayadas et al., 2014; Nathan, 2006; Jönsson et al., 2011). Neutrophils migrate to the site of injury and have the ability to neutralize pathogens and kill the bacteria by phagocytosing, degranulating, releasing a neutrophil extracellular trap, and releasing ROS (Kolaczkowska and Kubes, 2013; Mayadas et al., 2014; Nauseef and Borregaard, 2014). Neutrophils express LPS receptors, such as TLR4, which can induce systemic inflammation through activation of the TLR4 signaling pathway through, CD14 or MD-2 (Gomi et al., 2002; Pillay et al., 2010; Zanoni et al., 2011). Neutrophils can kill pathogenic organisms after recruitment to the site of injury and have the capacity to damage tissue. Upon exposure to LPS, peritoneal neutrophils become elevated and produce ROS contributing to persistent inflammation. Adhesion and migration of neutrophils after LPS exposure is facilitated by IL-1β production (Fermino et al., 2011). It has been reported that the depletion of neutrophils by anti-Ly6G or anti-Gr-1 antibody

hinders the onset of EAE, which is associated with antibody-dependent phagocytosis of neutrophils by macrophages and not the lack of Ly6G function (Daley et al., 2008).

Macrophages are derived from hematopoietic stem cells originating in the bone marrow and are expressed in all tissues of the body, and their designation is based on their location (Ahmadbeigi et al., 2013; Crocker and Gordon, 1985; King et al., 2009). For example, macrophages exist as microglia in the CNS, Kupffer cells in the liver, alveolar macrophages in the lungs, and peritoneal macrophages in the peritoneum, among others (Sawada et al., 2008). Macrophages are necessary for the effective functioning of the innate and adaptive immune responses, have a vital role in phagocytosis, and produce pro-inflammatory cytokines that contribute to inflammation (Korn et al., 2010).

In normal conditions, microglia in the CNS contributes to synaptic plasticity and are responsible for tissue repair, clearance of injury, and regulation of neurons (Ferrini and De Koninck, 2013; Ginhoux et al., 2010). The activity of microglia is regulated by neurons, astrocytes, T-cells, and the BBB and work collectively with peripheral macrophages. In the early stages of inflammation, levels of cellular markers such as CD45, CCR1, CCR5 are expressed in high levels in macrophages and low levels in microglia while TGF-β is expressed at high or low levels in macrophages or microglia, respectively. Macrophages and microglia fall into two categories, M1 or M2 (Mills et al., 2000). Macrophages or microglia in the resting state become activated through TLRs interacting with IFN-γ, immunoglobin, and complement to become pro-inflammatory M1 (Dong, 2008; Hanke and Kielian, 2011). Activated M1 will release pro-inflammatory cytokines and chemokines such as TNF, IL-1β, IL-6, IL-12, IL-23, CCL4, CCL5, CCL8, CXCL9, CXCL10, CXCL2, and CXCL4 that contribute to tissue damage demyelination,

and neuronal death in the CNS (Kim and De Vellis, 2005; Liu et al., 2013; Norden et al., 2015; Saijo and Glass, 2011). In contrast, IL-4, IL-10, IL-13, and TGF-β that are released by M2 microglia induce tissue repair, remodeling, and promote anti-inflammatory activities (Almolda et al., 2015; Franco and Fernández-Suárez, 2015; Miron et al., 2013; Shin et al., 2012). Furthermore, the differentiation of Th2 cells and regulatory T cells, which are regulated by M2, could suppress inflammation through reduced activity of NF-kB and enhanced phagocytic activity compared to M1 (Ghosh et al., 2016; Zhang et al., 2018). The imbalance between M1 and M2 correlates to the development of EAE, and it has been reported that treatment with M2 monocytes attenuated EAE symptoms and promoted the differentiation of oligodendrocytes to enhance the recovery phase of EAE (Jiang et al., 2014; Miron et al., 2013). Moreover, in the cuprizone model of EAE, microglia are present in the lesions of the CNS and are associated with the inflammatory process of MS. Though there is some uncertainty with the mechanisms linking microglia to MS pathogenesis, it is proposed that microglia create ROS that damage oligodendrocytes and astrocytes. Furthermore, microglia have been found to participate in the remyelination of the CNS through phagocytosis, and the remyelination process is insufficient in MS due to a blockage of OPC differentiation (Jiang et al., 2014; Miron et al., 2013). Additionally, microglia produce TNF, IGF-1, and FGF-2, which are necessary for the differentiation of OPCs. In the EAE model, it has been found that IL-4 increases the proliferation of oligodendrocytes suggesting the potential involvement of macrophages and microglia in the remyelination process (Keating et al., 2009). An additional role of microglia is to modulate the adaptive immune response by acting as APCs to recruit T cells in the CNS. It has been observed that monocytes have a strong

influence on the progression of EAE, and the deletion of monocytes cells in preclinical EAE was delayed symptom onset(Ajami et al., 2011; Iismaa et al., 2009). Additionally, the severity of clinical scoring is proportional to the number of infiltrating peripheral monocytes and the absence of monocytes contributes to reduced disease severity (Chrobok et al., 2017). Microglia play a prominent role in the early stages of EAE before the clinical onset and recruit monocytes during the chronic phase (Mikita et al., 2011; Zhu et al., 2007).

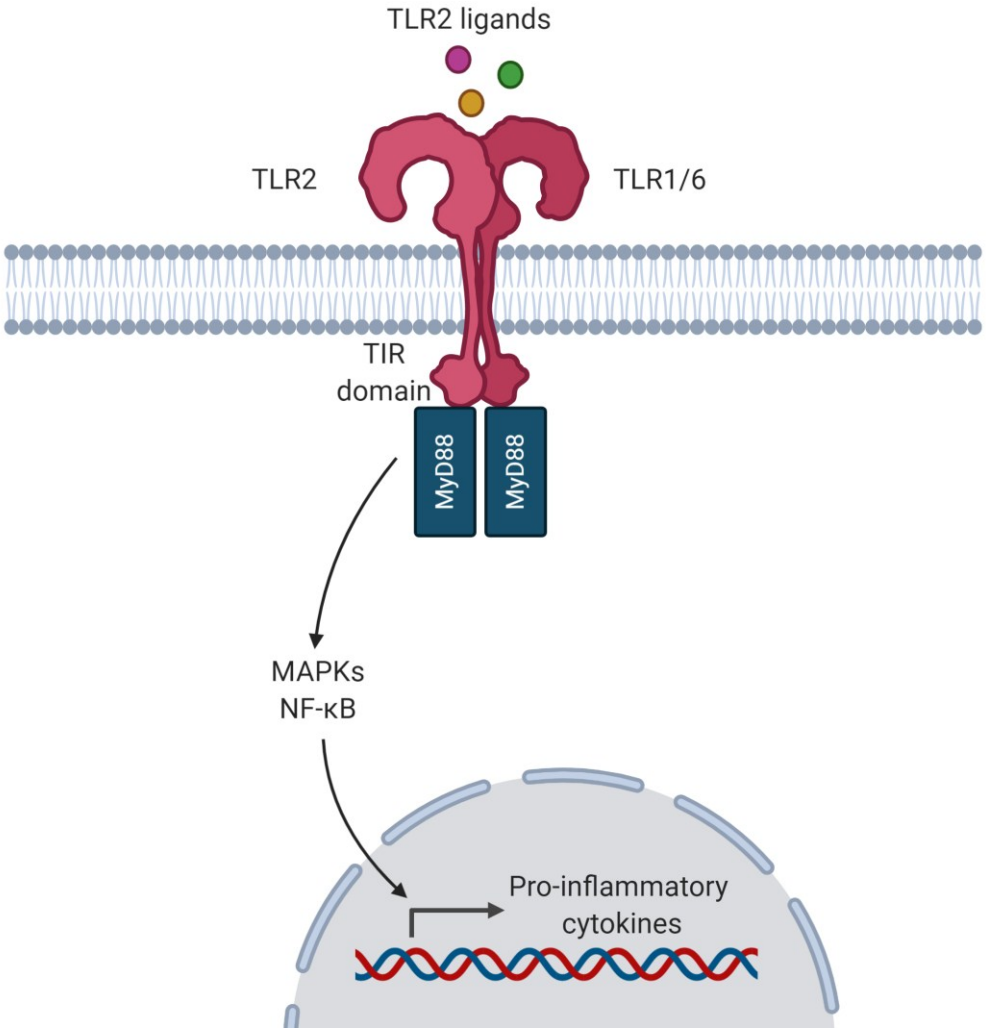
TLR2 ligands
TLR2
TLR1/6
TIR
domain
MyD88
MyD88
MAPKs
NF-κB
Pro-inflammatory
cytokines

Figure 1-1 Model for pro-inflammatory signaling through TLR2.

Simplified schematic representation of the pro-inflammatory signaling through TLR2 implicates the recruitment of the adaptors MyD88 to induce inflammatory cytokines through ERK, JNK, and NF-κB.

Adapted from Li et al., (2013b)

1.3.1.2 T cells and B cells

The role of the adaptive immune response in MS and EAE has been extensively studied, particularly the involvement of T cells and B cells in the pathogenesis of the disease. The modulation of $CD4^+$ T cell responses is the primary goal of therapeutic agents for EAE and MS; however, many other lymphocytes, such as $CD8^+$ T cells and B cells, are implicated in the disease and may be suitable targets (Bielekova et al., 2000; Rangachari et al., 2017).

It is well characterized that T cells, both $CD4^+$ and $CD8^+$ subtypes, are implicated in the pathology of MS (Legroux and Arbour, 2015; Rangachari et al., 2017). $CD4^+$ T cells, also known as helper T cells, are involved in the coordination of the immune system while $CD8^+$ T cells, also known as cytotoxic T cells, govern responses to intracellular pathogens and neoplastic cells. The T cell receptor (TCR) expressed on $CD4^+$ and $CD8^+$ T cells recognize antigens presented by major histocompatibility complex (MHC) class II and I, respectively. Naïve T cells must have two signals from APCs for activation: recognition of the peptide-MHC complex via TCR and communication with a coactivating receptor (CD28) along with a ligand (CD80, CD86). This process ultimately stimulates an intracellular signaling pathway leading to the maturation, proliferation, and secretion of cytokines by T cells (Dong, 2008; Legroux and Arbour, 2015). It is believed that $CD4^+$ T-cells mediate the disease pathogenesis of MS, especially Th1 and Th17 cells. The secretion of IL-6, TGF-β, and IL-23 and the transcription factors RORγt, RORα, and STAT3 induce the differentiation of naive CD4+ to Th17, which exacerbates the disease development by producing IL-17A, IL-17F, IL-

21, IL-22, IL-26 secretion (Dong, 2008). It has been reported that in the EAE model, $CD4^+$ T cells secrete IFN-γ and IL-17 by Th1 and Th17 cells, which coincided with increased production of pro-inflammatory cytokines IL-1β, IL-6 and TNF by microglia (Hemmer et al., 2015; Murphy et al., 2010). Blocking $CD4^+$ T cells in MS patients by an anti-CD4 depleting antibody had no impact on disease severity, while non-specific immunosuppressive therapy reduced the disease severity by preventing cytokine release and hindering disease progression (Jones et al., 2010; Van Oosten et al., 1997).

B cells have negative regulatory functions on inflammation during the course of EAE and MS through their production of anti-inflammatory cytokines, such as IL-10. Multiple subtypes of B cells exist, including B10 cells, which produce IL-10 (Shen and Fillatreau, 2015) and high levels of Th17 cells are present in MS and are related to disease severity (Axtell et al., 2010). B cells are APCs that originate in the bone marrow and are specialized in the secretion of antibodies that have a vital role in MS (Claes et al., 2015; Lebien and Tedder, 2008; Matsushita et al., 2006; Pierson et al., 2014). B cells have been reported to play an important role in modulating Th1 and Th2 cytokines production in EAE (Matsushita et al., 2006).

1.4 Voltage-gated sodium channels

Several underlying mechanisms that involve the interaction between immune cells and neurons are believed to impact the development of MS. Nav channels may play a central role in this interaction due to the expression in both types of cells (Eijkelkamp et al., 2012; Stys et al., 2006).

Nav channels are transmembrane proteins that conduct sodium across the cellular membrane (Catterall et al., 2005a; Chen et al., 2018a). They are found in both excitable

cells, such as neurons and myocytes and non-excitable cells, such as immune cells (Savio-Galimberti et al., 2012). In neuronal cells, the distribution of Nav channels along the axon is essential for the generation and propagation of action potentials, whereas in non-excitable cells such as glial cells, they are believed to regulate energy supply and cell motility (Brackenbury et al., 2010).

Each Nav channel is composed of one of ten known α-subunits isoforms and one or two regulatory β-subunits (β1, β2 and/or β3) (Brackenbury and Isom, 2011; Catterall, 2000). The α-subunit consists of four homologous domains (I-IV), each of which comprises six transmembrane segments (S1-S6). The S4 in each domain acts as a voltage sensor that contains a high concentration of positively charged amino acids, functioning as the core of the voltage sensor responsible for activation of the voltage-dependent channel (Figure 1.2) (Kwong and Carr, 2015; Patino and Isom, 2010). Furthermore, the α-subunit is sufficient to conduct sodium alone when it is expressed, whereas β-subunits are required for cell adhesion and channel localization and regulate the rate of activation and inactivation of the α-subunit (McEwen and Isom, 2004; O'Malley and Isom, 2015).

Nav channels have three states in terms of conductivity: a resting state in which the channel's gate is closed, an open state that occurs upon depolarization, and a deactivating state that occurs gradually after depolarization in a single step (Ahern, 2013; Eijkelkamp et al., 2012; McCusker et al., 2012).

A

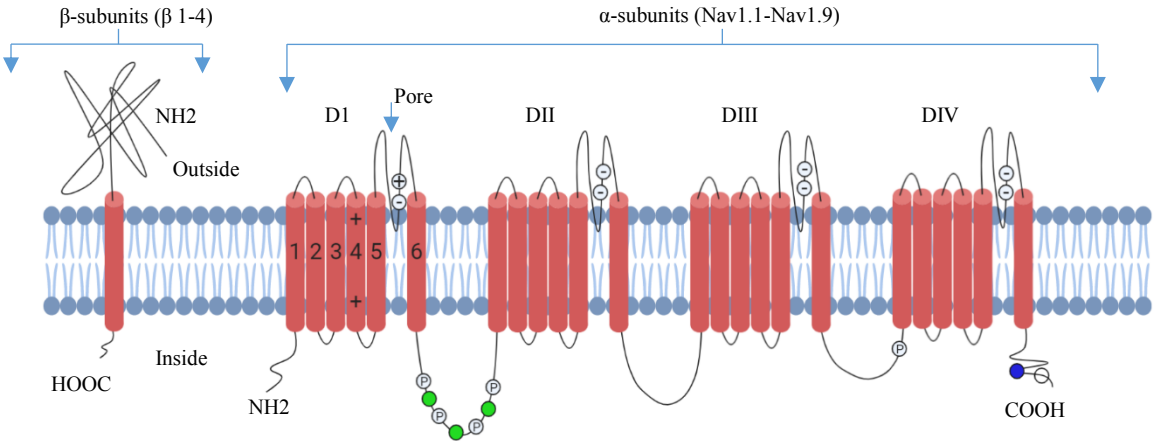
β-subunits (β 1-4)
α-subunits (Nav1.1-Nav1.9)
NH2
Outside
D1
Pore
DII
DIII
DIV
1 2 3 4 5
6
Inside
HOOC
NH2
COOH

B

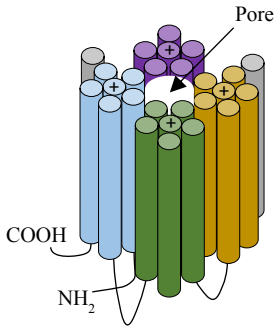
Pore
COOH
NH2

Figure 1-2 Structure of voltage-gated sodium channels.

A) Schematic representation of the voltage-gated sodium channels. α-subunits have four domains starting with the first domain at the N-terminus on the left to the fourth domain at the C-terminus on the right (D I -D IV) and β-subunit. The fourth α-helical transmembrane segment of each domain contains positively charged amino acids as represented in this schematic by the" +" symbol. P represents phosphorylation sites, and green circles represent RXR, a motif that mediates the localization of proteins in the ER (ER retention motif).

B**)** Schematic 3D representation of Nav channels.

Adapted from Fraser et al. (2014)

1.4.1 Nav channel heterogeneity

There are ten genes that encode Nav α-subunit proteins Nav1.1-Nav1.9 and Nav2.1 (Nax) (Catterall, 2000; Catterall et al., 2005a; O'Malley et al., 2009). Nav1.1, Nav1.2, Nav1.3, and Nav1.6, encoded by the genes *SCN1A*, *SCN2A*, *SCN3A*, and *SCN8A*, respectively, are mainly expressed in the CNS, however, with variable spatial (cell type and subcellular) and temporal (developmental) distribution (Catterall et al., 2005b; De Lera Ruiz and Kraus, 2015). Nav1.1 is prominently expressed in inhibitory gamma-aminobutyric acidergic neurons (Catterall et al., 2005a; Payandeh et al., 2011), Nav1.2 is prominently expressed in unmyelinated axons and dendrites in the cortex and the hippocampus (Boiko et al., 2001; Lossin et al., 2012), while Nav1.3 has a wide expression in the human brain (Estacion et al., 2010; Holland et al., 2008).

Nav1.6 is expressed in several different types of cells across the CNS, such as Purkinje cells, pyramidal cells, and glial cells (Boiko et al., 2001; Burgess et al., 1995a; O'Brien and Meisler, 2013). It is also expressed in the PNS and in myelinated neurons in which this channel is highly concentrated at the nodes of Ranvier (Kearney, 2002; Wagnon and Meisler, 2015).

Nav1.4, encoded by *SCN4A*, is mainly expressed in striated muscle tissue (Jurkat-Rott et al., 2010), whereas Nav1.5, encoded by *SCN5A*, is the dominant channel in the cardiac muscle (Black et al., 2009a; Estacion et al., 2010). Nav1.7, Nav1.8, and Nav1.9, encoded by *SCN9A*, *SCN10A*, and *SCN11A*, respectively, are expressed predominantly in the PNS (Eijkelkamp et al., 2012; Gong et al., 1999; Zakon, 2012).

Finally, based on sensitivity to tetrodotoxin (TTX), a potent non-specific Nav channel blocker, Nav channels are divided into (Chen et al., 2002; Hains et al., 2003;

Koopmann et al., 2006) TTX-sensitive (TTX-S) channels, which can be blocked by nanomolar concentrations of TTX includes Nav1.1, Nav1.2, Nav1.3, Nav1.4, Nav1.6, and Nav1.7 subtypes. TTX-resistant (TTX-R) channels, which require a higher amount of TTX (micromolar) to be blocked and include Nav1.5, Nav1.8, and Nav1.9 subtypes (Bagal et al., 2015; Catterall et al., 2005b; Black et al., 2004; Savio-Galimberti et al., 2012).

1.4.2 Nav channels in disease

Nav channels have been linked to a broad range of diseases in the nervous system, such as multiple sclerosis (MS), neuropathic pain, epilepsy, and brain cancer (Black and Waxman, 2013; Eijkelkamp et al., 2012). Scientists have used animal models to better understand the role of Nav channels in the pathogenesis of neuronal disorders by manipulating the encoding genes of these channels. In demyelination diseases, Nav1.2, Nav1.5, Nav1.6, and Nav1.8, have been linked to the axonal degeneration and loss. (Table 2)

Table 2 Channelopathies that have been associated with Nav channel expression

Nav channel	Encoding gene	The primary site of expression	TTX Sensitivity	Diseases /Phenotypes	References
α-subunits					
Nav1.1	*SCN1A*	CNS, PNS	sensitive	Epilepsy, neurodegeneration Panayiotopoulos syndrome	(Claes et al., 2003; Meisler and Kearney, 2005)
Nav1.2	*SCN2A*	CNS, PNS	sensitive	MS, early infantile epileptic encephalopathy, and familial autism.	(Berkovic et al., 2004; Schattling et al., 2016; Sugawara et al., 2001)
Nav1.3	*SCN3A*	CNS, PNS	sensitive	focal epilepsy in children	(Bartolomei et al., 1997; Hains et al., 2003; Vanoye et al., 2014)
Nav1.4	*SCN4A*	Skeletal muscle	sensitive	Hyperkalemic periodic paralysis	(Kuzmenkin et al., 2002; Raja Rayan and Hanna, 2010)
Nav1.5	*SCN5A*	Cardiac muscle	resistant	Brugada syndrome (idiopathic ventricular fibrillation), MS and arrhythmias	(Black et al., 2009b; Detta et al., 2015; Pappalardo et al., 2014)
Nav1.6	*SCN8A*	CNS, PNS	sensitive	Mental retardation, ataxia, tremors, MS and other movement disorders	(Alrashdi et al., 2019; Meisler et al., 2004; Veeramah et al., 2012)
Nav1.7	*SCN9A*	PNS	sensitive	familial rectal pain, and small fiber neuropathy	(Cummins et al., 2004; Dib-Hajj et al., 2005; Yang et al., 2004)
Nav1.8	*SCN10A*	PNS	resistant	peripheral pain syndromes Pain sensation, inflammatory pain, MS	(Lai et al., 2002; Shields et al., 2015)
Nav1.9	*SCN11A*	PNS	resistant	Loss of pain perception and pain sensitization	(Priest et al., 2005; Zhang et al., 2013)
Nax	*SCN6A and SCN7A*	Brain	unknown	Temporal lobe epilepsy	(Gorter et al., 2010; Noda and Hiyama, 2015)

Nav channel	Encoding gene	The primary site of expression	Diseases /Phenotypes	References
β-subunits				
Navβ.1	*SCN1B*	CNS, PNS, glia, cardiac muscles	Brugada syndrome, and epileptic syndromes	(O'Malley et al., 2009; Pertin et al., 2005)
Navβ.2	*SCN2B*	CNS, PNS cardiac tissue	inflammatory pain, MS	(O'Malley et al., 2009)
Navβ.3	*SCN3B*	CNS, PNS	Temporal epilepsy	(Casula et al., 2004; Van Gassen et al., 2009)
Navβ.4	*SCN4B*	CNS, PNS	Huntington's disease	(Medeiros-Domingo et al., 2007; Oyama et al., 2006)

1.4.3 Inflammation, demyelination and ion channel redistribution

Immune cells secrete several molecules, including cytokines, chemokines, glutamate, ROS, reactive nitrogen species (RNS) including nitric oxide (NO), some of which are neurotoxic and can disrupt the normal metabolism within neurons and promote inflammation (Bagasra et al., 1995; Bitsch, 2000; Van Horssen et al., 2011). NO has been shown to act as a double edge sword in MS as it might induce disruption of the BBB, demyelination, and axonal degeneration, while also having potentially beneficial immunomodulatory effects (Engelhardt and Ransohoff, 2012; Smith and Lassmann, 2002). The beneficial or harmful effect of NO relies on its level within the tissue and the existence of other molecules at the site of inflammation, such as superoxide anions. In normal conditions, NO is involved in neurotransmission and regulation of gene expression, which control the perception of pain, aggression, and depression (Kumar et al., 2017). In the context of MS, it has been reported that NO plays a protective role in the suppression of T cells by inhibiting their proliferation in EAE (Van Der Veen et al., 2004). However, the adverse effect of NO appears when it is released in high amounts by macrophages and microglia in MS and EAE at the site of inflammation concurrently with superoxide anions, leading to the production of highly toxic compounds such as peroxynitrite (Kumar et al., 2017). The production of peroxynitrite leads to the impairment of oligodendrocytes via damage to the mitochondrial DNA and membrane leading to the accumulation of mitochondrial DNA mutations and misfolded proteins (Friese et al., 2014; Lan et al., 2017).

Mitochondria are key regulators of axonal survival as they regulate the production of energy that is essential for ion channel function and distribution along the axon (Friese

et al., 2014; Nikić et al., 2011). Abnormal mitochondria function, which in turn results in reduced ATP production, causes increased levels of intercellular sodium by disabling the Na^+/K^+ ATPase (Friese et al., 2014; Kann and Kovács, 2007). The energy imbalance and loss of myelin in chronic CNS inflammation result in the maldistribution of several ion channels, including Nav channels, K^+ channels and Ca^{2+} channels and impairs their function (Craner et al., 2004a; Howarth et al., 2012). The impairment of function and distribution of these ion channels along the axon causes disturbances in ion concentrations, mainly of Na^+, K^+, and Ca^{2+}, across the neuronal membrane, which have a neurotoxic effect that impairs axonal conduction (Craner et al., 2004b). Increased intracellular Ca^{2+} is eventually fatal to the cell as degradative enzymes and NO synthase is activated, which leads to apoptosis of the neuron (Friese et al., 2014). Furthermore, intracellular accumulation of Ca^{2+} within the axons can cause oncotic cell swelling that leads to neuronal death (Schattling et al., 2012). Neurons have a buffering mechanism to prevent the adverse effects of the intracellular accumulation of Na^+ and Ca^{2+} by increasing activation of pro-survival genes and inhibition of Wallerian degeneration (Howarth et al., 2012). However, persistent inflammation, which is exacerbated by neuronal and oligodendrocytes necrosis, might inhibit these buffering mechanisms and thus provoke axonal damage (Dendrou et al., 2015; Saxena and Caroni, 2007).

1.4.4 Nav channels and axonal degeneration in MS

Nav channels have been proposed to play a significant role in the pathogenesis of demyelinating diseases. As mentioned before, expression of Nav channels (Nav1.1, Nav1.2, Nav1.3, Nav1.6, Nav1.7, Nav1.8, and Nav1.9) across the CNS and the PNS is regulated in a spatial (by cell type and subcellular localization) and a temporal (by

developmental time point) manner (Catterall et al., 2005b; Israel et al., 2019). The most studied Nav channels in MS and EAE are the Nav1.2 and Nav1.6 isoforms because they have been linked to the demyelination process and are found to be abnormally distributed in the lesions (Bouafia et al., 2014; Craner et al., 2004a; Waxman, 2006). Moreover, Nav1.5, which is best known as the cardiac muscle isoform, has been shown to be expressed in the astrocytes in acute and chronic MS lesions (Pappalardo et al., 2014; Yang et al., 2004). Finally, Nav1.8, which is mainly expressed in the PNS, is proposed to be involved in cerebellar dysfunction in MS and EAE (Han et al., 2016; Schaecher et al., 2001). In addition to the involvement of the Nav channel α-subunits, the β2-subunit has been reported to play a key role in the progression of MS (Chen et al., 2002; O'Malley et al., 2009).

1.4.4.1 Nav1.2 and Nav1.6 in EAE and MS

In normal conditions, Nav1.2 is predominantly expressed in the CNS in pre-myelinated axons, immature nodes of Ranvier during development, and non-myelinated axons in adults. In immature axons, the main function of Nav1.2 is to support action potential generation before the deposition of myelin (Gong et al., 1999; Kaplan et al., 2001). Nav1.6 gradually replaces Nav1.2 during axonal myelination and dominates in mature nodes of Ranvier, possibly because Nav1.6 produces a higher persistent current than Nav1.2 (Craner et al., 2004a; Waxman, 2006). Interestingly, Nav1.6 is expressed in non-neuronal cells, such as microglia and macrophages, as well as in invasive cancer cell lines. Nav channels in these non-excitable cells are believed to contribute to their motility by having their activity linked to the actin cytoskeleton dynamics and enabling the

formation of podosomes and invadopodia in macrophages (Carrithers et al., 2009a) although the mechanism by which Navs influence the actin network remains unclear.

Nav1.2 is co-expressed with the Na^+/Ca^{2+} exchanger (NCX) in demyelinated axons that have no signs of injury, whereas Nav1.6 co-localizes with NCX in demyelinated axons during an axonal injury in MS and EAE (Bouafia et al., 2014; Craner et al., 2004c; Waxman, 2008). In a study by Craner (Craner et al., 2004b), it was shown that co-localization of Nav1.6 and NCX was found only in damaged axons. These were identified using antibodies against beta-amyloid precursor protein (β-APP), an indicator of imminent degeneration of the demyelinated axons (Craner et al., 2004a). In contrast, Nav1.2 expression with NCX did not correlate with the presence of β-APP (Craner et al., 2004d; Waxman, 2008). The persistent influx of Na^+ through Nav1.6 channel has been suggested to reverse the function of NCX, leading to the accumulation of intracellular Ca^{2+} ions in the axon that results in axonal degradation (Bouafia et al., 2014; Craner, 2003). It is important to note that this hypothesis is based on co-localization experiments. Reduced expression of Nav1.6 should theoretically result in improved axonal health in the context of MS, but this has not been shown directly. Craner (Craner et al., 2005) showed that in EAE and MS, the expression of Nav1.6 is upregulated in activated microglia and macrophages. Increased activation of microglia and macrophages in MS has been linked to the axonal degeneration via induction of phagocytosis (Craner et al., 2005; Jacobsen et al., 2002), antigen presentation (Lo et al., 2012), cell migration (Black et al., 2009a; Hernandez-Plata et al., 2012; Persson et al., 2014a), stimulation of $CD4^+$ T cell proliferation, and production of pro-inflammatory cytokines and chemokine (Amor et al., 2014a; Black et al., 2009a).

Research has shown that blocking of Nav1.6 by TTX in rats and the lack of Nav1.6 in mice results in a significant reduction in phagocytic function of activated microglia by 40% and reduced infiltration of inflammatory cells by 75% (Craner et al., 2005). The reduced microglial phagocytic activity was associated with the decrease in proinflammatory cytokines production, including IL-1α, IL-1β and tumor necrosis factor (TNF) (Black et al., 2009a).

The expression of Nav1.2 along injured demyelinated axons in EAE resembles the distribution of this channel on pre-myelinated and non-myelinated axons (Boiko et al., 2001; Kaplan et al., 2001). Like in normal unmyelinated axons, it is speculated that Nav1.2 is important for conducting action potentials in non-damaged axons in MS, although with lower spike frequencies than Nav1.6 (Craner et al., 2004c; Waxman, 2006). Nav1.2 has less influence on Na^+ influx compared to Nav1.6, which might reduce the damage of axons and enhances their survival in MS and EAE (Rush et al., 2005). Studies have shown that Nav1.2 plays a compensatory role for partial loss of Nav1.6 and may be able to conduct signals in the demyelinated axon (Craner et al., 2004b; Van Wart and Matthews, 2006). In contrast, recent work by Schattling et al. (2016) has examined the impact in EAE mice of increased Nav1.2 activity on neuronal degeneration by inserting a human gain-of-function mutation in *Scn2a*. Although this increase of Nav1.2 activity was not associated with alteration of the immune response in EAE, it increased the intracellular Na^+ concentration, which was associated with increased neurodegeneration. Such evidence suggests that the development of a selective blocker of Nav1.6 might be of potential benefit for neuroprotection without a major impact on the immune system. However, researchers have not shown an impact of Nav1.2 gain of

function mutation on the expression of other Nav channels. In contrast, the generation of human Nav1.6 gain-of-function mutation in mice was found not to be suitable to study the role of Nav1.6 in EAE due to the spontaneous motor seizure phenotypes that could interfere with the EAE clinical symptoms (Wagnon et al., 2015). Our work implicates the Nav1.6 isoform as a primary contributor to axonal degeneration following demyelination in EAE (Alrashdi et al., 2019) (Chapter 2).

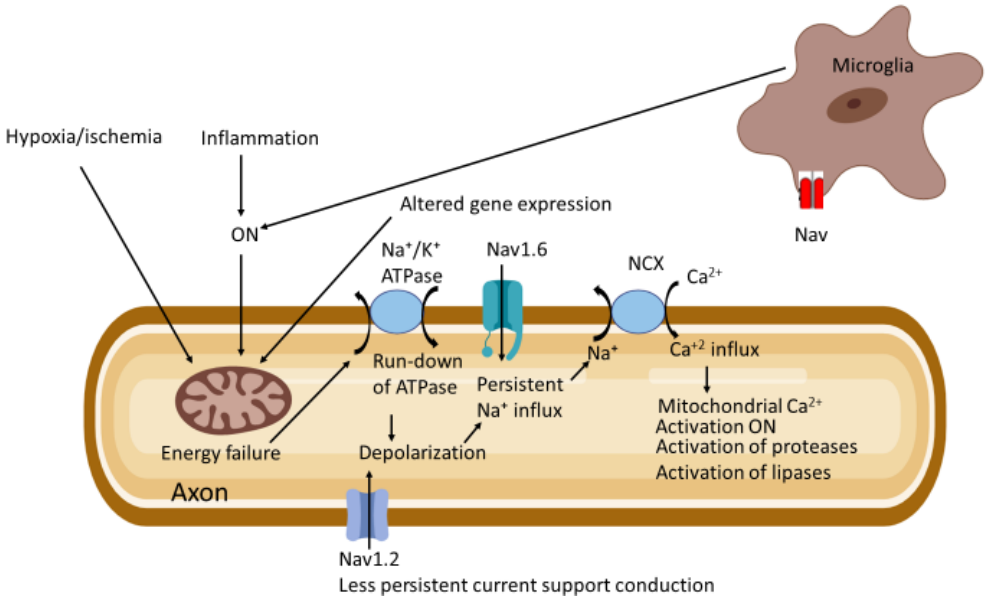
Microglia
Hypoxia/ischemia
Inflammation
ON
Altered gene expression
Nav
Na+/K+
ATPase
Nav1.6
NCX
Ca2+
Run-down
of ATPase
Persistent
Na+ influx
Na+
Ca+2 influx
Mitochondrial Ca2+
Activation ON
Activation of proteases
Activation of lipases
Energy failure
Depolarization
Axon
Nav1.2
Less persistent current support conduction

Figure 1-3 Model of functional effects of expression of Nav1.2 and Nav1.6 channels along demyelinated axons.

Schematic shows that Nav1.2 distributes along the demyelinated axon to restore the conduction of nerve impulse. The persistent current produced by Nav1.6 causes a reversal of the functioning of the Na^+-Ca^{2+} exchanger that leads to the accumulation of intracellular toxic calcium that triggers axonal injury. Mitochondrial dysfunction induced by NO, alterations of mitochondrial gene expression, and hypoxia/ischemia results from perivascular inflammation that promotes axonal energy failure to subsequently compromise the function of the Na^+/K^+ ATPase that reduces the ability of the axon to sustain resting potential and export Na^+. Resulting from the accumulation of Ca^{2+} inside the axon, calcium-induced calcium release (CICR) from internal stores and activation of NO synthase, proteases and lipases occur. Nav channels contribute to the activation of microglia and macrophages that release NO and participate in phagocytosis.

Adapted from (Waxman, 2006).

1.4.4.2 Nav1.5 in EAE and MS

Nav1.5 was long recognized as the exclusive cardiac muscle Nav isoform and was generally not believed to be expressed in other tissues (Black et al., 1995; Pappalardo et al., 2014). However, Fraser et al. (2004) have shown that the Nav1.5 channel is also expressed in normal human T-lymphocytes and modulates their motility. Furthermore, in MS and EAE, it has been shown that the expression of Nav1.5 is upregulated in reactive astrocytes within acute and chronic lesions (Craner et al., 2005). These observations implicate Nav1.5 in immune regulation. Nav1.5 expression was correlated with the severity of the disease in the EAE model, as it increased during relapses and decreased during remission (Pappalardo et al., 2014). Astrocytes are glial cells that represent the most abundant cell type in the CNS. These cells assist in maintaining homeostasis at synaptic connections, are an essential component of the BBB, and may regulate blood flow in response to synaptic activity (Blackburn et al., 2009). The selective upregulation of Nav1.5 on reactive astrocytes in MS patients compared to the minimal change of other Nav channels suggests a potential role of Nav1.5 in the pathogenesis of the disease (Black et al., 2010), but more direct functional data would be important to define this channel's role. However, the normal role of Nav channels in astrocytes is not well understood. Nav channels translocate to the plasma membrane and help to produce a persistent Na^+ current (Blackburn et al., 2009). Such Na^+ influx in the astrocytes is critical for the function of Na^+/K^+ ATPase activity that, in turn, regulates the ionic homeostasis in the CNS (Barker and Ullian, 2010; De Pittà et al., 2016). The correlation between the elevation of Na^+ concentration in MS lesions and upregulation of Nav1.5 on astrocytes suggests that such upregulation could be a compensation mechanism to

maintain the ionic homeostasis in areas of CNS injury (Black et al., 2010), but again does not provide direct evidence of a specific role for the of Nav1.5. Conclusive results on Nav1.5 function would require gene deletion or similar studies.

1.4.4.3 Nav1.8 in EAE and MS

Nav1.8 is mainly expressed in the PNS in nociceptive trigeminal and dorsal root ganglia neurons. However, in MS and EAE, Nav1.8 is ectopically expressed in Purkinje cells of the cerebellum, suggesting an important role of this channel in the pathogenesis of MS (Han et al., 2016). Craner et al., (2003) showed that the increase of Nav1.8 mRNA (*Scna10*) and protein levels in Purkinje cells are positively correlated with the severity and duration of EAE (Craner, 2003). Consistent with this observation, (Shields et al., 2012) reported that the cerebellar ectopic expression of Nav1.8 is linked to the disruption of the normal function of Purkinje cells and to the coordination of motor behavior that is responsible for aspects of symptom development in EAE (Shields et al., 2012). Overexpression of Nav1.8 in Purkinje cells in vitro causes an increase of action potential firing in these cells (Renganathan et al., 2003; Shields et al., 2012). The severity of EAE progression was significantly reduced in Nav1.8 knockout mice and in wild-type mice that were treated with Nav1.8 selective blockers (Shields et al., 2015).

1.4.4.4 Nav channel β2 subunit in EAE and MS

The β2 subunit of Nav channels, encoded by *SCN2B*, is a membrane glycoprotein that plays a critical role in the expression and localization of Nav channels on the neuronal cell membrane and in regulating the Na^+ current in CNS and PNS (Chen et al., 2002; Lopez-Santiago et al., 2006). Moreover, β2 subunits function as cell adhesion molecules that mediate interaction with the extracellular matrix and may play a role in

cell migration (McEwen and Isom, 2004). Expression of the β2 subunit in the nervous system changes during development in mice and rats as it starts before birth but reaches its maximum 21 days after birth and persists in adulthood, with its highest expression in cortex, hippocampus, and cerebellum (Sashihara et al., 1995). The known importance of Nav channels in demyelination diseases suggests the corresponding importance of the β2 subunit due to its role in Nav channel expression. Lopez-Santiago et al. (2006); O'Malley et al. (2009) showed that the absence of the β2 subunit in mice reduces the severe clinical symptoms and axonal degeneration in EAE. This protective effect is independent of the immune response, and it is attributed to the down-regulation of Nav1.6, thus reducing the harmful effect of Na^+ accumulation in axons (O'Malley et al., 2009). Moreover, the expression of *Scn2b* mRNA decreases in the late stages of EAE, which is suggested to be a compensatory mechanism in the neurons to down-regulate the harmful Nav1.6 overexpression (Nicot et al., 2003).

In summary, understanding the individual role of each Nav channel subunit is highly important in the development of a precise therapy that targets the harmful Nav isoforms and activates the beneficial ones. The neuronal, glial and immune effector cell expression of these molecules need to be considered to get a proper understanding of their impacts on the disease.

1.5 Rationale and Objectives

Axonal degeneration is a non-reversible process in MS that leads to several neurological disabilities. However, the mechanisms underlying axonal degeneration remain unclear. Several studies have suggested that Nav channels – and the isoform Nav1.6, in particular – are associated with axonal loss following demyelination. As such,

it has been hypothesized that damage to the axon might be caused by the persistent influx of sodium through Nav1.6. This increase in axonal sodium load is postulated to result in the Na^{+}/Ca^{2+} exchanger to operate in reverse as it works to remove this sodium and therefore produces an influx of damaging Ca^{2+} ions. However, this hypothesis has not been tested directly. For this reason, I investigated the role of the Nav1.6 channel as a primary contributor to axonal dysfunction following the demyelination process in chronic EAE while hypothesizing, that in mice subjected to EAE, axons selectively depleted of Nav1.6 will show significantly less axonal death than control (Chapter 2).

As such, the **FIRST OBJECTIVE** of this study was to examine the effects of targeted deletion of Nav1.6 on axonal loss in optic neuropathy.

To this end, I have used *Scn8a*$^{flox/flox}$ and *Scn8a*$^{+/+}$ (control) mice that are intravitreally injected with adeno-associated virus serotype 2 (AAV2) harboring the Cre recombinase and GFP under the control of the CMV promoter in the left eye and either non-injected or injected with AAV2/GFP in the right eye. EAE was induced in these mice and I was able to examine the role of Nav1.6 on retinal ganglion cells (RGCs) death and optic nerve axonal degeneration in the chronic phase of the disease. To be clear, tissue-specific targeting in the retina and optic nerve was used by using Cre-loxP system for two reasons: First, *Scn8a*-null mice (devoid of Nav1.6 in the whole body) die around 21 days post-partum. That makes them unsuitable for EAE. Second, there is no well-characterized drug appropriate for long-term blocking of Nav1.6 and inflammatory status. Our results have shown depletion of Nav1.6 from the retina was associated with a decrease in the demyelination and axolytic fibers in the optic nerve and consistent with Nav1.6 promoting inflammation and being a primary enabler of axonal degeneration following

demyelination. Having seen the impact of individual axons of selective Nav1.6 deletion led me to extend my study further to investigate the impact of this channel in disease progression and immune modulation.

The **SECOND OBJECTIVE** was to determine if Nav1.6 regulates mediators of autoimmune inflammation and to investigate the immune cell response in peripheral blood and CNS in the presence of normal and low expression of Nav1.6. Therefore, *Scn8a*$^{dmu/+}$ heterozygous mice for a null-allele of *Scn8a* that have reduced expression of Nav1.6 in comparison to their WT littermates were used in this study. I hypothesized that *Scn8a*$^{dmu/+}$ will show a decrease in inflammation in chronic EAE and in response to the LPS challenge (Chapter 3). I induced EAE in *Scn8a*$^{dmu/+}$ mice, with reduced Nav1.6 levels, and in *Scn8a*$^{+/+}$ littermate controls. Behavioral observations in *Scn8a*$^{dmu/+}$ mice revealed improved motor capacity during the early chronic phase when compared to +EAE/*Scn8a*$^{+/+}$ littermate controls. Inflammation was also found to be reduced in *Scn8a*$^{dmu/+}$ mice. Significantly lower levels of IL-6 were found in +EAE/*Scn8a*$^{dmu/+}$ vs +EAE/*Scn8a*$^{+/+}$ littermate controls, in the remission and chronic phases. Furthermore, *Scn8a*$^{dmu/+}$ mice displayed reduced inflammation in response to LPS challenge.

Toll-like receptors (TLRs) are a family of extracellular, intracellular, or soluble pattern recognition receptors (PRRs). They play a crucial role in the innate immune system and have recently been implicated in the etiology of MS by modulating adaptive immunity. TLR2 is activated by a broad range of ligands and its activation has been implicated in disease in MS and EAE.

TLR2 is an extracellular receptor that is well known to recognize a wide range of microbial ligands, including lipoteichoic acid, zymosan, lipoproteins, and peptidoglycan

(Chen et al., 2009). In both MS and EAE, the expression of TLR2 has been shown to be implicated in disease in MS and EAE and be upregulated in the CNS on oligodendrocytes and peripheral blood monocytes (Reynolds et al., 2010; Zekki et al., 2006). However, the exact role of TLR2 in the inflammatory response has been controversial and not completely defined in the context of EAE. **Therefore, the THIRD OBJECTIVE** of my research was to determine the impact of TLR2 on the axonal loss in the optic nerve and inflammatory response during EAE and its role in the axonal damage in the CNS. I hypothesized that mice with knocked out TLR2 will display attenuated EAE progression and reduced inflammation in EAE. **(Chapter 4).** EAE was induced in $TLR2^{-/-}$ and WT strains. Our results showed that the clinical score in $TLR2^{-/-}$ mice was significantly lower during the chronic phase compared to the control. The frequencies of $Gr\text{-}1^{+}/CD11b^{+}$ cells of the spleen and the brain were significantly lower in $TLR2^{-/-}$ mice at day 40 post-EAE induction compared to the control.

Chapter 2 Nav1.6 promotes inflammation and neuronal degeneration in a mouse model of multiple sclerosis.

This chapter appeared in the following publication:

https://jneuroinflammation.biomedcentral.com/articles/10.1186/s12974-019-1622-1

Barakat Alrashdi, Bassel Dawod, Andrea Schampel, Sabine Tacke, Stefanie Kuerten, Jean S. Marshall & Patrice D. Côté

Nav1.6 promotes inflammation and neuronal degeneration in a mouse model of multiple sclerosis. *Journal of Neuroinflammation* **16,** 215 (2019) doi:10.1186/s12974-019-1622-1).

2.1 Abstract

Background: In multiple sclerosis (MS) and in the experimental autoimmune encephalomyelitis (EAE) model of MS, the Nav1.6 voltage-gated sodium (Nav) channel isoform has been implicated as a primary contributor to axonal degeneration. Following demyelination Nav1.6, which is normally co-localized with the Na^+/Ca^{2+} exchanger (NCX) at the nodes of Ranvier, associates with β-APP, a marker of neural injury. The persistent influx of sodium through Nav1.6 is believed to reverse the function of NCX, resulting in increased influx of damaging Ca^{2+} ions. However, direct evidence for the role of Nav1.6 in axonal degeneration is lacking.

Methods: In mice floxed for *Scn8a*, the gene that encodes the α subunit of Nav1.6, subjected to EAE we examined the effect of eliminating Nav1.6 from retinal ganglion cells (RGC) in one eye using an AAV vector harbouring Cre and GFP, while using the contralateral either injected with AAV vector harboring GFP alone or non-targeted eye as control.

Results: In retinas, the expression of *Rbpms*, a marker for retinal ganglion cells, was found to be inversely correlated to the expression of *Scn8a*. Furthermore, the gene expression of the pro-inflammatory cytokines *Il6* (IL-6) and *Ifng* (IFN-γ), and of the reactive gliosis marker *Gfap* (GFAP) were found to be reduced in targeted retinas. Optic nerves from targeted eyes were shown to have reduced macrophage infiltration and improved axonal health.

Conclusion: Taken together, our results are consistent with Nav1.6 promoting inflammation and contributing to axonal degeneration following demyelination.

Keywords

Multiple sclerosis, inflammation, experimental autoimmune encephalitis, optic neuritis, sodium channel, *Scn8a*, Nav1.6, retinal ganglion cells, optic nerve, adeno-associated virus, conditional knockout.

Highlights

- Retinas from eyes subjected to selective Nav1.6 targeting have increased retinal ganglion cell survival and reduced inflammation and reactive gliosis.
- Optic nerves from eyes subjected to selective Nav1.6 targeting have reduced demyelination and axonal loss.
- Findings support the hypothesis that Nav1.6 in the EAE model of MS promotes inflammation and neuronal death.

2.2 Introduction

Multiple sclerosis (MS) is a chronic inflammatory and neurodegenerative disorder of the central nervous system (CNS), affecting more than 2.5 million people worldwide (Milo and Kahana, 2010; Mohr, 2011). It is believed that the main trigger of the disease might be an inflammatory autoimmune response within the nervous system that causes tissue damage, including demyelination and axonal damage (Constantinescu et al., 2011; de Leeuw et al., 2014; Trapp et al., 1998b). The neuroinflammation may be latent in the beginning but eventually progresses into a relapsing-remitting phase, at which point it is possible to lose and regain myelin (Bjartmar et al., 2003). In the early stages of the disease, axonal demyelination, with the axon remaining viable, is associated with variable degrees of inflammation and astrogliosis (Mancardi et al., 2001). However, permanent neurological deficits become increasingly prominent as the neuroaxonal degeneration progresses (Friese et al., 2014).

Voltage-gated sodium (Nav) channels have been implicated in etiology of MS and EAE as a key factor in causing axonal degeneration. The Nav1.x channel family consists of nine different pore-forming alpha-subunits (Nav1.1 – Nav1.9), which assemble with two of five non-pore-forming beta-subunits (β1, β1B, β2, β3, β4). These channels are present in motor and sensory axons in the peripheral nervous system (PNS) and cluster at nodes of Ranvier in CNS axons (Krzemien et al., 2000). The Nav1.6 isoform, in particular, has been associated with axonal loss following demyelination in both EAE (Craner, 2003; Craner et al., 2004b) and MS (Craner et al., 2004c). In axons, Nav1.6 has been shown to co-localize with the Na^{+}/Ca^{2+} exchanger (NCX) and β-APP, an indicator

of imminent degeneration. In addition, the co-localization between Nav1.6 and NCX was found only in axons that express β-APP, an indicator of defective transport which is commonly used as a marker of axonal damage(Ferguson et al., 1997).However, in axons with damaged myelin expressing diffused Nav channels, axons expressing only the Nav1.2 isoform did not co-localize with β-APP while virtually all β-APP-expressing axons were expressing Nav1.6, along or without Nav1.2 (Craner et al., 2004b).

In this study, we examined how deleting Nav1.6 from a population of retinal ganglion cells in EAE mice, a common animal model of MS (Bettelli, 2007b; Constantinescu et al., 2011) affects disease progression. Intra-animal comparisons revealed enhanced RGC survival, reduced inflammation, and improved axonal health in the Nav1.6-targeted eye versus the control eye. Taken together, our data support the hypothesis that Nav1.6 contributes to the pathophysiology of EAE, and by extension of MS and possibly other neurodegenerative disorders.

2.3 Materials and methods

2.3.1 Mice

A total of 36 mice were used in this study: C57BL/6 (Charles River, Saint-Constant, QC) (n = 16), and *Scn8a*$^{flox/flox}$ homozygous for alleles of *Scn8a* harbouring loxP sequences flanking the first exon (n = 20; a generous gift of Dr. Miriam Meisler, University of Michigan U.S.A. (Levin and Meisler, 2004)). Mice were housed in groups of 3 to 5 under a 12-hour light-dark cycle with free access to food and water in HEPA ventilated cages at the Carleton Animal Care Facility (CACF) facility at Dalhousie University. All animal procedures were completed in accordance with animal care guidelines established by the Canadian Council on Animal Care and in accordance to the

ARVO Statement for the Use of Animals in Ophthalmic and Vision Research. Protocols were reviewed and approved by the Dalhousie University Committee on Laboratory Animals (Protocol Nos. 17-012 and 19-050).

2.3.2 Intravitreal injection of AAV

Adeno-associated virus serotype 2 (AAV2) has been shown to preferentially target ganglion cells in the retina (de Leeuw et al., 2014). Using a 31 gauge needle and 10 ul syringe (Hamilton Company, Reno, NV, USA), we have intravitreally injected the left eye of 7 week old *Scn8a*$^{flox/flox}$ (n = 11; Fig 2.1A Day 0; 1.5 µL of 5 x 10^{12} viral genome copy number per mL) harbouring the Cre-recombinase and enhanced GFP (eGFP, Cat no. SL100814, Signagen Laboratories, Rockville, MD) under the control of the cytomegalovirus (CMV) promoter in the left eye and the fellow eye was injected with AAV2-GFP alone (n = 4; Cat no. SL100812, Signagen Laboratories) or left non-injected (n = 7). The injection site was located posterior to the super temporal limbus and the injection was performed at a depth of approximately 1 mm. This procedure was performed in a biocontainment room under ketamine/xylazine anesthesia (ketamine, 100 mg/kg body weight; xylazine, 10 mg/kg body weight). GFP-production was used as a marker of AAV2 transduction of RGCs and was visualized in vivo by confocal scanning laser ophthalmoscopy (CSLO) before and after EAE induction (measured at days 15, 30, 68, and 78 after AAV2 injection; Fig. 2.1A).

2.3.3 EAE induction and clinical score assessments

EAE was induced in 18-24 g female mice aged 10 to 12 weeks (total n = 22). C57BL/6 (n = 10) and in *Scn8a*$^{flox/flox}$ mice (n = 12) were immunized for EAE induction, while C57BL/6 (n = 6) and *Scn8a*$^{flox/flox}$ (n = 3) were left untreated as controls. EAE mice

were injected subcutaneously with 200 µL of MOG_{35-55} peptide solution suspended in CFA with a concentration of 2 mg/mL (kit EK-2110, Hooke Laboratories, Lawrence, MA) (Kuerten et al., 2007). PTX (200 ng per mouse dissolved in PBS) was injected intraperitoneally on the day of immunization and after two days. Mice were monitored daily for weight changes and for clinical signs of EAE and all scoring was done after removing cage cards by persons unaware of the animal groups as described by Miller et al. (Miller et al., 2010). Scoring was performed according to the following criteria: 1. flaccid tail; 2. hindlimb weakness and poor righting ability; 3. inability to right and paralysis in one hindlimb; 4. both hindlimbs paralyzed with or without forelimb paralysis and incontinence; 5. moribund. Mice that reached a score of 4 before the end of the study (41 or 50 days post-EAE) were sacrificed and discarded from the study. The mice included in the study displayed a clinical score between 2.5 and 3.5 and were sacrificed in the chronic phase at 41 days (n = 8) or 50 days (n = 4) post EAE induction.

2.3.4 In vivo imaging

GFP-producing RGCs were visualized by confocal scanning laser ophthalmoscopy (CSLO; Spectralis HRA, Heidelberg Engineering, Germany) at days 15, 30, 68, and 78 post AAV2 injection according to Smith and Chauhan (Smith and Chauhan, 2015). Briefly, mice were anesthetized with an initial induction of 3-4% isoflurane (vol) and the eyes were dilated with topical mydriatics (1% tropicamide and 2.5% phenylephrine hydrochloride, Alcon Canada Inc., Mississauga, ON). Corneal hydration was maintained with ophthalmic liquid gel (Novartis Pharmaceuticals Canada Inc., Dorval, QC, Canada) and a contact lens (Cantor and Nissel, Brackley, UK). CSLO imaging was performed for each animal with an auxiliary +25 diopter lens attached to the

camera objective. Baseline images focused at the level of the nerve fiber layer were first acquired with infrared (820 nm) illumination. The camera adjusted to obtain the optimal fluorescence images (488 nm excitation, 500-550 nm emission band pass filter) at the GCL layer. Each image was taken averaged 16 times using automatic real-time eye tracking software.

2.3.5 Immunohistochemistry

To quantify and visualize RGCs, the whole-mount retinas were incubated for 6 days at 4°C with primary antibody against the mouse RNA-binding protein with multiple splicing (RBPMS; 1:1000 dilution, guinea pig anti-RBPMS, PhosphoSolutions, Aurora, CO, USA), which is uniquely expressed in RGCs (Rodriguez et al., 2014) . This was followed by incubation with 1:400 Alexa Fluor® 488 conjugated rabbit anti-GFP (Molecular Probes, Eugene, OR, USA) and Cy3 conjugated donkey anti-guinea pig secondary antibody (Jackson Immuno Research Laboratories Inc., West Grove, PA, USA) overnight at 4°C. After that, the retina was rinsed in PBS for 10 min, then incubated in the nuclear counterstain TO-PRO-3 iodide (Thermo Fisher Scientific, Waltham, MA) for 15 min. Retinas were flattened with RGCs facing up, mounted with anti-fade fluorescent mounting medium (Sigma-Aldrich, St-Louis, MO), and cover slipped. Images were taken using a 20 X objective with a confocal microscope (Nikon C1, Nikon Canada Inc., Toronto, ON). Three images with an area of 330.32 x 330.32 µm from each retina were used for RGC quantification: near the optic disk, near the periphery and at an intermediate distance. Image J was used to perform RGC counts.

2.3.6 Hematoxylin and Eosin (H&E) staining of the optic nerve

Optic nerves were collected from mice, embedded in paraffin, and sectioned longitudinally. The sections were dehydrated for 2h at room temperature, after that fixed for 10 min with 4% paraformaldehyde (PFA), dehydrated for 2 min by a series of graded ethanol solutions, incubated for 5-7 min in hematoxylin and transferred to distilled water. The sections were incubated for 1 min in eosin, dehydrated in gradient ethanol series and mounted. Images were captured using a transmitted light microscope and analyzed with AxioVision 4.7 software (Carl Zeiss, Jena, Germany). The average number of cell nuclei per mm^2 was determined for each optic nerve.

2.3.7 Electron microscopy

Mice were sacrificed during the chronic phase of EAE at day 41 (n = 7), and day 50 (n = 4) and optic nerve tissue was harvested from both groups of mice C57BL/6 and 'floxed' alleles of *Scn8a*. Tissues were processed as described by Kuerten et al. (Kuerten et al., 2011). Tissues were fixed overnight in 2.5% glutaraldehyde in 0.1M sodium cacodylate buffer, rinsed with 0.1M sodium cacodylate buffer, fixed for 2 hrs with 1% osmium tetroxide, and then rinsed quickly with distilled water. Samples were then placed in 0.25% uranyl acetate at 4^oC, dehydrated in graded acetone solutions, embedded with Epon Araldite resin and placed in a 60°C oven for 48 hours to harden. The samples were sectioned transversally using an ultra-microtome (Reichert Ultracut R, Leica, Germany) at a thickness of 50 nm. Images were captured on a Zeiss 906 electron microscope (Carl Zeiss NTS GmbH, Oberkochen, Germany) equipped with a digital EM camera. To demonstrate the extent of the axonal loss and myelin pathology we measured the g-ratio by dividing the axon diameter by the diameter of the myelinated nerve fiber (Guy et al.,

1991; Kuerten et al., 2007). Only axonal g-ratios three standard deviations above (remyelinating) or below (demyelinating) the average of the non-EAE reference group were counted. Axonal damage, including axolytic axons and neurofilament pathology, was determined qualitatively. A person unaware of the nature of the samples performed the analysis.

2.3.8 Quantitative reverse-transcription polymerase chain reaction (qRT-PCR)

Following euthanasia, samples were quickly removed from the mice and submerged in RNA later (Qiagen, Hilden, Germany). Total RNA was extracted using RNeasy Plus Mini Kit (Qiagen) according to manufacturer's instructions. Concentration of RNA samples were measured using an Epoch spectrophotometer and Take3™ Micro-Volume Plate (Biotek, VT, USA). The ratio of 260/280 was used to evaluate the purity of RNA samples. RNA samples were reverse transcribed to cDNA using QuantiTect® Reverse Transcription Kit (Qiagen). The resulting cDNA samples were diluted 1:4 and used in qRT-PCR with the primer sets from Table 3 to measure the expression of mRNAs.

Table 3 qPCR primers:

Gene	Primer sequence or company (catalog number)
Hprt	Bio-Rad (Cat no. 10025636)
Gapdh	Bio-Rad (Cat no. 10025637)
Il6	Qiagen (Cat no. PPM03015A)
Gfap	Forward (5'-3') AGGGGCAGATTTAGTCCAAC Reverse (5'-3') AGGGAGTGGAGGAGTCATTC
Scn8α	Forward (5'-3') GCAAGCTCAAGAAACCACCC Reverse (5'-3') CCGTAGATGAAAGGCAAACTCT
Rbpms	Forward (5'-3') AGAGCTGTACCTGCTCTTCAGACC Reverse (5'-3') GCCTCTGCTTCTGAGCGACTGTC
Ifng	Bio-Rad (Cat no.10025636)

2.3.9 Flow Cytometry

Optic nerves were harvested, and the cells were dissociated by passing the tissues through metallic mesh followed by enzymatic digestion using 10µg/ml collagenase D and 100µg/ml DNase I. Single-cell suspensions were incubated with antibodies to define various types of immune cells, such as macrophages ($F4/80^+/CD11b^+$, 1:300 dilution Bioscience, USA). Cells were then washed using flow cytometry wash buffer (PBS supplemented with 1% BSA). Stained samples were harvested using BD FACS Canto™ II (BD Life Sciences, San Jose, CA, USA). All analysis and gating were done using BD FACS Diva software and FlowJo V10.2.

2.3.10 Statistics

Statistical analyses were performed using a paired Student's *t*-test. Error bars represent the standard error of the mean (SEM). GraphPad Prism software was used for statistical analyses (Ver. 5.0, GraphPad Software, La Jolla, CA, USA). * $P < 0.05$, ** $P < 0.01$.

2.4 Results

In MS and EAE, the clinical symptoms are associated with and caused by the progression of the axonal degeneration (Friese et al., 2014; Waxman, 2006). To test the role of Nav1.6 in axonal degeneration, we used mice that have the first exon of the Nav1.6 gene, *Scn8a*, flanked between two LoxP sites, ie. 'floxed' (Levin and Meisler, 2004), which allows the gene to be knocked out locally in the presence of Cre-recombinase. A recombinant adeno-associated virus serotype 2 (AAV2), which preferentially targets ganglion cells in the retina, was used to deliver an expression vector containing Cre-GFP (AAVCre) or, as a control, GFP alone (AAVGFP) under the control

of a cytomegalovirus promoter (Fig. 2.1A). Subsequent to intravitreal injection of the virus, GFP labeling was detectable *in vivo* by CSLO fluorescence imaging and the transduced cells were counted at 15, 30, 68, and 78 days post AAVCre injection (Fig. 2.1BC). Smith and Chauhan (2018) reported that AAV2 transduction of inner retinal cells stabilizes at 35 days; consequently, it was estimated that near maximal RGC transduction would be attained by 44 day post-AAV2 injection and this time was chosen to induce EAE. Interestingly, the number of transduced cells continued to increase at days 68 (EAE day 25) and 78 (EAE day 35). The clinical symptoms of EAE-induced mice started to appear 8 days post immunization, and all mice (C57BL/6 and flox mice) subjected to EAE displayed a typical clinical course with loss of body weight and motor impairment (Supplemental Figure 2.1).

To determine the effect of targeting *Scn8a* the RGC population in chronic-phase EAE, we immunostained flat-mount retinas against RBPMS, a highly specific marker of RGCs (Kwong et al., 2010). Control non-EAE/non-AAV-treated mice (-EAE/-AAV, Fig. 2. 2A) exhibited a dense population of RGCs, while +EAE/non-AAV-treated retinas (+EAE/-AAV, Fig. 2.2B), and EAE retinas from eyes intravitreally injected with a control GFP vector (+EAE/+AAVGFP, Fig.2. 2C) revealed massive RGC loss. In control GFP retinas, speckled GFP staining was observed, which occasionally co-localized with enlarged and degenerating RGC soma. The extent of the cell loss in +EAE/+AAVGFP control is quantified in (Fig. 2. 2E) and corresponds to 307.7 ± 83.5 cells/mm^2 (n = 3) vs 3633 ± 431.3 (n = 3) cells/mm^2 in non-EAE/-AAV controls. In +EAE/+AAVCre mice (Fig. 2.2D) large RGC loss was also observed but to a lesser extent than in contralateral +AAVGFP control retinas (589.2 ± 47.0; p = 0.0346; n = 3; Fig. 2. 2E). Furthermore, in

+AAVCre retinas, the RGC cells with morphologically normal cell bodies were to a large extent GFP-positive. To determine the extent to which AAVCre impacted the expression of Nav1.6 and RGC survival, we compared the expression of *Scn8a* (the gene that encodes the α subunit of Nav1.6) and Rbpms (RBPMS) in retinas of EAE mice from AAVCre-injected eyes against, within the same animal, either the AAVGFP-treated or the non-injected contralateral eyes (Fig.2. 2F). *Scn8a* expression in AAVCre-injected retinas was reduced to 44.8% ± 8.62 of levels found in non-injected contralateral retinas ($n = 4$) and to 62.43% ± 11.38 of levels found in AAVGFP-injected contralateral retinas ($n = 4$). In the same samples, Rpbms expression was, on the other hand, increased to 194.8% ± 31.91 of levels found in non-injected contralateral retinas and to 190.1% ± 13.81 of levels found in AAVGFP-injected contralateral retinas. Since the AAVCre-injected eyes displayed a similar effect relative to non-injected or to +AAVGFP contralateral control eyes, we combined the two groups for subsequent analysis (referred to -AAVCre).

To assess the role of Nav1.6 in stimulating inflammation in EAE retina, we performed real time PCR analysis for *Il6* (IL-6), *Ifng* (IFN-gamma), *Tnf* (TNF) pro-inflammatory cytokines, the *Il10* anti-inflammatory cytokine and *Gfap* (GFAP), a marker for reactive gliosis. The expression of *Tnf* and *Il10* was below the threshold of detection in all conditions (not shown) and the expression of *Il6, Ifng* and *Gfap* in non-EAE mice was negligeable to low (Fig 3A-C). *Il6* was found to be significantly reduced ($p = 0.0022$) in all +EAE/+AAVCre (0.7697 ± 0.07507, $n = 8$) relative to contralateral control retinas (2.031 ± 0.3726, -AAVCre, $n = 8$; Fig. 2.3A). In addition, the expresson of *Ifng* was significantly reduced ($p = 0.0186$) in +EAE/+AAVCre (0.1753 ± 0.05959; $n = 4$)

versus +EAE/+AAVGFP control retinas (0.3032 ± 0.03948; $n = 4$; Fig. 2.3B). *Gfap* was also significantly reduced ($p = 0.0080$) in +EAE/+AAVCre (0.006452 ± 0.001426; $n = 8$) in comparison to contralateral control retinas (0.02773 ± 0.006676; -AAVCre, $n = 8$; Fig. 2. 3C)

We then performed a histological examination of the optic nerves and found increased cell infiltration in +EAE non-injected or AAVGFP controls relative to naïve -EAE/-AAVCre with cell clusters commonly visible (indicated by arrowheads in Fig. 2.4A). AAVCre-treated retinas, on the other hand, had reduced cell infiltration (Fig. 2.4AB). The total number of optic nerve nuclei was significantly lower ($p = 0.0492$) in +EAE/+AAVCre (132.4 ± 16.54; $n = 7$) versus control +EAE/-AAVCre mice (220.0 ± 41.91; $n = 7$; Fig. 2.4AD).

The number of infiltrating macrophages, determined by flow cytometry as the percentage of F4-80$^+$, CD11b$^+$ of total CD45$^+$ cells, was found to be similar in -EAE/+AAVCre and in -EAE/-AAVCre (Fig. 2.4D). The level of optic nerve infiltrating macrophages was found significantly reduced ($p = 0.0015$) in +EAE/+AAVCre (2.958 ± 0.4188; $n = 8$) vs +EAE/-AAVCre (4.818 ± 0.6789; $n = 8$; Fig. 2.4D).

Next, myelin and axonal pathology were assessed by comparing electron micrographs of optic nerve transversal sections from naïve (-EAE/-AAVCre, Fig. 2.5A), to +EAE/-AAVCre (Fig 2.5B) and +EAE/+AAVCre (Fig. 2.5C) optic nerves. We found that axon density was severely reduced in +EAE/-AAVCre optic nerves compared to naïve optic nerves and pathological features such as demyelinating, demyelinated and axolytic axons were frequently observed. In comparison, the axon density in

+EAE/+AAVCre optic nerves was visibly increased and pathological features were less common.

A quantification of the electron micrographs revealed that axolytic fibers, visually identified based on the absence of discernable neurofilaments, presence of swollen mitochondria and unraveling myelin (Fig. 2.5BC), were significantly ($p = 0.042$) less common in +EAE/+AAVCre optic nerves (2.573 ± 0.4507; $n = 11$) than in their -AAVCre contralateral counterparts (4.136 ± 0.8918; n=11; Fig. 2.6A). Demyelinated fibers, visually identified based on the presence of an intact axon but devoid of myelin, were also less frequent ($p = 0.0470$) in +EAE/+AAVCre (12.28 ± 2.716 ; $n = 11$) than in their -AAVCre contralateral counterparts (19.06 ± 2.813; $n = 11$; Fig. 2.6B).

In the remaining fibers that were not visually identified as either axolytic or demyelinated, myelin pathology was quantified by using the g-ratio (Guy et al., 1991), dividing the axonal diameter by the diameter of the axon plus myelin sheath. The optimal g-ratio in optic nerve in naïve -EAE/-AAVCre flox mice was established at 0.77 ± 0.060 S.D. ($n = 3$) which was similar to wild-type C57BL/6 at 0.76 ± 0.070 S.D. ($n = 6$). A conservative margin of ± 3 standard deviations from the mean of normal -EAE/-AAVCre flox mice was used as the cutoff to assign a diagnosis of demyelinating (< 0.59) or remyelinating (> 0.95), with intermediate g-ratios being considered as optimally myelinated. Using these parameters, we found no remyelinating fibers in any group (not shown), while all (100%) of the quantified axonal fibers in non-EAE animals were optimally myelinated. In the EAE-treated groups -AAVCre mice had significantly fewer ($p = 0.0427$) optimally myelinated fibers (87.08 ± 3.669; $n = 11$) than +AAVCre mice (92.72 ± 2.283; $n = 11$; Fig. 2.6C). None (0%) of the non-EAE had demyelinating fibers.

In the +EAE/+AAVCre group the proportion of demyelinating axons was found significantly ($p = 0.0311$) reduced (7.308 ± 2.276; n=11) relative to their -AAVCre contralateral counterparts (13.17 ± 3.632; $n = 11$; Fig. 2.6d).

2.5 Discussion

Myelin, in addition to its electrical insulating properties, is essential to the organization of the nodes of Ranvier which ensure the efficient propagation of the action potential by saltatory conduction (Buffington and Rasband, 2013; Giuliodori and DiCarlo, 2004). In demyelinating diseases, including MS, myelin loss leads to a disruption of the molecular cues and anchors that maintain the integrity of the nodes and, in turn, the membrane proteins of the axons become displaced and their expression dysregulated. Among these proteins, the voltage-gated sodium channel Nav1.6 is believed to play an important role in the axonal degradation that eventually follows demyelination or cycles of demyelination. Interestingly, demyelination does not only cause the dispersal of the pre-existing channels that were present at the nodes of Ranvier but in fact increases the density of the Nav channels in animal models (England et al., 1991; Foster et al., 1980; Novakovic et al., 1998) and in MS lesions (Moll et al., 1991). The co-localization of Nav1.6, the Na^+/Ca^{2+} exchanger (NCX) and markers of axonal injury has led to the hypothesis that the persistent influx of Na^+ through Nav1.6 channel in MS, and in the EAE animal model of MS, causes the NCX to operate in reverse, leading to the toxic accumulation of intracellular Ca^{2+} ions that results in cell death and axonal degradation (Bouafia et al., 2014; Craner, 2003; Stys et al., 1992; Waxman, 2006). Alternatively, Nav1.6 has been implicated in the release of Ca^{2+} from intra-axonal stores (Stirling and Stys, 2010). The role of Nav1.6 in degeneration has been difficult to verify

directly since *Scn8a*/Nav1.6-null mice (i.e., whole-body mutants) die around 21 days post-partum, which make them unsuitable for EAE induction (Burgess et al., 1995b; Kohrman et al., 1996). We chose to target *Scn8a* specifically in the retina and optic nerve for studying demyelination and axonal loss since optic neuritis is prominent and well-characterized in EAE mice (Quinn et al., 2011; Soares et al., 2013). We targeted *Scn8a* in a single optic nerve by intravitreal injection of an adeno-associated virus harbouring the Cre recombinase and enhanced GFP (eGFP) genes under the control of the CMV promoter (AAV2-Cre-GFP) in mice homozygous for the floxed *Scn8a* allele (Levin and Meisler, 2004). *Scn8a* was targeted in retinal ganglion cells by using the serotype 2 variant of the adeno-associated virus (AAV2), which has been shown to transduce approximately 34% of the RGC population when administered by intravitreal injection, although it should be noted that in this study by Smith and Chauhan (Smith and Chauhan, 2018) the DCX promoter was used while we have used the CMV promoter. Subsequently, to induce EAE we used MOG_{35-55} as the antigen since it induces chronic monophasic EAE in C57BL/6 mice (Kuerten et al., 2007; Stromnes and Goverman, 2006b). The contralateral eye was used as an internal control, which was either injected with and AAV vector expressing GFP alone (AAVGFP) or left non-injected. This approach allows us to compare Cre-targeted and control samples that are exposed to the same disease micro-environment; a significant advantage since the EAE disease severity can vary considerably between animals (Constantinescu et al., 2011). Furthermore, the absence (*Il6* and *Ifng)* or near absence (*Gfap*) of expression in the non-EAE +AAVCre control strongly suggests that the effects observed in the +EAE/+AAVCre mice are

indeed due to the inactivation of *Scn8a*/Nav1.6 and not to a non-specific effect of the AAV2 virus.

Inner-retinal cell targeting was confirmed by eGFP expression, as detected by CSLO in vivo imaging (Smith and Chauhan, 2018) which allowed us to longitudinally track the number of Nav1.6 knockout cells. Following injection, the number of RGCs targeted increased in a linear fashion until day 78 consistently with the observations of (Smith and Chauhan, 2018). Immunostaining against RBPMS of flat-mounted retinas from 41 days post-EAE induction revealed a massive loss of RGCs, in accordance with previously reported RGC loss in EAE-associated optic neuritis (Quinn et al., 2011; Shindler et al., 2008). The co-localization of the remaining morphologically normal appearing RBPMS-positive RGC cell bodies with GFP strongly suggests that the elimination of Nav1.6 within neurons promotes cell survival. Real-time quantitative assessment of *Rbpms* and *Scn8a* retinal expression revealed that within each animal, the AAV2Cre+ retina expressed less *Scn8a* and more *Rbpms* than the retina from the non-injected or +AAVGFP contralateral eyes. Furthermore, when comparead as groups, the AAV2Cre+ eyes differed significantly from the non-injected and +AAVGFP contralateral eyes. Taken together, these observations corroborate the hypothesis that Nav1.6 exacerbates RGC death in EAE.

The main trigger of MS is believed to be an inflammatory autoimmune response within the CNS that causes tissue destruction including demyelination and axonal damage (Constantinescu et al., 2011). Inflammation in the CNS is generally initiated by microglia, the resident macrophages, and other immune cells that can cross the blood-brain barrier (BBB), such as macrophages, T cells, and B cells that exacerbate the

inflammatory response (Engelhardt and Ransohoff, 2012). Furthermore, this inflammation can lead to the disruption of BBB and increase the infiltration of immune cells into the CNS (Barnett et al., 2006; Duffy et al., 2014; Wojkowska et al., 2014). Quantitative RT-PCR expression analyses revealed that the reduction of *Scn8a* expression in the AAVCre+ eye versus the control contralateral eye was associated with decreased retinal expression of pro-inflammatory cytokines *Il6* (IL-6) and (*Ifng)*, robust indicators of inflammation. Antibody blockade studies of IL-6 and knockout studies of IFN-γ have revealed that these cytokines are implicated in the induction of EAE (Lin and Edelson, 2017; Matsuki et al., 2006; Serada et al., 2008) Furthermore, a notable reduction within individual mice of reactive gliosis as indicated by a marker of fibrillary acidic protein (*Gfap*) (Horstmann et al., 2013), was also observed in AAVCre+ eye compared to the fellow eye. A recent study by Wilmes et al. (Wilmes et al., 2018) showed that in acute and chronic phases of EAE, a glia scar is formed by reactive astrocytes. It has been shown that increased expression of GFAP in Müller cells is an indicator for the activation of astrocytes and the loss of RGC, which may be triggered by inflammation and apoptosis (Horstmann et al., 2013). Several underlying mechanisms that involve the interaction between the immune cells and the neurons are believed to impact the development of the disease and Nav channels may play a central role in this interaction due to their expression in both types of cells (Eijkelkamp et al., 2012; Waxman, 2006). Nav1.6, in particular, is expressed in non-neuronal cells, such as astrocytes, microglia, and macrophages as well as in invasive cancer cell lines, where they are believed to contribute in the ability of these cells to mobilize by activating the actin cytoskeleton leading to the formation of podosomes and invadopodia (Black et al., 2009a; Carrithers et

al., 2009b; Craner et al., 2005; Pappalardo et al., 2016). In the context of this study, the presence of Nav1.6 in non-neuronal cells raises the question as to whether our observations result from deleting Nav1.6 in RGCs or if the presence of +AAVCre/Nav1.6-null non-neuronal cells might be impacting the results. Of the total number of retinal cells transduced by AAV2 approximately 65% are ganglion cells, while approximately 9% are Müller cells (Hellström et al., 2009) and in the EAE chronic phase (41 days following induction) all the observed AAVCre+ cells also stained positively for RBPMS (Fig 2.2d). Therefore, while we cannot completely eliminate the possibility that cells other than RGCs, such as Müller cells, might contribute to the reduction in retinal inflammation we believe this contribution to be minimal. Nav1.6 expressed in neurons, therefore, appears to promote inflammation in EAE, although it is unclear if this is due to the increased axonal degeneration or to a more direct influence of Nav1.6 on immune cells.

A prominent feature of the optic neuritis associated with EAE and MS is the thinning of the retinal nerve fiber layer and loss of axons which can result in permanent vision disruptions (Shindler et al., 2008). Even in axons that survive demyelination after the inflammation resolves only limited remyelination usually occurs causing a decrease in the action potential conduction and nerve atrophy (Kolbe et al., 2009). We observed by histological staining that +AAVCre optic nerves were thicker had fewer infiltrating immune cells than EAE+ optic nerves from -AAVCre eyes and that the amount of infiltrating macrophages, as estimated by flow cytometry (F4-80^{+} CD11b^{+}), was reduced in the optic nerve from +AAV2Cre optic nerves. Horstmann et al. (Horstmann et al., 2016) showed that at day 60, during the late stage of EAE, an increased microglial cell

response was associated with increased RGCs loss and increased cell infiltration in the optic nerve, which was consistent with our findings.

Ultrastructural analysis of axonal damage in optic nerve revealed axonal degeneration, accompanied with degeneration of the myelin sheath, which is the main feature of the disease. Our observation showed that the optic nerves from AAVCre+ eyes have decreased demyelination and fewer axolytic fibers compared to the control fellow eye. This is consistent with O'Malley et al. (O'Malley et al., 2009) who found that sodium channel β subunits knockout mice show reduced axonopathy following induction of EAE. Moreover, O'Malley et al. (2009) showed that the lack of *Scn2B* (β2) subunit in mice reduces the severe clinical symptoms and axonal degeneration in EAE. This protective effect is independent of the immune response and it was attributed to the downregulation of Nav1.6, thus reducing the harmful effect of $Ca2^{+}$ accumulation in axons.

Nav channel involvement in the etiology of MS has long been recognized. For example, pharmacological treatment using broad spectrum blockers including phenytoin, lidocaine, carbamazepine, flecainide, safinamide, and TTX have shown efficacy in animal models of anoxia and NO-mediated damage anoxia and in EAE mice (Bechtold et al., 2004; Garthwaite et al., 2002; Kapoor et al., 2003; Morsali et al., 2013; Stys et al., 1991, 1992). However, the efforts to target Nav channels for the treatment of degenerative diseases in humans have faced challenges due to the complex structure of these channels, the lack of selective pharmaceutical inhibitors, and their broad expression on neuronal and non-neuronal cells. Clinical trials conducted with lamotrigine (Kapoor et al., 2010) and phenytoin (Raftopoulos et al., 2016; Waxman, 2008) have yielded

equivocal results indicating that more research is required to clarify how blocking Nav channel isoforms expressed in excitable and non-excitable cells impacts disease progression (Yang et al., 2013a). 4,9-Anhydrotetrodotoxin (4,9-ah-TTX), a metabolite of TTX, blocks Nav1.6 in the nanomolar range with minimal effect on other TTX-sensitive channels (Rosker et al., 2007a; Teramoto and Yotsu-Yamashita, 2015). Hargus et al. (Hargus et al., 2013) have shown that 4,9-ahTTX selectively blocks Nav1.6 but not Nav1.2 currents and was able to suppress neuronal hyperexcitability in a mouse model of epilepsy. Recently, the microRNA miR-30b-5p was shown to downregulate Nav1.6 in a rat model of neuropathic pain and was used to attenuate neuropathic pain induced by oxaliplatin (Li et al., 2019a). As such, new blocking or downregulation strategies for Nav1.6 may soon become available and could offer interesting therapeutic options for MS.

2.6 Conclusion

The molecular mechanism of axonal degeneration in MS is highly complex and involves several neurological and immunological elements. Here we demonstrate for the first time that a 'null' genetic lesion in neuronal Nav1.6 has a neuroprotective effect *in vivo*. Our results corroborate previous findings that Nav1.6 is a promoter of neuronal degeneration and inflammation in EAE (Craner et al., 2005), suggesting that it plays a corresponding role in MS and possibly in other degenerative neurological diseases. Our results suggest that downregulating or blocking Nav1.6, specifically on neuronal cells would be neuroprotective and could widen the therapeutic window for other therapies. However, based on its ubiquitous localization at axon initial segments and nodes of Ranvier and on the phenotype displayed in *Scn8a* mouse mutants such as juvenile

lethality in null mice and severe ataxia in channel gating mutants (Meisler et al., 2001), Nav1.6 plays an essential physiological role and targeting this isoform involves inherent risks. Nevertheless, there is evidence that other isoforms, such as Nav1.2, can effectively compensate for the loss of Nav1.6. During postnatal development, Nav1.2 is normally expressed along the optic nerve to be replaced later, at advanced stages of development, with Nav1.6 (Boiko et al., 2001; Kaplan et al., 2001). Studies have shown that Nav1.2 plays a compensatory role for partial loss of Nav1.6 and may be able to conduct signals in the demyelinated axon (Craner et al., 2004d; Van Wart and Matthews, 2006). As such, a mechanistic basis upon which the targeting of Nav1.6 may provide an effective treatment exists and it will be of primary interest to study the compensatory role of this channel in the context of EAE and MS.

Acknowledgments

We thank Dr. Ian Haidl, Alexander Edgar, Maria Vaci, Gayathri Ponneri, and Dr. Corey Smith for technical assistance. We thank Jordan Warford for technical advice. We also thank Dr. Balwantray Chauhan and Dr. Arunika Gunawardena for access to their respective imaging equipment.

Funding

This work was supported by the Nova Scotia Research Foundation (to PDC), the Dalhousie Medical Research Foundation/Gillian's Hope MS Research Grant (to PDC), and Jouf University, Saudi Arabia (to BA). BA is a recipient of a postgraduate scholarship from the Saudi Cultural Bureau (Canada) and Al Jouf University.

Authors' contributions

BA generated EAE mice and performed AAV injections, CSLO imaging, tissue collection, ELISA, qPCR, immunohistochemistry, histological staining, data analysis and wrote the manuscript draft. BD performed the EAE clinical score analysis, flow cytometry panel design and analysis, and helped edit early versions of the manuscript. ST and AS made the g-ratio measurements. PDC assembled the figures. PDC, SK, and JM critically revised draft versions of the manuscript. All authors read the final version of the manuscript.

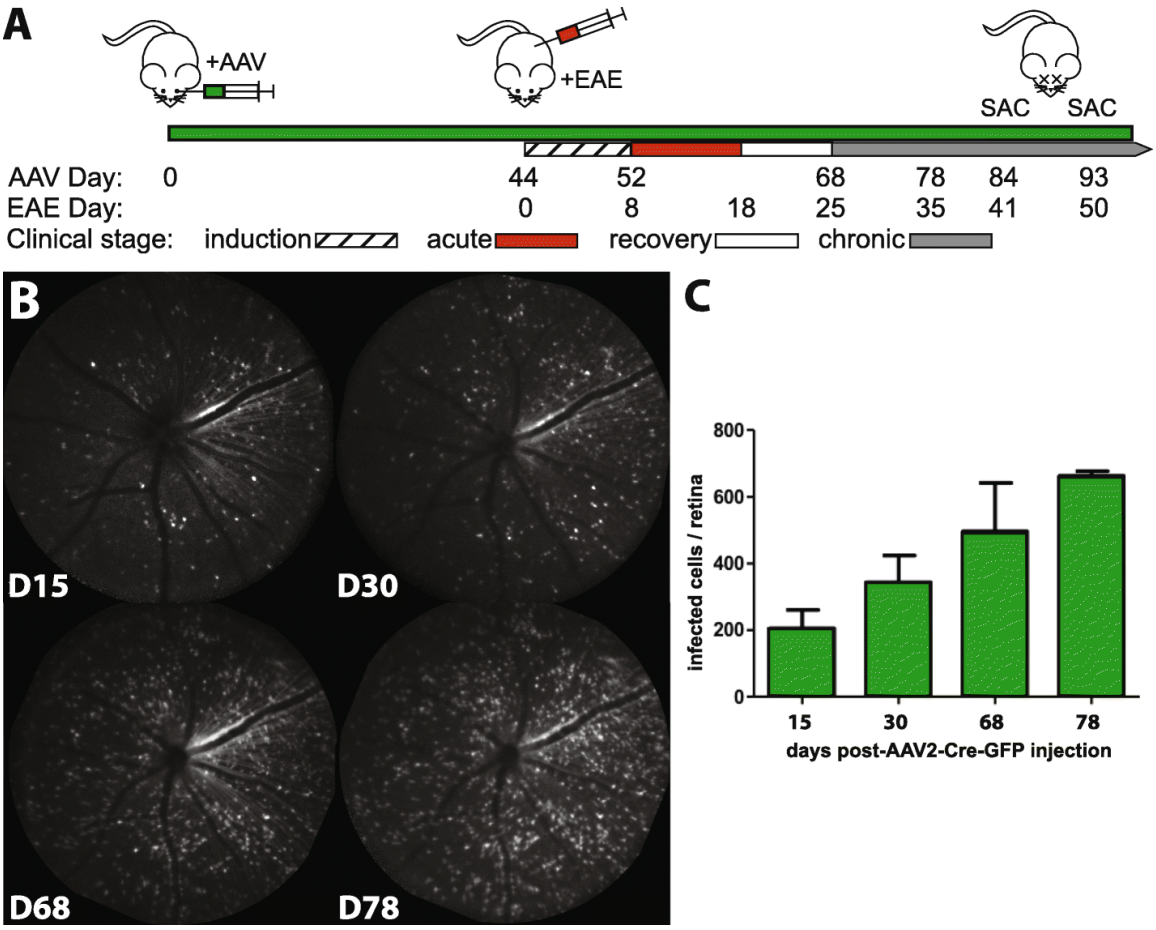
A
+AAV
+EAE
SAC
SAC
AAV Day: 0 44 52 68 78 84 93
EAE Day: 0 8 18 25 35 41 50
Clinical stage: induction acute recovery chronic
B
D15
D30
D68
D78
C
infected cells / retina
800
600
400
200
0
15
30
68
78
days post-AAV2-Cre-GFP injection

Figure 2-1 Experimental timeline and AAV transduction of inner retinal cells.

A) Experimental timeline with intravitreal injection of the AAV2-Cre-GFP or AAV2-GFP virus (+AAV), as well as the induction and clinical stages of EAE in *Scn8a*-flox mice. B) Representative confocal scanning laser ophthalmoscopy (CSLO) images of GFP-labeled inner retinal cells in a single animal up to 78 days post-AAVCre injection. C) Quantification of AAV transduction progression ($n = 4$).

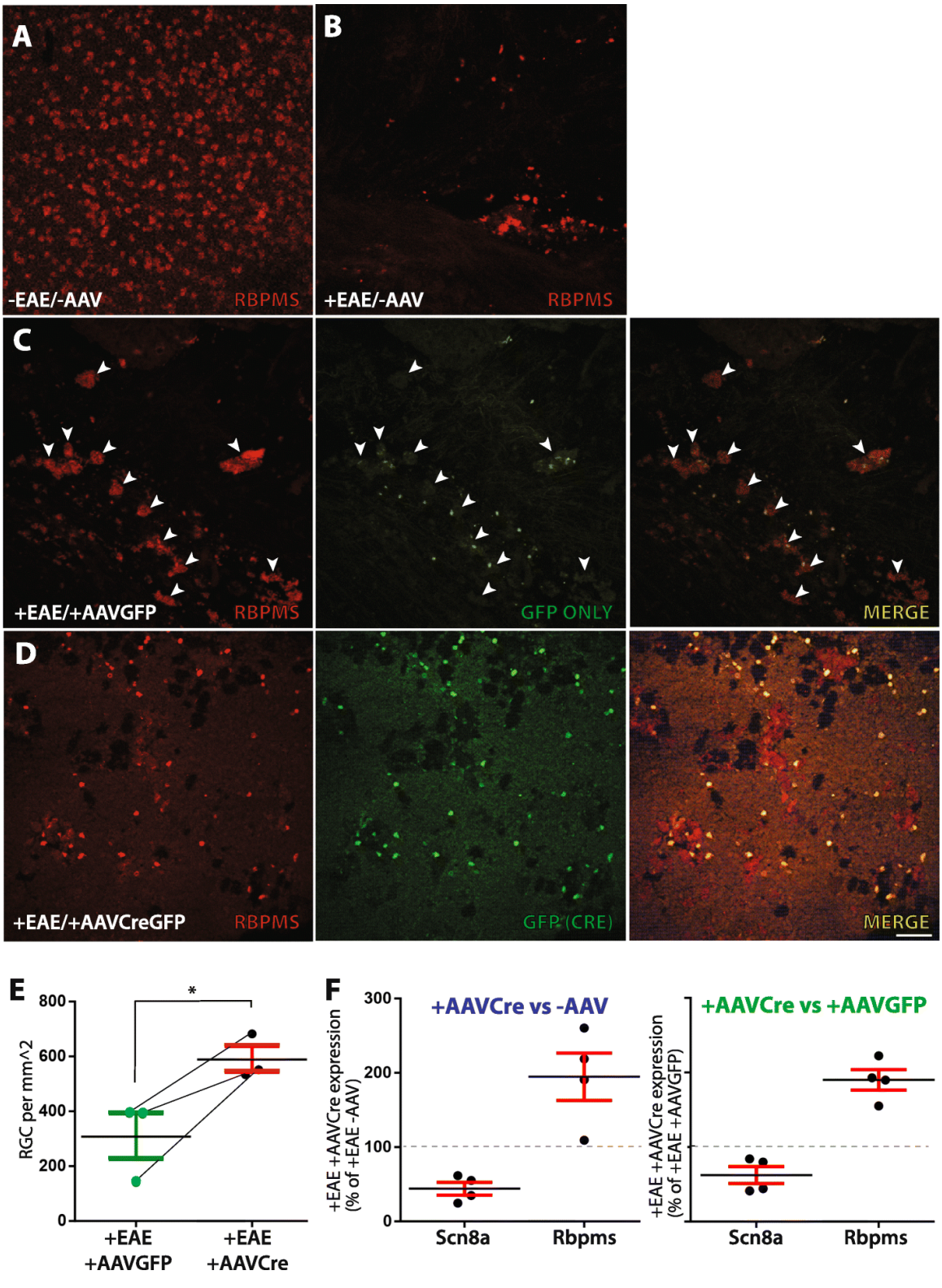
A
-EAE/-AAV
RBPMS
B
+EAE/-AAV
RBPMS
C
+EAE/+AAVGFP
RBPMS
GFP ONLY
MERGE
D
+EAE/+AAVCreGFP
RBPMS
GFP (CRE)
MERGE
E
RGC per mm^2
800
600
400
200
0
*
+EAE
+AAVGFP
+EAE
+AAVCre
F
+AAVCre vs -AAV
+EAE +AAVCre expression
(% of +EAE -AAV)
300
200
100
0
Scn8a
Rbpms
+AAVCre vs +AAVGFP
+EAE +AAVCre expression
(% of +EAE +AAVGFP)
Scn8a
Rbpms

Figure 2-2 Chronic stage EAE mice have increased RGC survival in retinas with reduced *Scn8a* (Nav1.6).

A**)** Population of RGCs (RBPMS-positive) in a normal (−EAE/−AAVCre) retina is shown in comparison to B**)** a representative image of an uninjected (−AAV) EAE mouse, and **C)** a representative image of a EAE mouse retina from a control AAVGFP-treated eye (+EAE/+AAVGFP) showing RBPMS-positive degenerating RGCs (white arrowheads) with GFP occasionally co-localizing with cell remnants. D**)** A representative image of an EAE mouse retina from an AAVCre-treated eye (+EAE/+AAVCreGFP) showing normal appearing GFP-positive RGCs. E**)** RGC quantification in +EAE retinas treated with AAVGFP ($n = 3$) or AAVCreGFP ($n = 3$). Lines link data points for retinas from the same animal. F**)** Percent of expression change for *Scn8a* and *Rbpms* in AAVCre-treated (+EAE/+AAVCreGFP; $n = 4$) eyes relative to their contralateral control uninjected (+EAE/−AAV; $n = 4$) or GFP (+EAE/+AAVGFP; $n = 4$) eye. Scale bar = 50 μm. Data are presented as the mean ± SEM. $*P \leq 0.05$, paired *t*-test.

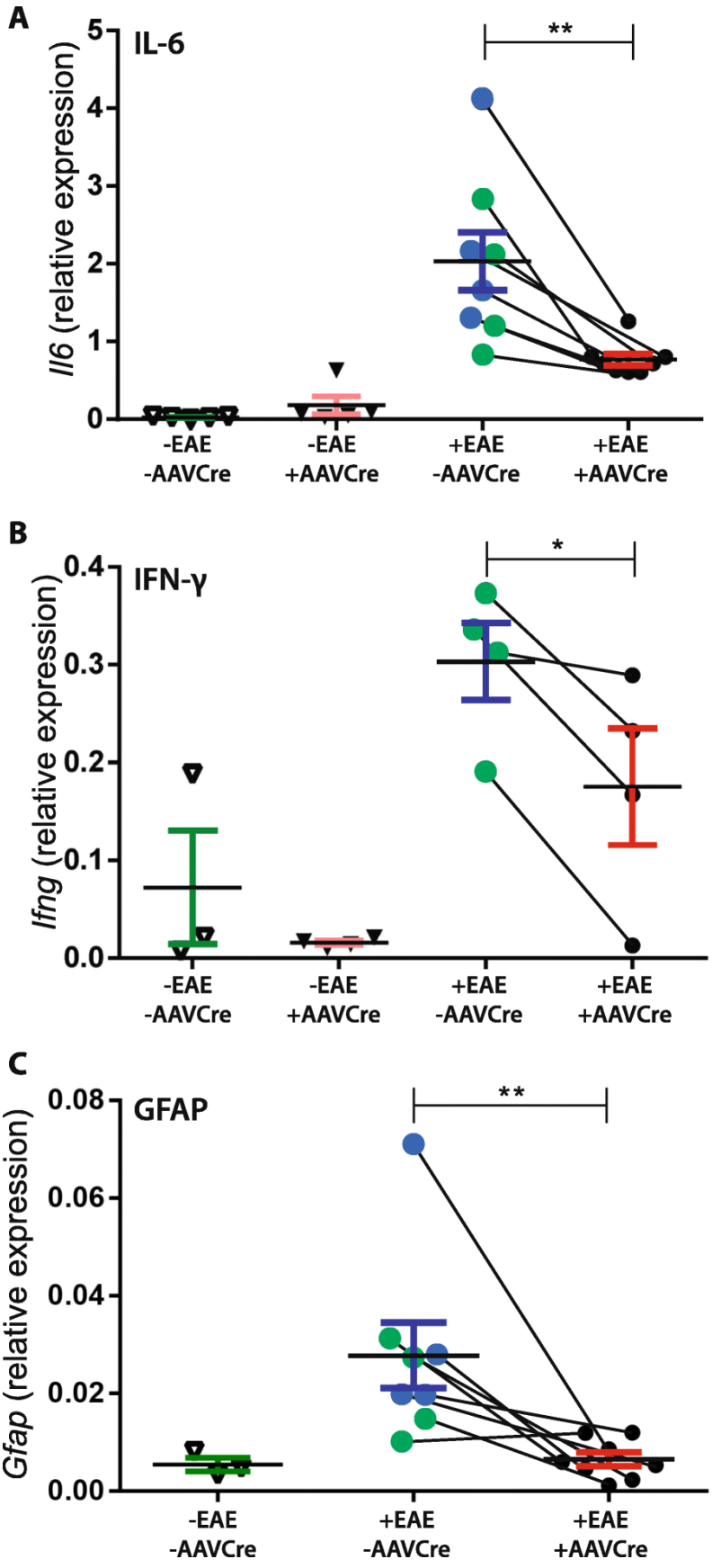
A
IL-6
Il6 (relative expression)
**
5
4
3
2
1
0
-EAE -AAVCre
-EAE +AAVCre
+EAE -AAVCre
+EAE +AAVCre
B
IFN-γ
Ifng (relative expression)
*
0.4
0.3
0.2
0.1
0.0
-EAE -AAVCre
-EAE +AAVCre
+EAE -AAVCre
+EAE +AAVCre
C
GFAP
Gfap (relative expression)
**
0.08
0.06
0.04
0.02
0.00
-EAE -AAVCre
+EAE -AAVCre
+EAE +AAVCre

Figure 2-3 Nav1.6 promotes inflammation in EAE mice. Expression in the retina of the markers of inflammation.

A**)** *Il6* (gene that encodes IL-6) and B**)** *Ifng* (IFN-γ) is compared between untreated (−EAE) or EAE-induced (+EAE) mice. The eyes of untreated (−EAE) mice are either left uninjected (−AAVCre, open triangles) or injected with AAVCreGFP (+AAVCre, closed triangles). In the EAE-induced mice, a comparison is made between AAVCreGFP-injected (+AAVCre, black dots) and the contralateral eye, which is either left uninjected (blue dots) or injected with a GFP-only control (AAVGFP, green dots). C**)** Analysis of the marker of reactive gliosis *Gfap* (Glial Fibrillary Acidic Protein). Lines link data points for retinas from the same animal. Data are presented as the mean ± SEM. $*P \leq 0.05$, $**P \leq 0.01$, paired *t*-test.

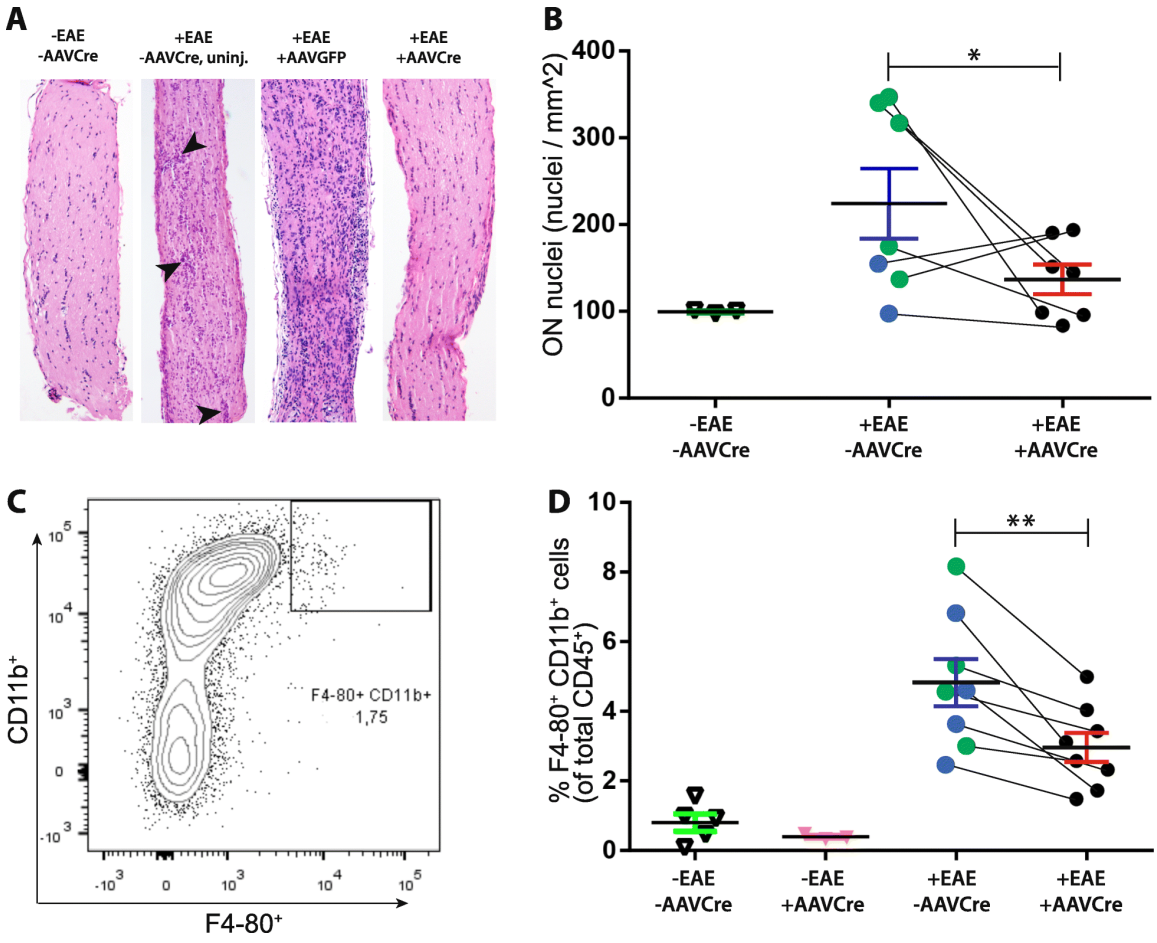
A
-EAE
-AAVCre
+EAE
-AAVCre, uninj.
+EAE
+AAVGFP
+EAE
+AAVCre
B
ON nuclei (nuclei / mm^2)
400
300
200
100
0
*
-EAE
-AAVCre
+EAE
-AAVCre
+EAE
+AAVCre
C
CD11b+
F4-80+ CD11b+
1,75
F4-80+
D
% F4-80+ CD11b+ cells
(of total CD45+)
10
8
6
4
2
0
**
-EAE
-AAVCre
-EAE
+AAVCre
+EAE
-AAVCre
+EAE
+AAVCre

Figure 2-4 Targeting of Nav1.6 results in reduced infiltration of myeloid cells in EAE optic nerves.

A**)** Hematoxylin and eosin-stained optic nerves from control non-EAE-induced/uninjected eye (−EAE/−AAVCre) and from EAE-induced (+EAE) mice with eyes left uninjected (−AAVCre, uninj), injected with AAVGFP (+AAVGFP), or injected with AAVCreGFP (+AAVCre). Arrowheads indicate cellular aggregates. B**)** Quantification of optic nerve nuclei from non-EAE-induced/uninjected eyes (−EAE/−AAVcre, open triangles) and from EAE-induced mice where a comparison is made between AAVCreGFP-injected (+AAVCre, black circles; $n = 7$) and the contralateral eye, which is either left uninjected (blue circles; $n = 2$) or injected with AAVGFP (green circles; $n = 5$). C**)** Representative dot plot flow cytometry analysis showing the gating strategy used to identify the macrophage population expressing marker $CD11b^+$ $F4–80^+$ from a population of $CD45^+$ cells isolated from optic nerves. D**)** Flow cytometry analysis for $CD11b^+$ $F4–80^+$ macrophages. Lines link data points for retinas from the same animal. Scale bar, 500 μm. Data are presented as the mean ± SEM. $*P \leq 0.05$, $**P \leq 0.01$, paired *t*-test. Data represents the combination of three separate experiments where each experiment consists of pooled from 4 mice for each group.

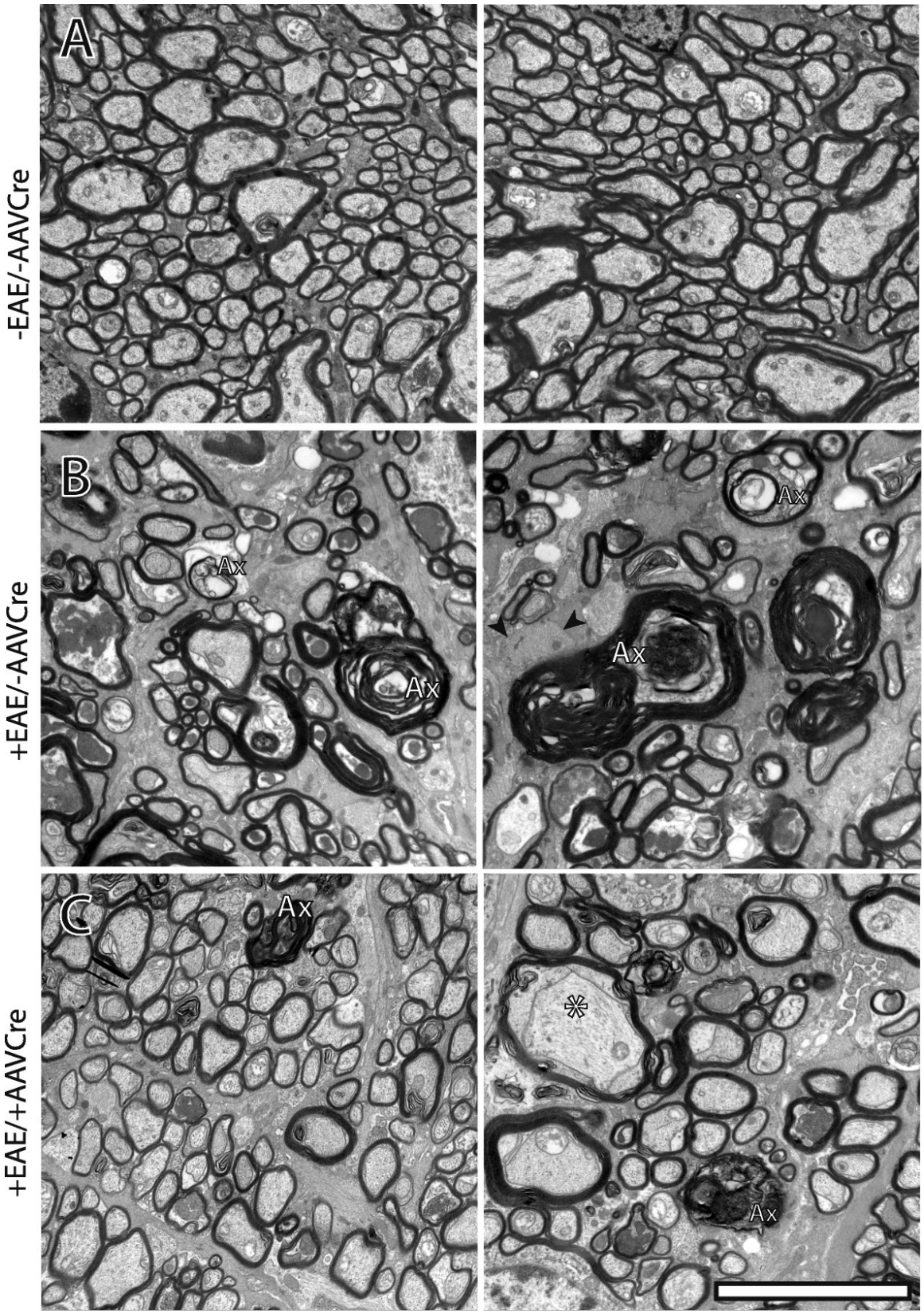
-EAE/-AAVCre
+EAE/-AAVCre
+EAE/+AAVCre
A
B
C
Ax
Ax
Ax
Ax
Ax
Ax

Figure 2-5 The axonal pathology is improved in optic nerves with reduced Nav1.6 levels.

Representative ultra-thin transversal sections of optic nerves were obtained from control non-EAE-treated/uninjected mice (A, −EAE/−AAVCre), EAE-treated/uninjected (B, +EAE/−AAVCre), and EAE-treated/AAV2Cre-injected (C, +EAE/+AAVCre). Images in B and C are of retinas from the same animal. Ax, axolytic; *, demyelinating. Scale bar, 5 μm.

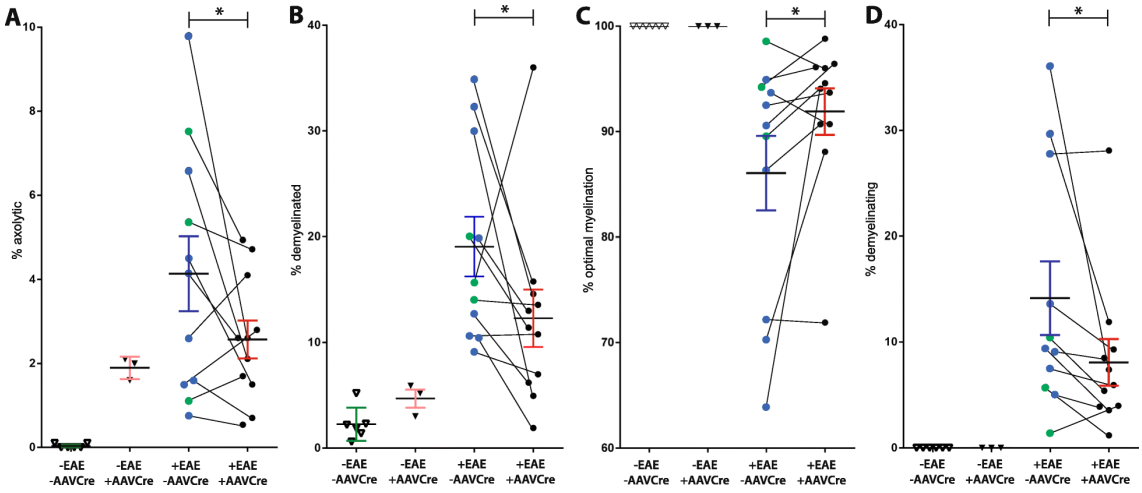
A
% axolytic
B
% demyelinated
C
% optimal myelination
D
% demyelinating
*
-EAE -AAVCre
-EAE +AAVCre
+EAE -AAVCre
+EAE +AAVCre

Figure 2-6 Reduced Nav1.6 levels in the optic nerve are associated with decreased demyelination and reduced axonal damage.

Electron micrographs of optic nerves from control non-EAE-induced (−EAE) or EAE-induced (+EAE) mice were analyzed. The non-EAE-induced optic nerves are from eyes either left uninjected (−AAVCre, open triangles) or injected with AAVCreGFP (+AAVCre, closed triangles). In the EAE-induced mice, a comparison is made between AAVCreGFP-injected (+AAVCre, black circles) and the contralateral eye, which is either left uninjected (blue dots) or injected with a GFP-only control AAV (green circles). We examined the frequency of A) axolytic axons and B) demyelinated axons (axons completely devoid of myelin). Based on the g-ratio (see "Materials and methods" section, we also examined the frequency of C) optimally myelinated and D) demyelinating axons. Data are presented as the mean ± SEM. $*P \leq 0.05$; paired *t*-test. Data represents the combination of three separate experiments where each experiment consists of pooled from 4 mice for each group.

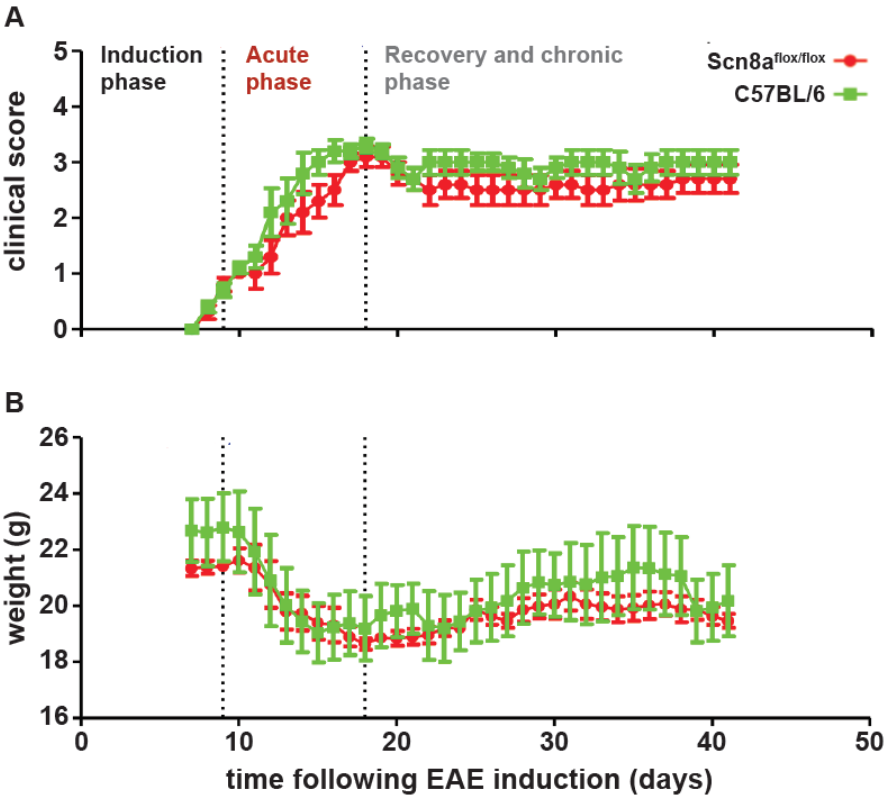
A
Induction phase
Acute phase
Recovery and chronic phase
Scn8a flox/flox
C57BL/6
clinical score
0
1
2
3
4
5
B
weight (g)
16
18
20
22
24
26
0
10
20
30
40
50
time following EAE induction (days)

S Figure 2.1. Clinical score and weight progression of Scn8a 'floxed' and wild-type C57BL/6 mice.

Eight to ten-week-old female mice were immunized with MOG_{35-55} with CFA and PTX. The progression of the clinical score A) and weight profile B) are similar for Scn8a homozygous 'floxed' (Scn8aflox/flox on C57BL/6 genetic background) mice that were used in this stud and for control wild type C57BL/6 mice (n = 10 for each group). Data represents the combination of three separate experiments where each experiment consists of pooled from 4 mice for each group.

Chapter 3 Mice heterozygous for the sodium channel Scn8a (Nav1.6) have reduced inflammatory responses during EAE and following LPS challenge

This chapter is under review at Frontiers in Immunology as following:

Barakat Al Rashdi, Bassel Dawod, Sabine Tacke, Stefanie Kuerten, Patrice D. Côté*, Jean S. Marshall*

*equal contribution

Running title:

Nav1.6 promotes inflammation in EAE and LPS

3.1 Abstract

Voltage gate sodium (Nav) channels contribute to axonal damage following demyelination in experimental autoimmune encephalomyelitis (EAE), a rodent model of multiple sclerosis (MS). The Nav1.6 isoform has been implicated as a primary contributor in this process. However, the role of Nav1.6 in immune processes, critical to the pathology of both MS and EAE, has not been extensively studied. EAE was induced with myelin oligodendrocyte (MOG_{35-55}) peptide in *Scn8a*$^{dmu/+}$ mice, which have reduced Nav1.6 levels. *Scn8a*$^{dmu/+}$ mice demonstrated improved motor capacity during the recovery and early chronic phases of EAE relative to wild-type animals. In the optic nerve, myeloid cell infiltration and the effects of EAE on the axonal ultrastructure were also significantly reduced in *Scn8a*$^{dmu/+}$ mice.

Analysis of innate immune parameters revealed reduced plasma IL-6 levels and decreased percentages of Gr-1^{high}/CD11b^{+} and Gr-1^{int}/CD11b^{+} myeloid cells in the blood during the chronic phase of EAE in *Scn8a*$^{dmu/+}$ mice. Elevated levels of the anti-inflammatory cytokines IL-10, IL-13, and TGF-β1 were also observed in the brains of untreated *Scn8a*$^{dmu/+}$ mice. A lipopolysaccharide (LPS) model was used to further evaluate inflammatory responses. *Scn8a*$^{dmu/+}$ mice displayed reduced inflammation in response to LPS challenge. To further evaluate if this was an immune cell-intrinsic difference or the result of changes in the immune or hormonal environment, mast cells were derived from the bone marrow of *Scn8a*$^{dmu/+}$ mice. These mast cells also produced lower levels of IL-6, in response to LPS, compared with those from wild type mice. Our results demonstrate that in addition to its recognized impact on axonal damage, Nav1.6 impacts multiple aspects of the innate inflammatory response.

Keywords:

Multiple sclerosis, inflammation, experimental autoimmune encephalomyelitis, sodium channel, lipopolysaccharide, mast cells.

Highlights

- The recruitment of myeloid cells was significantly reduced and levels of IL-10 increased in EAE *Scn8a*$^{dmu/+}$ mice.
- *Scn8a*$^{dmu/+}$ mice had significantly lower levels of plasma IL-6 during remission and chronic phases, which was associated with less inflammation.
- *Scn8a*$^{dmu/+}$ mice demonstrated reduced inflammatory and cytokine responses to LPS challenge.
- Our results suggest a potential general role for Nav1.6 in regulating the inflammatory process.

3.2 Introduction

Multiple sclerosis (MS) is an inflammatory demyelinating disease that affects the central nervous system (CNS) (Waxman, 2006) where it causes myelin loss that eventually leads to permanent disability in the majority of patients. Although the root causes of this disease are still unknown, a combination of environmental and genetic factors are thought to be involved (Constantinescu et al., 2011; Mohr, 2011). T and B cell function, as well as innate immune responses, are believed to play an important role in neuronal damage and loss of the myelin in the CNS (Pierson et al., 2014).

Numerous studies have reported that T cells play a potential role in the immune pathogenesis of MS by crossing through the blood-brain barrier (BBB), which then triggers autoimmune inflammation that destroys myelin (Duffy et al., 2014; Wojkowska et al., 2014). Autoreactive T cells produce cytokines that attract inflammatory cells into the CNS, including B cells, natural killer (NK) cells, and monocytes/macrophages. In MS, activated autoreactive myelin-specific $CD4^+$ T cells are able to initiate a chronic inflammatory response by migrating into CNS compartments. Autoreactive $CD4^+$ T cells cause neurodegeneration leading to a decrease in the neuronal count and grey matter volume (Bartholomäus et al., 2009; Ignjatović et al., 2012). Activated macrophages also directly or indirectly cause damage to the CNS by phagocytosing the myelin sheath (Barnett et al., 2006). The innate immune and inflammatory processes required to initiate and sustain disease are driven by a variety of cytokines and chemokines that include a pro-inflammatory cytokine cascade involving TNF and IL-6 (Dendrou et al., 2015). These cytokines activate immune effector cells and promote their migration partly through the enhanced expression of adhesion molecules on vascular endothelium

(Dendrou et al., 2015; Stadelmann et al., 2011). A number of regulatory cytokines, such as IL-10 help modulate the inflammatory process (Croxford et al., 2001; Kwilasz et al., 2015).

Nav channels are transmembrane proteins that can be found in both excitable and non-excitable cells (Savio-Galimberti et al., 2012). Each Nav channel is composed of one of ten known α-subunit isoforms and one or two regulatory β-subunits (β1, β2 and/or β3) (Catterall et al., 2005a). In excitable cells, these channels allow sodium to enter a cell in response to an increase of the voltage across the cell membrane and are essential for the generation of the action potential. In MS, the usually tightly regulated placement and concentration of Nav channels along the axon are profoundly altered following the loss of myelin (Craner et al., 2004c). Our previous work showed that an increase in Nav1.6 in EAE and is consistent with the hypothesis that Nav1.6 promotes inflammation and is an important factor in eventual neuron death.

While the physiological role of Nav channels in neuronal cells is well characterized (Catterall, 2013), these channels are also expressed in many other non-excitable cell types such as glia, immune cells, and cancer cells (Besson et al., 2015) in which their function is not well defined (Black and Waxman, 2013; Pappalardo et al., 2016). Nav1.6 is expressed in non-neuronal cells such as astrocytes, microglia, and macrophages as well as in invasive cancer lines (Black et al., 2009a; Carrithers et al., 2009b; Craner et al., 2005; Pappalardo et al., 2016). A significant increase in Nav1.6 expression occurs in activated microglia and macrophages in EAE and MS (Craner et al., 2005). Also, Nav1.6 has been found to play an important role in initiating microglial migration (Black and Waxman, 2013) by promoting the extension of lamellipodia of

ATP-activated microglia via modulation of intracellular Ca^{2+} levels and a Rac1-ERK1/2 pathway (Persson et al., 2014a).

In the current study EAE, a rodent model of MS, was induced by immunization with MOG_{35-55} in conjunction with CFA+PTX and PTX to induce an immune response against myelin. Our previous work showed that Nav1.6 contributes to the inflammation in CNS tissue (optic nerve) in EAE. Here we extend this investigation by seeking to determine if reduced levels of Nav1.6 regulate inflammation in EAE or, more generally, in the LPS model of systemic inflammation. We show that in the peripheral blood and optic nerve, the percentage of $Gr\text{-}1^+/CD11b^+$ cells, and levels of inflammatory cytokines, during EAE, were reduced in the *Scn8a*$^{dmu/+}$ mice, which express reduced levels of Nav1.6. Notably, untreated *Scn8a*$^{dmu/+}$ mice had levels of the anti-inflammatory cytokines of IL-10, IL-13, and TGF-β1 in the brain that exceeded wild type levels. In addition, *Scn8a*$^{dmu/+}$ mice displayed a reduced inflammatory reaction to LPS. *In vitro*, bone marrow-derived mast cells from *Scn8a*$^{dmu/+}$ mice also produced lower levels of IL-6 in response to LPS. Our results demonstrate that a reduction in Nav1.6/*Scn8a* expression has a significant inhibitory effect on the inflammatory response in these models.

3.3 Materials and methods

3.3.1 Mice

Two groups of female mice (n = 44), including *Scn8a*$^{dmu/+}$ heterozygous (n = 22) and *Scn8a*$^{+/+}$ wild-type (WT) littermates (n = 22), were used in this study. The *Degenerating muscle* (*dmu*) mutation consists of a single nucleotide deletion in the sequence coding for the first interdomain loop of Nav1.6, leading to a premature stop codon. Homozygous *dmu* mice are not suitable for the induction of EAE due to lethality

at approximately three weeks of age (De Repentigny, 2001). Heterozygous *dmu* mice, however, have a similar life-span to wild-type mice and do not exhibit any overt motor dysfunction (Côté et al., 2005). All animal experiments were approved by the Dalhousie University Committee on Laboratory Animals. This study was carried out by the recommendations in compliance with the Canadian Council for Animal Care guidelines.

3.3.2 EAE induction and clinical score

EAE was induced in *Scn8a*$^{dmu/+}$ heterozygous (n = 10) and *Scn8a*$^{+/+}$ mice (n = 10). Female mice were injected subcutaneously (s.c.) with 200 μg of MOG_{35-55} suspended in CFA. PTX (200 ng/mouse) was then injected intraperitoneally (i.p) on the day of immunization and two days later. Mice were monitored daily for clinical signs of EAE and body weight loss during the course of the disease. Scoring was done by a person blinded to the animal groups, with scores as (1) flaccid tail; (2) hind limb weakness and poor righting ability; (3) inability to right and paralysis in one hind limb; (4) both hind limbs paralyzed with or without forelimb paralysis and incontinence; and (5) moribund. Once mice reached a score of 2 to 3, they were monitored twice daily for dehydration and body weight. These mice were given food supplements (hydration gel and wet chow-slurry), provided with elongated water bottle sipper tubes and/or injected subcutaneously (s.c.) with normal saline as required. Animals exhibiting severe weakness of one or both hindlimbs or paralysis of either or both hind limbs were hand-fed chow-slurry. Animals whose weight fell below 80% of their original body weight were euthanized.

3.3.3 Blood collection and tissues sampling

Heparinized blood samples were collected from *Scn8a*$^{dmu/+}$ and *Scn8a*$^{+/+}$ mice (*n* = 14 each) by facial vein puncture on days 0, 6, 13, 21, and 35 post-immunization. The mice were sacrificed at 35 days post-EAE induction (Figure 1). Using flow cytometry, CNS tissues (optic nerve and brain) were studied to define various types of immune cells such as macrophages, myeloid cells, T lymphocytes ($CD4^+$ and $CD8^+$), and B lymphocytes ($CD19^+$). The optic nerves were assessed further by histological staining. ELISA was used to measure the level of several cytokines such as IL-10, IL-13, IL-4, TGF-β1, IL-6, and TNF in the brain and IL-6 in the plasma.

3.3.4 Staining of surface markers and flow cytometry

Peripheral blood, spleen, and CNS tissues (optic nerve and brain) from *Scn8a*$^{dmu/+}$ and *Scn8a*$^{+/+}$ mice (*n* = 14 each) were harvested at different time points. The peripheral blood mononuclear cells were isolated from heparinized blood samples using Ficoll. Cells from spleen and CNS tissues were dissociated by passing through wire mesh followed by addition of an equal volume of 2X enzymatic digestion mix to a final concentration of 10 µg/ml (collagenase D and 100 µg/ml DNase I, Roche Diagnostics, Mannheim, Germany), before incubation in a water bath at 37°C to prepare a single-cell suspension. The cells were centrifuged at 400 x g for 5 minutes at 4°C and resuspended in 0.5 ml of ammonium chloride lysis buffer (eBioscience, San Diego) on ice for 5 minutes to lyse red blood cells. The cells were centrifuged and resuspended in 1 mL of PBS. Next, the cells were filtered through the mesh for CNS and washed with an additional 1 mL of PBS and counted. Cells were then centrifuged at 400 x g for 10 minutes at 4°C and resuspended in a 1/1000 dilution of fixable viability dye (FVD)

eFluor450 (eBioscience, San Diego, CA) in PBS for 30 minutes. The cells were then washed with PBS and stained with specific monoclonal antibodies (mAbs) to define various types of immune cells such as macrophages ($F4/80^{+}/CD11b^{+}$), monocytes ($Gr\text{-}1^{int}/CD11b^{+}$) neutrophils ($Gr\text{-}1^{high}/CD11b^{+}/F4/80^{-}$ or $CD45^{+}/CD11b^{+}/Ly6G^{+}$), T lymphocytes ($CD4^{+}$, $CD8^{+}$) and B cells ($CD19^{+}$). After incubation, the cells were washed using wash buffer (PBS supplemented with 1% FBS), centrifuged again, and fixed in 1% paraformaldehyde (PFA) in PBS and kept at 4°C. Compensation controls were prepared using compensation beads (eBioscience) mixed with individual dilutions of each antibody used as above in IMF and fixed in 1% PFA. The unstained controls were not incubated with FVD. Stained samples were acquired within 24 hours using a BD FACS Canto™ II cytometer (BD Bioscience, San Jose, CA). All analysis and gating were done using BD FACS Diva software and FlowJo V10.2 (BD Biosciences).

3.3.5 ELISA

Concentrations of cytokines (IL-6, TNF, IL-10, IL-13, IL-4, and TGF-β1) in plasma samples or homogenized brain were determined using ELISA. We extracted the protein from the brain tissue of EAE mice by homogenizing the samples, using a Qiagen Tissue Ruptor device, in RIPA buffer with protease inhibitor for 1 minute on ice. Samples were centrifuged at 10,000 x g for 10 min, supernatants were collected, and total protein was measured using a Bradford protein assay (Bio-Rad, Mississauga). Levels of cytokines were normalized to total protein concentration. ELISA was then performed according to manufacturer instructions. Briefly, plates were coated with 2.5 μg/ml capture antibody (eBioscience) diluted in borate buffer (pH 8.2). Plates were blocked with blocking buffer (2% BSA in PBS) before samples were added to the plates and

incubated overnight at 4°C. Next, biotinylated secondary antibodies (eBioscience) were added to the plate, followed by the addition of streptavidin-horseradish peroxidase. 3,3′,5,5′-Tetramethylbenzidine or substrate solution (TMB) (eBioscience) was added to the plate and incubated for 10–15 minutes before the reaction was stopped using 2N H_2SO_4 and the plate measured using an Epoch microplate spectrophotometer (Biotek, Winooski, VT).

3.3.6 Quantitative reverse-transcription polymerase chain reaction (qRT-PCR)

Tissue samples harvested from *Scn8a*$^{dmu/+}$ and *Scn8a*$^{+/+}$ mice (n = 8 each) were immersed in RNAlater (Qiagen, Hilden, Germany). Brain samples were transferred from RNAlater solution (Qiagen, Hilden, Germany) into 700 µL of QIAzol Lysis Reagent (Qiagen). The tissue was homogenized using a Qiagen Tissue Ruptor device. After 5 minutes of incubation at room temperature, 140 µL of chloroform was added to the homogenate, shaken vigorously and centrifuged at 10,000 x g for 15 minutes at 4°C. The upper aqueous layer was extracted, combined with an equal volume of RNase-free 70% ethanol, and RNA was isolated using a Qiagen RNA Mini spin column according to the manufacturer's protocol. The concentration of RNA in each sample was determined and RNA integrity was determined using a 1% agarose gel to confirm the 2:1 ratio of 28S:18S RNA intensity. RNA samples were reverse transcribed to cDNA using a QuantiTect® Reverse Transcription Kit (Qiagen). The resulting cDNA samples were diluted 1:4 and used in qPCR to measure the expression of mRNAs, identifying genes that were implicated in impulse conduction such as Nav1.6 (*Scn8a*) during the clinical course of chronic EAE (Table 4). mRNA expression of the genes of interest was

normalized to the geometric mean of the reference *Gapdh* and *Hprt* Cq value expressed as $2^{-\Delta Cq}$ where the Δ Cq= Cq gene of interest – Cq references genes.

Table 4 qPCR primers:

Gene	Primer sequence or company (catalog number)
Hprt	Bio-Rad (Cat no. 10025636)
Gapdh	Bio-Rad (Cat no. 10025637)
Scn8a	Forward (5'-3') GCAAGCTCAAGAAACCACCC Reverse (5'-3') CCGTAGATGAAAGGCAAACTCT

3.3.7 Hematoxylin and eosin staining of the optic nerve

Optic nerves were collected from *Scn8a*$^{dmu/+}$ and *Scn8a*$^{+/+}$ mice (n = 8 each) and fixed with 10% formalin, embedded in paraffin, and sectioned (5μm) longitudinally. The sections were dehydrated for 2 h at room temperature and fixed for 10 min with 4% paraformaldehyde (PFA) followed by dehydration for 2 min by a series of graded ethanol solutions. The sections were incubated for 5-7 min in hematoxylin and transferred to distilled water. The sections were incubated for 1 min in eosin and dehydrated in a gradient ethanol series before mounting. Images were taken with a Zeiss microscope and software (AxioVision 4 4.7). Infiltration score was assessed by two investigators blinded to the nature of the samples according to (Shindler et al., 2008) as follows: no infiltration = 0; mild cellular infiltration = 1; moderate infiltration = 2; severe infiltration = 3; massive infiltration = 4. The average number of cell nuclei per mm^2 was determined for each optic nerve.

3.3.8 Electron microscopy

Optic nerve tissues were collected from *Scn8a*$^{+/+,}$ and *Scn8a*$^{dmu/+}$ mice (n = 13 each) sacrificed in the chronic phase, 35 days after induction of EAE. Tissues were then

processed according to the process outlined by Alrashdi *et al.*(2019). To demonstrate the axonal loss and myelin pathology, we used a g-ratio that was determined by dividing the axon diameter by the diameter of the myelinated nerve fiber (Guy et al., 1991; Kuerten et al., 2007). Only axonal g-ratios three standard deviations above (remyelinating) or below (demyelinating) the average of the non-EAE reference group were counted. A conservative margin of ± 3 standard deviations from the mean of normal healthy mice before EAE was used as the cut-off to assign a diagnosis of demyelinating (< 0.55) or remyelinating (> 0.95). The analysis was conducted by an individual that was blinded to the samples.

3.3.9 Lipopolysaccharide (LPS) injection

Scn8a$^{dmu/+}$ and *Scn8a*$^{+/+}$ mice (n = 12 each were injected intraperitoneally (i.p.) with 100 µL of 50 µg/mL LPS from *Escherichia coli* 055 B5 (Sigma-Aldrich, Mississauga) or sterile vehicle control (saline). After 16 hours, mice were euthanized and the peritoneal cells were harvested by lavage.

3.3.10 Peritoneal cavity cells harvesting and flow cytometry

Peritoneal cells from *Scn8a*$^{dmu/+}$ and *Scn8a*$^{+/+}$ mice (n = 16 each) were harvested by i.p. injection and recovery of 4 ml PBS, 0.5% bovine serum albumin, 5 mM EDTA. Mouse peritoneal cavity cells (PCC) were counted. Cells were centrifuged at 400 x g for 5 minutes at 4°C and resuspended in a 1/1000 dilution of fixable viability dye (FVD) eFluor 450 (eBiosciences) in PBS for 20 minutes. Then the cells were washed with wash buffer (PBS + 2% FBS + 20 mM NaN_3), centrifuged and resuspended in antibody cocktails containing anti-CD19-BV510 (clone 6D5, BioLegend), anti-CD11b-PE-eFL610 (clone M1/70, eBiosciences), CD117 (c-kit)-PE (clone 2B8, BioLegend), anti-

CD4-APC (clone GK1.5, eBiosciences), anti-FcεRI-APC eFL780 (clone Mar-1, eBioscience), anti-CD8a-BV650 (clone 53-6.7, BD Biosciences), anti-CD3-BV711 (clone 145-2C11, BD Biosciences), anti-Siglec-F-PE-CF594 (clone E50-2440, BD Bioscience), anti-CD11b-PE (clone M1/70, eBiosciences), anti-F4/80-PE-Cy7 (clone BM8, eBioscience), anti-Ly6C-APC-eF780 (clone HK1.4, eBioscience), or anti-Ly6G-BV605 (clone 1A8, BD Biosciences) for 30 minutes. Stained fixed cells were acquired for analysis using a BD LSRFortessa and results were analyzed using FlowJo (Ashland, OR) software. A visual representation of the gating strategy used to identify the cell populations in the mouse peritoneum is provided (Supplementary Figure 2).

3.3.11 Generation of murine mast cells

Bone marrow-derived mast cells (BMMCs) were generated from the bone marrow of C57BL/6 and *Scn8a*$^{dmu/+}$ heterozygous mice, as previously described (Tertian et al., 1981). Briefly, mice were sacrificed, the whole femurs and tibias were isolated, and the bone marrow cells were flushed out. The cell suspension was cultured at 0.5–1 × 10^6 cells/ml in BMMC cell culture media consisting of RPMI 1640 (Life Technologies) supplemented with 10% FCS 10% concentrated WEHI-3 cell-conditioned medium 1% penicillin/streptomycin (Life Technologies), 10^{-7} M prostaglandin E2, and 50 μM 2-β-mercaptoethanol (2-ME). The media was changed twice per week. BMMCs were assessed for purity after four weeks by Alcian blue (pH 0.3) staining of fixed cytocentrifuge preparations and checked for maturity by the expression of c-kit and IgE receptors using flow cytometry. Once the BMMC population reached a purity of >95% (5–8 weeks), they were used in subsequent experiments.

3.3.12 Mast cell activation

Cells were counted and then resuspended in resting media overnight (BMMC medium with 1.5 ng/mL recombinant IL-3 instead of WEHI-3 conditioned medium). Activation of BMMC was performed in resting medium with 100 μg/mL of soybean trypsin inhibitor (Sigma-Aldrich), three doses of LPS (100 μg/mL, 10 μg/mL, and 1μg/mL), 0.1 μM calcium ionophore (A23187), or in media alone at 10^6 cells/mL for 24 h at 37°C. Supernatant samples were collected and stored at −20°C until assayed.

3.3.13 Statistical analysis

All statistical analyses were performed by unpaired Student's *t*-tests, Kruskal-Wallis tests, or two-way ANOVA with multiple comparison tests, as indicated and dependent upon appropriate data distribution. Error bars represent the standard error of the mean (SEM). GraphPad Prism software was used for statistical analyses (Ver. 5.0, GraphPad Software, La Jolla, CA).

3.4 Results

To evaluate the impact of reduced expression of *Scn8a*, the gene that encodes the α subunit of the Nav1.6 channel, on inflammation in the EAE model, we used *Scn8a*$^{dmu/+}$ heterozygous mice and wild type *Scn8a*$^{+/+}$ littermates housed in the same cage environment. Mice were immunized with MOG_{35-55}, followed by intraperitoneal (i.p.) injection with PTX (Fig. 3.1A). The clinical symptoms in all mice subjected to EAE induction appeared 8 days post-immunization. Behavioral observations of *Scn8a*$^{dmu/+}$ mice revealed less impact of this treatment on motor capacity during the recovery and early chronic phase of EAE when compared with wild type animals (Fig. 3.1B). However, the severity of these symptoms returned to those observed in wild type mice later in the chronic phase (Fig. 3.1B).

Real-time qPCR analysis was used to determine how brain *Scn8a* mRNA expression fluctuates in response to EAE in *Scn8a*$^{dmu/+}$ and *Scn8a*$^{+/+}$ mice. In *Scn8a*$^{+/+}$ mice we found that in chronic EAE *Scn8a* expression (normalized to two reference genes) was reduced to 71% of their non-EAE level (0.035 ± 0.004 vs. 0.049 ± 0.0122), while the *Scn8a* expression in *Scn8a*$^{dmu/+}$ in chronic EAE was reduced to 55% of non-EAE levels (0.017 ± 0.005 vs. 0.031 ± 0.013). In chronic EAE, *Scn8a* expression in *Scn8a*$^{dmu/+}$ was reduced to 49% of *Scn8a*$^{+/+}$ levels ($P = 0.028$, Fig. 3.1C). *Scn8a* mRNA was not detectable by real-time qPCR in leukocytes derived from the spleen or peritoneum (not shown).

To characterize the immune cell populations in the blood under normal and pathological conditions, we performed flow cytometry longitudinally throughout EAE. All blood leukocytes were first identified using the general marker CD45 (Supplementary

Fig. 3.1) before determining the percentage of (Gr-1^{high} /CD11b^{+}, Gr-1^{int} /CD11b^{+}), T cells (CD4^{+} or CD8^{+}), and B cells (CD19^{+}) (Fig 3. 2). At 35 days post-induction, representing the chronic phase of EAE, we found a significant reduction (P = 0.027) in the percentage of (Gr-1^{high} /CD11b^{+}) granulocytes in *Scn8a*$^{dmu/+}$ mice only reaching 59% of that seen in *Scn8a*$^{+/+}$ mice (23.34 ± 5.469%, n = 8 vs 39.41 ± 3.549%, n = 8; Fig. 3.2A).We also found a significant reduction (P = 0.035) in the percentage of (Gr-1int /CD11b+) monocytes in *Scn8a*$^{dmu/+}$ mice ,only reaching 64% of that seen in Scn8a+/+ mice (14.40 ± 3.317%, n = 8 vs 25.84 ± 3.606%, n = 8; Fig.3.2B). In chronic EAE, we found no significant differences in the frequency of CD4^{+} and CD8^{+} T cells in both groups (Fig. 3. 2C, D). However, in chronic EAE the percentage of CD19^{+} B cells was significantly higher (P = 0.034) in *Scn8a*$^{dmu/+}$ relative to *Scn8a*$^{+/+}$ (39.61 ± 8.078%, n = 8 vs 18.25 ± 4.177%, n =8; Fig 3.2E).

The expression of Nav1.6 also influenced the presence of inflammation-related cytokines in the plasma (Fig. 3.3). Following EAE induction, the pro-inflammatory cytokine IL-6 was found to be significantly reduced in *Scn8a*$^{dmu/+}$ to 3% of *Scn8a*$^{+/+}$ at day 21 (0.63 ± 0.62 pg/mL, n = 8 vs 21.51 ± 9.51 pg/mL, n = 8, *P* = 0.046) and to 26% of *Scn8a*$^{+/+}$ at day 35 (15.70 ± 7.51 pg/mL, n = 8 vs 61.01 ± 17.39 pg/mL, n = 10, *P* = 0.043). The proinflammatory cytokines TNF and IL-1β and the anti-inflammatory cytokine IL-10 were, however, undetectable in both groups at all time points (not shown).

Next, we turned to the CNS and examined how Nav1.6 influences immune cell infiltration in the optic nerve. Longitudinal sections of optic nerves were stained with H&E and cell infiltration was analyzed in *Scn8a*$^{+/+}$ and *Scn8a*$^{dmu/+}$ mice. The total number of nuclei within the optic nerve was significantly higher in *Scn8a*$^{+/+}$ mice (*P* =

0.041) and numerous cell clusters were seen versus non-EAE *Scn8a*$^{+/+}$ mice. In contrast, *Scn8a*$^{dmu/+}$ optic nerves were relatively devoid of clusters, and total nuclei counts were equivalent to non-EAE *Scn8a*$^{dmu/+}$ mice (Fig. 3.4A, B). To further analyze the infiltrating cells in the optic nerve and the brain, flow cytometry was performed. The percentage of (Gr-1^{+}/CD11b^{+}) granulocytes was significantly less (P = 0.0100) in the *Scn8a*$^{dmu/+}$ mice reaching 54% of that observed in *Scn8a*$^{+/+}$ mice (12.58 ± 3.840%, n=8 vs 23.33 ± 3.840%, n = 10) at the chronic stage of EAE (Fig.3.4C). The percentage of Gr-1^{+}/CD11b^{+} granulocytes in the brain was also found to be reduced in the *Scn8a*$^{dmu/+}$ vs *Scn8a*$^{+/+}$ mice but without reaching significance (Fig.3.4D). The CD8^{+}, CD4^{+}, and B cell populations in the optic nerve and brain did not change significantly between both groups of mice (data not shown).

To assess the effects of Nav1.6 in myelin sheath pathology, we performed optic nerve ultra-structure analysis (Fig. 3.5). We found that nerves from healthy *Scn8a*$^{+/+}$ and *Scn8a*$^{dmu/+}$ (non-EAE) controls had a similar appearance with axons generally appearing rounded throughout the optic nerve (Fig. 3.5 A and B). Interestingly, the g-ratio (25, see Materials and Methods) of healthy *Scn8a*$^{dmu/+}$ was found to be significantly lower than in healthy *Scn8a*$^{+/+}$ optic nerves (P = 0.0196; 0.7572 ± 0.058884; n = 483 vs 0.7668 ± 0.060645; n = 375; Fig. 3.5C). However, in *Scn8a*$^{+/+}$ mice at 35 days post-EAE induction, the axons generally appeared deformed. Several pathological features could be identified in EAE mice, including demyelinated and axolytic fibers, though the frequency of these features did not differ significantly between *Scn8a*$^{+/+}$ and *Scn8a*$^{dmu/+}$ optic nerves. However, a representation of the distribution of the axonal area (measured inside the myelin sheath) revealed that more axons in *Scn8a*$^{+/+}$ mice were between 4-10 μm²

compared to *Scn8a*$^{dmu/+}$ mice and only *Scn8a*$^{+/+}$ had very enlarged axons between the sizes of 7 and 10 μm² (Fig. 3.5D). The g-ratio post-EAE was significantly higher in *Scn8a*$^{dmu/+}$ vs *Scn8a*$^{+/+}$ mice (P = < 0.0001; 0.8097 ± 0.002624; n = 618 vs 0.7944 ± 0.002803; n = 622; Fig 3.5D). No demyelinating axons were observed in either group (not shown). However, *Scn8a*$^{dmu/+}$ mice had significantly increased remyelination (P = 0.0400; 1.200 ± 0.4899 %, n = 5 vs 0.0 ± 0.0 %; n =5) in *Scn8a*$^{+/+}$ mice Fig. 3.5E).

In the brain, we analyzed pro-inflammatory and anti-inflammatory cytokine levels by ELISA in healthy control and chronic phase-EAE mice. In chronic EAE, the pro-inflammatory cytokine TNF and IL-6 responses were both modestly reduced in *Scn8a*$^{dmu/+}$ relative to *Scn8a*$^{+/+}$ mice but neither change reached significance. The anti-inflammatory cytokines IL-10, TGF-β1, and IL-13, were also examined in the brain by ELISA in non-EAE and in chronic-phase EAE mice. Surprisingly, the levels of IL-10 in non-EAE *Scn8a*$^{dmu/+}$ mice were found to be 3.7 fold higher than control non-EAE *Scn8a*$^{+/+}$ values (209.6 ± 44.33 pg/mL, n = 7 vs 57.28 ± 6.285 pg/mL; n = 7, P = 0.0002; Fig. 3.6C). Similarly, levels of TGF-β1 in non-EAE *Scn8a*$^{dmu/+}$ mice were 45-fold higher than control levels (1722 ± 143.3 pg/mL; n = 3 vs 37.79 ± 4.597 pg/mL; n = 4; P = 0.0057; Fig 3.6B). In both *Scn8a*$^{dmu/+}$ and *Scn8a*$^{+/+}$ mice, the level of IL-10 was lower in chronic-phase EAE while the level of TGF-β1was found to be significantly lower only in *Scn8a*$^{dmu/+}$. As opposed to IL-10 and TGF-β1, we did not find a significant difference for IL-13 in untreated animals. However, in chronic EAE, IL-13 was significantly higher in *Scn8a*$^{dmu/+}$ mice than in *Scn8a*$^{+/+}$ mice (181.9 ± 39.93 pg/mL, n = 6 vs 101.2 ± 33.15 pg/mL, n = 6, P = 0.048).

Having demonstrated that mice with reduced levels of Nav1.6 display a reduced inflammatory reaction in the EAE model of CNS inflammation, we aimed to define whether Nav1.6 might be generally involved in the regulation of neutrophils and macrophages in response to inflammatory stimuli, such as LPS insult. Neutrophils are a major immune cell type recruited during acute inflammation. Analysis of peritoneal cavity cells (PCC) following an intraperitoneal injection of LPS (5 μg/animal) resulted in a significant increase in the number of neutrophils after 16 hours in *Scn8a*$^{+/+}$ mice. However, this neutrophil response was significantly lower in *Scn8a*$^{dmu/+}$ than in *Scn8a*$^{+/+}$ mice at 16 h post-LPS (10.77 % ± 3.566, $n = 8$ vs 27.65% ± 6.989, n = 8, $P = 0.0199$, Fig. 3.7A). The resting monocytes were reduced in *Scn8a*$^{+/+}$ mice at 16 h post-LPS ($P = 0.0054$), whereas a more modest reduction was observed in the *Scn8a*$^{dmu/+}$ mice post-LPS without reaching statistical significance (Fig. 3.7B).

To determine if the reduced inflammatory response to LPS in *Scn8a*$^{dmu/+}$ was also observed *in vitro* in the absence of systemic influences, we analyzed the response of primary cultured immune cells outside of the mouse in vivo environment. Mast cells derived from the long term (6 to 8 week) culture of bone marrow (BMMC) were therefore exposed to LPS for 24 hours (McCurdy et al., 2001). BMMC derived from *Scn8a*$^{dmu/+}$ and *Scn8a*$^{+/+}$ mice were treated with three different concentrations of LPS (100, 10, 1 μg/mL) and the production of IL-6 was determined. We observed significantly lower levels of IL-6 in *Scn8a*$^{dmu/+}$ BMMCs treated with 100 μg/mL LPS at 24 hours (0.2888 ± 0.0618 ng/ml, $n = 5$ vs 0.6389 ± 0.1089 ng/ml, $n = 5$, $P = 0.044$, Fig. 3.8) post-treatment.

3.5 Discussion

While the adaptive immune system has been the primary research focus in MS, the role of the innate immune system is attracting an increasing interest due to its importance for the generation of acquired immunity and for the inflammatory response that impacts the progression of the disease (Hossain et al., 2015). Inflammation is a primary hallmark of MS and is characterized by the infiltration of different types of leukocytes into the CNS, leading to the disruption of the BBB and axonal damage (Foster et al., 1980). Immune cells secrete multiple mediators of inflammation, including cytokines, chemokines, glutamate, reactive oxygen, and nitrogen species, some of which are neurotoxic and can disrupt the normal metabolism within neurons (Burgess et al., 1995b; García-Vallejo et al., 2014; Van Wart and Matthews, 2006).

In MS and in the EAE model, neuronal Nav channel expression is dysregulated and they are known to become abnormally distributed along axons following demyelination. As a result, these channels have been hypothesized to cause sodium-calcium exchangers to operate in reverse such that they extrude excess axoplasmic sodium while calcium is imported, which eventually results in neuronal death by apoptosis (Craner et al., 2004c). However, Nav channels, including Nav1.6, are also present in immune cells where an understanding of their role remains limited and their involvement in the etiology of MS and EAE is not well characterized. Macrophages and microglia express different types of Nav channels, and which have been implicated in different functions of these cells, including motility and migration (Black et al., 2009a; Morsali et al., 2013). A study by Black *et al.* (20) reported that Nav1.6 and Nav1.5 regulate phagocytosis in human macrophages and cellular movement through their

association with the F-actin cytoskeleton and also regulate podosomes formation. In EAE and MS, Craner *et al.* (2005) showed that the expression of Nav1.6 is upregulated in activated microglia and macrophages. Increased activation of microglia and macrophages in MS has been linked to the axonal degeneration via induction of phagocytosis (Black et al., 2009a; Craner et al., 2005; Jacobsen et al., 2002), antigen presentation(Lo et al., 2012), cell migration(Black et al., 2009a; Persson et al., 2014a), stimulation of $CD4^+$ T cell proliferation, and production of pro-inflammatory cytokines and chemokines (Amor et al., 2014b; Black et al., 2009a).

To evaluate the role of Nav1.6 in the inflammatory response during EAE, we used *Scn8a*$^{dmu/+}$, which are heterozygous for a null allele of *Scn8a* and express low levels of *Scn8a*, the gene that encodes the alpha subunit of Nav1.6. The heterozygous mice that had a single mutation in Nav1.6 resulting in a decreased expression of the channel protein did not show any neurological deficit; however, they presented with behavioral and emotional changes (Meisler et al., 2004). It has been reported that Nav1.2 compensates for partial reductions of Nav1.6 in heterozygous mice indicating that Nav1.6 is unable to fully occupy the nodal membrane, which allows Nav1.2 to function and stabilize at the node of Ranvier. In addition, the similarity between the properties of Nav1.6 and Nav1.2 and their clustering indicates a binding competition at the node (Vega et al., 2008).

Mice were immunized with MOG_{35-55} as the antigen to induce chronic monophasic EAE (Kuerten et al., 2007; Stromnes and Goverman, 2006b). The *Scn8a*$^{dmu/+}$ and control *Scn8a*$^{+/+}$ littermates were housed in the same room and in the same cages to ensure that they shared the same environment. Clinical symptoms started at day 8 post-EAE and progressed similarly in both groups, consistent with the study of Horstmann et

al. (Horstmann et al., 2013). However, during the recovery phase (days 19-26), the clinical scores in *Scn8a*$^{dmu/+}$ mice were significantly lower than *Scn8a*$^{+/+}$ mice and the average clinical scores were 2.5, which an indicator for the ability of the mouse to walk and move around the cage than *Scn8a*$^{+/+}$ mice that showed the average clinical score was 3, which means the mice had a deficit in walking and moving around the cage indicating that *Scn8a*$^{dmu/+}$ had improved motor function during this period.

During EAE, peripheral blood Gr-1^{+}/CD11b^{+} myeloid cells were significantly reduced in *Scn8a*$^{dmu/+}$ in the EAE chronic phase. Several studies have reported that the expansion of Gr-1^{+}/CD11b^{+} cells in the peripheral blood in the early chronic phase of EAE is associated with the pathogenesis of EAE (Shindler et al., 2008). Neutrophil depletion using anti-Ly6G or anti-Gr-1 antibody hinders the onset of EAE (Bucher et al., 2015; Daley et al., 2008). The infiltration of these cells into the CNS was also investigated. Gr-1^{+}/CD11b^{+} cells were significantly reduced in the optic nerve of *Scn8a*$^{dmu/+}$ mice in keeping with their reduced numbers in the peripheral blood.

Levels of the cytokine IL-6 were significantly reduced in the plasma of *Scn8a*$^{dmu/+}$ mice during the recovery and the chronic phases of EAE. IL-6 is a hallmark cytokine of inflammation that induces the acute phase response and promotes the development of plasma cells from B cells. Notably, a higher level of CD19^{+} B cells was observed in *Scn8a*$^{dmu/+}$ mice. Notably, B cells have been implicated in the pathogenesis of the disease. It has been observed that CD19 knockout mice exhibit a more severe disease state highlighting the crucial role of CD19 on B cells in modulating the production of several cytokines (Matsushita et al., 2006). B cells are also implicated in

the recovery phase of EAE because of their ability to produce IL-10 that resolves inflammation; however, they are not required for its initiation (Fillatreau et al., 2002).

Ultrastructural analysis of axonal pathology in chronic phase EAE optic nerves revealed a higher g-ratio in *Scn8a*$^{dmu/+}$ mice post-EAE than *Scn8a*$^{+/+}$ mice and the distribution of the axonal area was shifted to the right in *Scn8a*$^{+/+}$ mice. In addition, based on g-ratio, remyelination occurred in *Scn8a*$^{dmu/+}$, while remyelination was completely absent in *Scn8a*$^{+/+}$ mice. In the CNS, remyelination may occur but is not sufficient to fully restore normal CNS function following demyelination (Patani et al., 2007), suggesting perhaps that partial blockade of *Scn8a* function or expression may be sufficient to enhance function through remyelination. Determination of the specific role that Nav1.6 may have in regulating remyelination, and whether the channels involved are of neuronal or glial origin, will require further investigation.

Interestingly, the infiltration of Gr-1$^+$/CD11b$^+$ cells and the level of the pro-inflammatory cytokine TNF in the brain increased markedly after EAE in *Scn8a*$^{+/+}$ mice, effects that were considerably less pronounced in the *Scn8a*$^{dmu/+}$ mice. TNF has been reported to cause apoptosis of oligodendrocytes and to induce the release of glutamate from astrocytes that leads to damage of oligodendrocytes and neurons (Jurewicz et al., 2005). It has also been reported that in cultured cortical neurons, TNF and IL-1β elevate Nav currents via the upregulation of TTX-sensitive Navs via a p38 MAPK dependent pathway (Chen et al., 2017). When combined with our results, these observations suggest the possible presence of bidirectional regulation between Nav channels and TNF. Additionally, treatment with anti-TNF-receptor IgG prevented the development of clinical signs of active EAE (Körner et al., 1995). A recent study by Ding et al. (2019)

has demonstrated that Nav1.6 upregulation in neuropathic pain caused by nerve injury might be through the activation of the TNF/STAT3 pathway. Our observed pathological improvements in *Scn8a*$^{dmu/+}$, including improved motor function and reduced myeloid cell infiltration in the optic nerve, could, therefore, plausibly be a result of Nav1.6 influence on TNF expression.

In examining anti-inflammatory cytokines, we observed that the level of IL-13 was significantly increased in chronic phase EAE *Scn8a*$^{dmu/+}$ mice. Most striking, however, was the presence of dramatically higher levels of IL-10 and TGF-β1in untreated (non-EAE) *Scn8a*$^{dmu/+}$ mice vs non-EAE *Scn8a*$^{+/+}$ controls. The Th2 subset of T cells are known to produce cytokines such as IL-4, IL-13, and IL-10 (Mosmann and Sad, 1996), which can ameliorate EAE by inhibiting Th1-like responses through the reduction of IFN-γ, TNF and IL-12 levels (Bitan et al., 2010). In addition, IL-10 inhibits a variety of innate immune and inflammatory events including upregulation of adhesion molecule expression, proinflammatory cytokine and chemokine production (58). IL-13 can also promote the polarization of macrophages to less inflammatory M2 phenotype (Benoit et al., 2008; Zhang et al., 2017). In our study, the strong expression of anti-inflammatory cytokines in the CNS prior to disease onset could have had a protective effect that resulted in the reduction of inflammation in chronic phase EAE *Scn8a*$^{dmu/+}$ mice.

To determine if heterozygous *Scn8a*$^{dmu/+}$ mice displayed reduced innate immune system-mediated inflammation outside of the context of EAE, the intraperitoneal LPS administration model was employed. LPS is an outer membrane Gram-negative bacterial product that acts as a pathogen-associated molecular pattern(Willis and Whitfield, 2013). Neutrophils and monocyte recruitment and cytokine production, together with enhanced

phagocytic activity, are key characteristics of the LPS model *in vivo* (Nathan, 2006). Upon exposure to LPS, neutrophils recruited to the site of injection produce ROS contributing to persistent inflammation (McDonald et al., 2010). Our results demonstrate that significantly lower neutrophil recruitment in *Scn8a*$^{dmu/+}$ than in *Scn8a*$^{+/+}$ mice at 16-hour post-LPS, suggesting that Nav1.6 may play a role in directly or indirectly facilitating migration. In this context, it is noteworthy that Craner *et al.* (Craner et al., 2005) has shown that the expression of Nav1.6 is upregulated in activated microglia and macrophages in response to LPS (Craner et al., 2005). Furthermore, increased activation of microglia and macrophages in MS has been linked to axonal degeneration via induction of pro-inflammatory cytokines (Black et al., 2009a; Craner et al., 2005). It was shown additionally that blocking of Nav1.6 by TTX in rat microglia or the lack of Nav1.6 in microglia isolated from *Scn8a*$^{med/med}$ (Nav1.6-null) mice, both have a significant negative impact on the phagocytic function of activated microglia by 40% and 65%, respectively (Craner et al., 2005).

Mast cells are innate immune cells known to respond to LPS, their localization in the leptomeninges has suggested a possible contribution of these cells in the regulation immune cell trafficking through the BBB (Kumar and Sharma, 2010). Bone marrow-derived mast cells (BMMC) were used as an *in vitro* model of inflammatory mediator responses, which could be assessed independently from neuronal mediators and impacts. Mast cells derived from *Scn8a*$^{dmu/+}$ produced lower levels of IL-6 than cells derived from *Scn8a*$^{+/+}$ animals in response to LPS stimulation. Although it has been reported that voltage-gated sodium channel mRNA is expressed in mast cells derived from human lung, skin, and cord blood (Bradding et al., 2003), only *SCN10A* (Nav1.8) and

SCN11A/SCN12A (Nav1.9) was detected. Similarly, in our study, the expression of *Scn8a* in BMMC derived from *Scn8a*$^{dmu/+}$ or *Scn8a*$^{+/+}$ by RT-qPCR and droplet digital PCR analysis was below the level of detection. This raises the possibility that reduced IL-6 from *Scn8a*$^{dmu/+}$-derived BMMCs is the result of a developmental requirement for Nav1.6 in the maturation of BMMCs.

Taken together, these results indicate that a reduction in *Scn8a* expression has a significant impact on the inflammatory response both in EAE and in response to LPS, even in isolated immune cells.

It is increasingly evident that abnormal activity and altered expression of Nav channels not only in neurons but also in immune cells are central to the pathophysiology of MS (Bouafia et al., 2014; Craner et al., 2004d). Our study provides evidence that reduced *Scn8a* expression *in vivo* is associated with several indicators of reduced inflammation and damage EAE including improved motor capacity during the recovery and early chronic phase, a decrease in neutrophil infiltration, reduced proinflammatory IL-6 in the blood, and decreased infiltration of myeloid cells within the optic nerve. Overall, this is the first in *vivo* study to report changes in the regulation of inflammation related to a reduced level of *Scn8a* in EAE. The decreased in *vivo* and in *vitro* response to LPS in *Scn8a*$^{dmu/+}$ we observed suggests that Nav1.6 could be a general regulator of inflammation with impacts in multiple settings and not limited to models of neuronal damage.

Acknowledgments

We thank Dr. Ian Haidl for critical reading of the manuscript. Thank you, Alexander Edgar, Maria Vaci, and Nong Xu for technical assistance. We also thank Derek Rowter for support in Fortessa acquired samples.

Funding

The Nova Scotia Research Foundation supported this work (to PDC), the Dalhousie Medical Research Foundation/Gillian's Hope MS Research Grant (to PDC), The Canadian Institutes of Health Research (CIHR) grant (to JSM) grant number THC-135230 and MOP-93517, and Jouf University, Saudi Arabia (to BA). BA is a recipient of a postgraduate scholarship from the Saudi Cultural Bureau (Canada) and Al Jouf University.

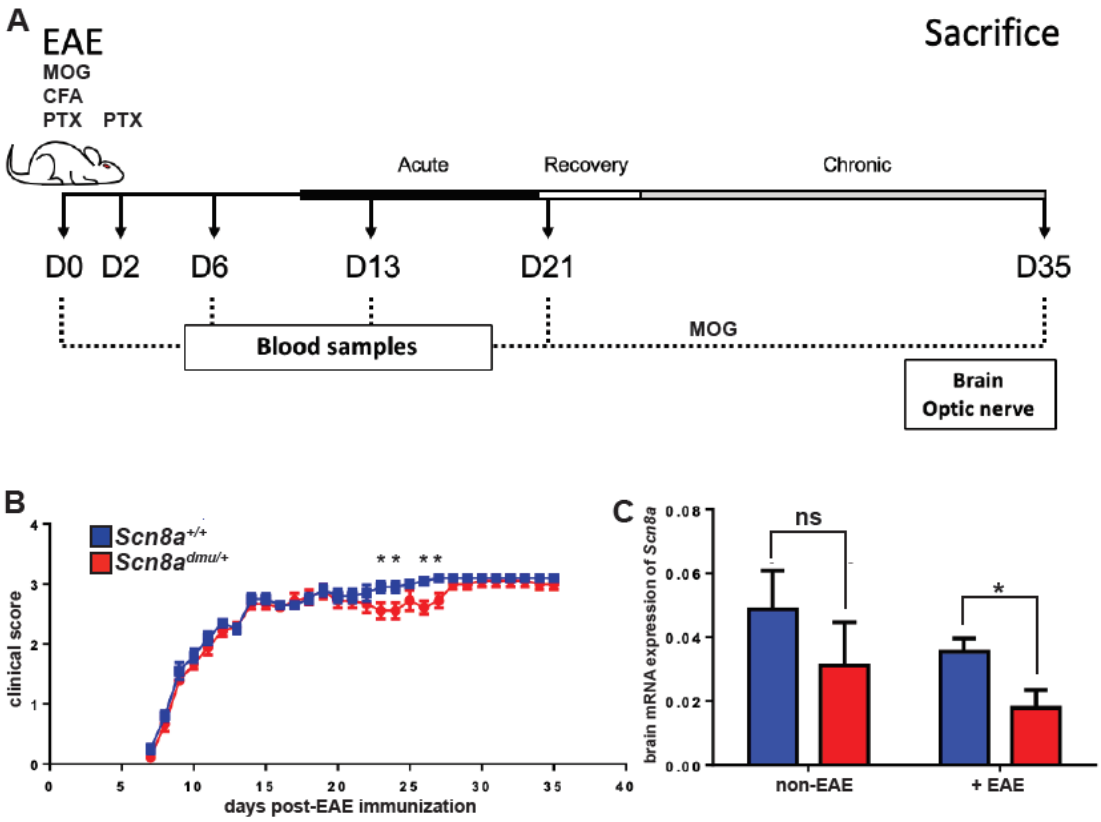
A
EAE
MOG
CFA
PTX PTX
Sacrifice
Acute
Recovery
Chronic
D0 D2 D6 D13 D21 D35
Blood samples
MOG
Brain
Optic nerve
B
Scn8a+/+
Scn8admu/+
clinical score
days post-EAE immunization
C
brain mRNA expression of Scn8a
ns
*
non-EAE
+ EAE

Figure 3-1 *Scn8a*$^{dmu/+}$ heterozygous mice have improved motor function during the EAE recovery and early chronic phase.

A) Schematic illustration of the experimental design to evaluate the role of reduced Nav1.6 channels in EAE. Two groups of mice, *Scn8a*$^{dmu/+}$ heterozygous and *Scn8a*$^{+/+}$ littermates were used in this study. EAE was induced at day 0 in *Scn8a*$^{+/+}$ and *Scn8a*$^{dmu/+}$ mice by immunization with MOG/CFA followed by PTX and injected at day 2 with PTX only. Mice were sacrificed 35 days post-EAE induction. The clinical score of mice in both *Scn8a*$^{+/+}$ and *Scn8a*$^{dmu/+}$ mice was recorded daily, starting at day 8 post EAE induction. Blood samples were collected at days 0 (pre-immunization), 6, 13, 21, and 35. On day 35, mice were sacrificed, and optic nerves and brains were collected. B) The clinical score of *Scn8a*$^{+/+}$ (n = 10) and *Scn8a*$^{dmu/+}$ (n = 10) mice post -EAE induction revealed a typical progression of MOG-induced EAE but with significantly improved motor function in *Scn8a*$^{dmu/+}$ in the recovery and chronic stage. C) RNA was extracted from brains of healthy (non-EAE) or chronic stage (35 day) EAE-induced (+EAE) mice. The expression of *Scn8a* in EAE *Scn8a*$^{dmu/+}$ was downregulated significantly compared to *Scn8a*$^{+/+}$ EAE mice. Data are presented as the mean ± SEM. Two-way ANOVA was used to compare the statistical differences among groups, with the Šídák post hoc test. **P* < 0.05, ns, not significant.

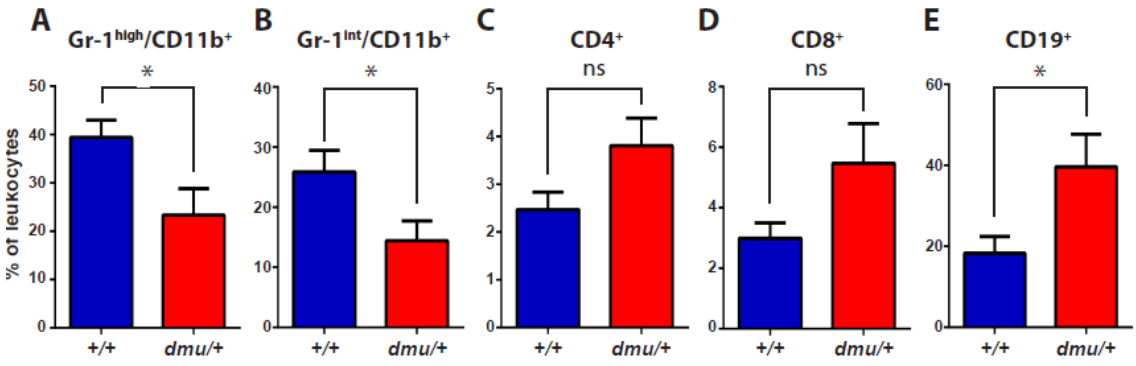
A
Gr-1highCD11b+
*
B
Gr-1intCD11b+
*
C
CD4+
ns
D
CD8+
ns
E
CD19+
*
% of leukocytes
+/+
dmu/+

Figure 3-2 *Scn8a*$^{dmu/+}$ heterozygous mice have a lower frequency of Gr-1^{high}/CD11b^{+} and Gr-1^{int}/CD11b^{+} but a higher frequency of CD19^{+} cells in the blood during the chronic phase of EAE.

Immune cell frequency in peripheral blood at 35 days post-EAE from *Scn8a*$^{+/+}$ (blue bars, n=8) and *Scn8a*$^{dmu/+}$ (red bars, n = 8) mice. The frequency of A) Gr-1 ^{high}/ CD11b^{+}, B) Gr-1^{int} /CD11b^{+}, C) CD4^{+}, D) CD8^{+} and E) CD19^{+} cells at days 35 post-EAE induction. Data are presented as the mean ± SEM. **P* < 0.05, ns, not significant, unpaired *t*-test.

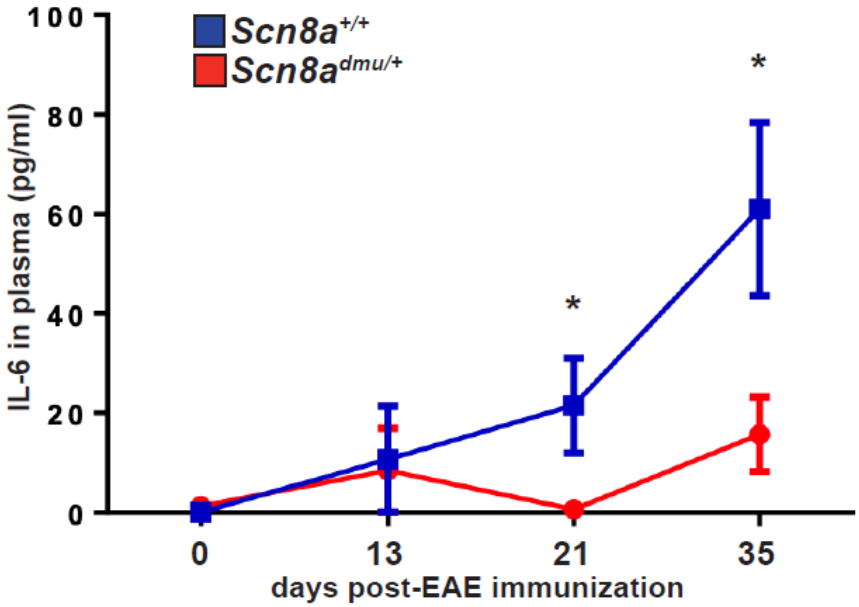
Scn8a+/+
Scn8admu/+
IL-6 in plasma (pg/ml)
100
80
60
40
20
0
*
*
0
13
21
35
days post-EAE immunization

Figure 3-3 Nav1.6 regulates levels of the pro-inflammatory cytokine IL-6 in plasma during the recovery and chronic phases of EAE.

The level of IL-6 was measured in the plasma of *Scn8a*$^{+/+}$ (n = 10) and *Scn8a*$^{dmu/+}$ (n = 8) mice post EAE induction by ELISA. Data are presented as the mean ± SEM. Two-way ANOVA with Tukey's post hoc test was used to compare the statistical differences among groups *$P < 0.05$.

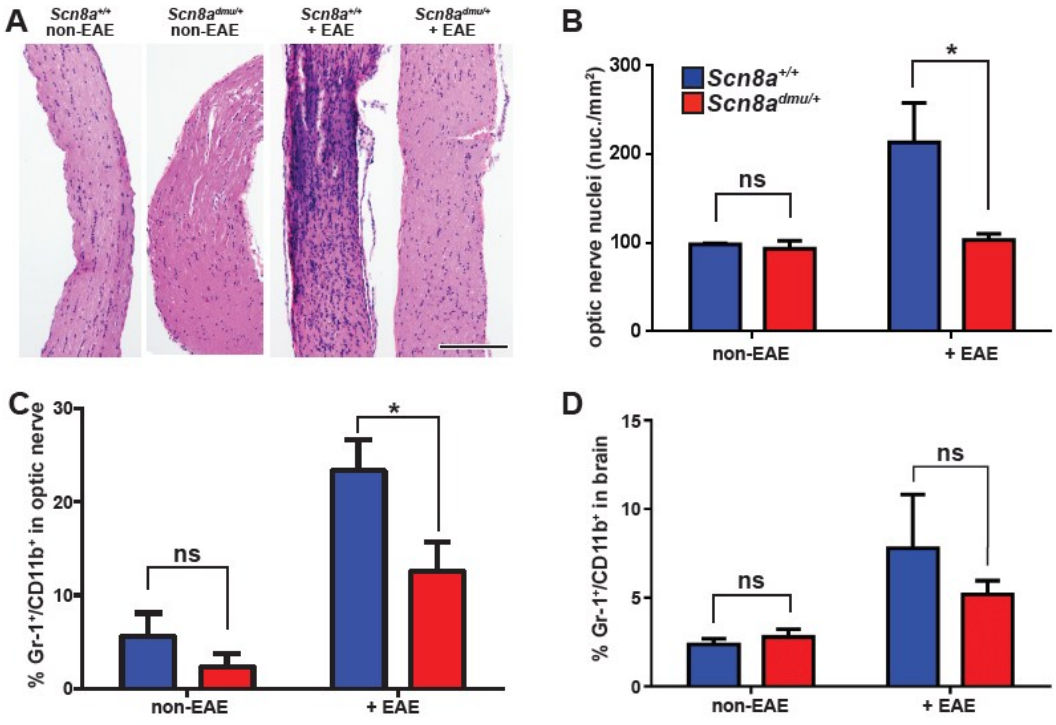
A
Scn8a+/+ non-EAE
Scn8admu/+ non-EAE
Scn8a+/+ + EAE
Scn8admu/+ + EAE
B
optic nerve nuclei (nuc./mm2)
Scn8a+/+
Scn8admu/+
ns
*
non-EAE
+ EAE
C
% Gr-1+/CD11b+ in optic nerve
ns
*
non-EAE
+ EAE
D
% Gr-1+/CD11b+ in brain
ns
ns
non-EAE
+ EAE

Figure 3-4 *Scn8a*$^{dmu/+}$ heterozygous mice have decreased optic nerve infiltration of Gr-1^{+}/CD11b^{+} cells during the chronic phase of EAE.

H&E-stained longitudinal optic nerve sections (A) and quantification of nuclei per mm^2 (B). Flow cytometry analysis of infiltration of Gr-1^{+}/CD11b^{+} in the optic nerves (C) and the brains (D) of healthy (non-EAE) and chronic-phase EAE (+EAE, day 35) *Scn8a*$^{+/+}$ and *Scn8a*$^{dmu/+}$ mice. Scale bar = 500 μm. Data are presented as the mean ± SEM. **P* < 0.05 ns, not significant, unpaired *t*-test.

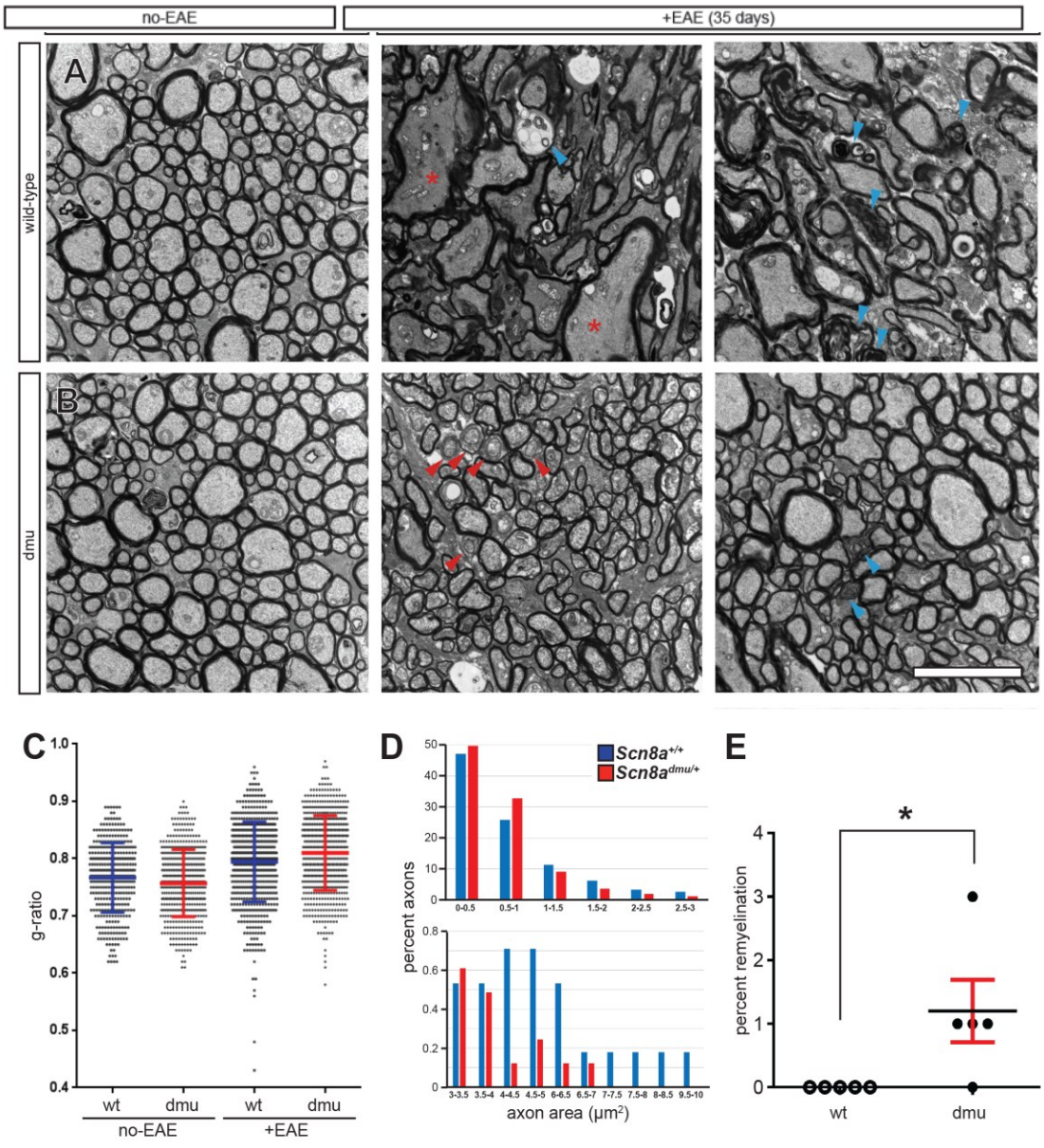
no-EAE
+EAE (35 days)
wild-type
dmu
A
B
C
g-ratio
wt
dmu
wt
dmu
no-EAE
+EAE
D
Scn8a+/+
Scn8admu/+
percent axons
axon area (μm2)
E
percent remyelination
wt
dmu

Figure 3-5 Improved axonal pathology in optic nerves of *Scn8a*$^{dmu/+}$ heterozygous mice during the chronic phase of EAE.

Representative EM micrographs of healthy (non-EAE) and 35 day EAE (+EAE) optic nerves from A) *Scn8a*$^{+/+}$ and B) *Scn8a*$^{dmu/+}$ mice. Red asterisks indicate enlarged fibers, blue arrowheads show axolytic fibers and red arrowheads show remyelinating fibers. C) Summary data for g-ratios from pooled axonal measurements of healthy and EAE optic nerves from *Scn8a*$^{+/+}$ and *Scn8a*$^{dmu/+}$ mice (error bars are ± SD). D) Distribution of the axonal area in 35 day post-EAE (error bars are ± SEM). E) Frequency of remyelination. Scale bar, 5μm. *, $P < 0.05$, unpaired t-test.

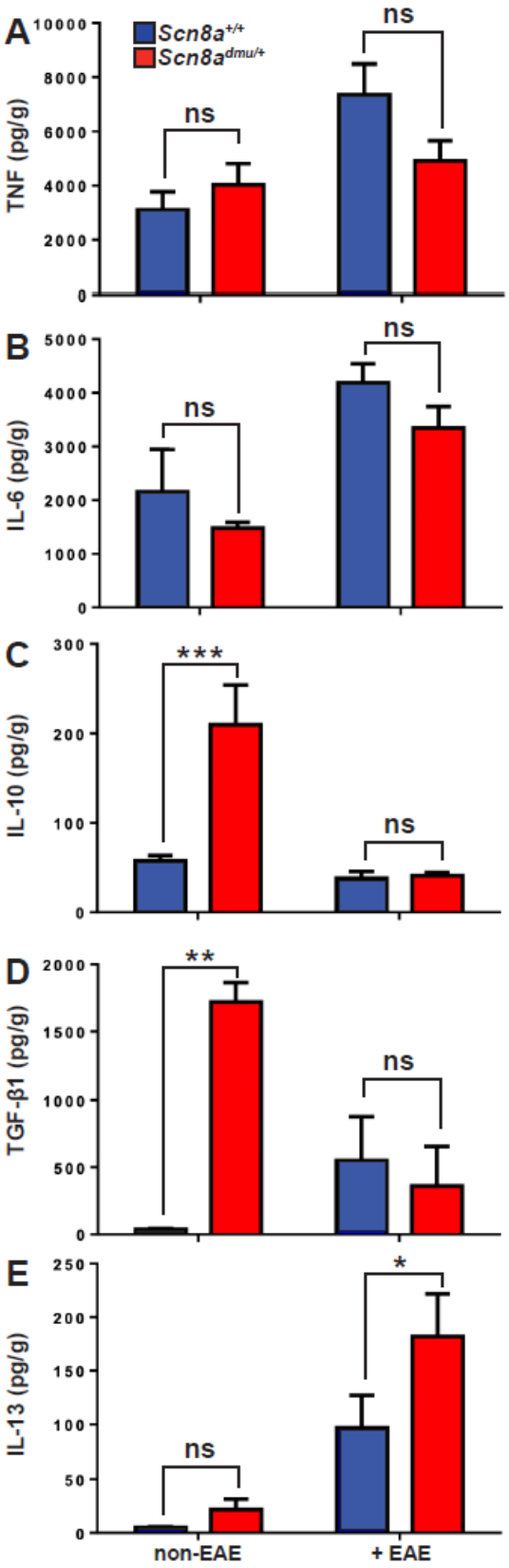
A
B
C
D
E
Scn8a+/+
Scn8admu/+
TNF (pg/g)
IL-6 (pg/g)
IL-10 (pg/g)
TGF-β1 (pg/g)
IL-13 (pg/g)
ns
***
**
*
non-EAE
+ EAE

Figure 3-6 Healthy (non-EAE) *Scn8a*$^{dmu/+}$ heterozygous mice express higher levels of regulatory cytokines while IL-13 is increased during the chronic phase of EAE.

The levels of A) TNF and B) IL-6 were measured in the brains of *Scn8a*$^{+/+}$ and *Scn8a*$^{dmu/+}$ mice before (*Scn8a*$^{+/+}$, n = 4 vs *Scn8a*$^{dmu/+}$, n = 4) and after EAE (day 35; *Scn8a*$^{+/+}$, n = 7 vs *Scn8a*$^{dmu/+}$, n = 8). The levels of C) IL-10, D) TGF-β1, and E) IL-13 were measured in the brains of *Scn8a*$^{+/+}$ and *Scn8a*$^{dmu/+}$ mice before EAE (*Scn8a*$^{+/+}$, n = 4-7 vs *Scn8a*$^{dmu/+}$, n = 3-7) and after EAE (day 35; *Scn8a*$^{+/+}$, n = 7 vs *Scn8a*$^{dmu/+}$, n = 7). Data are presented as the mean ± SEM of cytokine level per gram of brain tissue. **P* < 0.05, ** *P* < 0.01 ,*** *P* < 0.001, ns, not significant, unpaired *t*-test.

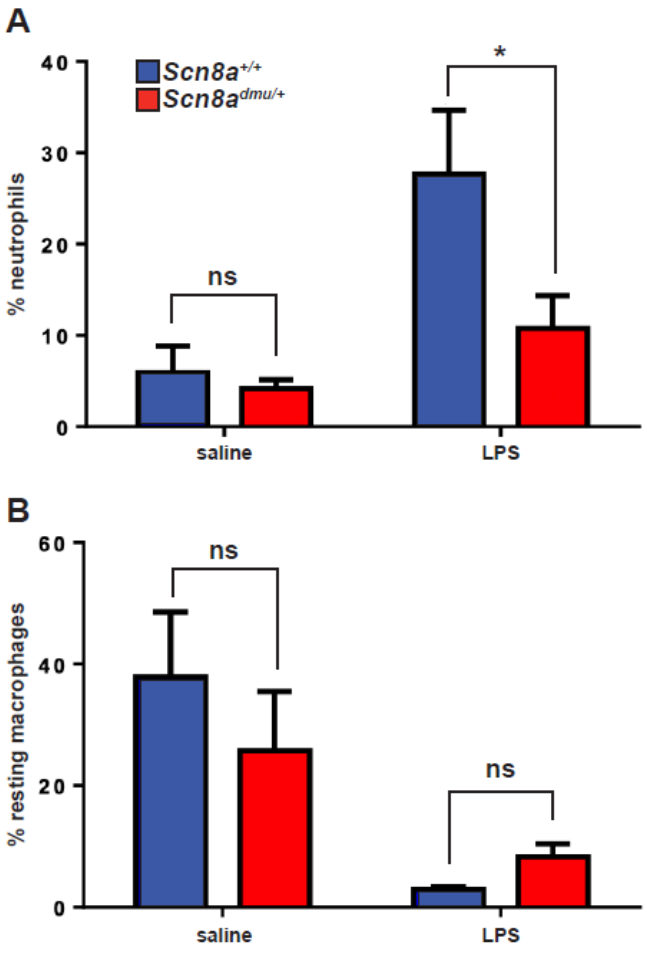
A
Scn8a+/+
Scn8admu/+
% neutrophils
40
30
20
10
0
ns
*
saline
LPS
B
% resting macrophages
60
40
20
0
ns
ns
saline
LPS

Figure 3-7 *Scn8a*$^{dmu/+}$ heterozygous mice display decreased infiltration of neutrophils in the peritoneum post-LPS stimulation.

The frequency of neutrophils (A)and resting macrophages (B) were analyzed by flow cytometry in the peritoneal lavage of WT and dmu mice before (*Scn8a*$^{+/+}$ n = 4 vs *Scn8a*$^{dmu/+}$ n = 4) and 16 hours post-LPS stimulation (*Scn8a*$^{+/+}$ n = 8 vs *Scn8a*$^{dmu/+}$ n = 8). Data are presented as the mean ± SEM. **P* < 0.05, unpaired t-test. Data represent two separate experiments combined with each experiment (B, D) consisting of cells pooled 4 mice for each group.

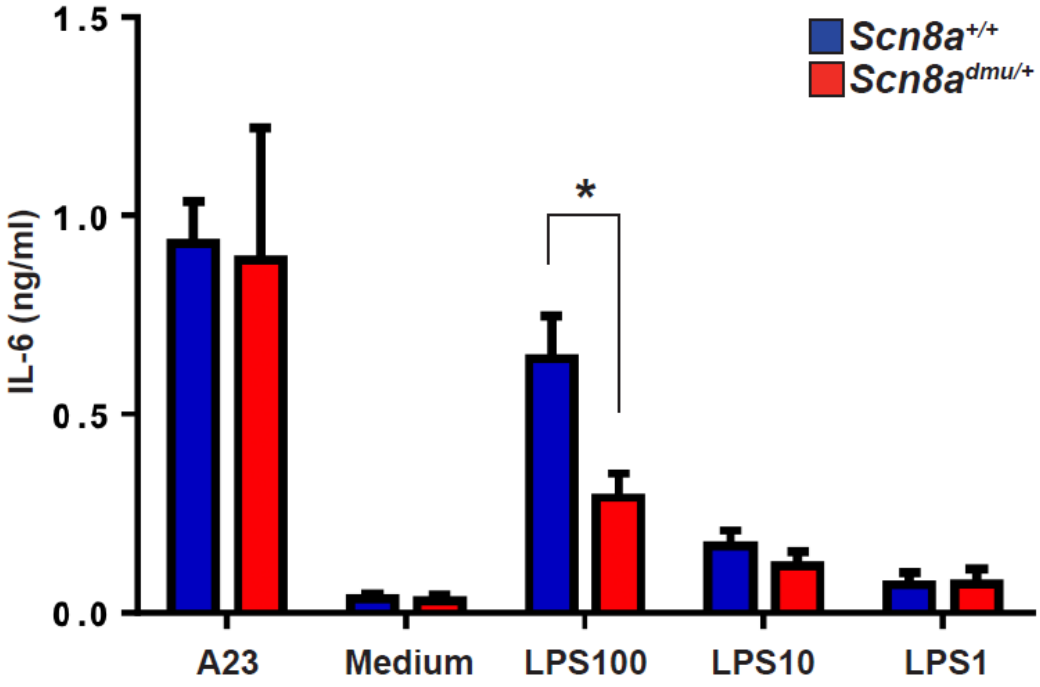
Scn8a+/+
Scn8admu/+
IL-6 (ng/ml)
1.5
1.0
0.5
0.0
*
A23
Medium
LPS100
LPS10
LPS1

Figure 3-8 Mast cells from *Scn8a*$^{dmu/+}$ heterozygous mice produce lower levels of IL-6 in response to LPS stimulation *in vitro*.

Bone marrow-derived mast cells (BMMC) were cultured and stimulated with 100, 10, 1, and 0 μg/ml of LPS or 0.5 μM calcium ionophore (A23187) in the medium for 24 hours. The concentration of IL-6 secreted by *Scn8a*$^{+/+}$ (n = 5) and *Scn8a*$^{dmu/+}$ (n = 5) BMMC was measured by ELISA. Data are presented as the mean ± SEM. **P* < 0.05, Kruskal-Wallis test. Data represent four separate experiments combined with each experiment consisting of cells pooled 4 cell cultures for each group.

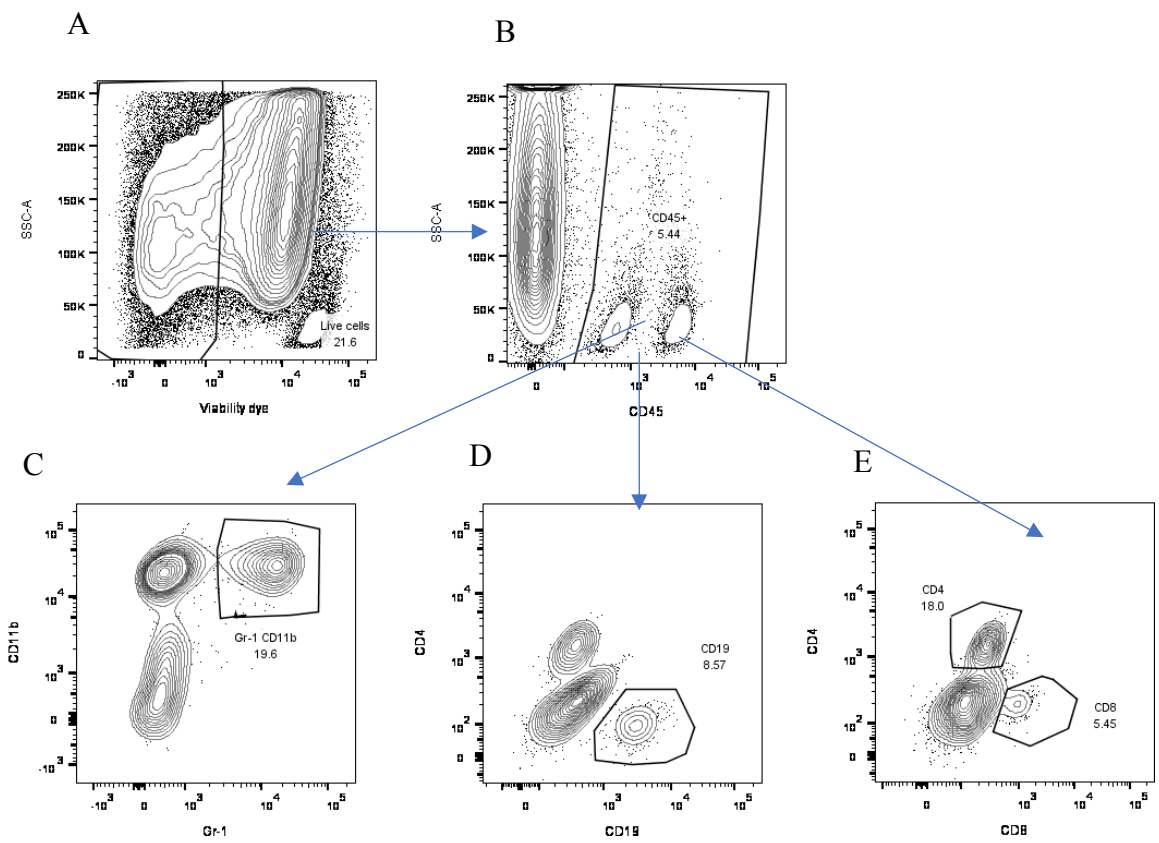
A
B
C
D
E
SSC-A
Viability dye
Live cells
21.6
CD45+
5.44
CD45
CD11b
Gr-1
Gr-1 CD11b
19.6
CD4
CD19
8.57
CD4
18.0
CD8
5.45
CD8

Figure S 3.1 Gating strategy used to identify immune cells population present in mouse blood and brain.

A) Starting from the upper left panel and going down following the arrows shows flow cytometric analysis of leukocytes isolated from a representative mouse brain 35 days post-EAE. B) Cells were examined by the side scatter (SSC) versus CD45 staining. C) Show distribution of Ly-6G^{+}-neutrophils. D) B cells subsets identified by expression CD19^{+} E) Distributions of T cells CD4^{+}and CD8^{+}.

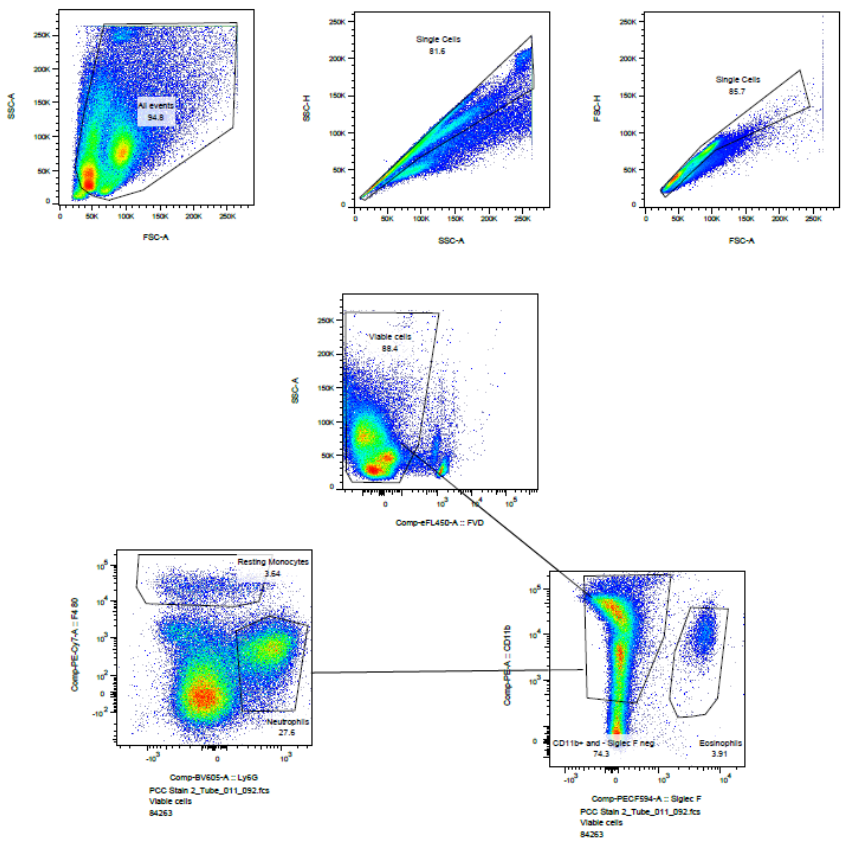
All events
54.8
SSC-A
FSC-A
Single Cells
81.6
SSC-H
SSC-A
Single Cells
85.7
FSC-H
FSC-A
Viable cells
88.4
SSC-A
Comp-eFL450-A :: FVD
Resting Monocytes
3.64
Neutrophils
27.6
Comp-PE-Cy7-A :: F4.80
Comp-BV605-A :: Ly6G
PCC Stain 2_Tube_011_092.fcs
Viable cells
84263
CD11b+ and - Siglec F neg
74.3
Eosinophils
3.91
Comp-PE-A :: CD11b
Comp-PECF594-A :: Siglec F
PCC Stain 2_Tube_011_092.fcs
Viable cells
84263

Figure S3.2 Gating strategy used to characterize the cell population in the mouse peritoneum.

Cells were harvested from the peritoneal cavity by lavage, counted, and centrifuged prior to staining with specific antibodies. Staining is shown for a saline mouse at 16 hours. After FSC /SSC scatter gating, a sequential gating strategy was used to determine populations expressing specific markers: neutrophils (CD11 b^{+} F4/80 $^{-}$ $Ly6G^{+}$), resting monocytes ($CD11b^{+}$ F4/80 ^{hi} $Ly6G^{-}$).

Chapter 4 Toll-Like Receptor 2 mediates axonal loss and inflammatory processes in the chronic phase of EAE.

This manuscript is in preparation to submit as the following:

Barakat Al Rashdi, Bassel Dawod, Ian D. Haidl, Sabine Tacke, Stefanie Kuerten, Patrice D. Côté, Jean S. Marshall

Running title:
Toll-Like Receptor 2 enhance inflammation in EAE

4.1 Abstract

Multiple sclerosis (MS) is an autoimmune, inflammatory demyelinating disease that affects the central nervous system (CNS). Although the etiology of MS remains unclear, it is well accepted that both genetic predisposition and the environment are critical factors. While the adaptive immune system has been the primary research focus in MS, the role of the innate immune system is attracting increased interest. Toll-like receptors (TLRs) are a major family of pattern recognition receptors (PRRs). TLR2 is activated by a broad range of ligands. TLR2 activation has been implicated in several diseases, including MS and experimental autoimmune encephalomyelitis (EAE)but, its exact role has been controversial and not well defined in the context of EAE. We, therefore, investigated EAE associated disease progression and inflammation in $TLR2^{-/-}$ and WT mice, focusing on the nature of the inflammatory response. EAE was induced in $TLR2^{-/-}$ and WT groups by injecting mice subcutaneously with myelin oligodendrocyte MOG_{35-55} peptide and Mycobacterium tuberculosis H37RA. PTX was injected intraperitoneally on the day of immunization and again 2 days later. Our results showed that the clinical score in $TLR2^{-/-}$ mice was significantly lower during the early chronic phase, compared to wild type mice. The frequencies of $Gr\text{-}1^{+}/CD11b^{+}$ cells in the blood, spleen, and brain were significantly lower in $TLR2^{-/-}$ mice at day 40 post- EAE induction compared to the control ($p<0.01$). $TLR2^{-/-}$ mice exhibited decreased proinflammatory cytokines, such as CXCL1, in the plasma and IL-6 ($p<0.01$) in the brain. These data demonstrate reduced inflammation and decreased disease severity, during EAE, in the absence of TLR2. Overall, these results suggest that TLR2 activation plays an important role in the pathogenesis of MS and EAE by mediating the production of proinflammatory

cytokines, which exacerbate the EAE symptoms, potentially via their impact on myeloid cellsand astroglial cells.

Keywords:

Multiple sclerosis, inflammation, experimental autoimmune encephalitis, optic neuritis, Toll-like receptors, myeloid cells, optic nerve, brain, cytokines.

Highlights

- TLR2$^{-/-}$ mice exhibited reduced recruitment of myeloid cells in the context of EAE
- TLR2$^{-/-}$ mice had significantly lower levels of plasma CXCL1 during chronic phases of EAE.
- TLR2$^{-/-}$ mice exhibit a decrease in clinical and inflammatory scores in correlation with decreased demyelination in the CNS.
- Our results suggest TLR2 signaling plays an important role in the pathogenesis of EAE and by regulating the inflammatory response during the disease.

4.2 Introduction

Multiple sclerosis (MS) is a chronic demyelinating disease that affects the central nervous system (CNS). Although the etiology of MS is still unknown, it is well accepted that genetic factors and environmental factors increase disease risk (Bettelli, 2007a; Currier and Eldridge, 1982). MS is generally thought to be triggered by an autoimmune response that attacks the healthy myelin sheath, which protects axons (Mohr, 2015). The mechanisms associated with MS and experimental autoimmune encephalomyelitis (EAE), an animal model resembling MS, are primarily attributed to the adaptive immune system (Hemmer et al., 2015). T cells, especially effector T helper cells, including Th1 and Th17, react to self-myelin resulting in demyelination of axons, which leads to axonal degeneration and irreversible neurological disabilities (Petermann and Korn, 2011). The contribution of the innate immune system in the pathogenesis of MS has recently gained greater attention from researchers in this field. The innate immune system can contribute to the disease through multiple mechanisms, including impacts on antigen-presenting cells (APC) that subsequently modulate T-cell responses (Hossain et al., 2015).

Toll-like receptors (TLRs) are a family of extracellular, intracellular, or soluble pattern recognition receptors (PRRs) that are crucial for innate immune responses. TLRs recognize several ligands, DAMPs or exogenous PAMPs including LPS, PTX, and tuberculosis toxins, and upon activation regulate different signaling pathways that lead to the maturation of DCs and differentiation of T cell subsets (Janeway and Medzhitov, 2002; Kawai and Akira, 2011; Qureshi and Medzhitov, 2003). Humans express eleven types of TLRs (TLR1 to TLR11), and mice express twelve (TLR1 to TLR 9 and TLR 11 to TLR 13) (Akira et al., 2006; Kawai and Akira, 2010). Recent studies have suggested

that TLRs have a role in MS initiation, relapse of the disease, and CNS damage (Miranda-Hernandez and Baxter, 2013). TLR2 is an extracellular receptor expressed in numerous cells including monocytes, microglia, Schwann cells, endothelial cells in CNS, neurons, dendritic cells (DC), B cells, and T cells (Aravalli et al., 2007; Bsibsi et al., 2002; Medzhitov, 2001). In MS and EAE, the expression of TLR2 has been shown to be upregulated in the CNS on oligodendrocytes and in peripheral blood monocytes (Aravalli et al., 2007; Prinz et al., 2006; Sloane et al., 2010). TLR2 has been found to suppress the maturation and remyelination of OPC, thereby provoking a deterioration of MS symptoms (Sloane et al., 2010).

TLR2 is expressed as a homodimer or heterodimer with TLR1 or TLR6 (Medzhitov, 2001). In MS patients, endogenous ligands of TLR2 have been identified in regions of the CNS, such as the spinal cord and brain (Palle and Buch, 2014; Schrijver, 2001). In this context, it is noteworthy that the ectodomain of TLR2, which can be found as a soluble protein (sTLR2) in body fluids including plasma, cerebrospinal fluid (CSF), and breast milk (LeBouder et al., 2003), has been proposed to act as a decoy receptor that can compete with TLR2 for ligands to regulate signaling (LeBouder et al., 2003).

In EAE, TLR2 interacting with endogenous ligands such as hyaluronan, and HMGB1 can enhance inflammation and exacerbate clinical symptoms. The inhibition of these ligands reduces disease severity. In both the adoptive cell transfer and active induction of EAE, TLR2 deficient mice show an attenuated progression of the disease (Miranda-Hernandez et al., 2011). The mechanism of TLR2 promotion of EAE/MS appears to be dependent on the type and dose of ligands binding to the receptor (Okun et al., 2011).

Exogenous ligands for TLR2 include bacterial peptidoglycan and Pam_3CSK_4 lipopeptide. Peptidoglycan was found to enhance the induction of EAE through binding to TLR2 (Visser et al., 2005). Conversely, low doses of zymosan, a fungal beta glycan, reduces or reverses the relapsing paralysis in EAE by enhancing the differentiation of regulatory T cells (Tregs) (Li et al., 2013a). Notably, the previous investigation of the role of TLR2 in EAE primarily evaluated inflammation in the spinal cord and peripheral organs while the role of TLR2 in optic nerve degeneration and inflammation of the brain was not fully defined.

In this study, we aimed to investigate the role of TLR2 in the initiation and development of EAE in the optic nerve and brain by using TLR2 knockout and WT mice. We hypothesized that the absence of the TLR2 receptor would reduce inflammation in the brain and mediate axonal damage in the optic nerve in the chronic phase of EAE. Our results indicate that TLR2 knockout mice displayed less inflammation and a reduction of $Gr\text{-}1^+/CD11b^+$ in the blood, spleen, and CNS combined with a decreased level of chemokines in the plasma and pro-inflammatory cytokines in the brain. These results suggest that TLR2 signaling plays an important role in the pathogenesis of EAE by regulating the production of pro and anti-inflammatory cytokines and chemokines, including CXCL1 in the plasma and IL-6, IL-13 in the brain and enhances axonal survival in the optic nerve.

4.3 Materials and methods

4.3.1 Mice

Female mice (10–12 weeks old) (n = 49), C57BL/6 Charles River Laboratory (Montreal, QC, Canada) and B6.129-Tlr2tm1Kir/J ($TLR2^{-/-}$) mice were bred from stock

obtained from the Jackson Laboratory (Bar Harbour, ME, USA) for use in this study. All animal experiments were approved by the Dalhousie University Committee on Laboratory Animals and conducted according to the guidelines from the Canadian Council for Animal Care.

4.3.2 Animal models and experimental design

Three major treatment groups of mice were analyzed: An EAE group, an EAE-control group, and a TLR2 ligand treatment group. EAE was induced as previously described by (Alrashdi et al., 2019). Briefly, It was induced in $TLR2^{-/-}$ and WT mice by subcutaneously injecting 200 µl of MOG_{35-55} combined with CFA (2 mg/ml) (kit EK-2110, Hooke Laboratories, Lawrence, MA)(Svensson et al., 2002). The mice were also injected intraperitoneally with PTX (200 ng/mouse) on the day of the initial immunization and two days later. For the EAE control group, $TLR2^{-/-}$ and WT mice used as antigen controls received CFA plus PTX but not MOG_{35-55}. The third group of mice was also EAE treated to induce stimulated with the TLR2 ligand, Pam_3CSK_4 (20 µg, i.p.) on days -1, 1, 3 and 5 of EAE induction, similar to what has been used by Chen et al. (Chen et al., 2009). EAE mice were monitored daily for symptoms of EAE and changes in body weight beyond day 40.

4.3.3 Blood collection and tissue sampling

On days 0, 6, 13, and 21, facial vein puncture was performed to collect the blood sample's final heparin concentration. Heart puncture was performed at the endpoint of the study 40 days post-EAE (Fig 4.1). Plasma was collected from each animal for chemokine and cytokines measurements. Flow cytometry was used to analyze blood, optic nerve,

and brain samples to identify subtypes of cells, including myeloid cells, T lymphocytes ($CD4^+$ and $CD8^+$), and B lymphocytes ($CD19^+$).

4.3.4 Extracellular staining and flow cytometry

Peripheral blood plus 20 µL of heparin as anti-coagulant was collected at day 40 post-EAE. Furthermore, spleen and brain tissue were harvested at the chronic phase of EAE. The peripheral blood mononuclear cells were isolated using Ficoll. Red blood cells were lysed using ACK buffer (0.15 M ammonium chloride (cat. #A4514, Sigma Aldrich), 0.01 M potassium bicarbonate (cat. #P7682, Sigma Aldrich), 0.07 mM EDTA (cat. #15575, Invitrogen) for 10 minutes at room temperature. Cells from spleen and brain tissues were disassociated through 70µm wire mesh and followed by addition of an equal volume of 2X enzymatic digestion mix to a final concentration of 10 µg/ml (collagenase D and 100 µg/ml DNase I, Roche Diagnostics, Mannheim, Germany), before incubation in a water bath at 37°C to degrade the tissue and prepare a single-cell suspension. Cells were then centrifuged at 400 x g for 5 minutes at 4°C, resuspended in 0.5 ml of ACK, and placed on ice for 5 minutes to lyse red blood cells. Cells were washed, counted, then centrifuged at 400 x g for 10 minutes at 4°C and resuspended in a 1/1000 of fixable viability dye (FVD) eFluor450 (eBioscience, San Diego, CA) in PBS for 30 minutes. The cells were washed with IMF and brain tissue was stained with specific monoclonal antibodies (mAbs) to label various immune cells such as macrophages ($F4/80^+/CD11b^+$), granulocytes (Gr-1+/$CD11b^+$), T lymphocytes ($CD4^+$, $CD8^+$) and B cells ($CD19^+$). After incubation, cells were washed with flow cytometry wash buffer (PBS supplemented with 2% FBS), centrifuged again, fixed in 1% paraformaldehyde (PFA) in PBS and kept at 4°C.

Compensation controls were prepared using compensation beads (Invitrogen, Carlsbad, CA) mixed with individual dilutions of each antibody used as above in IMF. All beads and cells for compensation were incubated with dye or antibody cocktail for 30 minutes on ice and then washed with IMF, centrifuged, and fixed in 1% PFA. The unstained controls were not incubated with FVD. Stained samples were acquired within 24 hours using a BD FACS Canto™ II cytometer (BD Biosciences, San Jose, CA). All analysis and gating were done using BD FACS Diva software and FlowJo V10.2(Ashland, OR) software.

4.3.5 ELISA

ELISA was used to detect levels of the chemokine CXCL1 and cytokines, including IL-6 and IL-10 in the plasma and TNF, IL-10, IL-6, IL-13, and TGF-β1 in the brain. We extracted the protein from the brain tissue of EAE mice by homogenizing the samples, using a Qiagen Tissue Ruptor device, in RIPA buffer with EDTA-free protease inhibitor tablets from (Sigma) for 1 minute on ice. Samples were centrifuged at 10,000 x g for 10 min, supernatants were collected, and total protein was measured using a Bradford protein assay (Bio-Rad, Mississauga). Levels of cytokines were normalized to total protein concentration. ELISA was performed according to the manufacturer's instructions. Briefly, 2.5 μg/ml of capture antibody (CXCL1, IL-6, TNF, IL-10, IL-13, and TGF-β1) (eBioscience) diluted in borate buffer (pH 8.2) was used to coat each ELISA plate. Blocking buffer (2% BSA in PBS) was added to the plates before the addition of samples. After incubation overnight at 4°C, biotinylated secondary antibodies and Streptavidin-horseradish peroxidase were added. TMB solution (eBioecience) was added to the plate and incubated for 10–15 min before the reaction was stopped using 2N

H_2SO_4 and the plate measured using an Epoch microplate spectrophotometer (Biotek, VT).

4.3.6 Luminex multiplex assay

Luminex analyses were performed on the plasma and brain tissue according to the manufacturer's instructions. Brain and plasma samples were centrifuged at 16000 x g for 5 minutes, diluted 2-fold in Calibrator Diluent RD6-52 and then analyzed by using Multi-Analyte Mouse Magnetic Luminex Assay (R&D system, Minneapolis, MN, USA) and Bio-Rad Bio-Plex analyzer. The instrument sets were used: 50µL sample volume, Bio-Plex MagPlex Beads (Magnetic) bead type, and doublet discriminator gates set between 8000 and 23000. The assay used detected the cytokines TNF, IL-10, IL-6, IL-13, and TGFβ-1 and chemokines CXCL1 and CCL2.

4.3.7 Quantitative reverse-transcription polymerase chain reaction (qRT-PCR)

Brain tissue was collected from TLR2 knockout mice and wildtype mice and submerged in RNA later (Qiagen, Hilden, Germany). 700 µL of a phenol/guanidine based QIAzol Lysis Reagent was added to samples (Qiagen, Maryland). Next, tissues were homogenized using a Qiagen Tissue Ruptor device and incubated for 5 minutes at room temperature. 140 µL of chloroform was added to the homogenate, shaken vigorously and centrifuged at 10000 x g for 15 minutes at 4°C. The upper aqueous layer was extracted, an equal volume of RNase-free 70% ethanol was added, and centrifugation at 7500 x g for 15 seconds occurred at room temperature on an RNase Mini spin column using Qiagen kits. RNA was isolated according to the manufacturer's protocol. RNA concentrations were measured using an Epoch spectrophotometer, and Take3™ Micro-Volume Plate (Biotek), and analysis was performed using Gen 5 software. The ratio of

A260/280 was used to identify the purity of RNA samples, and 1.8-2.2 was considered good quality RNA. The RNA integrity was determined, RNA samples were reverse transcribed to cDNA using a QuantiTect® Reverse Transcription Kit (Qiagen). The resulting cDNA samples were diluted 1:4, and qPCR was performed to measure the expression of mRNAs for implicated in the inflammatory response, including *Il1b* and *IL-10* in the chronic phase of EAE (Table 5). The relative mRNA expression of the genes of interest was normalized to the geometric mean of the reference genes *Gusb* and *Hprt* Cq value expressed as $2^{-\Delta Cq}$ where the Δ Cq= Cq gene of interest – Cq references genes.

Table 5 qPCR primers:

Gene	Primer sequence or company (catalog number)
Hprt	Bio-Rad (Cat no. 10025636)
TBP	Bio-Rad (Cat no. 10025637)
Ilb	Qiagen (Cat no. PPM03015A)
Il10	Qiagen (Cat no. PPM03015A)

4.3.8 Electron microscopy

Optic nerve tissues were collected from both groups of C57BL/6 and TLR2-/- mice that were sacrificed in the chronic phase, 40 days after induction of EAE. Tissues were then processed according to the process outlined by Kuerten et al., (2011). Glutaraldehyde 2.5% in 0.1M sodium cacodylate buffer was used for the fixation of tissues overnight. Tissues were then rinsed with 0.1M sodium cacodylate buffer, fixed for 2 hrs with 1% osmium tetroxide, and then quickly rinsed with distilled water. Samples were then placed in 0.25% uranyl acetate at 4oC, dehydrated in graded acetone solutions, embedded with Epon Araldite resin and placed in a 60°C oven for 48 hours to harden. An ultra-microtome (Reichert Ultracut R, Leica, Germany) was used to transversally section

samples to a thickness of 50 nm. A digital EM camera (MegaView III, Olympus Soft Imaging Systems GmbH, Münster, Germany) was used to take images. To demonstrate the axonal loss and myelin pathology, we used a g-ratio that was determined by dividing the axon diameter by the diameter of the myelinated nerve fiber (Guy et al., 1991; Kuerten et al., 2007). Only axonal g-ratios three standard deviations above (remyelinating) or below (demyelinating) the average of the non-EAE reference group were counted. Axonal damage, including axolytic axons and neurofilament pathology, was determined qualitatively. The analysis was conducted by an individual that was blind to the nature of the samples.

4.3.9 Statistical analysis

All statistical analyses were performed by two-way ANOVA with multiple comparison tests with Tukey's post hoc test and unpaired Student's *t*-tests, as indicated in the legend of the figure. Error bars represent the standard error of the mean (SEM). GraphPad Prism software was used for statistical analyses (Ver. 5.0, GraphPad Software, La Jolla, CA).

4.4 Results

To address the impact of TLR2 deficiency on the immunological mechanisms involved in the course of EAE, with a focus on the chronic phase, we induced monophasic chronic EAE in both C57BL/6 and TLR2$^{-/-}$ mice by immunization with the MOG_{35-55}, followed by intraperitoneal (i.p.) injection with PTX along with CFA (Figure 4.1A). As such, four experiments comparing WT and TLR2$^{-/-}$ were conducted to determine the role of TLR2 in chronic EAE including, untreated control, MOG_{35-55}-immunized (+EAE), adjuvant control without MOG_{35-55} (+CFA+PTX), and TLR2

activator Pam_3CSK_4 with EAE (+EAE+Pam3). The clinical symptoms appeared nine days post-immunization in all EAE mice (Fig. 4.1B). However, $TLR2^{-/-}$+EAE mice exhibited a significant improvement in clinical signs during the chronic phase between 28-37 days post-EAE immunization compared to WT+EAE (Fig. 4.1B). The +CFA+PTX mice ($TLR2^{-/-}$ and WT) showed no clinical signs of disease for the duration of the experiment. Finally, the clinical signs of all WT+EAE+Pam3-treated mice were not significantly different from those of WT+EAE (Figure 4.1B).

We assessed the inflammatory status and immune profile of our EAE-treated groups by examining the circulating immune cells in the peripheral blood of chronic phase EAE (day 40). The frequency but, not the absolute cell number of $Gr\text{-}1^{high}$ /$CD11b^+$ cells in $TLR2^{-/-}$+EAE mice was significantly lower ($P = 0.0259$) and only reached 59% of that seen in WT+EAE mice (10.60 ± 2.341, $n = 8$ vs 21.31 ± 1.784 %, $n = 8$; Fig. 4. 2A). Our results showed that the activation of TLR2 in WT+EAE+Pam3 significantly increased the total cell number but not the frequency of $Gr\text{-}1^{high}$ /$CD11b^+$ cells in the blood compared to WT+EAE ($P = 0.0012$; 709410 ± 72236, $n = 4$ vs 280650 ± 49752, $n = 8$; Fig 4.2A). Whereas, $TLR2^{-/-}$+EAE+Pam3 mice showed no significant difference compared to $TLR2^{-/-}$+EAE either in the frequency or the absolute number of circulating $Gr\text{-}1^{high}$ /$CD11b^+$ cells. In contrast, no significant differences in the frequency or the total number of $CD4^+$ and $CD8^+$ cells were observed in any of the conditions (Fig. 4. 2B and C). The frequency of $CD19^+$ B cells was significantly higher ($P = 0.0148$) in $TLR2^{-/-}$ +EAE vs WT+EAE (49.54 ± 4.161, $n = 8$ vs 35.69 ± 4.225%, $n = 8$; Fig 4.2D) but the absolute number of cells was not significantly different. In addition, $TLR2^{-/-}$ mice activated with Pam_3CSK_4 showed significantly lower the absolute number but, not

frequencies of Gr-1^{high}/CD11b^{+} compared to TLR2 stimulation by Pam_3CSK_4 in WT mice (P = 0.0136; 709410 ± 72236 , n = 4 vs 328156 ± 35565, n = 4; Fig 4.2A). Finally, a comparison between control groups WT+CFA+PTX and TLR2$^{-/-}$+CFA+PTX showed no significant differences in the frequencies of immune cells Gr-1^{high}/CD11b^{+}, CD4^{+}, CD8^{+}, and CD19^{+}.

To investigate whether TLR2 expression modulates the inflammatory response systemically, we measured the level of pro-inflammatory cytokine IL-6, the anti-inflammatory cytokine IL-10, and the chemokine CXCL1, a chemoattractant of neutrophils (Ahuja and Murphy, 1996), in the plasma of mice (Fig. 4.3). Following EAE induction, IL-6 in TLR2$^{-/-}$ was reduced to half of WT levels, although this difference was not significant. In Pam3-treated +EAE mice, the levels of IL-6 in WT+EAE+Pam3 were 2.5 fold higher than in WT+EAE (P = 0.0010; 222.4 ± 34.39, n =5 vs 554.3 ± 56.40 pg/ml, n = 4), while TLR2$^{-/-}$+EAE+Pam3 did not show a significant increase vs TLR2$^{-/-}$ +EAE. Furthermore, the levels IL-6 in WT+EAE+Pam3 were significantly higher than in TLR2$^{-/-}$+EAE+ Pam3 (P = 0.0001; Fig. 4.3A). Comparisons of levels of IL-10 did not reveal significant differences between WT+EAE and TLR2$^{-/-}$+EAE in all conditions (Fig. 4.3B). Levels of CXCL1 were significantly lower in TLR2$^{-/-}$+EAE vs WT+EAE (P = 0.0152; 121.6 ± 33.82, n = 4 vs 244.4 ± 9.655 pg/mL, n = 4). The proinflammatory cytokines TNF, IL-1β, IL-17, and GM-CSF along with the anti-inflammatory cytokines IL-13 and IL- 4 were below the limit of detection for WT and TLR2$^{-/-}$ in all conditions (not shown).

In spleen, similarly, to circulating levels in the blood, the infiltration of Gr-1^{+}/CD11b^{+}, CD4+, and CD19^{+} cells were increased in both WT+EAE and TLR2$^{-/-}$+EAE.

The frequency, but not the absolute number of Gr-1^{high} /CD11b^{+} cells, was significantly lower in TLR2$^{-/-}$+EAE vs WT+EAE mice (P = 0.0016; 8.16 ± 1.753, n = 8 vs 16.28 ± 1.367 %, n = 8). However, the comparison between WT+EAE+Pam3 and TLR2$^{-/-}$ +EAE+Pam3 mice showed significantly lower frequencies and total cells number of Gr-1^{high} /CD11b^{+} cells in TLR2$^{-/-}$+EAE+Pam3 mice compared to WT+EAE+Pam3 (P = 0.0131; 2.323 ± 0.4935, n = 4 vs 11.83 ± 3.101 %, n = 4; Fig 4.4A). CD4^{+} cells were significantly higher in frequency, but not absolute number, in WT+EAE+Pam3 compared to WT+EAE mice (P = 0.0487; 15.65 ± 1.854 , n = 4 vs 6.541 ± 0.6836 % , n = 8) and there was a significant increase in TLR2$^{-/-}$+EAE+Pam3 vs TLR2$^{-/-}$+EAE (P = 0.0025; 19.75 ± 5.320, n = 4 vs 7.344 ± 1.086 % , n = 8; Fig 4.4B). CD8^{+} did not show significant differences in all conditions (Fig. 4.4C and D). In addition, CD19^{+} cell frequency but, not the absolute number, were significantly elevated in TLR2$^{-/-}$+EAE compared to WT+EAE (P = 0.0018; 59.16 ± 2.982, n = 8 vs 39.66 ± 4.865%, n = 8; Fig 4.4D).

Based on our results revealing improved clinical scores of TLR2$^{-/-}$ vs WT during the chronic phase and consistent observations of reduced circulating Gr-1^{high}/CD11b^{+} in the blood and infiltration of the spleen along with decreases of CXCL1 levels in the plasma, we sought to investigate the effect of the absence of TLR2 on the CNS. The infiltration of Gr-1^{+}/CD11b^{+} cells was significantly lower in the brains of TLR2$^{-/-}$+EAE vs WT+EAE (P = 0.0373; 2.648 ± 0.7137, n = 8 vs 6.513 ± 1.474%, n = 8; and Fig. 4.5A). Comparisons of CD4^{+} (Fig. 4.5B), CD8^{+} (Fig. 4.5C) and CD19^{+} (Fig. 4.5D) cell frequency did not reveal significant differences between WT and TLR2$^{-/-}$ in all conditions. Moreover, Pam3 did not significantly impact the infiltration of Gr-

1^+/CD11b$^+$, CD4$^+$ T cells, CD8 $^+$ T cells, and CD19$^+$ B cells in the brains of WT+EAE or TLR2$^{-/-}$ +EAE mice (Fig. 4.5 A-D).

To evaluate the role of TLR2 in inflammation in EAE brains, we performed real-time PCR analysis for the IL-1β pro-inflammatory cytokine transcript (*Il1b*) and the IL-10 anti-inflammatory cytokine transcript (*Il10*). *Il1b* expression was found to be significantly lower in TLR2$^{-/-}$+EAE mice during the chronic phase of EAE in comparison to WT+EAE (P = 0.0334; 0.7734 ± 0.1057, n = 3 vs 1.316 ± 0.04371, n = 3; Fig. 4.6A) and, conversely, the expression of *Il10* was found to be significantly higher in TLR2$^{-/-}$ +EAE mice in comparison to WT+EAE (P = 0.0144; 2.303 ± 0.1749, n = 3 vs 1.081 ± 0.2715, n = 3; Fig. 4.6B). No significant difference was found for the expression of *Il1b* and *Il10* between +EAE and +EAE+Pam3 for both WT and TLR2$^{-/-}$ (not shown).

To complement our investigation of inflammation in the brain, we measured the pro-inflammatory cytokines IL-6 and TNF at the protein level in untreated mice and chronic phase TLR2$^{-/-}$+EAE, and WT+EAE mice and found IL-6 to be significantly decreased in TLR2$^{-/-}$+EAE mice relative to WT+EAE (P = 0.0001; 123.5 ± 3.247, n = 4 vs 209.2 ± 6.373 pg/mL, n = 5; Fig. 4.7A), while the TNF did not show the difference between groups (Fig. 4.7B). The levels of the anti-inflammatory cytokines IL-13, IL-10, and TGF-β1, were also examined in the brains of untreated and chronic-phase EAE mice. IL-13 was dramatically and significantly increased 60-fold in TLR2$^{-/-}$+EAE vs WT+EAE (P 0.0059; 33.17 ± 10.25, n = 4 vs 0.5175 ± 0.1871 pg/mL, n = 4; Fig. 4.7C). The observed difference level of IL-10 (Fig. 4.7D) and TGF-β1 (Fig. 4.7E) in TLR2$^{-/-}$+EAE vs WT+EAE did not reach significance in both groups.

To determine the impact of TLR2 on the axonal degeneration we analyzed the optic nerve, a well characterized component of the CNS frequently used to assess axonal and myelin pathology post-EAE. In comparison, the axon density in TLR2$^{-/-}$+EAE optic nerves was visibly increased and pathological features were less common compared to WT+EAE (Fig. 4.8).

The ultrastructure of transversally sectioned optic nerves was assessed for axonal demyelination and degeneration by using the g-ratio. Based on the g-ratio, we found that the level of demyelination was significantly lower in TLR2$^{-/-}$+EAE vs WT+EAE (P = 0.0398; 0.6223 ± 0.2857, n = 4 vs 2.031 ± 0.4561, n = 4; Fig 4.9AB). Demyelinated fibers, visually identified based on the presence of an intact axon but devoid of myelin, showed no significant difference was found in both groups (Fig. 4.9C). Visual assessment of sections revealed the presence of axolytic (degenerated) fibers in WT while none were detected in TLR2$^{-/-}$ mice (P = 0.0149; 1.397 ± 0.4133, n = 4 vs 0.0 ± 0.0, n = 4; Fig 4. 9D).

4.5 Discussion

The pathogenesis of MS and EAE is characterized by complex interactions between the nervous system and the immune system. Axonal loss and persistent inflammation caused by the infiltration of immune cells into the CNS are hallmarks of MS and EAE (Amor et al., 2014a; Bjartmar et al., 2003). The activation of TLRs by its ligands enables immune cells to produce pro-inflammatory cytokines and enhance the function of APCs that have the capacity to promote T-cell activity to recognize antigens (Akira and Takeda, 2004).

It has been reported that TLR2 activation hinders remyelination (Esser et al., 2018), possibly through the blockade of oligodendrocyte progenitor maturation by the interaction of hyaluronan and TLR2 (Sloane et al., 2010). Following the initial acute-remission phase of EAE, the symptoms have been found to be milder in TLR2-deficient mice than WT controls, which highlights a potential role for TLR2 in the progression of EAE (Marta, 2009; Miranda-Hernandez et al., 2011). The disease progression, at least in early stages, may involve endogenous TLR2 ligands produced during initial tissue damage. Consistent with the findings of Miranda-Hernandez et al. (2011) who found a reduction of the clinical score in TLR2 knockout mice from day 16 until day 40 post-EAE, and we found that TLR2 deficient mice presented with a lower clinical score of EAE compared to WT mice in the chronic phase.

The literature on the role of TLR2 in the inflammatory process of EAE has been inconsistent (Kremer et al., 2011). Prinz et al. (2006) did not find any difference between TLR2 knockout and WT mice in EAE. Prinz et al. (2006) used MOG_{35-55} peptide in female strain mice. Miranda-Hernandez et al. used MOG_{35-55} peptide and female mice, similar to our study. Our results are more consistent with Miranda-Hernandez and Baxter (2013), who found a reduction of clinical score in TLR2 knockout mice starting on day 16 until day 40 post-EAEand we observed the reduction during the chronic phase of EAE. The EAE induction protocol, animal age, strain and sex, and microbiome differences between facilities could contribute to these differences.

It is noteworthy that for inducing EAE, we used complete Freund's adjuvant (CFA), which includes killed Mycobacterium tuberculosis, a ligand for TLR2, TLR4, and TLR9 (Lim, 2003; Means et al., 1999).CFA is able to disrupt blood-brain barriers and

enhance the production of inflammatory cytokines in circumventricular organs through microglia in the CNS (Reiber et al., 1984). However, the use of CFA+PTX alone in our study without MOG35-55 as control has not changed the clinical score and infiltration of immune cells in the CNS and periphery. Our observation that TLR2- deficient mice had improved motor function during the early chronic phase of the disease may be attributed to the reduced circulation and infiltration of myeloid cells in the periphery and CNS. Miranda-Hernandez and Baxter (2013) have reported that TLR2-deficient mice that were injected with leukocytes transferred from EAE-induced C57BL/6 attenuated the disease compared to WT that were injected with leukocytes transferred from EAE-induced C57BL/6, similar to active of EAE in the deficiency TLR2 and WT. These results confirm the involvement of TLR2 in the development of EAE.

Neutrophils represent a high percentage of leukocytes in the CNS and are key mediators of the inflammatory process (Rumble et al., 2015). There are two subpopulations of $CD11b^{+}Gr\text{-}1^{+}$ cells in mice, $Gr\text{-}1^{high}$ and $Gr\text{-}1^{int}$, which have been shown to have pro- and anti-inflammatory roles, respectively, in several disease models including cancer, mycobacterial infections, and EAE (Pastor et al., 2009). In EAE, neutrophils have been found to be elevated in the blood plasma and CNS (Naegele et al., 2012; Rumble et al., 2015) and have been implicated in the development and progression of the disease, but their exact role remains unclear. Neutrophils ($Gr\text{-}1^{high}/CD11b^{+}$) cells increase in mice during inflammatory responses (Pastor et al., 2009) and could be used to monitor the development of immune-mediated diseases, including EAE (Yi et al., 2012). Our data showed that circulating myeloid cells, including $Gr\text{-}1^{high}/CD11b^{+}$, were increased in the peripheral blood, spleen, and brain during the chronic phase of EAE,

which is in agreement with Yi et al. (2012) who found an increase of Gr-1^{high}/CD11b^{+} in chronic EAE. Furthermore, we activated TLR2 in WT+EAE by its ligand Pam3 to confirm its role in disease progression and found an increase in the absolute number but not the frequency of circulating Gr-1^{high}/CD11b^{+} cells in the blood along with high infiltration of the frequency and the total cell number in the spleen compared to un-activated WT+EAE mice. However, we did not observe a significant difference in the infiltration of Gr-1^{high}/CD11b^{+} cells into the CNS, suggesting that the Pam3 did not cross the blood-brain barrier (BBB). Activation of TLR2 by exogenous ligands is not sufficient to trigger the antigen-specific T cells that contribute to CNS damage. It has been reported that both endogenous and exogenous ligands are necessary for the activation of TLR2 to trigger the inflammatory response (Reynolds et al., 2010). Moreover, the activation of TLR2 in the CNS is implicated in the innate inflammatory response, but it does not affect the adaptive immune response or the course of EAE (Luz et al., 2015).

CD19^{+} B cells modulate the production of several cytokines such as TNF, IFN-γ, IL-12p40, IL-10, and IL-6 under normal conditions. It has been shown that CD19 has multiple roles in the development of EAE (Matsushita et al., 2006). Mice lacking the CD19 cell surface marker (CD19$^{-/-}$ mice) exhibit a more severe disease state compared to WT mice indicating the role of CD19 in reducing disease severity (Bouaziz et al., 2008; Musette and Bouaziz, 2018). This can perhaps be explained by CD19^{+} B cells having a role in the recovery phase of EAE by producing IL-10, which is required to suppress the inflammatory response (Bouaziz et al., 2008; Kalampokis et al., 2013; Yang et al., 2013b). In EAE, CD19^{+} B cells regulate the balance of pro- and anti-inflammatory cytokines produced by Th1 and Th2 (Matsushita et al., 2006). Our findings indicate that

higher levels of $CD19^+$ B cells in the periphery and CNS could play a regulatory role by reducing inflammation in TLR2 knockout mice.

It has been reported that levels of CXCL1, a major neutrophil chemoattractant, are elevated in the CNS of EAE mice (Grist et al., 2018; Rumble et al., 2015). In the plasma of $TLR2^{-/-}$ mice, we found that levels of the chemokine CXCL1 were significantly reduced along with slight reductions of IL-6 during the chronic phase of EAE. Our results are consistent with findings from (Reynolds et al., 2010) that show a decrease of $CD4^+$ T cell in EAE mice, specifically Th17, infiltration into the CNS, and also show a decrease in IL-6 production, which most likely contributes to the attenuated disease severity in TLR2 knockout mice. Inhibition of CXCL1 reduces the accumulation of myeloid cells in the blood leading to subsequent amelioration of disease severity in EAE (Fischer et al., 2000; Grist et al., 2018). CXCR2, a chemokine receptor for CXCL1 and a major neutrophil chemokine receptor, promotes the migration of neutrophils to injured areas of the CNS in EAE (Kerstetter et al., 2009; Zhou et al., 2003) and CXCR2 knockout mice injected with MOG_{35-55} display a reduction in the development and severity of EAE (Zhou et al., 2003). This suggests that the improvement of clinical symptoms in $TLR2^{-/-}$ mice during the chronic phase of EAE could be attributed to a decrease in inflammatory status due to a decrease in circulating $Gr\text{-}1^{high}/CD11b^+$ neutrophils and in IL-6 levels, with increased levels of $CD19^+$ B cells. Finally, our inability to detect TNF, IL-1β, IL-17, GM-CSF, IL-13 and IL-4 cytokines in plasma during EAE is consistent with the findings from (Miranda-Hernandez et al., 2011).

By examining anti-inflammatory cytokines, we observed that the level of IL-13 was significantly elevated in the brain of $TLR2^{-/-}$+EAE mice compared to WT+EAE

mice. The Th2 subset of T cells produce cytokines such as IL-4, and IL-13 (Kasper and Shoemaker, 2010; Mosmann and Sad, 1996), which can ameliorate EAE by inhibiting Th1-like responses through reducing IFN-γ, TNF and IL-12 levels (Bitan et al., 2010). Therefore, the strong expression of IL-13 in the CNS could have a potential protective effect in reducing inflammation in the chronic phase of EAE in $TLR2^{-/-}$ mice.

Myelin is essential for the function and molecular organization of axons allowing the propagation of action potentials at high speed with reduced energy consumption (Saab et al., 2013). Disruption in the myelin sheath is believed to eventually lead to axonal loss (Bjartmar et al., 2003); however, axonal degeneration in the EAE model has been observed to occur before the inflammatory and demyelination processes suggesting that the process is more complex. Indeed, it has been suggested that axonal damage in the optic nerve during the acute phase of EAE occurs via retrograde degeneration, which leads to retinal ganglion cells (RGC) loss following disease progression and glial cell damage (Hein et al., 2012). The extent of demyelination and axonal loss in the optic nerve was found to be lower in TLR2 knockout mice compared to WT. This strongly suggests that TLR2 enhances the immune and glial response in EAE, a process dependent on inflammatory cytokine release via the MAPK and NF-κB pathways. The TLR2-dependent immune response may, therefore, interfere with the maturation and remyelination of oligodendrocyte precursor cells in EAE, thereby provoking a deterioration of symptoms (Sloane et al., 2010).

In conclusion, in this study, we provide evidence indicating that signaling via TLR2 plays a major role in the progression of the EAE clinical course. $TLR2^{-/-}$ mice with EAE had significantly improved motor behavior with reduced demyelination and axonal

damage in the optic nerve. Our results suggest that reduced symptoms in TLR2$^{-/-}$ mice could involve the reduction of inflammation and activation of myeloid cells with elevated levels of CD19^{+} cells through the modulation of pro-inflammatory cytokines in the periphery and brain. Furthermore, we provide evidence that the activation of TLR2 in the periphery enhances disease progression, but we were unable to confirm any exacerbation of disease severity through exogenous Pam3 activation of TLR2.

Further research should focus on identifying the mechanism of CNS damage through TLR2 signaling via endogenous or exogenous ligands.

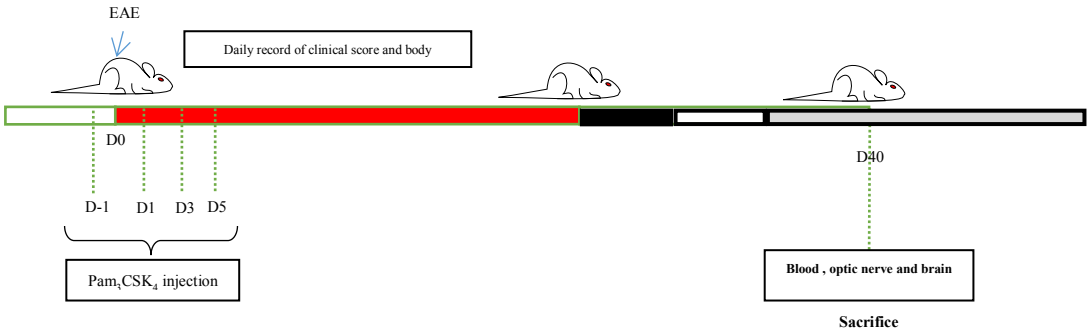
EAE
Daily record of clinical score and body
D0
D-1
D1
D3
D5
D40
Pam3CSK4 injection
Blood , optic nerve and brain
Sacrifice

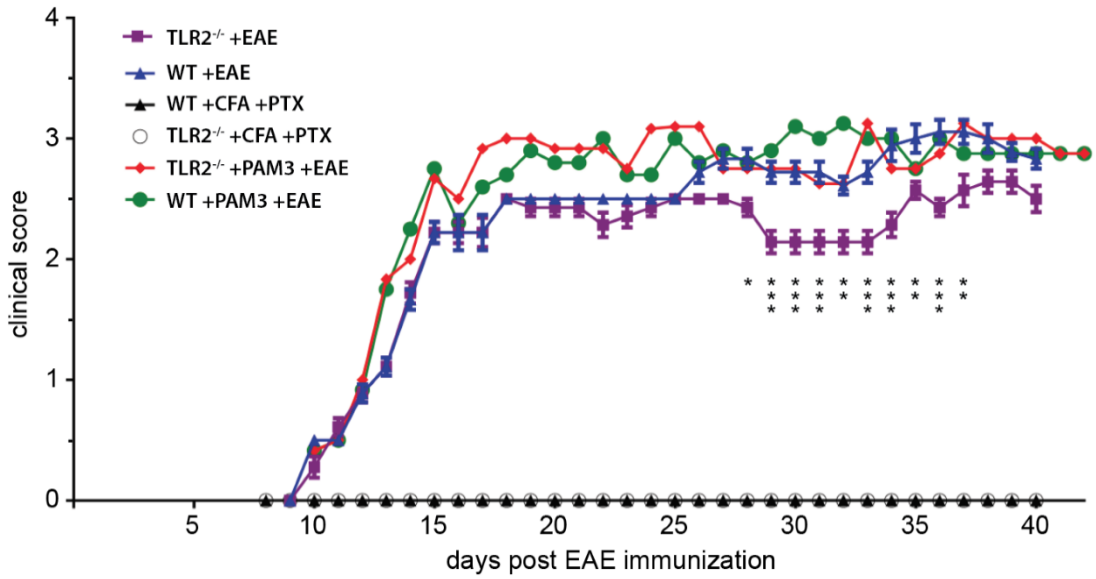
TLR2-/- +EAE
WT +EAE
WT +CFA +PTX
TLR2-/- +CFA +PTX
TLR2-/- +PAM3 +EAE
WT +PAM3 +EAE
clinical score
days post EAE immunization
0
1
2
3
4
5
10
15
20
25
30
35
40

Figure 4-1 TLR2$^{-/-}$ mice have improved motor function during the early chronic phase.

(A) Schematic diagram of the experimental design to evaluate the role of TLR2 in EAE. Two strains of mice, WT and TLR2$^{-/-}$ were used in this study. EAE was induced at day 0 in WT and TLR2$^{-/-}$ mice by immunization with MOG_{35-55}/CFA, followed by PTX and injected at day 2 with PTX only. Mice were sacrificed 40 day post-EAE induction. The clinical score of mice in both WT and TLR2$^{-/-}$ mice was recorded daily, starting at day 8 post-EAE induction. Control mice received only CFA and PTX. PAM_3CSK_4 was injected as indicated (20 µg /injection). Blood samples were collected at days 6, 13, 21, and 40. On the day of sacrifice, optic nerves and brains were collected. (B) The clinical score post-EAE induction of WT (n =10) and TLR2$^{-/-}$ (n =10),WT+CFA+PTX (n=3), TLR2$^{-/-}$ +CFA+PTX (n =3), WT+ PAM_3CSK_4 (n = 5) and TLR2$^{-/-}$+ PAM_3CSK_4 (n =5) . Two-way ANOVA was used to compare the statistical differences among groups, with the Šídák post hoc test and the lines represent mean ± SEM. * P< 0.05, ** $P < 0.01$,*** $P < 0.001$.

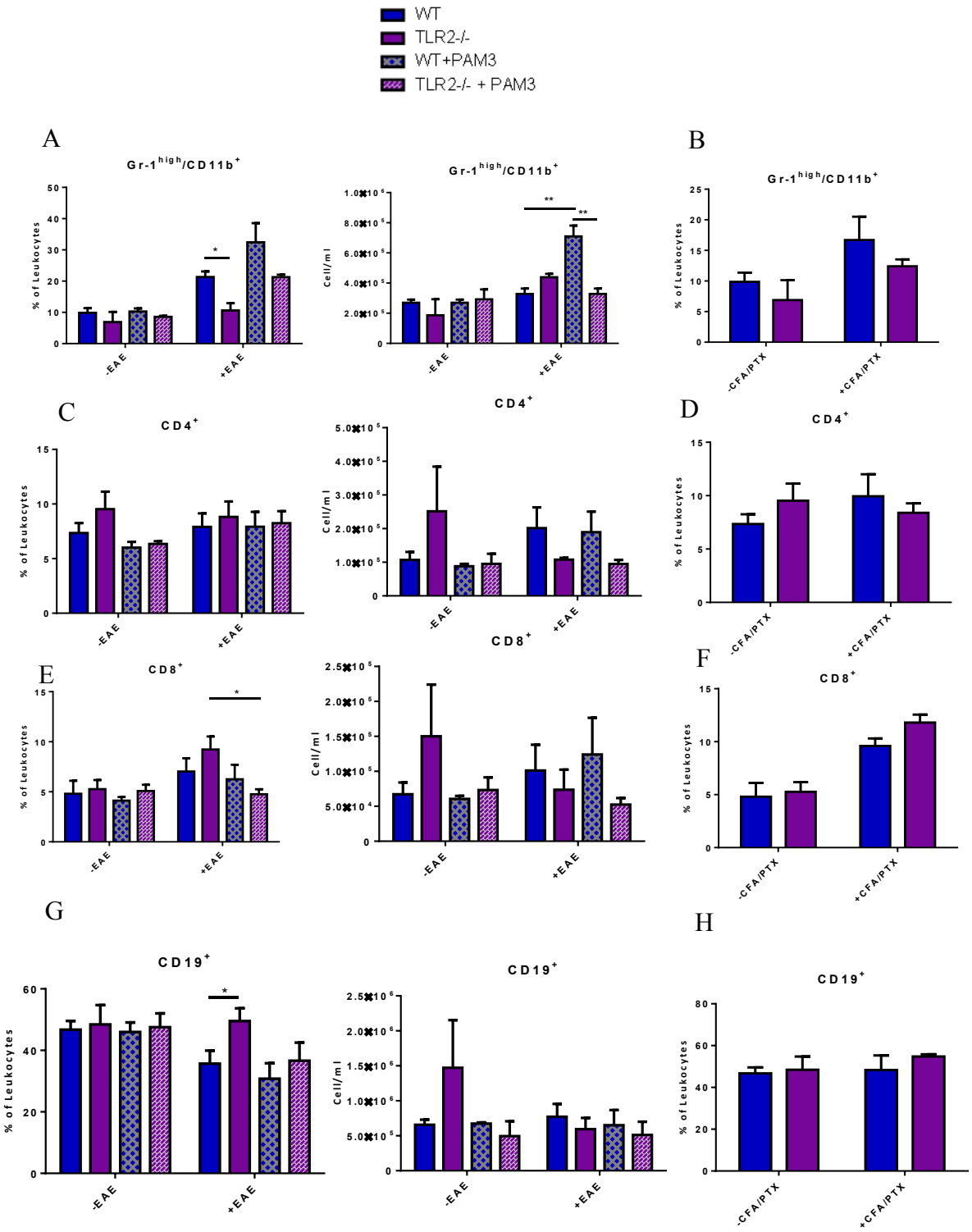
WT
TLR2-/-
WT+PAM3
TLR2-/- + PAM3
A
Gr-1high/CD11b+
% of Leukocytes
Cell/ml
-EAE
+EAE
B
-CFA/PTX
+CFA/PTX
C
CD4+
D
E
CD8+
F
G
CD19+
H

Figure 4-2 TLR2$^{-/-}$ mice have a lower frequency of Gr-1^{high}/CD11b^{+} and a higher frequency of CD19^{+} cells in the blood in the chronic phase of EAE.

Blood was collected from the heart puncture of each animal at day 40 post-EAE from WT (blue bars, n=8) and TLR2$^{-/-}$ (purple bars, n = 8) mice, WT+CFA+PTX (n =2), TLR2$^{-/-}$ +CFA+PTX (n =3), WT+ PAM_3CSK_4 (n = 4) and TLR2$^{-/-}$+ PAM_3CSK_4 (n = 4). (A and B) Frequency and the absolute number of myeloid Gr-1^{+}/CD11b^{+} leukocytes in the CD45^{+} gate. (C and D) Frequency and absolute number of CD4^{+} (E and F) Frequency and the absolute number of CD8^{+} and G and H) frequency and absolute number of CD19^{+} cells at days 40 post-EAE induction. Data are presented as the mean ± SEM. Two-way ANOVA with Tukey's post hoc test was used to compare the statistical differences among group *$P < 0.05$, ** $P < 0.01$,*** $P < 0.001$. Data represents the combination of three separate experiments where each experiment consists of pooled from 4 mice for each group.

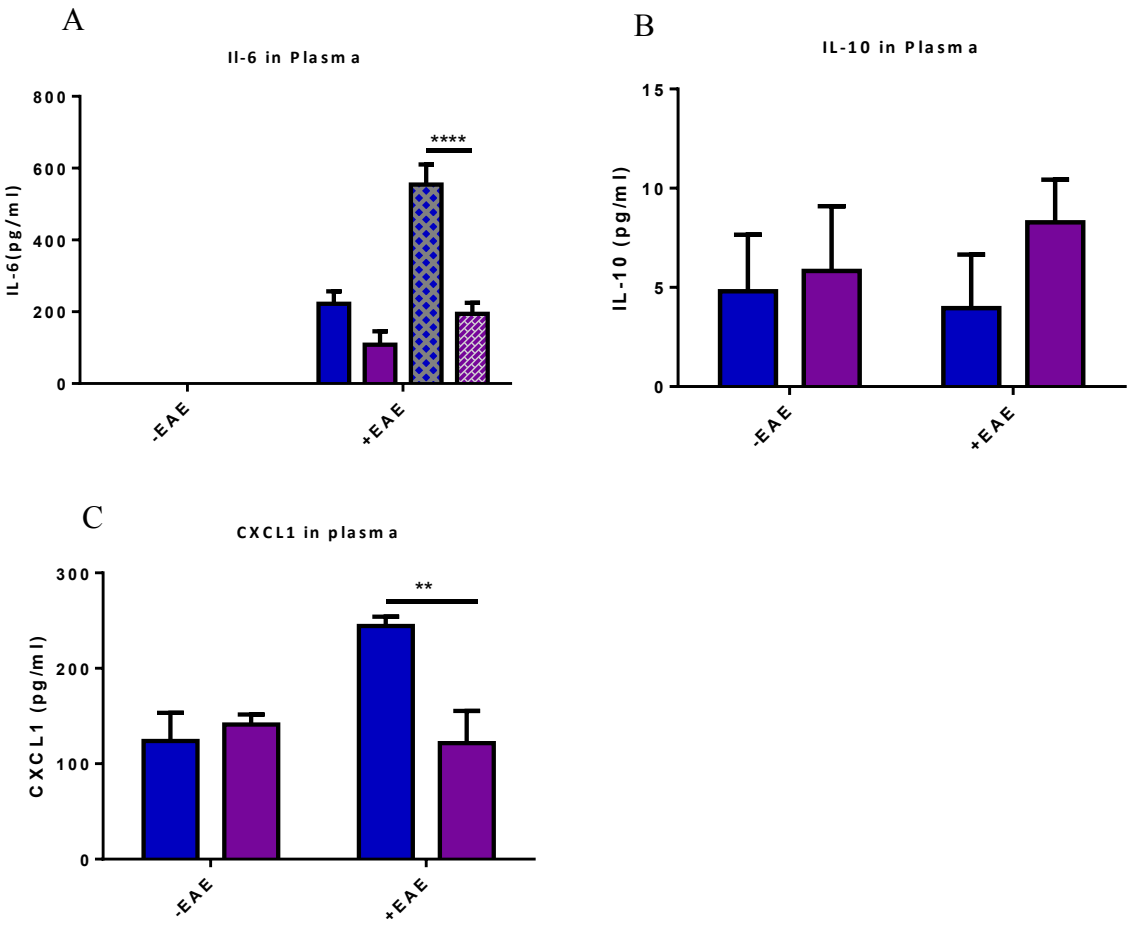
A
Il-6 in Plasma
IL-6(pg/ml)
800
600
400
200
0
****
-EAE
+EAE
B
IL-10 in Plasma
IL-10 (pg/ml)
15
10
5
0
-EAE
+EAE
C
CXCL1 in plasma
CXCL1 (pg/ml)
300
200
100
0
**
-EAE
+EAE

Figure 4-3 TLR2 regulates levels of the pro-inflammatory cytokine IL-6 and chemokine CXCL1 in plasma during the chronic phases of EAE.

(A) The level of IL-6 were measured in the plasma of WT (n= 5) and TLR2$^{-/-}$ (n = 4) mice, WT+ PAM_3CSK_4 (n = 4) and TLR2$^{-/-}$ + PAM_3CSK_4 (n = 4). (B and C) The level of IL-10 and CXCL1 was measured in the plasma of non-EAE WT (n=4) and TLR2$^{-/-}$ (n = 4) and WT (n= 4) and TLR2$^{-/-}$ (n = 4) mice post-EAE induction by ELISA. Data are presented as the mean ± SEM. Two-way ANOVA with Tukey's post hoc test was used to compare the statistical differences among groups**$P < 0.05$, **** $P < 0.01$.

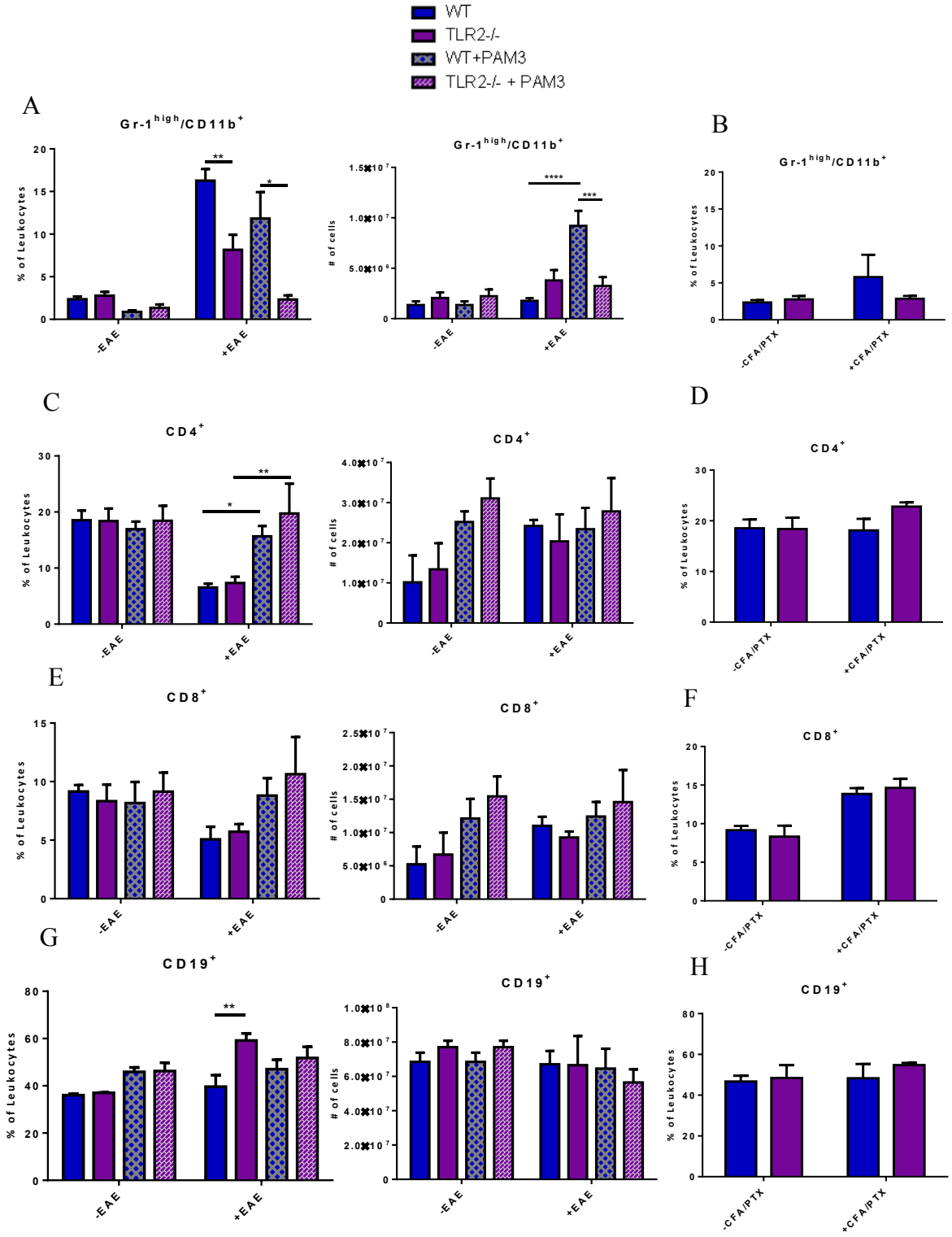
WT
TLR2-/-
WT+PAM3
TLR2-/- + PAM3
A
Gr-1high/CD11b+
% of Leukocytes
# of cells
-EAE
+EAE
B
-CFA/PTX
+CFA/PTX
C
CD4+
D
E
CD8+
F
G
CD19+
H

Figure 4-4 TLR2$^{-/-}$ mice have a lower frequency of Gr-1^{high}/CD11b^{+} and higher frequency of CD19^{+} cells in the spleen during the EAE chronic phase.

WT (blue bars, n=8) and TLR2$^{-/-}$ (purple bars, n = 8) mice, WT+CFA+PTX (n =2), TLR2$^{-/-}$ +CFA+PTX (n =3), WT+ PAM_3CSK_4 (n = 4) and TLR2$^{-/-}$+ PAM_3CSK_4 (n = 4). The frequency and absolute number of (A and B) Gr-1 ^{high}/ CD11b^{+}, (C and D) CD4^{+} (E and F) CD8^{+} , and G and H) CD19^{+} cells at day 40 post-EAE induction . Data are presented as the mean ± SEM. Two-way ANOVA with Tukey's post hc test was used to compare the statistical differences among group*$P < 0.05$, ** $P < 0.01$,**** $P < 0.001$. Data represents the combination of three separate experiments where each experiment consists of pooled from 4 mice for each group.

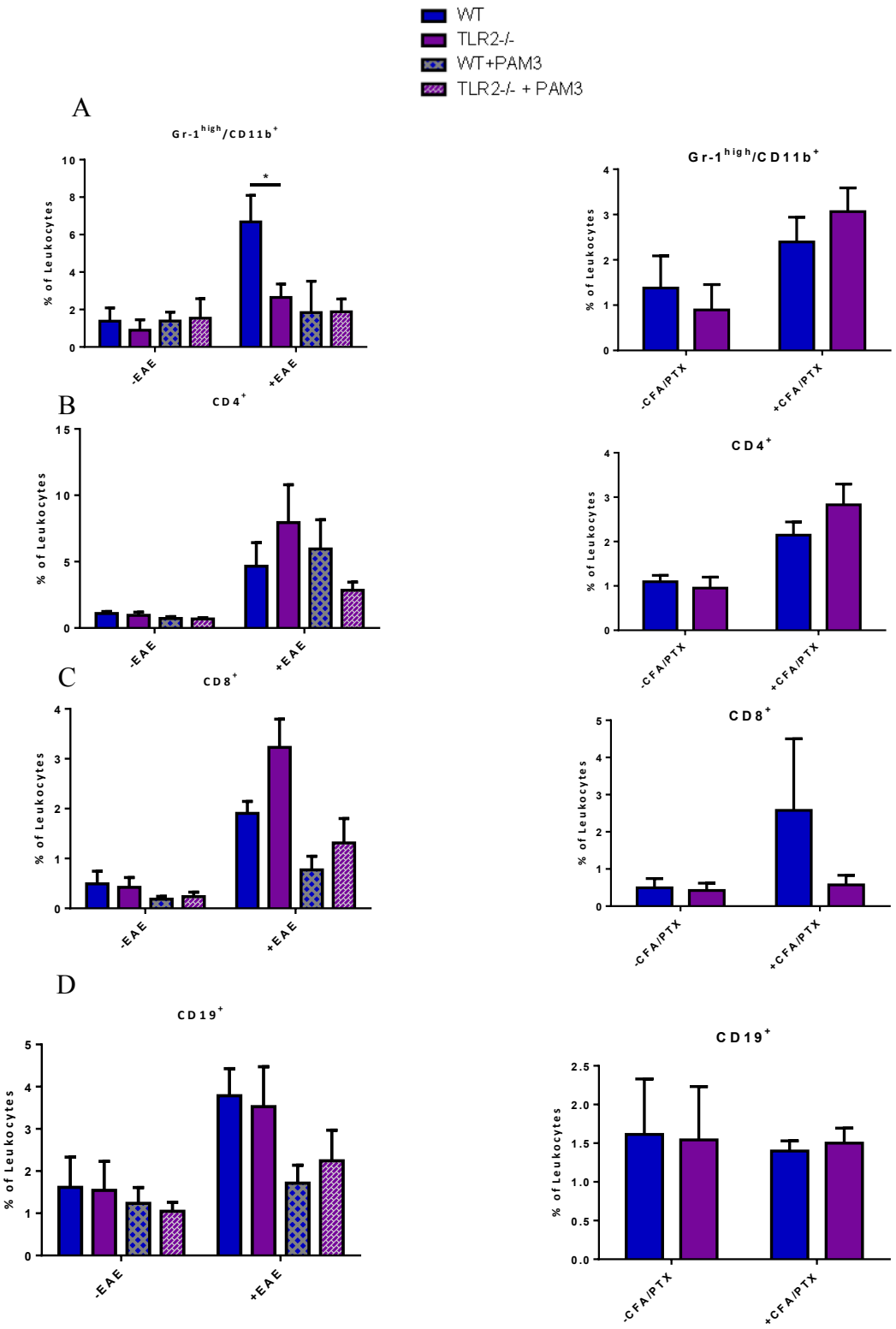
WT
TLR2-/-
WT+PAM3
TLR2-/- + PAM3
A
Gr-1high/CD11b+
% of Leukocytes
-EAE
+EAE
-CFA/PTX
+CFA/PTX
B
CD4+
C
CD8+
D
CD19+

Figure 4-5 TLR2$^{-/-}$ mice have a lower frequency of Gr-1^{high}/CD11b^{+} cells in the brain during the chronic phase of EAE.

WT (blue bars, n=8) and TLR2$^{-/-}$ (purple bars, n = 8) mice, WT+CFA+PTX (n =2), TLR2$^{-/-}$ +CFA+PTX (n =3), WT+ PAM_3CSK_4 (n = 4) and TLR2$^{-/-}$+ PAM_3CSK_4 (n = 4). The frequency of (A) Gr-1 $^{high/}$ CD11b^{+}, (B) CD4^{+}, (C) CD8^{+}, and E) and CD19^{+} cells at day 40 post-EAE induction. Data are presented as the mean ± SEM. Two-way ANOVA with Tukey's post hoc test was used to compare the statistical differences among groups *P < 0.05.


WT
TLR2-/-

A

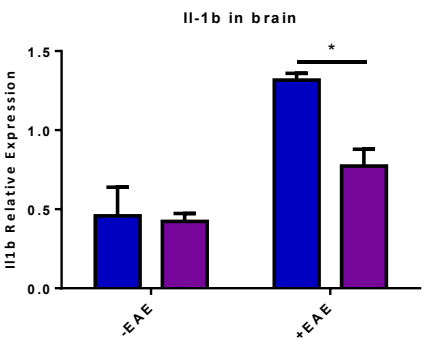
Il-1b in brain
Il1b Relative Expression
1.5
1.0
0.5
0.0
*
-EAE
+EAE

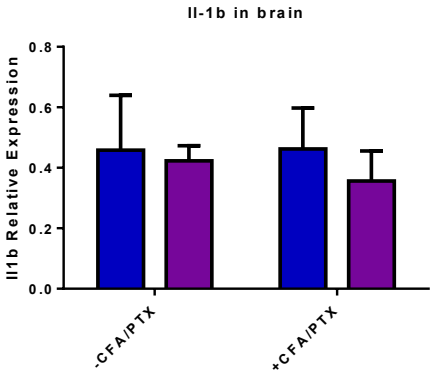
Il-1b in brain
Il1b Relative Expression
0.8
0.6
0.4
0.2
0.0
-CFA/PTX
+CFA/PTX

B

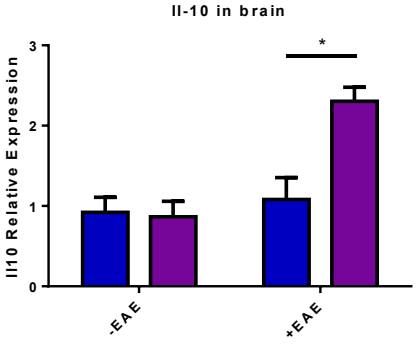
Il-10 in brain
Il10 Relative Expression
3
2
1
0
*
-EAE
+EAE

Figure 4-6 TLR2 promotes inflammation in EAE mice.

Expression in the brain of the markers of inflammation A) *Il1b* (a gene that encodes (IL-1β) and B) *Il10* (a gene encodes (IL-10) were compared between untreated (-EAE) or EAE-induced (+EAE) mice. Data are presented as the mean ± SEM. Two-way ANOVA with Tukey's post hoc test was used to compare the statistical differences among groups $*P < 0.05$.

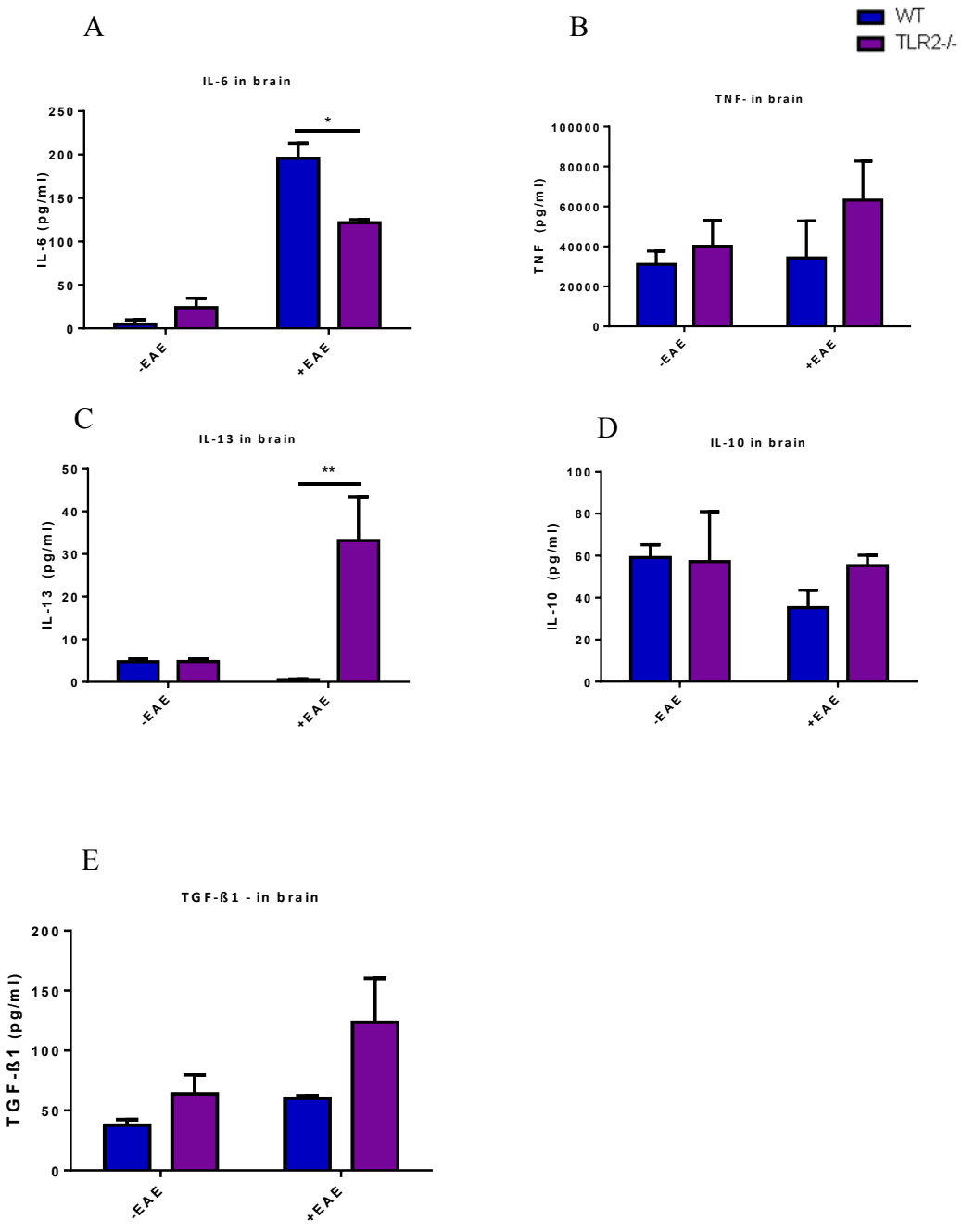
A
IL-6 in brain
IL-6 (pg/ml)
250
200
150
100
50
0
*
-EAE
+EAE
B
WT
TLR2-/-
TNF- in brain
TNF (pg/ml)
100000
80000
60000
40000
20000
0
-EAE
+EAE
C
IL-13 in brain
IL-13 (pg/ml)
50
40
30
20
10
0
**
-EAE
+EAE
D
IL-10 in brain
IL-10 (pg/ml)
100
80
60
40
20
0
-EAE
+EAE
E
TGF-ß1 - in brain
TGF-ß1 (pg/ml)
200
150
100
50
0
-EAE
+EAE

Figure 4-7 Reduced level of the pro-inflammatory cytokine IL-6 reduced in and increased levels of regulatory cytokine IL-13 in the TLR2$^{-/-}$ brain during the chronic phase of EAE.

The levels of A) IL-6 and B) TNF were measured in the brains of WT and TLR2$^{-/-}$mice before (WT, n = 4 vs TLR2$^{-/-}$, n = 4) and after EAE (day 40; WT, n = 5 vs TLR2$^{-/-}$, n = 4). The levels of C) IL-13, D) IL-10, and E) TGF-β1 were measured in the brains of WT and TLR2$^{-/-}$mice before EAE (WT, n = 4-5 vs TLR2$^{-/-}$, n = 3-4) and after EAE (day 40 ; WT, n = 4-7 vs TLR2$^{-/-}$, n = 4-6). Data are presented as the mean ± SEM of cytokine level per gram of brain tissue. Two-way ANOVA with Tukey's post hoc test was used to compare the statistical differences among groups *$P < 0.05$, ** $P < 0.01$.

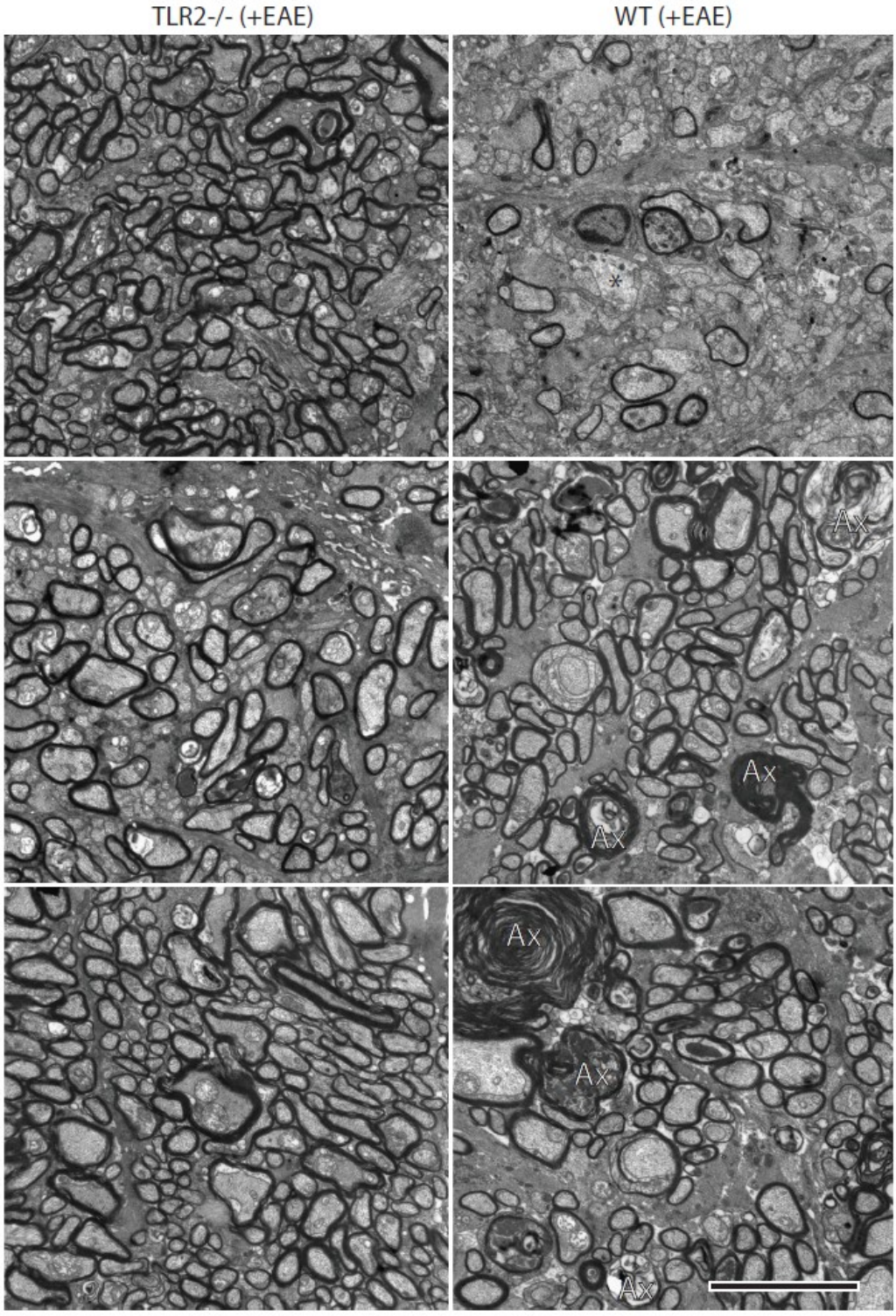
TLR2-/- (+EAE)
WT (+EAE)
*
Ax
Ax
Ax
Ax
Ax

Figure 4-8 The axonal pathology is improved in optic nerves in the absence of TLR2 expression.

Representative ultra-thin transversal sections of optic nerves were obtained (A, +EAE+TLR2$^{-/-}$) (B, +EAE+WT). Ax, axolytic; *, demyelinating. Scale bar, 5 μm.

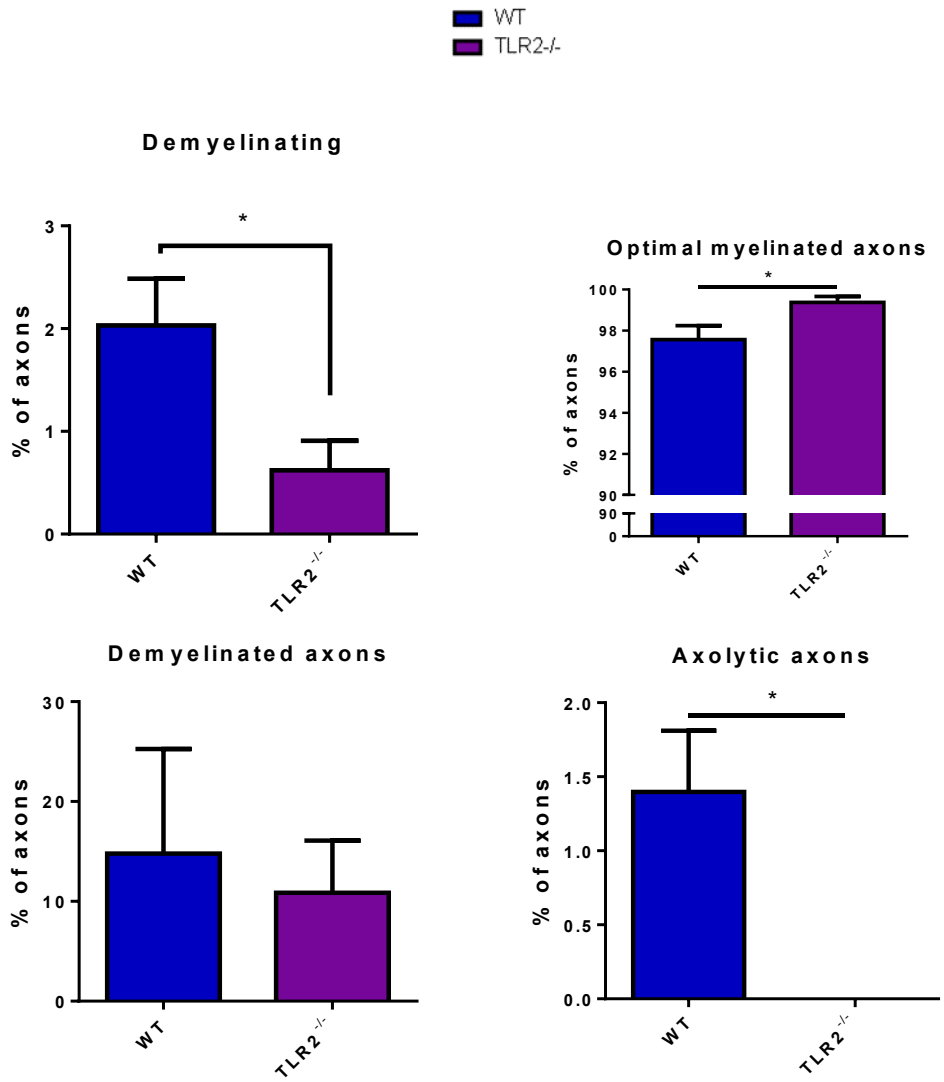
WT
TLR2-/-
Demyelinating
% of axons
3
2
1
0
*
WT
TLR2 -/-
Optimal myelinated axons
% of axons
100
98
96
94
92
90
90
0
*
WT
TLR2 -/-
Demyelinated axons
% of axons
30
20
10
0
WT
TLR2 -/-
Axolytic axons
% of axons
2.0
1.5
1.0
0.5
0.0
*
WT
TLR2 -/-

Figure 4-9 TLR2-deficient mice have decreased demyelination and reduced axonal damage in the optic nerve.

Electron micrographs of optic nerves from (+EAE) mice were analyzed. Based on the g-ratio (see Materials and Methods), the frequency of A) demyelinating axons and B) optimally myelinated was determined. We also examined the frequency of axons completely devoid of myelin (C) and axolytic axons (D). Data are presented as the mean ± SEM and an unpaired *t*-test was used for statistical analysis * $P \leq 0.05$.

Chapter 5 General discussion and conclusion

MS is a chronic illness that has a substantial negative influence on well-being and quality of life. Inflammation in MS and EAE is stimulated and regulated by a wide array of molecules. This study investigated the role of two crucial molecules involved in the pathogenesis and regulation of EAE: The Nav 1.6 isoform, a primary contributor to axonal loss in EAE, and Toll-like receptor 2, a key element of the innate immune system vital for EAE development. I used the MOG_{35-55} peptide to actively induce the chronic phase of EAE because this peptide is a unique myelin autoantigen that causes an encephalitogenic T cell and a demyelinating autoantibody response that represents the MS disease state.

5.1 Nav1.6 in axonal degeneration and inflammation

The first objective of this study aimed to examine whether a deficiency (Chapter 2) or reduction of expression of (Chapter 3) Nav1.6 improves axonal survival and disease development in EAE. I have provided evidence that Nav1.6 promotes neuronal degeneration and that the channel activity is also linked to the inflammatory response. Assessing the impact of eliminating this sodium channel in the CNS (chapter 2) was complicated by the fact that mice with full-body, homozygous knockouts of the *Scn8a* gene, such as $Scn8a^{dmu/dmu}$ or $Scn8a^{med/med}$ (Meisler et al., 2001; De Repentigny, 2001) suffer from paralysis and death after three weeks of age, thus precluding EAE experiments. Therefore, another strategy was devised where Cre recombinase, along with the GFP marker, was delivered to RGCs of $Scn8a^{flox/flox}$ mice using the AAV (serotype 2) vector. Since AAV2 preferentially targets RGCs and reduced expression of *Scn8a* in a sub-population of these cells, I was able to assess the impact of Nav1.6 on axonal homeostasis, in the context of EAE. In addition, this approach proved advantageous since

it allowed me to use the contralateral eye, either left un-injected or injected with a AAV2 containing only the GFP gene, as a control in the same disease microenvironment as the experimental Cre-targeted eye.

The results of these studies showed that the depletion (Chapter 2) or reduction (Chapter 3) of Nav1.6 expression improves axonal health, as shown by a reduction of demyelination and a decreased number of axolytic fibers within the optic nerve. In Chapter 3, the reduction of the expression of this channel was also found to enhance the remyelination of axons (interestingly, remyelination was not observed in Cre-targeted optic nerves in Chapter 2). This work is the first to show *in vivo* that a reduction of Nav1.6 expression improves EAE pathology.

Kearney (2002) showed that a reduction of Nav1.6 expression to 50% of WT in heterozygous *Scn8a*$^{medJ/+}$ mice (*medJ* is a hypomorphic allele of *Scn8a* that with a splice donor mutation in exon 3, which results in abnormal splicing of the transcripts due to exon skipping) do not have overt neurological deficits, whereas a reduction of expression of this channel to 12% in homozygous *Scn8a*$^{medJ/medJ}$ is associated with neurological symptoms such as dystonia and muscle weakness. Furthermore, a decrease of Nav1.6 expression to 6% is lethal and the range of minimal channel expression for survival to adulthood is between 6% to 12%. However, 12% expression in *Scn8a*$^{medJ/medJ}$ (where these mice are crossed to mice harbouring the dominant H allele of the *Scnm1* modifier gene, which ensures that a higher proportion of the transcripts encoded by the *medJ* allele are correctly spliced) results in dystonia and muscle weakness. Taken together, my observations in *Scn8a*$^{dmu/+}$ mice along with the results from Kearney (2002) suggest that there may be an optimal level of Nav1.6 expression between approximately 25% and

50% of WT levels that should be aimed for to reduce EAE (and MS) symptoms and to promote remyelination to maintain and restore nerve conduction. It has been reported that Nav1.2, which is not associated with axonal degeneration and immune cells infiltration in EAE (Craner et al., 2004b; Schattling et al., 2016), at least partially compensates for reductions of Nav1.6 in heterozygous mice for a null mutation in *Scn8a* mice*,* indicating that if Nav1.6 is unable to fully occupy the nodal membrane, Nav1.2 may be expressed at higher levels in the nodes to maintain saltatory conduction (Vega et al., 2008). In addition, the similarity between the properties of Nav1.6 and Nav1.2 and their clustering indicates a binding competition at the node (Vega et al., 2008).

The work reported in this thesis also indicates that Nav1.6 promotes the production of inflammatory cytokines, as indicated by reductions in the expression of *Il6* (IL-6)*, Ifng* (IFN-γ), and gliosis measured by quantification of GFAP (*Gfap)* in the retina. While I cannot eliminate the possibility that cells other than RGCs, such as Müller cells and microglia, might contribute to the reduction in retinal inflammation and axonal loss, I believe this contribution to be minimal when considering previous evidence. A study conducted by Kaspar et al. (2002) investigated the cellular selectivity of AAV2 in the brain of a transgenic reporter mouse by quantitating cells with both NeuN, a marker of neurons, and beta-galactosidase to indicate AAV2-infected cells. The researchers found that neurons and not glial cells were targeted by AAV2, confirming the previously-reported tropism of AAV serotype 2 towards neurons (Bartlett et al., 1998)

The *neuronal* Nav1.6 channel, therefore, seems to promote inflammation in EAE. It is unclear if this is due to the increased axonal degeneration or if these neuronal channels exert a more direct influence on immune cells. To address this, a strategy that

would include knocking out macrophage function in EAE mice in combination with a knockout of neuronal Nav1.6 could provide insight. If axons continue to degenerate, we would conclude that neuronal Nav1.6 is responsible for neuronal loss.

The work contained within Chapter 3 of this thesis further explored the link between Nav1.6 and inflammatory mediators. At the histological level, I found that the infiltration of immune cells was significantly decreased in the optic nerves from *Scn8a*$^{dmu/+}$ mice with EAE. I found that, in the optic nerve, the frequency of neutrophil infiltration was reduced in comparison to WT+EAE. Axonal damage may be driven by inflammatory immune cells. Nav1.6 is expressed in multiple immune cells including neutrophils and macrophages and participates in the modulation of microglial activation (Black and Waxman, 2013; Craner et al., 2005; Hossain et al., 2018b), this channel should certainly be considered as a primary enhancer of the immune response. In addition to optic nerve infiltration, the reduction of expression of Nav1.6 influences peripheral inflammation by reducing the circulation of Gr-1^{high}/CD11b^{+} and Gr-1^{int}/CD11b^{+} cells in the blood and decreasing the level of IL-6 in the plasma. In this context, it is noteworthy that it has recently been reported that there is a high expression of Nav1.6 in the microglia of mice and post-mortem in patients with Parkinson's disease (Hossain et al., 2018b) thereby strengthening the link between Nav1.6 and microglial activation.

In the work pursued for **Chapter 3**, I was struck by the following observation: untreated *Scn8a*$^{dmu/+}$ mice had levels of IL-10 and TGF-β1 anti-inflammatory cytokines in the brain that far exceeded wild type levels. Increases of such anti-inflammatory cytokines in mice with reduced Nav1.6 poses new questions: What is the role of Nav1.6 channel in relation to the expression of anti-inflammatory cytokines? Also, might it be

possible to target Nav1.6 in order to increase the production of anti-inflammatory mediators in the early stages of EAE, which may offer protection against the disease in mice (and potentially for human MS)? Thus, it may be beneficial to follow this direction to identify how Nav1.6 activity modulates secretion of IL-10, TGF-β1, and IL-13 in the brain, the latter which was found to be increased following EAE induction.

Ultimately, these results taken together provide support the hypothesis that Nav1.6 promotes inflammation and contributes to axonal degeneration following demyelination.

The observed reduction in neuroinflammation in both optic nerve-targeted *Scn8a*$^{flox/flox}$ and *Scn8a*$^{dmu/+}$ mice prompted me to ask whether Nav1.6 has a broader regulatory role in the immune system. To address this, I used lipopolysaccharide (LPS) from *E. Coli*, a widely used inducer of systemic inflammation, in *Scn8a*$^{dmu/+}$ mice. The mice displayed a reduced inflammatory reaction to LPS. It is known that upon exposure to LPS, neutrophils recruited to the site of injection produce ROS contributing to persistent inflammation (McDonald et al., 2010)**.** Our results demonstrate that significantly lower neutrophil recruitment in *Scn8a*$^{dmu/+}$ than in *Scn8a*$^{+/+}$ mice at 16-hour post-LPS, suggesting that Nav1.6 may play a role in directly or indirectly in facilitating migration. It will be of interest to investigate the role of such sodium channels in regulating the migration and extravasation of neutrophils in response to an infection, and the associated noncanonical molecular pathways.

With regard to how Nav1.6 may influence cell signaling, we know that inflammation, cell proliferation, and cell death are influenced by the activity and signaling of MAPK pathways that include the extracellular-signal-related kinase (ERK),

c-Jun N-terminal kinase, p38, and ERK5/big mitogen-activated protein kinase (Gasser et al., 2010; Persson et al., 2014b). Interestingly, Nav1.6 and p38 are found in CNS neurons and expressed in a variety of CNS tissues, indicating the involvement of p38 in the modulation of Nav1.6 (Black et al., 2018; Wittmack et al., 2005). There is colocalization of Nav1.6 and p38 in hippocampal neurons and following activation of p38 by stress the expression of Nav1.6 current is decreased (Gasser et al., 2010). Modulation of Nav1.6 activity may impact the functions of neurons and glial cells that restore proper axonal conduction. Following injuries, such as hypoxia and sciatic nerve transection, MAPKs are expressed to varying degrees in neurons (Black et al., 2018; Gasser et al., 2010; Wittmack et al., 2005). While the impact of MAPK on injury-induced gene expression regulation and signal transduction is well-known, the mechanism that contributes to kinases phosphorylating and modulating Nav channels is not well understood.

5.2 Therapeutic modulation of Nav channel function: past, present and future

Lidocaine, a non-selective intracellular Nav channel blocker usually used as a local anesthetic, has been shown to protect axons from NO-mediated axonal degeneration (Kapoor et al., 2003). Furthermore, lidocaine has been shown to improve some of the positive symptoms in MS patients, such as burning and tingling sensation, which are less responsive to non-steroidal anti-inflammatory drugs (Sakurai and Kanazawa, 1999). However, since lidocaine causes a complete loss of sensation the quality of life may not be improved (Putrenko et al., 2016).

Phenytoin and carbamazepine are other Nav channel blockers that have been shown to be protective in EAE by reducing axonal degeneration in the intact neuron, to reduce infiltration of inflammatory cells in CNS, and to produce an improvement in the

clinical outcome (Craner et al., 2005; Lo et al., 2003). The protective effect of these drugs was striking even when administered 7-10 days post EAE induction (Bechtold et al., 2004; Lo et al., 2003). However, research at Yale University in EAE mice by Black et al. (2007) showed that the acute withdrawal of phenytoin or carbamazepine exacerbated the symptoms 7 days after withdrawal. This observation caused the phenytoin clinical study to be halted, although tapering the withdrawal was later found to eliminate this inflammatory rebound effect in mice (Liu et al., 2014). Perhaps as a result of the trial being arrested, the inflammatory rebound has not been reported in any MS patient with Nav channel blocker withdrawal. While the mechanisms underlying such worsening of the disease are not well understood, it is speculated to be due to the infiltration of immune cells within the spinal cord in mice with EAE (Renno et al., 1995; Black and Waxman, 2007).

The risks of treatment with sodium channel non-specific blockers, such as lidocaine, phenytoin and carbamazepine have some common side effects that include involuntary movement, ataxia, nystagmus and visual impairments, drowsiness, fatigue, and impairment of cognitive function (Brodie, 2017; Perucca et al., 2000). In addition, some of the disadvantages of using such Nav channel blockers could be due to their non-selective blocking of all the subtypes of Nav channels that are expressed on both neuronal and immune cells, some of which are believed to have a compensatory role in MS such as Nav1.2 as discussed above. The TTX metabolite 4,9-Anhydrotetrodotoxin (4,9-ah-TTX) blocks Nav1.6 in the nanomolar range with minimal effect on other TTX-sensitive channels (Rosker et al., 2007b). Hargus et al. (2013) have shown that 4,9-ahTTX selectively blocks Nav1.6 but not Nav1.2 currents and was able to suppress neuronal

hyperexcitability in a mouse model of epilepsy. In light of the findings presented here, 4,9-ah-TTX could potentially be assessed in the EAE model, although the toxicity dose-response would have to be carefully determined due to the vital importance of Nav1.6 function. Furthermore, since the blockade of Nav1.6 would presumably have to be ongoing during the course of EAE development, the drug would have to be administered several times per day or continuously using an infusion pump. Ultimately, due to its toxicity, it is doubtful that 4,9-ahTTX will be practical for therapeutic use.

An alternative approach, to overcome the problem of using broad-spectrum Nav channel blockers, could be via the use of gene therapy methods to selectively reduce the expression of specific Nav channels. In a recent study by Chen et al. (2018b), the AAV-Cre serotype 2 was used to eliminate Nav1.6 specifically in dorsal root ganglion (DRG) in a spared nerve injury model to study the role of Nav1.6 in peripheral neuropathic pain. They showed that AAV-Cre-mediated Nav1.6 knockout, mostly in a large proportion of DRG neurons, significantly decreases the excitability of these neurons by reducing the accumulation of Nav1.6 at the node of Ranvier within the site of injury. Furthermore, a study by Xie et al. (2013) has shown that knockdown of Nav1.6 by small inhibitory (si) RNA-mediated knockdown reduces the inflammation and controls the development of pain in the PNS. In addition, Samad et al. (2013) have used (shRNA) to knockdown the Nav1.3 channel gene in dorsal ganglion cells. The knockdown of Nav1.3 resulted in the attenuation of pain in adult rats with neuropathic pain. This success of the Nav1.3-knockdown in the PNS offers hope that a similar strategy may be used in the CNS for Nav channels related to the MS. Finally, the use of micro RNAs may prove useful in regulating Nav1.6 expression, as recently miR-30b-5p was shown to downregulate

Nav1.6 in a rat model of neuropathic pain and was used to attenuate neuropathic pain induced by the chemotherapy drug oxaliplatin (Li et al., 2019) .

Taken together, the exacerbation of the clinical symptoms in EAE upon withdrawal of phenytoin and carbamazepine effectively rules out the use of non-specific Nav blockade for the treatment of MS. Therefore, developing more selective pharmaceutical therapies and genetic treatments which reduce Nav1.6 expression or function, could be the way to achieve future goals in Nav1.6-based clinical trials.

5.3 TLR2 and inflammation

The correlation between bacterial infections and MS relapse, as well as the elevation of TLR2 ligands in the brains and CSF of MS patients, suggest a role of TLR2 in the progression of the disease. Furthermore, TLR2 has been implicated in pain, which constitutes a major aspect of MS and EAE. In **Chapter 4** of this study, we provide evidence that the absence of TLR2 was associated with reduced inflammation at the periphery and in the CNS, which is marked by decreased myeloid cells, including Gr-1^{+}/$CD11b^{+}$, chemokines in the plasma, and pro-inflammatory cytokines in the brain.

TLR2 knockout mice following EAE showed a clinical score of 2 to 2.5 indicating reduced symptoms, a greater ability to mobilize in their cages, and a partial deficit in one hindleg in comparison to control mice who exhibited a higher clinical score of 3 to 3.5 which indicates severe motor deficits to almost complete paralysis. Furthermore, no change in the clinical score was noted in +EAE WT with the addition of the of Pam_3CSK_4 TLR2 agonist relative to +EAE WT.

In TLR2 knockout mice, Gr-1^{high}/$CD11b^{+}$ cells in the spleen were decreased and $CD19^{+}$ cells in the blood were increased, respectively, in the chronic phase of EAE

compared to WT mice. In our comparisons of TLR2 $^{-/-}$ and WT mice, no significant differences in Gr-1^{int}/CD11b^{+} monocytes, CD4^{+} and CD8^{+} T cells were observed for all groups. The stimulation of TLR2 by Pam_3CSK_4 in WT mice showed increased circulating Gr-1^{high}/CD11b^{+} as compared to WT mice without TLR2 activation, while TLR2 knockout mice with Pam_3CSK_4 had decreased Gr-1^{high} /CD11b^{+} compared to WT mice with TLR2 activation.

In the brain, Gr-1^{+}/CD11b^{+} cell infiltration was significantly less in TLR2 knockout mice compared to WT mice. However, the activation of TLR2 in the brain following EAE did not induce any significant changes in TLR2 knockout mice compared to WT. The levels of IL-6 in the brains of TLR2 knockout mice were significantly decreased, whereas IL-13 and IL-10 were significantly increased and marginally increased, respectively. From the EAE model, we can see how complex and interrelated these regulatory mechanisms can be when influenced by a variety of cell subsets at various disease stages. For example, if wild-type mice B cells become depleted due to CD20 mAb treatments one week prior to EAE induction, the encephalitogenic T cells undergo expansion in the CNS, leading to a worsening of EAE symptoms (Matsushita et al., 2008). It appears that this reaction may be caused by B10 cell depletion, as we can find nearly the same effects during selective B10 depletion using CD22 mAb (Kalampokis et al., 2013; Matsushita et al., 2010). The improvement in suggests that the improvement of clinical symptoms TLR2$^{-/-}$ in mice and decreased the inflammation during the chronic phase of EAE could be attributed to increased CD19^{+} and decreased Gr1^{+}/CD11b^{+}.

Overall, these results suggest that TLR2 activation plays an important role in the pathogenesis of MS and EAE by mediating the production of proinflammatory cytokines and suppressing the production of anti-inflammatory cytokines, which exacerbate the EAE symptoms. This occurs potentially via the effect on myeloid cells, such as myeloid cells $Gr1^+/CD11b^+$.

There are seemingly contradictory results in the recent literature regarding the activation of TLR2 in EAE. Peptidoglycan, a TLR2 ligand found in the gram-positive bacterial wall, has been found to enhance the induction of EAE (Visser et al., 2005) while low doses of zymosan, a fungal beta glycan, can reduce or even reverse the relapsing paralysis by promoting the differentiation of Tregs (Li et al., 2013a). This latter result appears to be due to the development of TLR2 tolerance in EAE (Anstadt et al., 2016). It has been reported that the repeated signaling of low doses of TLR2 ligands can reduce the responsiveness of the receptor for further signaling via other ligands besides changing the effector immune cells into regulatory phenotype. Consequently, dampening the signaling via the use of a low dose of TLR2 ligands may potentially attenuate the progression of MS (Anstadt et al., 2016).

5.4 The Potential link between Nav channels and TLR

In non-neuronal cells, there is a distinct possibility that the current density of ion channels, including Nav channel currents, may be associated with TLR4 activation. It is known that TLR4 agonists, such as M3G, elicit a substantial increase in the current density of Nav channels including Nav1.6, Nav1.7 and Nav1.9, but not Nav1.8 (Chow et al., 1999). There could be an association between Nav and TLR4 signaling, as it has been observed that increases in TLR4 expression following exposure to LPS in mouse

macrophage cultures promote downstream signaling components such as NFkB, p38 MAPK, JNK and ERK (Lee et al., 2008; Lu et al., 2008). Increased firing of these channels may contribute to opioid-induced tactile allodynia. These opioid metabolite-induced changes in neuronal excitability can be pharmacologically inhibited by the state-dependent sodium channel blocker, carbamazepine. In Chapter 3, I reported that in the presence of reduced Nav1.6 levels, LPS – also frequently a bacterial ligand for TLR2 (Li et al., 2013b) – resulted in reduced inflammation in *vivo* and in *vitro*. I believe, based on the observation that there is a high likelihood of interaction between Nav1.6 and TLR2, which should be further investigated.

5.5 Limitations of this study

5.5.1 Mouse model for MS

Several elements, mechanisms, and treatments of MS have been identified and studied by researchers using EAE (Constantinescu et al., 2011). This model mimics many features of MS, including inflammation, demyelination, axonal loss, gliosis and optic neuritis. However, there is no perfect animal model that entirely stimulates the immunological and neuropathological changes related to the initiation and development of MS (Lassmann and Bradl, 2017). Firstly, the development of EAE is preformed through known antigen injection, whereas in humans, the disease develops spontaneously without a clearly defined antigen. Additionally, it is believed that predominately $CD4^+$ T cells contribute to the development of EAE, while $CD8^+$ T cells are the primary contributor to the progression of the disease in humans (Mix et al., 2010). Moreover, the animal model exhibits differences in inflammatory lesions and activation of autoreactive T cells compared to MS (Höftberger et al., 2015). As such, some medications found to be

effective in EAE were not beneficial for treating MS patients such as monoclonal anti-IL-12p40 (Segal et al., 2008) and anti-TNF therapy (Kemanetzoglou and Andreadou, 2017; The Lenercept Multiple Sclerosis Study Group and The University of British Columbia MS/MRI Analysis Group., 1999). Despite these limitations, the EAE model was, I believe, the most appropriate choice for my study since it recapitulates many aspects of the chronic phase of MS including demyelination, optic neuritis, and axonal loss

5.5.2 Investigating other immune cells

In the current study, I focused on the role of neutrophils and macrophages. However, it might be important to address the role of Nav1.6 on other cells, such as Tregs and microglial subtypes in order to study the influence of Nav1.6 in microglial activation following EAE and LPS stimulation (Black et al., 2009b; Hossain et al., 2018b). It has been hypothesized that Nav1.6 participates in the modulation of microglial activation and function in EAE. It would, therefore, be desirable to further investigate the role of Nav1.6 microglia beyond the work of Craner et al. (2005).

5.6 Future directions

The work presented in this thesis answered several questions about the contribution of Nav1.6 in neuronal death following demyelination in the chronic EAE and the role of this channel for regulating the inflammation in EAE and LPS model. In addition, it answered several questions regarding the role of TLR2 in EAE. However, many vital questions are still unanswered and need further investigation. Additional research is required to determine whether Nav1.6 could enhance remyelination in an alternate EAE model such as the cuprizone model or using a Lysophosphatidylcholine (LPC) mouse model of focal demyelination. The molecular mechanisms underlying the

changes in the expression of various subtypes of ion channels in the demyelinated lesion should also be investigated. Therefore, developing selective pharmaceutical therapies and genetic treatments could be the way to facilitate these efforts and to achieve future goals including working towards Nav1.6-based clinical therapy.

Further research should focus on identifying the mechanism of CNS damage through TLR2 signaling via endogenous or exogenous ligands. In addition, it is proposed that soluble TLR2, which is found in body fluids such as plasma, CSF, and breast milk, may act as a decoy receptor and compete for TLR2 ligands to subsequently attenuate the disease severity (Dulay et al., 2009; Hossain et al., 2018a; LeBouder et al., 2003). Thus, additional studies should investigate the role of soluble TLR2 in the progression of EAE.

In the presence of infection, TLR2 has the capacity to signal as a heterodimer with TLR1 and TLR6, eliciting the innate immune response and subsequently the adaptive immune response to engulf pathogens (West et al., 2011). Infections may predispose individuals to MS by reducing Treg cell function (Hossain et al., 2015). Replicating the findings herein in the cuprizone and lysolecithin models of demyelination/remyelination will further confirm that targeting the TLR2 pathway with therapeutic agents is potentiality e a valid therapeutic strategy in humans.

5.7 Conclusion

In addressing Objectives 1 and 2, my findings demonstrate that selective targeting of *Scn8a* in RGCs is associated with a reduction of markers of gliosis (GFAP) and inflammation (IL-6). Mice with reduced Nav 1.6 expression display less demyelination and less axonal loss in the optic nerve following EAE induction (Figure 5.1). In addition, my results suggest a potential role of Nav1.6 in regulating the inflammatory process

during both EAE and the response to LPS challenge. These observations characterize the contribution of Nav1.6 to the sequence of events that lead to neuronal death following myelin loss in EAE.

In investigations relating to Objective 3, my results showed that in mice lacking TLR2 signaling is associated with a reduced inflammatory response, which was marked by a reduction of IL-6 and TNF production in the CNS (Figure 5.2). Overall, these results suggest that TLR2 signaling plays an important role in the pathogenesis of EAE by mediating the production of several pro-inflammatory cytokines.

The uncovered links between Nav1.6 and TLR2 with inflammatory mediators will hopefully inform future efforts aimed at controlling the inflammation and axonal damage associated with MS. Taken together the findings reported in this thesis suggest novel opportunities to intervene in the development of MS and suggest a novel paradigm for the role of Nav1.6 in inflammation that would be of great interest to follow up in a clinical or therapeutic setting.

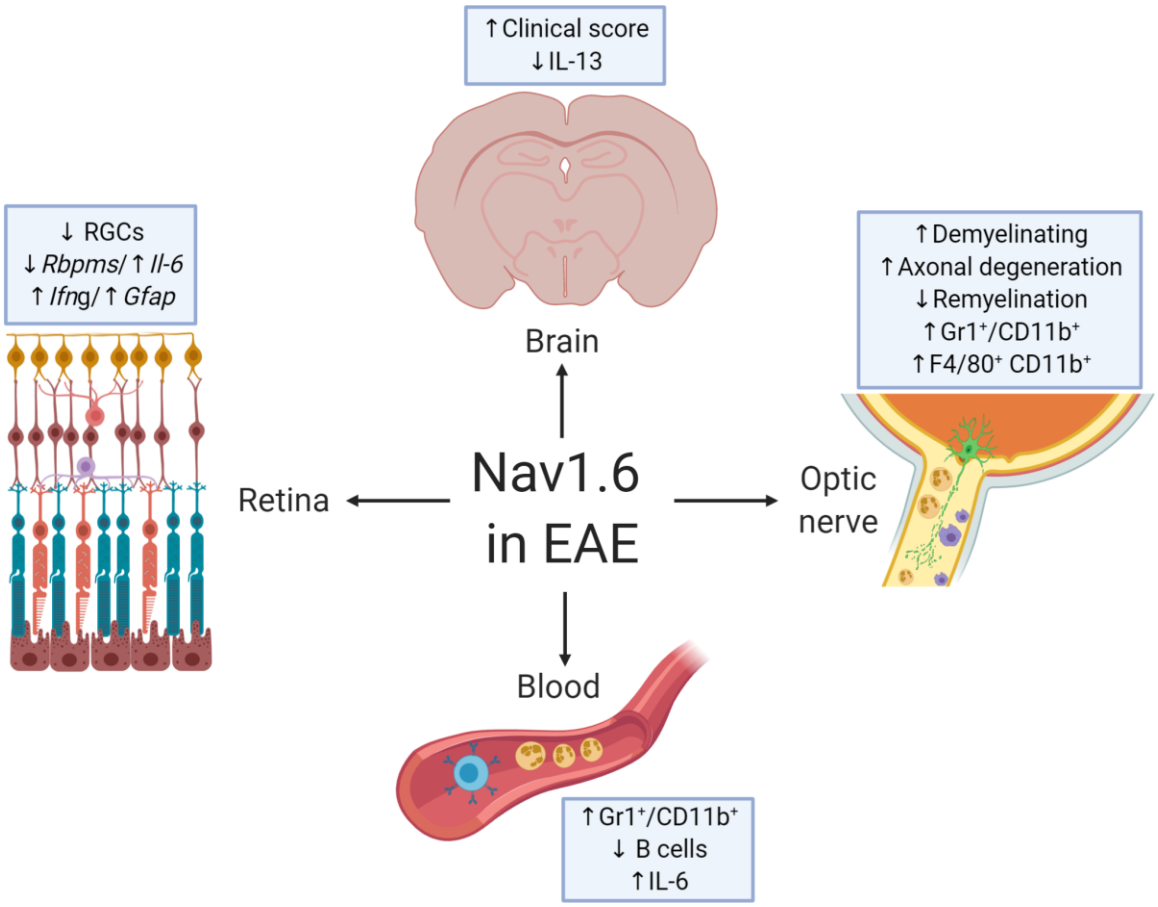
↑ Clinical score
↓ IL-13
Brain
↓ RGCs
↓ *Rbpms*/ ↑ *Il-6*
↑ *Ifng*/ ↑ *Gfap*
Retina
Nav1.6
in EAE
↑ Demyelinating
↑ Axonal degeneration
↓ Remyelination
↑ Gr1⁺/CD11b⁺
↑ F4/80⁺ CD11b⁺
Optic
nerve
Blood
↑ Gr1⁺/CD11b⁺
↓ B cells
↑ IL-6

Figure 5-1 Schematic diagram of the functional effects of Nav1.6 expression in axonal axons and inflammation in EAE

Diagram summarizing the contribution of the Nav1.6 voltage-gated sodium channel isoform to axonal damage in EAE and how it may impact the regulation of multiple aspects of the inflammatory response.

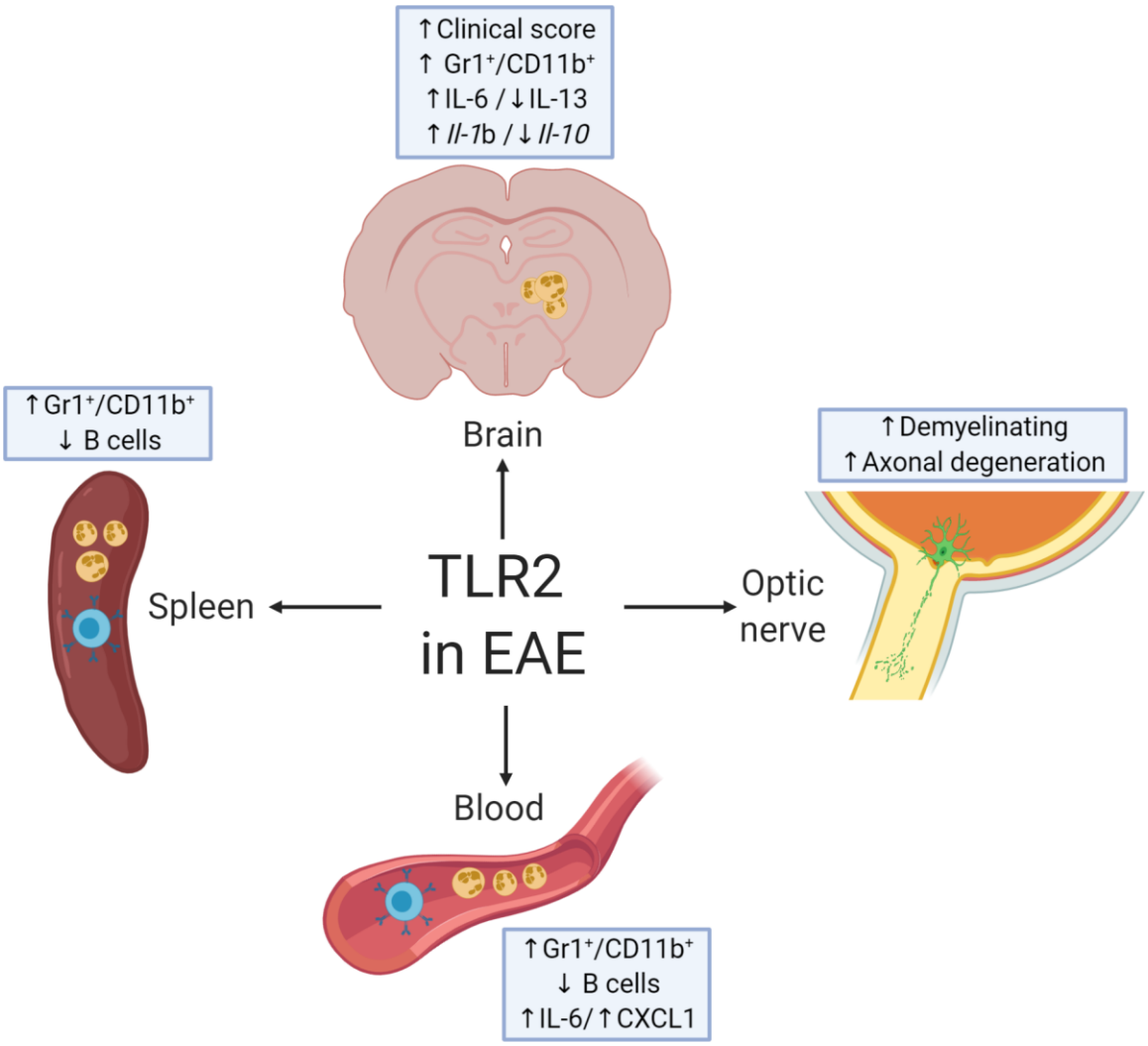
↑Clinical score
↑ Gr1+/CD11b+
↑IL-6 / ↓IL-13
↑ Il-1b / ↓ Il-10
Brain
↑Gr1+/CD11b+
↓ B cells
Spleen
TLR2
in EAE
↑Demyelinating
↑Axonal degeneration
Optic
nerve
Blood
↑Gr1+/CD11b+
↓ B cells
↑IL-6/ ↑CXCL1

Figure 5-2 Proposed model of functional effects of TLR2 expression in axonal axons and inflammation in EAE.

Diagram summarizing the contribution of TLR2 expression in the pathogenesis of EAE by mediating the production of proinflammatory cytokines, which exacerbate the EAE symptoms.

References

't Hart, B.A., Gran, B., and Weissert, R. (2011). EAE: Imperfect but useful models of multiple sclerosis. Trends Mol. Med. *17*, 119–125.

Ahern, C.A. (2013). What activates inactivation? J. Gen. Physiol. *142*, 97–100.

Ahmadbeigi, N., Soleimani, M., Vasei, M., Gheisari, Y., Mortazavi, Y., Azadmanesh, K., Omidkhoda, A., Janzamin, E., and Nardi, N.B. (2013). Isolation, characterization, and transplantation of bone marrow-derived cell components with hematopoietic stem cell niche properties. Stem Cells Dev. *22*, 3052–3061.

Ahuja, S.K., and Murphy, P.M. (1996). The CXC chemokines growth-regulated oncogene (GRO) α, GROβ, GROγ, neutrophil-activating peptide-2, and epithelial cell-derived neutrophil- activating peptide-78 are potent agonists for the type B, but not the type A, human interleukin-8 receptor. J. Biol. Chem. *271*, 20545–20550.

Ajami, B., Bennett, J.L., Krieger, C., McNagny, K.M., and Rossi, F.M. V (2011). Infiltrating monocytes trigger EAE progression, but do not contribute to the resident microglia pool. Nat. Neurosci. *14*, 1142–1150.

Akira, S. (2003). Toll-like receptor signaling. J. Biol. Chem. *278*, 38105–38108.

Akira, S., and Takeda, K. (2004). Toll-like receptor signalling. Nat. Rev. Immunol. *4*, 499–511.

Akira, S., Uematsu, S., and Takeuchi, O. (2006). Pathogen recognition and innate immunity. Cell *124*, 783–801.

Almolda, B., de Labra, C., Barrera, I., Gruart, A., Delgado-Garcia, J.M., Villacampa, N., Vilella, A., Hofer, M.J., Hidalgo, J., Campbell, I.L., et al. (2015). Alterations in microglial phenotype and hippocampal neuronal function in transgenic mice with astrocyte-targeted production of interleukin-10. Brain. Behav. Immun. *45*, 80–97.

Alrashdi, B., Dawod, B., Schampel, A., Tacke, S., Kuerten, S., Marshall, J.S., and Côté, P.D. (2019). Nav1.6 promotes inflammation and neuronal degeneration in a mouse model of multiple sclerosis. J. Neuroinflammation *16*.

Amankwah, N., Marrie, R.A., Bancej, C., Garner, R., Manuel, D.G., Wall, R., Finès, P., Bernier, J., Tu, K., and Reimer, K. (2017). Multiple sclerosis in Canada 2011 to 2031: Results of a microsimulation modelling study of epidemiological and economic impacts. Heal. Promot. Chronic Dis. Prev. Canada *37*, 37–48.

Amarante-Mendes, G.P., Adjemian, S., Branco, L.M., Zanetti, L.C., Weinlich, R., and Bortoluci, K.R. (2018). Pattern recognition receptors and the host cell death molecular machinery. Front. Immunol. *9*.

Amato, M.P., Bertolotto, A., Brunelli, R., Cavalla, P., Goretti, B., Marrosu, M.G., Patti, F., Pozzilli, C., Provinciali, L., Rizzo, N., et al. (2017). Management of pregnancy-related issues in multiple sclerosis patients: the need for an interdisciplinary approach. Neurol. Sci. *38*, 1849–1858.

Amor, S., Peferoen, L.A.N., Vogel, D.Y.S., Breur, M., van der Valk, P., Baker, D., and Van Noort, J.M. (2014a). Inflammation in neurodegenerative diseases - an update. Immunology *142*, 151–166.

Amor, S., Peferoen, L.A.N., Vogel, D.Y.S., Breur, M., van der Valk, P., Baker, D., and Van Noort, J.M. (2014b). Inflammation in neurodegenerative diseases - an update. Immunology *142*, 151–166.

Anstadt, E.J., Fujiwara, M., Wasko, N., Nichols, F., and Clark, R.B. (2016). TLR Tolerance as a Treatment for Central Nervous System Autoimmunity. J. Immunol. *197*, 2110–2118.

Aravalli, R.N., Peterson, P.K., and Lokensgard, J.R. (2007). Toll-like receptors in defense and damage of the central nervous system. J. Neuroimmune Pharmacol. *2*, 297–312.

Arnett, H.A., Mason, J., Marino, M., Suzuki, K., Matsushima, G.K., and Ting, J.P.Y. (2001). TNFα promotes proliferation of oligodendrocyte progenitors and remyelination. Nat. Neurosci. *4*, 1116–1122.

Ascherio, A. (2013). Environmental factors in multiple sclerosis. In Expert Review of Neurotherapeutics, pp. 3–9.

Axtell, R.C., De Jong, B.A., Boniface, K., Van Der Voort, L.F., Bhat, R., De Sarno, P., Naves, R., Han, M., Zhong, F., Castellanos, J.G., et al. (2010). T helper type 1 and 17 cells determine efficacy of interferon-B in multiple sclerosis and experimental encephalomyelitis. Nat. Med. *16*, 406–412.

Bagal, S.K., Marron, B.E., Owen, R.M., Storer, R.I., and Swain, N.A. (2015). Voltage gated sodium channels as drug discovery targets. Channels *9*, 360–366.

Bagasra, O., Michaels, F.H., Zheng, Y.M., Bobroski, L.E., Spitsin, S. V., Fu, Z.F., Tawadros, R., and Koprowski, H. (1995). Activation of the inducible form of nitric oxide synthase in the brains of patients with multiple sclerosis. Proc. Natl. Acad. Sci. U. S. A. *92*, 12041–12045.

Barker, A.J., and Ullian, E.M. (2010). Astrocytes and synaptic plasticity. Neuroscientist *16*, 40–50.

Barnett, M.H., Henderson, A.P.D., and Prineas, J.W. (2006). The macrophage in MS: Just a scavenger after all? Pathology and pathogenesis of the acute MS lesion. Mult. Scler. *12*, 121–132.

Barthelmes, J., Tafferner, N., Kurz, J., de Bruin, N., Parnham, M.J., Geisslinger, G., and Schiffmann, S. (2016). Induction of experimental autoimmune encephalomyelitis in mice and evaluation of the disease-dependent distribution of immune cells in various tissues. J. Vis. Exp. *2016*.

Bartholomäus, I., Kawakami, N., Odoardi, F., Schläger, C., Miljkovic, D., Ellwart, J.W., Klinkert, W.E.F., Flügel-Koch, C., Issekutz, T.B., Wekerle, H., et al. (2009). Effector T cell interactions with meningeal vascular structures in nascent autoimmune CNS lesions. Nature *462*, 94–98.

Bartlett, J.S., Samulski, R.J., and McCown, T.J. (1998). Selective and rapid uptake of adeno-associated virus type 2 in brain. Hum. Gene Ther.

Bartolomei, F., Gastaldi, M., Massacrier, A., Planells, R., Nicolas, S., and Cau, P. (1997). Changes in the mRNAs encoding subtypes I, II and III sodium channel alpha subunits following kainate-induced seizures in rat brain. J. Neurocytol. *26*, 667–678.

Baxter, A.G. (2007). The origin and application of experimental autoimmune encephalomyelitis. Nat. Rev. Immunol. *7*, 904–912.

Bechtold, D.A., Kapoor, R., and Smith, K.J. (2004). Axonal Protection Using Flecainide in Experimental Autoimmune Encephalomyelitis. Ann. Neurol. *55*, 607–616.

Beck, C.A., Metz, L.M., Svenson, L.W., and Patten, S.B. (2005). Regional variation of multiple sclerosis prevalence in Canada. Mult. Scler. *11*, 516–519.

Beecham, A.H., Patsopoulos, N.A., Xifara, D.K., Davis, M.F., Kemppinen, A., Cotsapas, C., Shah, T.S., Spencer, C., Booth, D., Goris, A., et al. (2013). Analysis of immune-related loci identifies 48 new susceptibility variants for multiple sclerosis. Nat. Genet. *45*, 1353–1362.

Bell, J.C., Liu, Q., Gan, Y., Liu, Q., Liu, Y., Shi, F.D., and Turner, G.H. (2013). Visualization of inflammation and demyelination in 2D2 transgenic mice with rodent MRI. J. Neuroimmunol. *264*, 35–40.

Benoit, M., Desnues, B., and Mege, J.-L. (2008). Macrophage Polarization in Bacterial Infections. J. Immunol. *181*, 3733–3739.

Berkovic, S.F., Heron, S.E., Giordano, L., Marini, C., Guerrini, R., Kaplan, R.E., Gambardella, A., Steinlein, O.K., Grinton, B.E., Dean, J.T., et al. (2004). Benign Familial Neonatal-Infantile Seizures: Characterization of a New Sodium Channelopathy. Ann. Neurol. *55*, 550–557.

Besson, P., Driffort, V., Bon, É., Gradek, F., Chevalier, S., and Roger, S. (2015). How do voltage-gated sodium channels enhance migration and invasiveness in cancer cells? Biochim. Biophys. Acta - Biomembr. *1848*, 2493–2501.

Bettelli, E. (2007a). Building different mouse models for human MS. Ann. N. Y. Acad. Sci. *1103*, 11–18.

Bettelli, E. (2007b). Building different mouse models for human MS. Ann. N. Y. Acad. Sci. *1103*, 11–18.

Bettelli, E., Pagany, M., Weiner, H.L., Linington, C., Sobel, R.A., and Kuchroo, V.K. (2003). Myelin oligodendrocyte glycoprotein-specific T cell receptor transgenic mice develop spontaneous autoimmune optic neuritis. J. Exp. Med. *197*, 1073–1081.

Bielekova, B., Goodwin, B., Richert, N., Cortese, I., Kondo, T., Afshar, G., Gran, B., Eaton, J., Antel, J., Frank, J.A., et al. (2000). Encephalitogenic potential of the myelin basic protein peptide (amino acids 83-99) in multiple sclerosis: Results of a phase II clinical trial with an altered peptide ligand. Nat. Med. *6*, 1167–1175.

Bitan, M., Weiss, L., Reibstein, I., Zeira, M., Fellig, Y., Slavin, S., Zcharia, E., Nagler, A., and Vlodavsky, I. (2010). Heparanase upregulates Th2 cytokines, ameliorating experimental autoimmune encephalitis. Mol. Immunol. *47*, 1890–1898.

Bitsch, A. (2000). Acute axonal injury in multiple sclerosis: Correlation with demyelination and inflammation. Brain *123*, 1174–1183.

Bjartmar, C., Wujek, J.R., and Trapp, B.D. (2003). Axonal loss in the pathology of MS: Consequences for understanding the progressive phase of the disease. J. Neurol. Sci. *206*, 165–171.

Black, J.A., and Waxman, S.G. (2013). Noncanonical roles of voltage-gated sodium channels. Neuron *80*, 280–291.

Black, J.A., Westenbroek, R.E., Catterall, W.A., and Waxman, S.G. (1995). Type II brain sodium channel expression in non-neuronal cells: embryonic rat osteoblasts. Mol. Brain Res. *34*, 89–98.

Black, J.A., Liu, S., Tanaka, M., Cummins, T.R., and Waxman, S.G. (2004). Changes in the expression of tetrodotoxin-sensitive sodium channels within dorsal root ganglia neurons in inflammatory pain. Pain *108*, 237–247.

Black, J.A., Liu, S., Carrithers, M., Carrithers, L.M., and Waxman, S.G. (2007). Exacerbation of experimental autoimmune encephalomyelitis after withdrawal of phenytoin and carbamazepine. Ann. Neurol. *62*, 21–33.

Black, J.A., Liu, S., and Waxman, S.G. (2009a). Sodium channel activity modulates multiple functions in microglia. Glia *57*, 1072–1081.

Black, J.A., Liu, S., and Waxman, S.G. (2009b). Sodium channel activity modulates multiple functions in microglia. Glia *57*, 1072–1081.

Black, J.A., Newcombe, J., and Waxman, S.G. (2010). Astrocytes within multiple sclerosis lesions upregulate sodium channel Nav1.5. Brain *133*, 835–846.

Black, J.A., Nikolajsen, L., Kroner, K., Jensen, T.S., and Waxman, S.G. (2018). Multiple sodium channel isoforms and mitogen-activated protein kinases are present in painful human neuromas. In Chasing Men on Fire: The Story of the Search for a Pain Gene, pp. 139–153.

Blackburn, D., Sargsyan, S., Monk, P.N., and Shaw, P.J. (2009). Astrocyte function and role in motor neuron disease: A future therapeutic target? Glia *57*, 1251–1264.

Boiko, T., Rasband, M.N., Levinson, S.R., Caldwell, J.H., Mandel, G., Trimmer, J.S., and Matthews, G. (2001). Compact myelin dictates the differential targeting of two sodium channel isoforms in the same axon. Neuron *30*, 91–104.

Botos, I., Segal, D.M., and Davies, D.R. (2011). The structural biology of Toll-like receptors. Structure *19*, 447–459.

Bouafia, A., Golmard, J.L., Thuries, V., Sazdovitch, V., Hauw, J.J., Fontaine, B., and Seilhean, D. (2014). Axonal expression of sodium channels and neuropathology of the plaques in multiple sclerosis. Neuropathol. Appl. Neurobiol. *40*, 579–590.

Bouaziz, J.D., Yanaba, K., and Tedder, T.F. (2008). Regulatory B cells as inhibitors of immune responses and inflammation. Immunol. Rev. *224*, 201–214.

Brackenbury, W.J., and Isom, L.L. (2011). Na+ channel β subunits: Overachievers of the ion channel family. Front. Pharmacol. *SEP*.

Brackenbury, W.J., Calhoun, J.D., Chen, C., Miyazaki, H., Nukina, N., Oyama, F., Ranscht, B., and Isom, L.L. (2010). Functional reciprocity between Na+ channel Nav1.6 and β1 subunits in the coordinated regulation of excitability and neurite outgrowth. Proc. Natl. Acad. Sci. U. S. A. *107*, 2283–2288.

Bradding, P., Okayama, Y., Kambe, N., and Saito, H. (2003). Ion channel gene expression in human lung, skin, and cord blood-derived mast cells. J. Leukoc. Biol. *73*, 614–620.

Brennan, C.A., and Anderson, K. V. (2004). D rosophila : The Genetics of Innate Immune Recognition and Response . Annu. Rev. Immunol. *22*, 457–483.

Brodie, M.J. (2017). Tolerability and Safety of Commonly Used Antiepileptic Drugs in Adolescents and Adults: A Clinician's Overview. CNS Drugs *31*, 135–147.

Brown, D.A., and Sawchenko, P.E. (2007). Time course and distribution of inflammatory and neurodegenerative events suggest structural bases for the pathogenesis of experimental autoimmune encephalomyelitis. J. Comp. Neurol. *502*, 236–260.

Bsibsi, M., Ravid, R., Gveric, D., and Van Noort, J.M. (2002). Broad expression of Toll-like receptors in the human central nervous system. J. Neuropathol. Exp. Neurol. *61*, 1013–1021.

Bucher, K., Schmitt, F., Autenrieth, S.E., Dillmann, I., Nürnberg, B., Schenke-Layland, K., and Beer-Hammer, S. (2015). Fluorescent Ly6G antibodies determine macrophage phagocytosis of neutrophils and alter the retrieval of neutrophils in mice. J. Leukoc. Biol.

Buffington, S.A., and Rasband, M.N. (2013). Structure and Function of Myelinated Axons. In Comprehensive Developmental Neuroscience: Patterning and Cell Type Specification in the Developing CNS and PNS, pp. 707–722.

Burda, J.E., and Sofroniew, M. V. (2014). Reactive gliosis and the multicellular response to CNS damage and disease. Neuron *81*, 229–248.

Burgess, D.L., Kohrman, D.C., Galt, J., Plummer, N.W., Jones, J.M., Spear, B., and Meisler, M.H. (1995a). Mutation of a new sodium channel gene, Scn8a, in the mouse mutant 'motor endplate disease.' Nat. Genet. *10*, 461–465.

Burgess, D.L., Kohrman, D.C., Galt, J., Plummer, N.W., Jones, J.M., Spear, B., and Meisler, M.H. (1995b). Mutation of a new sodium channel gene, Scn8a, in the mouse mutant 'motor endplate disease.' Nat. Genet. *10*, 461–465.

Carrithers, M.D., Chatterjee, G., Carrithers, L.M., Offoha, R., Iheagwara, U., Rahner, C., Graham, M., and Waxman, S.G. (2009a). Regulation of podosome formation in macrophages by a splice variant of the sodium channel SCN8A. J. Biol. Chem. *284*, 8114–8126.

Carrithers, M.D., Chatterjee, G., Carrithers, L.M., Offoha, R., Iheagwara, U., Rahner, C., Graham, M., and Waxman, S.G. (2009b). Regulation of podosome formation in macrophages by a splice variant of the sodium channel SCN8A. J. Biol. Chem. *284*, 8114–8126.

Casula, M.A., Facer, P., Powell, A.J., Kinghorn, I.J., Plumpton, C., Tate, S.N., Bountra, C., Birch, R., and Anand, P. (2004). Expression of the sodium channel β3 subunit in injured human sensory neurons. Neuroreport *15*, 1629–1632.

Catterall, W.A. (2000). From ionic currents to molecular mechanisms: The structure and function of voltage-gated sodium channels. Neuron *26*, 13–25.

Catterall, W.A. (2013). Voltage-Gated Sodium Channels: Structure, Function, and Pathophysiology. In Encyclopedia of Biological Chemistry: Second Edition, pp. 564–569.

Catterall, W.A., Goldin, A.L., and Waxman, S.G. (2005a). Nomenclature and structure-function relationships of voltage-gated sodium channels. Pharmacol. Rev. *57*, 397–409.

Catterall, W.A., Perez-Reyes, E., Snutch, T.P., and Striessnig, J. (2005b). International Union of Pharmacology. XLVIII. Nomenclature and structure-function relationships of voltage-gated calcium channels. Pharmacol. Rev. *57*, 411–425.

Centonze, D., Muzio, L., Rossi, S., Furlan, R., Bernardi, G., and Martino, G. (2010). The link between inflammation, synaptic transmission and neurodegeneration in multiple sclerosis. Cell Death Differ. *17*, 1083–1091.

Chen, C., Bharucha, V., Chen, Y., Westenbroek, R.E., Brown, A., Malhotra, J.D., Jones, D., Avery, C., Gillespie, P.J., Kazen-Gillespie, K.A., et al. (2002). Reduced sodium channel density, altered voltage dependence of inactivation, and increased susceptibility to seizures in mice lacking sodium channel β2-subunits. Proc. Natl. Acad. Sci. U. S. A. *99*, 17072–17077.

Chen, L., Huang, J., Zhao, P., Persson, A.K., Dib-Hajj, F.B., Cheng, X., Tan, A., Waxman, S.G., and Dib-Hajj, S.D. (2018a). Conditional knockout of Na V 1.6 in adult mice ameliorates neuropathic pain. Sci. Rep. *8*.

Chen, L., Huang, J., Zhao, P., Persson, A.K., Dib-Hajj, F.B., Cheng, X., Tan, A., Waxman, S.G., and Dib-Hajj, S.D. (2018b). Conditional knockout of NaV1.6 in adult mice ameliorates neuropathic pain. Sci. Rep. *8*.

Chen, Q., Davidson, T.S., Huter, E.N., and Shevach, E.M. (2009). Engagement of TLR2 Does not Reverse the Suppressor Function of Mouse Regulatory T Cells, but Promotes Their Survival. J. Immunol. *183*, 4458–4466.

Chen, W., Sheng, J., Guo, J., Peng, G., Hong, J., Li, B., Chen, X., Li, K., and Wang, S. (2017). Cytokine cascades induced by mechanical trauma injury alter voltage-gated sodium channel activity in intact cortical neurons. J. Neuroinflammation *14*.

Chow, J.C., Young, D.W., Golenbock, D.T., Christ, W.J., and Gusovsky, F. (1999). Toll-like receptor-4 mediates lipopolysaccharide-induced signal transduction. J. Biol. Chem. *274*, 10689–10692.

Chrobok, N.L., Jaouen, A., Fenrich, K.K., Bol, J.G.J.M., Wilhelmus, M.M.M., Drukarch, B., Debarbieux, F., and van Dam, A.M. (2017). Monocyte behaviour and tissue transglutaminase expression during experimental autoimmune encephalomyelitis in transgenic CX3CR1 gfp/gfp mice. Amino Acids *49*, 643–658.

Claes, L., Ceulemans, B., Audenaert, D., Smets, K., Löfgren, A., Del-Favero, J., Ala-Mello, S., Basel-Vanagaite, L., Plecko, B., Raskin, S., et al. (2003). De novo SCN1A mutations are a major cause of severe myoclonic epilepsy of infancy. Hum. Mutat. *21*, 615–621.

Claes, N., Fraussen, J., Stinissen, P., Hupperts, R., and Somers, V. (2015). B cells are multifunctional players in multiple sclerosis pathogenesis: Insights from therapeutic interventions. Front. Immunol. *6*.

Cohen, J.A., Barkhof, F., Comi, G., Hartung, H.P., Khatri, B.O., Montalban, X., Pelletier, J., Capra, R., Gallo, P., Izquierdo, G., et al. (2010). Oral fingolimod or intramuscular interferon for relapsing multiple sclerosis. N. Engl. J. Med. *362*, 402–415.

Coles, A. (2009). Multiple sclerosis: THE BARE ESSENTIALS. Pract. Neurol. *9*, 118–126.

Constantinescu, C.S., Farooqi, N., O'Brien, K., and Gran, B. (2011). Experimental autoimmune encephalomyelitis (EAE) as a model for multiple sclerosis (MS). Br. J. Pharmacol. *164*, 1079–1106.

Côté, P.D., De Repentigny, Y., Coupland, S.G., Schwab, Y., Roux, M.J., Levinson, S.R., and Kothary, R. (2005). Physiological maturation of photoreceptors depends on the voltage-gated sodium channel NaV1.6 (Scn8a). J. Neurosci. *25*, 5046–5050.

Cotsapas, C., and Mitrovic, M. (2018). Genome-wide association studies of multiple sclerosis. Clin. Transl. Immunol. *7*.

Craner, M.J. (2003). Abnormal sodium channel distribution in optic nerve axons in a model of inflammatory demyelination. Brain *126*, 1552–1561.

Craner, M.J., Newcombe, J., Black, J.A., Hartle, C., Cuzner, M.L., and Waxman, S.G. (2004a). Molecular changes in neurons in multiple sclerosis: Altered axonal expression of Nav1.2 and Nav1.6 sodium channels and Na+/Ca2+ exchanger. Proc. Natl. Acad. Sci. U. S. A. *101*, 8168–8173.

Craner, M.J., Hains, B.C., Lo, A.C., Black, J.A., and Waxman, S.G. (2004b). Co-localization of sodium channel Nav1.6 and the sodium-calcium exchanger at sites of axonal injury in the spinal cord in EAE. Brain *127*, 294–303.

Craner, M.J., Newcombe, J., Black, J.A., Hartle, C., Cuzner, M.L., and Waxman, S.G. (2004c). Molecular changes in neurons in multiple sclerosis: Altered axonal expression of Nav1.2 and Nav1.6 sodium channels and Na+/Ca2+ exchanger. Proc. Natl. Acad. Sci. *101*, 8168–8173.

Craner, M.J., Hains, B.C., Lo, A.C., Black, J.A., and Waxma, S.G. (2004d). Co-localization of sodium channel Nav1 . 6 and the sodium-calcium exchanger at ... Brain *127*, 294–303.

Craner, M.J., Damarjian, T.G., Liu, S., Hains, B.C., Lo, A.C., Black, J.A., Newcombe, J., Cuzner, M.L., and Waxman, S.G. (2005). Sodium channels contribute to microglia/macrophage activation and function in EAE and MS. Glia *49*, 220–229.

Crocker, P.R., and Gordon, S. (1985). Isolation and characterization of resident stromal macrophages and hematopoietic cell clusters from mouse bone marrow. J. Exp. Med. *162*, 993–1014.

Croxford, J.L., Feldmann, M., Chernajovsky, Y., and Baker, D. (2001). Different Therapeutic Outcomes in Experimental Allergic Encephalomyelitis Dependant Upon the Mode of Delivery of IL-10: A Comparison of the Effects of Protein, Adenoviral or Retroviral IL-10 Delivery into the Central Nervous System. J. Immunol. *166*, 4124–4130.

Cummins, T.R., Dib-Hajj, S.D., and Waxman, S.G. (2004). Electrophysiological properties of mutant Nav1.7 sodium channels in a painful inherited neuropathy. J. Neurosci. *24*, 8232–8236.

Currier, R.D., and Eldridge, R. (1982). Possible Risk Factors in Multiple Sclerosis as Found in a National Twin Study. Arch. Neurol. *39*, 140–144.

Daley, J.M., Thomay, A.A., Connolly, M.D., Reichner, J.S., and Albina, J.E. (2008). Use of Ly6G-specific monoclonal antibody to deplete neutrophils in mice. J. Leukoc. Biol. *83*, 64–70.

Dean, G., and Elian, M. (1997). Age at immigration to England of Asian and Caribbean immigrants and the risk of developing multiple sclerosis. J. Neurol. Neurosurg. Psychiatry *63*, 565–568.

Debanne, D. (2004). Information processing in the axon. Nat. Rev. Neurosci. *5*, 304–316.

Dendrou, C.A., Fugger, L., and Friese, M.A. (2015). Immunopathology of multiple sclerosis. Nat. Rev. Immunol. *15*, 545–558.

Detta, N., Frisso, G., and Salvatore, F. (2015). The multi-faceted aspects of the complex cardiac Nav1.5 protein in membrane function and pathophysiology. Biochim. Biophys. Acta - Proteins Proteomics *1854*, 1502–1509.

Dib-Hajj, S.D., Rush, A.M., Cummins, T.R., Hisama, F.M., Novella, S., Tyrrell, L., Marshall, L., and Waxman, S.G. (2005). Gain-of-function mutation in Nav1.7 in familial erythromelalgia induces bursting of sensory neurons. Brain *128*, 1847–1854.

Ding, H.H., Zhang, S.B., Lv, Y.Y., Ma, C., Liu, M., Zhang, K.B., Ruan, X.C., Wei, J.Y., Xin, W.J., and Wu, S.L. (2019). TNF-α/STAT3 pathway epigenetically upregulates Nav1.6 expression in DRG and contributes to neuropathic pain induced by L5-VRT. J. Neuroinflammation *16*.

Dong, C. (2008). TH17 cells in development: An updated view of their molecular identity and genetic programming. Nat. Rev. Immunol. *8*, 337–348.

Duffy, S.S., Lees, J.G., and Moalem-Taylor, G. (2014). The Contribution of Immune and Glial Cell Types in Experimental Autoimmune Encephalomyelitis and Multiple Sclerosis. Mult. Scler. Int. *2014*, 1–17.

Dulay, A.T., Buhimschi, C.S., Zhao, G., Oliver, E.A., Mbele, A., Jing, S., and Buhimschi, I.A. (2009). Soluble TLR2 Is Present in Human Amniotic Fluid and Modulates the Intraamniotic Inflammatory Response to Infection. J. Immunol. *182*, 7244–7253.

Eijkelkamp, N., Linley, J.E., Baker, M.D., Minett, M.S., Cregg, R., Werdehausen, R., Rugiero, F., and Wood, J.N. (2012). Neurological perspectives on voltage-gated sodium channels. Brain *135*, 2585–2612.

Engelhardt, B., and Ransohoff, R.M. (2012). Capture, crawl, cross: The T cell code to breach the blood-brain barriers. Trends Immunol. *33*, 579–589.

England, J.D., Gamboni, F., and Levinson, S.R. (1991). Increased numbers of sodium channels form along demyelinated axons. Brain Res. *548*, 334–337.

Esser, S., Göpfrich, L., Bihler, K., Kress, E., Nyamoya, S., Tauber, S.C., Clarner, T., Stope, M.B., Pufe, T., Kipp, M., et al. (2018). Toll-Like Receptor 2-Mediated Glial Cell Activation in a Mouse Model of Cuprizone-Induced Demyelination. Mol. Neurobiol. *55*, 6237–6249.

Estacion, M., Gasser, A., Dib-Hajj, S.D., and Waxman, S.G. (2010). A sodium channel mutation linked to epilepsy increases ramp and persistent current of Nav1.3 and induces hyperexcitability in hippocampal neurons. Exp. Neurol. *224*, 362–368.

Ferguson, B., Matyszak, M.K., Esiri, M.M., and Perry, V.H. (1997). Axonal damage in acute multiple sclerosis lesions. Brain *120*, 393–399.

Fermino, M.L., Da Polli, C., Toledo, K.A., Liu, F.T., Hsu, D.K., Roque-Barreira, M.C., Pereira-da-Silva, G., Bernardes, E.S., and Halbwachs-Mecarelli, L. (2011). LPS-induced galectin-3 oligomerization results in enhancement of neutrophil activation. PLoS One *6*.

Ferrini, F., and De Koninck, Y. (2013). Microglia control neuronal network excitability via BDNF signalling. Neural Plast. *2013*.

Fillatreau, S., Sweenie, C.H., McGeachy, M.J., Gray, D., and Anderton, S.M. (2002). B cells regulate autoimmunity by provision of IL-10. Nat. Immunol. *3*, 944–950.

Fischer, F.R., Santambrogio, L., Luo, Y., Berman, M.A., Hancock, W.W., and Dorf, M.E. (2000). Modulation of experimental autoimmune encephalomyelitis: Effect of altered peptide ligand on chemokine and chemokine receptor expression. J. Neuroimmunol. *110*, 195–208.

Foster, R.E., Whalen, C.C., and Waxman, S.G. (1980). Reorganization of the axon membrane in demyelinated peripheral nerve fibers: Morphological evidence. Science (80-.). *210*, 661–663.

Franco, R., and Fernández-Suárez, D. (2015). Alternatively activated microglia and macrophages in the central nervous system. Prog. Neurobiol. *131*, 65–86.

Fraser, S.P., Diss, J.K.J., Lloyd, L.J., Pani, F., Chioni, A.M., George, A.J.T., and Djamgoz, M.B.A. (2004). T-lymphocyte invasiveness: Control by voltage-gated Na+ channel activity. FEBS Lett. *569*, 191–194.

Fraser, S.P., Ozerlat-Gunduz, I., Brackenbury, W.J., Fitzgerald, E.M., Campbell, T.M., Coombes, R.C., and Djamgoz, M.B.A. (2014). Regulation of voltage-gated sodium channel expression in cancer: Hormones, growth factors and auto-regulation. Philos. Trans. R. Soc. B Biol. Sci. *369*.

Freeman, S.A., Desmazières, A., Fricker, D., Lubetzki, C., and Sol-Foulon, N. (2016). Mechanisms of sodium channel clustering and its influence on axonal impulse conduction. Cell. Mol. Life Sci. *73*, 723–735.

Friese, M.A., and Fugger, L. (2009). Pathogenic CD8 + T cells in multiple sclerosis. Ann. Neurol. *66*, 132–141.

Friese, M.A., Montalban, X., Willcox, N., Bell, J.I., Martin, R., and Fugger, L. (2006). The value of animal models for drug development in multiple sclerosis. Brain *129*, 1940–1952.

Friese, M.A., Schattling, B., and Fugger, L. (2014). Mechanisms of neurodegeneration and axonal dysfunction in multiple sclerosis. Nat. Rev. Neurol. *10*, 225–238.

Frohman, E.M., Racke, M.K., and Raine, C.S. (2006). Medical progress: Multiple sclerosis - The plaque and its pathogenesis. N. Engl. J. Med. *354*, 942–955.

Frohman, E.M., Costello, F., Stüve, O., Calabresi, P., Miller, D.H., Hickman, S.J., Sergott, R., Conger, A., Salter, A., Krumwiede, K.H., et al. (2008). Modeling axonal degeneration within the anterior visual system: Implications for demonstrating neuroprotection in multiple sclerosis. Arch. Neurol. *65*, 26–35.

García-Vallejo, J.J., Ilarregui, J.M., Kalay, H., Chamorro, S., Koning, N., Unger, W.W., Ambrosini, M., Montserrat, V., Fernandes, R.J., Bruijns, S.C.M., et al. (2014). CNS myelin induces regulatory functions of DC-SIGN-expressing, antigen-presenting cells via cognate interaction with MOG. J. Exp. Med. *211*, 1465–1483.

Garthwaite, G., Goodwin, D.A., Batchelor, A.M., Leeming, K., and Garthwaite, J. (2002). Nitric oxide toxicity in CNS white matter: An in vitro study using rat optic nerve. Neuroscience *109*, 145–155.

Van Gassen, K.L.I., De Wit, M., Van Kempen, M., Saskia Van Der Hel, W., Van Rijen, P.C., Jackson, A.P., Lindhout, D., and De Graan, P.N.E. (2009). Hippocampal Navβ3 expression in patients with temporal lobe epilepsy. Epilepsia *50*, 957–962.

Gasser, A., Cheng, X., Gilmore, E.S., Tyrrell, L., Waxman, S.G., and Dib-Hajj, S.D. (2010). Two Nedd4-binding motifs underlie modulation of sodium channel Na v1.6 by p38 MAPK. J. Biol. Chem. *285*, 26149–26161.

Ghosh, M., Xu, Y., and Pearse, D.D. (2016). Cyclic AMP is a key regulator of M1 to M2a phenotypic conversion of microglia in the presence of Th2 cytokines. J. Neuroinflammation *13*.

Ginhoux, F., Greter, M., Leboeuf, M., Nandi, S., See, P., Gokhan, S., Mehler, M.F., Conway, S.J., Ng, L.G., Stanley, E.R., et al. (2010). Fate mapping analysis reveals that adult microglia derive from primitive macrophages. Science (80-.). *330*, 841–845.

Giuliodori, M.J., and DiCarlo, S.E. (2004). Myelinated vs. unmyelinated nerve conduction: A novel way of understanding the mechanisms. Am. J. Physiol. - Adv. Physiol. Educ. *28*, 80–81.

Goldenberg, M.M. (2012). Multiple sclerosis review. P T *37*, 175–184.

Gomi, K., Kawasaki, K., Kawai, Y., Shiozaki, M., and Nishijima, M. (2002). Toll-Like Receptor 4-MD-2 Complex Mediates the Signal Transduction Induced by Flavolipin, an Amino Acid-Containing Lipid Unique to Flavobacterium meningosepticum . J. Immunol. *168*, 2939–2943.

Gong, B., Rhodes, K.J., Bekele-Arcuri, Z., and Trimmer, J.S. (1999). Type I and type II Na+ channel α-subunit polypeptides exhibit distinct spatial and temporal patterning, and association with auxiliary subunits in rat brain. J. Comp. Neurol. *412*, 342–352.

Gorter, J.A., Zurolo, E., Iyer, A., Fluiter, K., Van Vliet, E.A., Baayen, J.C., and Aronica, E. (2010). Induction of sodium channel Nax (SCN7A) expression in rat and human hippocampus in temporal lobe epilepsy. Epilepsia *51*, 1791–1800.

Grist, J.J., Marro, B.S., Skinner, D.D., Syage, A.R., Worne, C., Doty, D.J., Fujinami, R.S., and Lane, T.E. (2018). Induced CNS expression of CXCL1 augments neurologic disease in a murine model of multiple sclerosis via enhanced neutrophil recruitment. Eur. J. Immunol. *48*, 1199–1210.

Gudi, V., Gingele, S., Skripuletz, T., and Stangel, M. (2014). Glial response during cuprizone-induced de- and remyelination in the CNS: Lessons learned. Front. Cell. Neurosci. *8*.

Guy, J., Ellis, E.A., Hope, G.M., and Emerson, S. (1991). Maintenance of myelinated fibre g ratio in acute experimental allergic encephalomyelitis. Brain *114A*, 281–294.

Hafler, D.A., Buchsbaum, M., Johnson, D., and Weiner, H.L. (1985). Phenotypic and functional analysis of T cells cloned directly from the blood and cerebrospinal fluid of patients with multiple sclerosis. Ann. Neurol. *18*, 451–458.

Hafler, D.A., Compston, A., Sawcer, S., Lander, E.S., Daly, M.J., De Jager, P.L., De Bakker, P.I.W., Gabriel, S.B., Mirel, D.B., Ivinson, A.J., et al. (2007). Risk alleles for multiple sclerosis identified by a genomewide study. N. Engl. J. Med. *357*, 851–862.

Hains, B.C., Klein, J.P., Saab, C.Y., Craner, M.J., Black, J.A., and Waxman, S.G. (2003).

Upregulation of sodium channel Nav1.3 and functional involvement in neuronal hyperexcitability associated with central neuropathic pain after spinal cord injury. J. Neurosci. *23*, 8881–8892.

Han, C., Huang, J., and Waxman, S.G. (2016). Sodium channel Nav1.8: Emerging links to human disease. Neurology *86*, 473–783.

Hanke, M.L., and Kielian, T. (2011). Toll-like receptors in health and disease in the brain: mechanisms and therapeutic potential. Clin. Sci. *121*, 367–387.

Hargus, N.J., Nigam, A., Bertram, E.H., and Patel, M.K. (2013). Evidence for a role of Na v 1.6 in facilitating increases in neuronal hyperexcitability during epileptogenesis . J. Neurophysiol. *110*, 1144–1157.

Harrington, L.E., Hatton, R.D., Mangan, P.R., Turner, H., Murphy, T.L., Murphy, K.M., and Weaver, C.T. (2005). Interleukin 17-producing CD4+ effector T cells develop via a lineage distinct from the T helper type 1 and 2 lineages. Nat. Immunol. *6*, 1123–1132.

Harris, H.E., and Raucci, A. (2006). Alarmin(g) news about danger: Workshop on Innate Danger Signals and HMGB1. In EMBO Reports, pp. 774–778.

Hein, K., Gadjanski, I., Kretzschmar, B., Lange, K., Diem, R., Sättler, M.B., and Bähr, M. (2012). An optical coherence tomography study on degeneration of retinal nerve fiber layer in rats with autoimmune optic neuritis. Investig. Ophthalmol. Vis. Sci. *53*, 157–163.

Heinrich, P.C., Behrmann, I., Haan, S., Hermanns, H.M., Müller-Newen, G., and Schaper, F. (2003). Principles of interleukin (IL)-6-type cytokine signalling and its regulation. Biochem. J. *374*, 1–20.

Hellström, M., Ruitenberg, M.J., Pollett, M.A., Ehlert, E.M.E., Twisk, J., Verhaagen, J., and Harvey, A.R. (2009). Cellular tropism and transduction properties of seven adeno-associated viral vector serotypes in adult retina after intravitreal injection. Gene Ther. *16*, 521–532.

Hemmer, B., Kerschensteiner, M., and Korn, T. (2015). Role of the innate and adaptive immune responses in the course of multiple sclerosis. Lancet Neurol. *14*, 406–419.

Hernandez-Plata, E., Ortiz, C.S., Marquina-Castillo, B., Medina-Martinez, I., Alfaro, A., Berumen, J., Rivera, M., and Gomora, J.C. (2012). Overexpression of Na V1.6 channels is associated with the invasion capacity of human cervical cancer. Int. J. Cancer *130*, 2013–2023.

Höftberger, R., Leisser, M., Bauer, J., and Lassmann, H. (2015). Autoimmune encephalitis in humans: how closely does it reflect multiple sclerosis ? Acta Neuropathol. Commun. *3*, 80.

Holland, K.D., Kearney, J.A., Glauser, T.A., Buck, G., Keddache, M., Blankston, J.R., Glaaser, I.W., Kass, R.S., and Meisler, M.H. (2008). Mutation of sodium channel SCN3A in a patient with cryptogenic pediatric partial epilepsy. Neurosci. Lett. *433*, 65–70.

Van Horssen, J., Witte, M.E., Schreibelt, G., and de Vries, H.E. (2011). Radical changes in multiple sclerosis pathogenesis. Biochim. Biophys. Acta - Mol. Basis Dis. *1812*, 141–150.

Horstmann, L., Schmid, H., Heinen, A.P., Kurschus, F.C., Dick, H.B., and Joachim, S.C. (2013). Inflammatory demyelination induces glia alterations and ganglion cell loss in the retina of an experimental autoimmune encephalomyelitis model. J. Neuroinflammation *10*.

Horstmann, L., Kuehn, S., Pedreiturria, X., Haak, K., Pfarrer, C., Dick, H.B., Kleiter, I., and Joachim, S.C. (2016). Microglia response in retina and optic nerve in chronic experimental autoimmune encephalomyelitis. J. Neuroimmunol. *298*, 32–41.

Hossain, M.J., Tanasescu, R., and Gran, B. (2015). TLR2 - an innate immune checkpoint in multiple sclerosis. Oncotarget *6*, 35131–35132.

Hossain, M.J., Tanasescu, R., and Gran, B. (2017). Innate immune regulation of autoimmunity in multiple sclerosis: Focus on the role of Toll-like receptor 2. J. Neuroimmunol. *304*, 11–20.

Hossain, M.J., Morandi, E., Tanasescu, R., Frakich, N., Caldano, M., Onion, D., Faraj, T.A., Erridge, C., and Gran, B. (2018a). The soluble form of toll-like receptor 2 is elevated in serum of multiple sclerosis patients: A novel potential disease biomarker. Front. Immunol. *9*.

Hossain, M.M., Weig, B., Reuhl, K., Gearing, M., Wu, L.J., and Richardson, J.R. (2018b). The anti-parkinsonian drug zonisamide reduces neuroinflammation: Role of microglial Na v 1.6. Exp. Neurol. *308*, 111–119.

Howarth, C., Gleeson, P., and Attwell, D. (2012). Updated energy budgets for neural computation in the neocortex and cerebellum. J. Cereb. Blood Flow Metab. *32*, 1222–1232.

Iglesias, A., Bauer, J., Litzenburger, T., Schubart, A., and Linington, C. (2001). T- and B-cell responses to myelin oligodendrocyte glycoprotein in experimental autoimmune encephalomyelitis and multiple sclerosis. Glia *36*, 220–234.

Ignjatović, A., Stević, Z., Lavrnić, D., Nikolić-Kokić, A., Blagojević, D., Spasić, M., and Spasojević, I. (2012). Inappropriately chelated iron in the cerebrospinal fluid of amyotrophic lateral sclerosis patients. Amyotroph. Lateral Scler. *13*, 357–362.

Iismaa, S.E., Mearns, B.M., Lorand, L., and Graham, R.M. (2009). Transglutaminases and disease: Lessons from genetically engineered mouse models and inherited disorders. Physiol. Rev. *89*, 991–1023.

Imitola, J., Chitnis, T., and Khoury, S.J. (2005). Cytokines in multiple sclerosis: From bench to bedside. Pharmacol. Ther. *106*, 163–177.

Ioannou, M., Alissafi, T., Lazaridis, I., Deraos, G., Matsoukas, J., Gravanis, A., Mastorodemos, V., Plaitakis, A., Sharpe, A., Boumpas, D., et al. (2014). Correction: Crucial Role of Granulocytic Myeloid-Derived Suppressor Cells in the Regulation of Central Nervous System Autoimmune Disease. J. Immunol. *192*, 1334–1334.

Israel, M.R., Tanaka, B.S., Castro, J., Thongyoo, P., Robinson, S.D., Zhao, P., Deuis, J.R., Craik, D.J., Durek, T., Brierley, S.M., et al. (2019). NaV1.6 regulates excitability of mechanosensitive sensory neurons. J. Physiol. *597*, 3751–3768.

Jacobsen, F.A., Scherer, A.N., Mouritsen, J., Bragadóttir, H., Thomas Bäckström, B., Sardar, S., Holmberg, D., Koleske, A.J., and Andersson, Å. (2018). A Role for the Non-Receptor Tyrosine Kinase Abl2/Arg in Experimental Neuroinflammation. J. Neuroimmune Pharmacol. *13*, 265–276.

Jacobsen, M., Cepok, S., Quak, E., Happel, M., Gaber, R., Ziegler, A., Schock, S., Oertel, W.H., Sommer, N., and Hemmer, B. (2002). Oligoclonal expansion of memory CD8+ T cells in cerebrospinal fluid from multiple sclerosis patients. Brain *125*, 538–550.

Janeway, C.A., and Medzhitov, R. (2002). I Nnate I Mmune R Ecognition . Annu. Rev. Immunol. *20*, 197–216.

Jang, J.H., Shin, H.W., Lee, J.M., Lee, H.W., Kim, E.C., and Park, S.H. (2015). An Overview of Pathogen Recognition Receptors for Innate Immunity in Dental Pulp. Mediators Inflamm. *2015*.

Jiang, Z., Jiang, J.X., and Zhang, G.X. (2014). Macrophages: A double-edged sword in experimental autoimmune encephalomyelitis. Immunol. Lett. *160*, 17.

Jin, M.S., and Lee, J.O. (2008). Structures of the Toll-like Receptor Family and Its Ligand Complexes. Immunity *29*, 182–191.

Jones, J.L., Anderson, J.M., Phuah, C.L., Fox, E.J., Selmaj, K., Margolin, D., Lake, S.L., Palmer, J., Thompson, S.J., Wilkins, A., et al. (2010). Improvement in disability after alemtuzumab treatment of multiple sclerosis is associated with neuroprotective autoimmunity. Brain *133*, 2232–2247.

Jönsson, F., Mancardi, D.A., Kita, Y., Karasuyama, H., Iannascoli, B., Van Rooijen, N., Shimizu, T., Daëron, M., and Bruhns, P. (2011). Mouse and human neutrophils induce anaphylaxis. J. Clin. Invest. *121*, 1484–1496.

Jurewicz, A., Matysiak, M., Tybor, K., Kilianek, L., Raine, C.S., and Selmaj, K. (2005). Tumour necrosis factor-induced death of adult human oligodendrocytes is mediated by apoptosis inducing factor. Brain *128*, 2675–2688.

Jurkat-Rott, K., Holzherr, B., Fauler, M., and Lehmann-Horn, F. (2010). Sodium channelopathies of skeletal muscle result from gain or loss of function. Pflugers Arch. Eur. J. Physiol. *460*, 239–248.

Kalampokis, I., Yoshizaki, A., and Tedder, T.F. (2013). IL-10-producing regulatory B cells (B10 cells) in autoimmune disease. Arthritis Res. Ther. *15*.

Kann, O., and Kovács, R. (2007). Mitochondria and neuronal activity. Am. J. Physiol. - Cell Physiol. *292*.

Kaplan, M.R., Cho, M.H., Ullian, E.M., Isom, L.L., Levinson, S.R., and Barres, B.A. (2001). Differential control of clustering of the sodium channels Nav1.2 and Nav1.6 at developing CNS nodes of Ranvier. Neuron *30*, 105–119.

Kapoor, R., Davies, M., Blaker, P.A., Hall, S.M., and Smith, K.J. (2003). Blockers of sodium and calcium entry protect axons from nitric oxide-mediated degeneration. Ann. Neurol. *53*, 174–180.

Kapoor, R., Furby, J., Hayton, T., Smith, K.J., Altmann, D.R., Brenner, R., Chataway, J., Hughes, R.A., and Miller, D.H. (2010). Lamotrigine for neuroprotection in secondary progressive multiple sclerosis: a randomised, double-blind, placebo-controlled, parallel-group trial. Lancet Neurol. *9*, 681–688.

Kasper, L.H., and Shoemaker, J. (2010). Multiple sclerosis immunology: The healthy immune system vs the MS immune system. Neurology *74*, S2.

Kawai, T., and Akira, S. (2009). The roles of TLRs, RLRs and NLRs in pathogen recognition. Int. Immunol. *21*, 317–337.

Kawai, T., and Akira, S. (2010). The role of pattern-recognition receptors in innate immunity: Update on toll-like receptors. Nat. Immunol. *11*, 373–384.

Kawai, T., and Akira, S. (2011). Toll-like Receptors and Their Crosstalk with Other Innate Receptors in Infection and Immunity. Immunity *34*, 637–650.

Kearney, J.A. (2002). Molecular and pathological effects of a modifier gene on deficiency of the sodium channel Scn8a (Nav1.6). Hum. Mol. Genet. *11*, 2765–2775.

Keating, P., O'Sullivan, D., Tierney, J.B., Kenwright, D., Miromoeini, S., Mawasse, L., Brombacher, F., and La Flamme, A.C. (2009). Protection from EAE by IL-4Rα-/- macrophages depends upon T regulatory cell involvement. Immunol. Cell Biol. *87*, 534–545.

Kemanetzoglou, E., and Andreadou, E. (2017). CNS Demyelination with TNF-α Blockers. Curr. Neurol. Neurosci. Rep.

Kennedy, M.A. (2010). A Brief Review of the Basics of Immunology: The Innate and Adaptive Response. Vet. Clin. North Am. - Small Anim. Pract. *40*, 369–379.

Kerlero De Rosbo, N., Hoffman, M., Mendel, I., Yust, I., Kaye, J., Bakimer, R., Flechter, S., Abramsky, O., Milo, R., Karni, A., et al. (1997). Predominance of the autoimmune response to myelin oligodendrocyte glycoprotein (MOG) in multiple sclerosis: Reactivity to the extracellular domain of MOG is directed against three main regions. Eur. J. Immunol. *27*, 3059–3069.

Kerstetter, A.E., Padovani-Claudio, D.A., Bai, L., and Miller, R.H. (2009). Inhibition of CXCR2 signaling promotes recovery in models of multiple sclerosis. Exp. Neurol. *220*, 44–56.

Kigerl, K.A., Gensel, J.C., Ankeny, D.P., Alexander, J.K., Donnelly, D.J., and Popovich, P.G. (2009). Identification of two distinct macrophage subsets with divergent effects causing either neurotoxicity or regeneration in the injured mouse spinal cord. J. Neurosci. *29*, 13435–13444.

Kim, S.U., and De Vellis, J. (2005). Microglia in health and disease. J. Neurosci. Res. *81*, 302–313.

King, I.L., Dickendesher, T.L., and Segal, B.M. (2009). Circulating Ly-6C + myeloid precursors migrate to the CNS and play a pathogenic role during autoimmune demyelinating disease. Blood *113*, 3190–3197.

Kohrman, D.C., Smith, M.R., Goldin, A.L., Harris, J., and Meisler, M.H. (1996). A missense mutation in the sodium channel Scn8a is responsible for cerebellar ataxia in the mouse mutant jolting. J. Neurosci. *16*, 5993–5999.

Kolaczkowska, E., and Kubes, P. (2013). Neutrophil recruitment and function in health and inflammation. Nat. Rev. Immunol. *13*, 159–175.

Kolbe, S., Chapman, C., Nguyen, T., Bajraszewski, C., Johnston, L., Kean, M., Mitchell, P., Paine, M., Butzkueven, H., Kilpatrick, T., et al. (2009). Optic nerve diffusion changes and atrophy jointly predict visual dysfunction after optic neuritis. Neuroimage *45*, 679–686.

Koopmann, T.T., Bezzina, C.R., and Wilde, A.A.M. (2006). Voltage-gated sodium channels: Action players with many faces. Ann. Med. *38*, 472–482.

Korn, T., Mitsdoerffer, M., and Kuchroo, V.K. (2010). Immunological basis for the development of tissue inflammation and organ-specific autoimmunity in animal models of multiple sclerosis. Results Probl. Cell Differ. *51*, 43–74.

Körner, H., Goodsall, A.L., Lemckert, F.A., Scallon, B.J., Ghrayeb, J., Ford, A.L., and Sedgwick, J.D. (1995). Unimpaired autoreactive T-cell traffic within the central nervous system during tumor necrosis factor receptor-mediated inhibition of experimental autoimmune encephalomyelitis. Proc. Natl. Acad. Sci. U. S. A. *92*, 11066–11070.

Kremer, D., Aktas, O., Hartung, H.P., and Küry, P. (2011). The complex world of oligodendroglial differentiation inhibitors. Ann. Neurol. *69*, 602–618.

Krieg, A.M. (2002). C P G M Otifs in B Acterial Dna and T Heir I Mmune E Ffects . Annu. Rev. Immunol. *20*, 709–760.

Krzemien, D.M., Schaller, K.L., Levinson, S.R., and Caldwell, J.H. (2000). Immunolocalization of sodium channel isoform NaCh6 in the nervous system. J. Comp. Neurol. *420*, 70–83.

Kuerten, S., Kostova-Bales, D.A., Frenzel, L.P., Tigno, J.T., Tary-Lehmann, M., Angelov, D.N., and Lehmann, P. V. (2007). MP4- and MOG:35-55-induced EAE in C57BL/6 mice differentially targets brain, spinal cord and cerebellum. J. Neuroimmunol. *189*, 31–40.

Kuerten, S., Gruppe, T.L., Laurentius, L.M., Kirch, C., Tary-Lehmann, M., Lehmann, P. V., and Addicks, K. (2011). Differential patterns of spinal cord pathology induced by MP4, MOG peptide 35-55, and PLP peptide 178-191 in C57BL/6 mice. Apmis *119*, 336–346.

Kuhlmann, T., Ludwin, S., Prat, A., Antel, J., Brück, W., and Lassmann, H. (2017). An updated histological classification system for multiple sclerosis lesions. Acta Neuropathol. *133*, 13–24.

Kumar, V., and Sharma, A. (2010). Mast cells: Emerging sentinel innate immune cells with diverse role in immunity. Mol. Immunol. *48*, 14–25.

Kumar, H., Kawai, T., and Akira, S. (2011). Pathogen recognition by the innate immune system. Int. Rev. Immunol.

Kumar, S., Singh, R.K., and Bhardwaj, T.R. (2017). Therapeutic role of nitric oxide as emerging molecule. Biomed. Pharmacother. *85*, 182–201.

Kuzmenkin, A., Muncan, V., Jurkat-Rott, K., Hang, C., Lerche, H., Lehmann-Horn, F., and Mitrovic, N. (2002). Enhanced inactivation and pH sensitivity of Na+ channel mutations causing hypokalaemic periodic paralysis type II. Brain.

Kwilasz, A.J., Grace, P.M., Serbedzija, P., Maier, S.F., and Watkins, L.R. (2015). The therapeutic potential of interleukin-10 in neuroimmune diseases. Neuropharmacology *96*, 55–69.

Kwong, K., and Carr, M.J. (2015). Voltage-gated sodium channels. Curr. Opin. Pharmacol. *22*, 131–139.

Kwong, J.M.K., Caprioli, J., and Piri, N. (2010). RNA binding protein with multiple splicing: A new marker for retinal ganglion cells. Investig. Ophthalmol. Vis. Sci. *51*, 1052–1058.

Lai, J., Gold, M.S., Kim, C.S., Biana, D., Ossipov, M.H., Hunterc, J.C., and Porreca, F. (2002). Inhibition of neuropathic pain by decreased expression of the tetrodotoxin-resistant sodium channel, NaV1.8. Pain *95*, 143–152.

Lan, M., Tang, X., Zhang, J., and Yao, Z. (2017). Insights in pathogenesis of multiple sclerosis: Nitric oxide may induce mitochondrial dysfunction of oligodendrocytes. Rev. Neurosci. *29*, 39–53.

Lassmann, H., and Bradl, M. (2017). Multiple sclerosis: experimental models and reality. Acta Neuropathol. *133*, 223–244.

Lassmann, H., Brück, W., and Lucchinetti, C.F. (2007). The immunopathology of multiple sclerosis: An overview. In Brain Pathology, pp. 210–218.

Lebien, T.W., and Tedder, T.F. (2008). B lymphocytes: How they develop and function. Blood *112*, 1570–1580.

LeBouder, E., Rey-Nores, J.E., Rushmere, N.K., Grigorov, M., Lawn, S.D., Affolter, M., Griffin, G.E., Ferrara, P., Schiffrin, E.J., Morgan, B.P., et al. (2003). Soluble Forms of Toll-Like Receptor (TLR)2 Capable of Modulating TLR2 Signaling Are Present in Human Plasma and Breast Milk. J. Immunol. *171*, 6680–6689.

Lee, P.Y., Tsai, P.S., Huang, Y.H., and Huang, C.J. (2008). Inhibition of toll-like receptor-4, nuclear factor-κB and mitogen-activated protein kinase by lignocaine may involve voltage-sensitive sodium channels. Clin. Exp. Pharmacol. Physiol. *35*, 1052–1058.

de Leeuw, C.N., Dyka, F.M., Boye, S.L., Laprise, S., Zhou, M., Chou, A.Y., Borretta, L., McInerny, S.C., Banks, K.G., Portales-Casamar, E., et al. (2014). Targeted CNS delivery using human MiniPromoters and demonstrated compatibility with adeno-associated viral vectors. Mol. Ther. - Methods Clin. Dev. *1*, 5.

Legroux, L., and Arbour, N. (2015). Multiple Sclerosis and T Lymphocytes: An Entangled Story. J. Neuroimmune Pharmacol. *10*, 528–546.

De Lera Ruiz, M., and Kraus, R.L. (2015). Voltage-Gated Sodium Channels: Structure, Function, Pharmacology, and Clinical Indications. J. Med. Chem. *58*, 7093–7118.

Levin, S.I., and Meisler, M.H. (2004). Floxed allele for conditional inactivation of the voltage-gated sodium channel Scn8a (Nav1.6). Genesis *39*, 234–239.

Li, H., Gonnella, P., Safavi, F., Vessal, G., Nourbakhsh, B., Zhou, F., Zhang, G.X., and Rostami, A. (2013a). Low dose zymosan ameliorates both chronic and relapsing experimental autoimmune encephalomyelitis. J. Neuroimmunol. *254*, 28–38.

Li, J., Lee, D.S.W., and Madrenas, J. (2013b). Evolving Bacterial Envelopes and Plasticity of TLR2-Dependent Responses: Basic Research and Translational Opportunities. Front. Immunol. *4*.

Li, L., Shao, J., Wang, J., Liu, Y., Zhang, Y., Zhang, M., Zhang, J., Ren, X., Su, S., Li, Y., et al. (2019a). MiR-30b-5p attenuates oxaliplatin-induced peripheral neuropathic pain through the voltage-gated sodium channel Na v 1.6 in rats. Neuropharmacology *153*, 111–120.

Li, L., Shao, J., Wang, J., Liu, Y., Zhang, Y., Zhang, M., Zhang, J., Ren, X., Su, S., Li, Y., et al. (2019b). MiR-30b-5p attenuates oxaliplatin-induced peripheral neuropathic pain through the voltage-gated sodium channel Nav1.6 in rats. Neuropharmacology *153*, 111–120.

Li, S., Strelow, A., Fontana, E.J., and Wesche, H. (2002). IRAK-4: A novel member of the IRAK family with the properties of an IRAK-kinase. Proc. Natl. Acad. Sci. U. S. A. *99*, 5567–5572.

Lim, S.K. (2003). Freund adjuvant induces TLR2 but not TLR4 expression in the liver of mice. Int. Immunopharmacol. *3*, 115–118.

Lin, C.-C., and Edelson, B.T. (2017). New Insights into the Role of IL-1β in Experimental Autoimmune Encephalomyelitis and Multiple Sclerosis. J. Immunol. *198*, 4553–4560.

Linnington, C., Webb, M., and Woodhams, P.L. (1984). A novel myelin-associated glycoprotein defined by a mouse monoclonal antibody. J. Neuroimmunol. *6*, 387–396.

Liu, C., Li, Y., Yu, J., Feng, L., Hou, S., Liu, Y., Guo, M., Xie, Y., Meng, J., Zhang, H., et al. (2013). Targeting the Shift from M1 to M2 Macrophages in Experimental Autoimmune Encephalomyelitis Mice Treated with Fasudil. PLoS One *8*.

Lo, A.C., Saab, C.Y., Black, J.A., and Waxman, S.G. (2003). Phenytoin Protects Spinal Cord Axons and Preserves Axonal Conduction and Neurological Function in a Model of Neuroinflammation In Vivo. J. Neurophysiol. *90*, 3566–3571.

Lo, W.L., Donermeyer, D.L., and Allen, P.M. (2012). A voltage-gated sodium channel is essential for the positive selection of CD4 $^{+}$ T cells. Nat. Immunol. *13*, 880–887.

Lopez-Santiago, L.F., Pertin, M., Morisod, X., Chen, C., Hong, S., Wiley, J., Decosterd, I., and Isom, L.L. (2006). Sodium channel β2 subunits regulate tetrodotoxin-sensitive sodium channels in small dorsal root ganglion neurons and modulate the response to pain. J. Neurosci. *26*, 7984–7994.

Lossin, C., Shi, X., Rogawski, M.A., and Hirose, S. (2012). Compromised function in the Nav1.2 Dravet syndrome mutation R1312T. Neurobiol. Dis. *47*, 378–384.

Lu, Y.C., Yeh, W.C., and Ohashi, P.S. (2008). LPS/TLR4 signal transduction pathway. Cytokine *42*, 145–151.

Luz, A., Fainstein, N., Einstein, O., and Ben-Hur, T. (2015). The role of CNS TLR2 activation in mediating innate versus adaptive neuroinflammation. Exp. Neurol.

Lyons, J.A., San, M., Happ, M.P., and Cross, A.H. (1999). B cells are critical to induction of experimental allergic encephalomyelitis by protein but not by a short encephalitogenic peptide. Eur. J. Immunol. *29*, 3432–3439.

Madsen, L.S., Andersson, E.C., Jansson, L., Krogsgaard, M., Andersen, C.B., Engberg, J., Strominger, J.L., Svejgaard, A., Hjorth, J.P., Holmdahl, R., et al. (1999). A humanized model for multiple sclerosis using HLA-DR2 and a human T- cell receptor. Nat. Genet. *23*, 343–347.

Mancardi, G., Hart, B., Roccatagliata, L., Brok, H., Giunti, D., Bontrop, R., Massacesi, L., Capello, E., and Uccelli, A. (2001). Demyelination and axonal damage in a non-human primate model of multiple sclerosis. J. Neurol. Sci. *184*, 41–49.

Mangiardi, M., Crawford, D.K., Xia, X., Du, S., Simon-Freeman, R., Voskuhl, R.R., and Tiwari-Woodruff, S.K. (2011). An animal model of cortical and callosal pathology in multiple sclerosis. Brain Pathol. *21*, 263–278.

Marcus, J., Dupree, J.L., and Popko, B. (2002). Myelin-associated glycoprotein and myelin galactolipids stabilize developing axo-glial interactions. J. Cell Biol. *156*, 567–577.

Marrie, R.A., Fisk, J.D., Stadnyk, K.J., Yu, B.N., Tremlett, H., Wolfson, C., Warren, S., and Bhan, V. (2013). The incidence and prevalence of multiple sclerosis in Nova Scotia, Canada. Can. J. Neurol. Sci. *40*, 824–831.

Marta, M. (2009). Toll-like receptors in multiple sclerosis mouse experimental models. In Annals of the New York Academy of Sciences, pp. 458–462.

Marui, N., Offermann, M.K., Swerlick, R., Kunsch, C., Rosen, C.A., Ahmad, M., Wayne Alexander, R., and Medford, R.M. (1993). Vascular cell adhesion molecule-1 (VCAM-1) gene transcription and expression are regulated through an antioxidant-sensitive mechanism in human vascular endothelial cells. J. Clin. Invest. *92*, 1866–1874.

Matsuki, T., Nakae, S., Sudo, K., Horai, R., and Iwakura, Y. (2006). Abnormal T cell activation caused by the imbalance of the IL-1/IL-1R antagonist system is responsible for the development of experimental autoimmune encephalomyelitis. Int. Immunol. *18*, 399–407.

Matsushima, G.K., and Morell, P. (2006). The Neurotoxicant, Cuprizone, as a Model to Study Demyelination and Remyelination in the Central Nervous System. Brain Pathol. *11*, 107–116.

Matsushita, T., Fujimoto, M., Hasegawa, M., Komura, K., Takehara, K., Tedder, T.F., and Sato, S. (2006). Inhibitory role of CD19 in the progression of experimental autoimmune encephalomyelitis by regulating cytokine response. Am. J. Pathol. *168*, 812–821.

Mayadas, T.N., Cullere, X., and Lowell, C.A. (2014). The Multifaceted Functions of Neutrophils. Annu. Rev. Pathol. Mech. Dis. *9*, 181–218.

Mayo, S., and Quinn, A. (2007). Altered susceptibility to EAE in congenic NOD mice: Altered processing of the encephalitogenic MOG35-55 peptide by NOR/LtJ mice. Clin. Immunol. *122*, 91–100.

McCarthy, D.P., Richards, M.H., and Miller, S.D. (2012). Mouse models of multiple sclerosis: Experimental autoimmune encephalomyelitis and theiler's virus-induced demyelinating disease. Methods Mol. Biol. *900*, 381–401.

McCurdy, J.D., Lin, T.J., and Marshall, J.S. (2001). Toll-like receptor 4-mediated activation of murine mast cells. J. Leukoc. Biol. *70*, 977–984.

McCusker, E.C., Bagnéris, C., Naylor, C.E., Cole, A.R., D'Avanzo, N., Nichols, C.G., and Wallace, B.A. (2012). Structure of a bacterial voltage-gated sodium channel pore reveals mechanisms of opening and closing. Nat. Commun. *3*.

McDonald, B., Pittman, K., Menezes, G.B., Hirota, S.A., Slaba, I., Waterhouse, C.C.M., Beck, P.L., Muruve, D.A., and Kubes, P. (2010). Intravascular danger signals guide neutrophils to sites of sterile inflammation. Science (80-.). *330*, 362–366.

McEwen, D.P., and Isom, L.L. (2004). Heterophilic interactions of sodium channel β1 subunits with axonal and glial cell adhesion molecules. J. Biol. Chem. *279*, 52744–52752.

Means, T.K., Wang, S., Lien, E., Yoshimura, A., Golenbock, D.T., and Fenton, M.J. (1999). Human toll-like receptors mediate cellular activation by Mycobacterium tuberculosis. J. Immunol. *163*, 3920–3927.

Medeiros-Domingo, A., Kaku, T., Tester, D.J., Iturralde-Torres, P., Itty, A., Ye, B., Valdivia, C., Ueda, K., Canizales-Quinteros, S., Tusié-Luna, M.T., et al. (2007). SCN4B-encoded sodium channel β4 subunit in congenital long-QT syndrome. Circulation.

Medzhitov, R. (2001). Toll-like receptors and innate immunity. Nat. Rev. Immunol. *1*, 135–145.

Meisler, M.H., and Kearney, J.A. (2005). Sodium channel mutations in epilepsy and other neurological disorders. J. Clin. Invest. *115*, 2010–2017.

Meisler, M.H., Kearney, J., Escayg, A., MacDonald, B.T., and Sprunger, L.K. (2001). Sodium channels and neurological disease: Insights from Scn8a mutations in the mouse. Neuroscientist *7*, 136–145.

Meisler, M.H., Plummer, N.W., Burgess, D.L., Buchner, D.A., and Sprunger, L.K. (2004). Allelic mutations of the sodium channel SCN8A reveal multiple cellular and physiological functions. In Genetica, pp. 37–45.

Mendel, I., de Rosbo, N.K., and Ben-Nun, A. (1995). A myelin oligodendrocyte glycoprotein peptide induces typical chronic experimental autoimmune encephalomyelitis in H-2b mice: Fine specificity and T cell receptor Vβ expression of encephalitogenic T cells. Eur. J. Immunol. *25*, 1951–1959.

Mikita, J., Dubourdieu-Cassagno, N., Deloire, M.S., Vekris, A., Biran, M., Raffard, G., Brochet, B., Canron, M.H., Franconi, J.M., Boiziau, C., et al. (2011). Altered M1/M2 activation patterns of monocytes in severe relapsing experimental rat model of multiple sclerosis. Amelioration of clinical status by M2 activated monocyte administration. Mult. Scler. J. *17*, 2–15.

Miller, S.D., Karpus, W.J., and Davidson, T.S. (2010). Experimental autoimmune encephalomyelitis in the mouse. Curr. Protoc. Immunol.

Mills, C.D., Kincaid, K., Alt, J.M., Heilman, M.J., and Hill, A.M. (2000). M-1/M-2 Macrophages and the Th1/Th2 Paradigm. J. Immunol. *164*, 6166–6173.

Milo, R., and Kahana, E. (2010). Multiple sclerosis: Geoepidemiology, genetics and the environment. Autoimmun. Rev. *9*.

Miranda-Hernandez, S., and Baxter, A.G. (2013). Role of toll-like receptors in multiple sclerosis. Am. J. Clin. Exp. Immunol. *2*, 75–93.

Miranda-Hernandez, S., Gerlach, N., Fletcher, J.M., Biros, E., Mack, M., Körner, H., and Baxter, A.G. (2011). Role for MyD88, TLR2 and TLR9 but Not TLR1, TLR4 or TLR6 in Experimental Autoimmune Encephalomyelitis. J. Immunol. *187*, 791–804.

Miron, V.E., Boyd, A., Zhao, J.W., Yuen, T.J., Ruckh, J.M., Shadrach, J.L., Van Wijngaarden, P., Wagers, A.J., Williams, A., Franklin, R.J.M., et al. (2013). M2 microglia and macrophages drive oligodendrocyte differentiation during CNS remyelination. Nat. Neurosci. *16*, 1211–1218.

Mix, E., Meyer-Rienecker, H., Hartung, H.P., and Zettl, U.K. (2010). Animal models of multiple sclerosis-Potentials and limitations. Prog. Neurobiol. *92*, 386–404.

Mohr, D. (2015). The Stress and Mood Management Program for Individuals With Multiple Sclerosis.

Mohr, D.C. (2011). Psychiatric Disorders, Stress, and Their Treatment Among People with Multiple Sclerosis. In Psychological Co-Morbidities of Physical Illness, pp. 311–334.

Moll, C., Mourre, C., Lazdunski, M., and Ulrich, J. (1991). Increase of sodium channels in demyelinated lesions of multiple sclerosis. Brain Res. *556*, 311–316.

Morsali, D., Bechtold, D., Lee, W., Chauhdry, S., Palchaudhuri, U., Hassoon, P., Snell, D.M., Malpass, K., Piers, T., Pocock, J., et al. (2013). Safinamide and flecainide protect axons and reduce microglial activation in models of multiple sclerosis. Brain *136*, 1067–1082.

Mosmann, T.R., and Sad, S. (1996). The expanding universe of T-cell subsets: Th1, Th2 and more. Immunol. Today *17*, 138–146.

Murphy, Á.C., Lalor, S.J., Lynch, M.A., and Mills, K.H.G. (2010). Infiltration of Th1 and Th17 cells and activation of microglia in the CNS during the course of experimental autoimmune encephalomyelitis. Brain. Behav. Immun. *24*, 641–651.

Murray, P.D., Pavelko, K.D., Lin, X., Rodriguez, M., and Leibowitz, J. (1998). CD4+ and CD8+ T cells make discrete contributions to demyelination and neurologic disease in a viral model of multiple sclerosis. J. Virol. *72*, 7320–7329.

Musette, P., and Bouaziz, J.D. (2018). B cell modulation strategies in autoimmune diseases: New concepts. Front. Immunol. *9*.

Naegele, M., Tillack, K., Reinhardt, S., Schippling, S., Martin, R., and Sospedra, M. (2012). Neutrophils in multiple sclerosis are characterized by a primed phenotype. J. Neuroimmunol. *242*, 60–71.

Nathan, C. (2006). Neutrophils and immunity: Challenges and opportunities. Nat. Rev. Immunol. *6*, 173–182.

Nauseef, W.M., and Borregaard, N. (2014). Neutrophils at work. Nat. Immunol. *15*, 602–611.

Nicot, A., Ratnakar, P. V., Ron, Y., Chen, C.C., and Elkabes, S. (2003). Regulation of gene expression in experimental autoimmune encephalomyelitis indicates early neuronal dysfunction. Brain *126*, 398–412.

Nikić, I., Merkler, D., Sorbara, C., Brinkoetter, M., Kreutzfeldt, M., Bareyre, F.M., Brück, W., Bishop, D., Misgeld, T., and Kerschensteiner, M. (2011). A reversible form of axon damage in experimental autoimmune encephalomyelitis and multiple sclerosis. Nat. Med. *17*, 495–499.

Noda, M., and Hiyama, T.Y. (2015). The Nax channel: What it is and what it does. Neuroscientist *21*, 399–412.

Norden, D.M., Muccigrosso, M.M., and Godbout, J.P. (2015). Microglial priming and enhanced reactivity to secondary insult in aging, and traumatic CNS injury, and neurodegenerative disease. Neuropharmacology *96*, 29–41.

Noseworthy, J.H., Lucchinetti, C., Rodriguez, M., and Weinshenker, B.G. (2000). MS - Clinical course and diagnosis. N. Engl. J. Med. *343*, 938–952.

Novakovic, S.D., Levinson, S.R., Schachner, M., and Shrager, P. (1998). Disruption and reorganization of sodium channels in experimental allergic neuritis. Muscle and Nerve *21*, 1019–1032.

O'Brien, J.E., and Meisler, M.H. (2013). Sodium channel SCN8A (Nav1.6): properties and de novo mutations in epileptic encephalopathy and intellectual disability. Front. Genet. *4*.

O'Malley, H.A., and Isom, L.L. (2015). Sodium Channel β Subunits: Emerging Targets in Channelopathies. Annu. Rev. Physiol. *77*, 481–504.

O'Malley, H.A., Shreiner, A.B., Chen, G.H., Huffnagle, G.B., and Isom, L.L. (2009). Loss of Na^+ channel β2 subunits is neuroprotective in a mouse model of multiple sclerosis. Mol. Cell. Neurosci. *40*, 143–155.

Okun, E., Griffioen, K.J., and Mattson, M.P. (2011). Toll-like receptor signaling in neural plasticity and disease. Trends Neurosci. *34*, 269–281.

OLITSKY, P.K., and YAGER, R.H. (1949). Experimental disseminated encephalomyelitis in white mice. J. Exp. Med. *90*, 213–224.

Van Oosten, B.W., Lai, M., Hodgkinson, S., Barkhof, F., Miller, D.H., Moseley, I.F., Thompson, A.J., Rudge, P., McDougall, A., McLeod, J.G., et al. (1997). Treatment of multiple sclerosis with the monoclonal anti-CD4 antibody cM-T412: Results of a randomized, double-blind, placebo-controlled, MR- monitored phase II trial. Neurology *49*, 351–357.

Ousman, S.S., and David, S. (2000). Lysophosphatidylcholine induces rapid recruitment and activation of macrophages in the adult mouse spinal cord. Glia *30*, 92–104.

Owens, T., and Sriram, S. (1995). The immunology of multiple sclerosis and its animal model, experimental allergic encephalomyelitis. Neurol. Clin. *13*, 51–73.

Oyama, F., Miyazaki, H., Sakamoto, N., Becquet, C., Machida, Y., Kaneko, K., Uchikawa, C., Suzuki, T., Kurosawa, M., Ikeda, T., et al. (2006). Sodium channel β4 subunit: Down-regulation and possible involvement in neuritic degeneration in Huntington's disease transgenic mice. J. Neurochem. *98*, 518–529.

Palle, P., and Buch, T. (2014). Dispensable role for TLRs 2,3,4,7,9 in the mouse of multiple sclerosis. J. Neuroimmunol. *275*, 91.

Pappalardo, L.W., Liu, S., Black, J.A., and Waxman, S.G. (2014). Dynamics of sodium channel Nav1.5 expression in astrocytes in mouse models of multiple sclerosis. Neuroreport *25*, 1208–1215.

Pappalardo, L.W., Black, J.A., and Waxman, S.G. (2016). Sodium channels in astroglia and microglia. Glia *64*, 1628–1645.

Pastor, S., Minguela, A., Mi, W., and Ward, E.S. (2009). Autoantigen Immunization at Different Sites Reveals a Role for Anti-Inflammatory Effects of IFN-γ in Regulating Susceptibility to Experimental Autoimmune Encephalomyelitis. J. Immunol. *182*, 5268–5275.

Patani, R., Balaratnam, M., Vora, A., and Reynolds, R. (2007). Remyelination can be extensive in multiple sclerosis despite a long disease course. Neuropathol. Appl. Neurobiol. *33*, 277–287.

Patino, G.A., and Isom, L.L. (2010). Electrophysiology and beyond: Multiple roles of Na+ channel β subunits in development and disease. Neurosci. Lett. *486*, 53–59.

Payandeh, J., Scheuer, T., Zheng, N., and Catterall, W.A. (2011). The crystal structure of a voltage-gated sodium channel. Nature *475*, 353–359.

Persson, A.K., Estacion, M., Ahn, H., Liu, S., Stamboulian-Platel, S., Waxman, S.G., and Black, J.A. (2014a). Contribution of sodium channels to lamellipodial protrusion and Rac1 and ERK1/2 activation in ATP-stimulated microglia. Glia *62*, 2080–2095.

Persson, A.K., Estacion, M., Ahn, H., Liu, S., Stamboulian-Platel, S., Waxman, S.G., and Black, J.A. (2014b). Contribution of sodium channels to lamellipodial protrusion and Rac1 and ERK1/2 activation in ATP-stimulated microglia. Glia *62*, 2080–2095.

Pertin, M., Ji, R.R., Berta, T., Powell, A.J., Karchewski, L., Tate, S.N., Isom, L.L., Woolf, C.J., Gilliard, N., Spahn, D.R., et al. (2005). Upregulation of the voltage-gated sodium channel β2 subunit in neuropathic pain models: Characterization of expression in injured and non-injured primary sensory neurons. J. Neurosci. *25*, 10970–10980.

Perucca, E., Beghi, E., Dulac, O., Shorvon, S., and Tomson, T. (2000). Assessing risk to benefit ratio in antiepileptic drug therapy. Epilepsy Res. *41*, 107–139.

Petermann, F., and Korn, T. (2011). Cytokines and effector T cell subsets causing autoimmune CNS disease. FEBS Lett. *585*, 3747–3757.

Pierson, E.R., Stromnes, I.M., and Goverman, J.M. (2014). B Cells Promote Induction of Experimental Autoimmune Encephalomyelitis by Facilitating Reactivation of T Cells in the Central Nervous System. J. Immunol. *192*, 929–939.

Pillay, J., Ramakers, B.P., Kamp, V.M., Loi, A.L.T., Lam, S.W., Hietbrink, F., Leenen, L.P., Tool, A.T., Pickkers, P., and Koenderman, L. (2010). Functional heterogeneity and differential priming of circulating neutrophils in human experimental endotoxemia. J. Leukoc. Biol. *88*, 211–220.

De Pittà, M., Brunel, N., and Volterra, A. (2016). Astrocytes: Orchestrating synaptic plasticity? Neuroscience *323*, 43–61.

Piwko, C., Desjardins, O.B., Bereza, B.G., Machado, M., Jaszewski, B., Freedman, M.S., Einarson, T.R., and Iskedjian, M. (2007). Pain due to multiple sclerosis: Analysis of the prevalence and economic burden in Canada. Pain Res. Manag. *12*, 259–265.

Praet, J., Guglielmetti, C., Berneman, Z., Van der Linden, A., and Ponsaerts, P. (2014). Cellular and molecular neuropathology of the cuprizone mouse model: Clinical relevance for multiple sclerosis. Neurosci. Biobehav. Rev. *47*, 485–505.

Priest, B.T., Murphy, B.A., Lindia, J.A., Diaz, C., Abbadie, C., Ritter, A.M., Liberator, P., Iyer, L.M., Kash, S.F., Kohler, M.G., et al. (2005). Contribution of the tetrodotoxin-resistant voltage-gated sodium channel Nav1.9 to sensory transmission and nociceptive behavior. Proc. Natl. Acad. Sci. U. S. A. *102*, 9382–9387.

Prineas, J.W. (2001). Pathology of multiple sclerosis. Handb. Mult. Sclerosis, Third Ed. 289–324.

Prinz, M., Garbe, F., Schmidt, H., Mildner, A., Gutcher, I., Wolter, K., Piesche, M., Schroers, R., Weiss, E., Kirschning, C.J., et al. (2006). Innate immunity mediated by TLR9 modulates pathogenicity in an animal model of multiple sclerosis. J. Clin. Invest. *116*, 456–464.

Probert, L., Akassoglou, K., Pasparakis, M., Kontogeorgos, G., and Kollias, G. (1995). Spontaneous inflammatory demyelinating disease in transgenic mice showing central nervous system-specific expression of tumor necrosis factor α. Proc. Natl. Acad. Sci. U. S. A. *92*, 11294–11298.

Procaccini, C., De Rosa, V., Pucino, V., Formisano, L., and Matarese, G. (2015). Animal models of Multiple Sclerosis. Eur. J. Pharmacol. *759*, 182–191.

Putrenko, I., Ghavanini, A.A., SchöNiger, K.S.M., and Schwarz, S.K.W. (2016). Central Nervous System-Toxic Lidocaine Concentrations Unmask L-Type Ca2+ Current-Mediated Action Potentials in Rat Thalamocortical Neurons: An in Vitro Mechanism of Action Study. Anesth. Analg. *122*, 1360–1369.

Quinn, T.A., Dutt, M., and Shindler, K.S. (2011). Optic neuritis and retinal ganglion cell loss in a chronic murine model of multiple sclerosis. Front. Neurol. *AUG*.

Qureshi, S.T., and Medzhitov, R. (2003). Toll-like receptors and their role in experimental models of microbial infection. Genes Immun. *4*, 87–94.

Raddassi, K., Kent, S.C., Yang, J., Bourcier, K., Bradshaw, E.M., Seyfert-Margolis, V., Nepom, G.T., Kwok, W.W., and Hafler, D.A. (2011). Increased Frequencies of Myelin Oligodendrocyte Glycoprotein/MHC Class II-Binding CD4 Cells in Patients with Multiple Sclerosis. J. Immunol. *187*, 1039–1046.

Raftopoulos, R., Hickman, S.J., Toosy, A., Sharrack, B., Mallik, S., Paling, D., Altmann, D.R., Yiannakas, M.C., Malladi, P., Sheridan, R., et al. (2016). Phenytoin for neuroprotection in patients with acute optic neuritis: a randomised, placebo-controlled, phase 2 trial. Lancet Neurol. *15*, 259–269.

Raja Rayan, D.L., and Hanna, M.G. (2010). Skeletal muscle channelopathies: Nondystrophic myotonias and periodic paralysis. Curr. Opin. Neurol. *23*, 466–476.

Rangachari, M., and Kuchroo, V.K. (2013). Using EAE to better understand principles of immune function and autoimmune pathology. J. Autoimmun. *45*, 31–39.

Rangachari, M., Kerfoot, S.M., Arbour, N., and Alvarez, J.I. (2017). Editorial: Lymphocytes in MS and EAE: More than just a CD4 + world. Front. Immunol. *8*.

Ransohoff, R.M. (2012). Animal models of multiple sclerosis: The good, the bad and the bottom line. Nat. Neurosci. *15*, 1074–1077.

Reiber, H., Suckling, A.J., and Rumsby, M.G. (1984). The effect of Freund's adjuvants on blood-cerebrospinal fluid barrier permeability. J. Neurol. Sci. *63*, 55–61.

Renganathan, M., Gelderblom, M., Black, J.A., and Waxman, S.G. (2003). Expression of Nav1.8 sodium channels perturbs the firing patterns of cerebellar purkinje cells. Brain Res. *959*, 235–242.

De Repentigny, Y. (2001). Pathological and genetic analysis of the degenerating muscle (dmu) mouse: a new allele of Scn8a. Hum. Mol. Genet. *10*, 1819–1827.

Reynolds, J.M., Pappu, B.P., Peng, J., Martinez, G.J., Zhang, Y., Chung, Y., Ma, L., Yang, X.O., Nurieva, R.I., Tian, Q., et al. (2010). Toll-like receptor 2 signaling in CD4 + T lymphocytes promotes T helper 17 responses and regulates the pathogenesis of autoimmune disease. Immunity *32*, 692–702.

Reynolds, J.M., Martinez, G.J., Chung, Y., and Dong, C. (2012). Toll-like receptor 4 signaling in T cells promotes autoimmune inflammation. Proc. Natl. Acad. Sci. U. S. A. *109*, 13064–13069.

Rivers, T.M., Sprunt, D.H., and Berry, G.P. (1933). Observations on attempts to produce acute disseminated encephalomyelitis in monkeys. J. Exp. Med. *58*, 39–52.

Robinson, A.P., Harp, C.T., Noronha, A., and Miller, S.D. (2014). The experimental autoimmune encephalomyelitis (EAE) model of MS. utility for understanding disease pathophysiology and treatment. In Handbook of Clinical Neurology, pp. 173–189.

Rodriguez, A.R., de Sevilla Müller, L.P., and Brecha, N.C. (2014). The RNA binding protein RBPMS is a selective marker of ganglion cells in the mammalian retina. J. Comp. Neurol. *522*, 1411–1443.

Romme Christensen, J., Börnsen, L., Khademi, M., Olsson, T., Jensen, P.E., Sørensen, P.S., and Sellebjerg, F. (2013). CSF inflammation and axonal damage are increased and correlate in progressive multiple sclerosis. Mult. Scler. J. *19*, 877–884.

Rosker, C., Lohberger, B., Hofer, D., Steinecker, B., Quasthoff, S., and Schreibmayer, W. (2007a). The TTX metabolite 4,9-anhydro-TTX is a highly specific blocker of the Na v1.6 voltage-dependent sodium channel . Am. J. Physiol. Physiol. *293*, C783–C789.

Rosker, C., Lohberger, B., Hofer, D., Steinecker, B., Quasthoff, S., and Schreibmayer, W. (2007b). The TTX metabolite 4,9-anhydro-TTX is a highly specific blocker of the Nav1.6 voltage-dependent sodium channel. Am. J. Physiol. - Cell Physiol. *293*.

Rumble, J.M., Huber, A.K., Krishnamoorthy, G., Srinivasan, A., Giles, D.A., Zhang, X., Wang, L., and Segal, B.M. (2015). Neutrophil-related factors as biomarkers in EAE and MS. J. Exp. Med. *212*, 23–35.

Rush, A.M., Dib-Hajj, S.D., and Waxman, S.G. (2005). Electrophysiological properties of two axonal sodium channels, Nav1.2 and Nav1.6, expressed in mouse spinal sensory neurones. J. Physiol. *564*, 803–815.

Saab, A.S., Tzvetanova, I.D., and Nave, K.A. (2013). The role of myelin and oligodendrocytes in axonal energy metabolism. Curr. Opin. Neurobiol. *23*, 1065–1072.

Saijo, K., and Glass, C.K. (2011). Microglial cell origin and phenotypes in health and disease. Nat. Rev. Immunol. *11*, 775–787.

Sakurai, M., and Kanazawa, I. (1999). Positive symptoms in multiple sclerosis: Their treatment with sodium channel blockers, lidocaine and mexiletine. J. Neurol. Sci. *162*, 162–168.

Samad, O.A., Tan, A.M., Cheng, X., Foster, E., Dib-Hajj, S.D., and Waxman, S.G. (2013). Virus-mediated shRNA knockdown of Na v 1.3 in rat dorsal root ganglion attenuates nerve injury-induced neuropathic pain. Mol. Ther. *21*, 49–56.

Samoilova, E.B., Horton, J.L., Hilliard, B., Liu, T.S.T., and Chen, Y. (1998). IL-6-deficient mice are resistant to experimental autoimmune encephalomyelitis: Roles of IL-6 in the activation and differentiation of autoreactive T cells. J. Immunol. *161*, 6480–6486.

Sasai, M., and Yamamoto, M. (2013). Pathogen recognition receptors: Ligands and signaling pathways by toll-like receptors. Int. Rev. Immunol.

Sashihara, S., Oh, Y., Black, J.A., and Waxman, S.G. (1995). Na+ channel β1 subunit mRNA expression in developing rat central nervous system. Mol. Brain Res. *34*, 239–250.

Savio-Galimberti, E., Gollob, M.H., and Darbar, D. (2012). Voltage-gated sodium channels: Biophysics, pharmacology, and related channelopathies. Front. Pharmacol. *3 JUL*.

Sawada, M., Sawada, H., and Nagatsu, T. (2008). Effects of aging on neuroprotective and neurotoxic properties of microglia in neurodegenerative diseases. In Neurodegenerative Diseases, pp. 254–256.

Saxena, S., and Caroni, P. (2007). Mechanisms of axon degeneration: From development to disease. Prog. Neurobiol. *83*, 174–191.

Scalfari, A., Neuhaus, A., Daumer, M., Muraro, P.A., and Ebers, G.C. (2014). Onset of secondary progressive phase and long-term evolution of multiple sclerosis. J. Neurol. Neurosurg. Psychiatry *85*, 67–75.

Schaecher, K.E., Shields, D.C., and Banik, N.L. (2001). Mechanism of myelin breakdown in experimental demyelination: A putative role for calpain. Neurochem. Res. *26*, 731–737.

Schattling, B., Steinbach, K., Thies, E., Kruse, M., Menigoz, A., Ufer, F., Flockerzi, V., Brück, W., Pongs, O., Vennekens, R., et al. (2012). TRPM4 cation channel mediates axonal and neuronal degeneration in experimental autoimmune encephalomyelitis and multiple sclerosis. Nat. Med.

Schattling, B., Fazeli, W., Engeland, B., Liu, Y., Lerche, H., Isbrandt, D., and Friese, M.A. (2016). Activity of NaV1.2 promotes neurodegeneration in an animal model of multiple sclerosis. JCI Insight *1*.

Schrijver, I.A. (2001). Bacterial peptidoglycan and immune reactivity in the central nervous system in multiple sclerosis. Brain *124*, 1544–1554.

Serada, S., Fujimoto, M., Mihara, M., Koike, N., Ohsugi, Y., Nomura, S., Yoshida, H., Nishikawa, T., Terabe, F., Ohkawara, T., et al. (2008). IL-6 blockade inhibits the induction of myelin antigen-specific Th17 cells and Th1 cells in experimental autoimmune encephalomyelitis. Proc. Natl. Acad. Sci. *105*, 9041–9046.

Shen, P., and Fillatreau, S. (2015). Antibody-independent functions of B cells: A focus on cytokines. Nat. Rev. Immunol. *15*, 441–451.

Shields, S.D., Cheng, X., Gasser, A., Saab, C.Y., Tyrrell, L., Eastman, E.M., Iwata, M., Zwinger, P.J., Black, J.A., Dib-Hajj, S.D., et al. (2012). A channelopathy contributes to cerebellar dysfunction in a model of multiple sclerosis. Ann. Neurol. *71*, 186–194.

Shields, S.D., Butt, R.P., Dib-Hajj, S.D., and Waxman, S.G. (2015). Oral administration of PF-01247324, a subtype-selective Nav1.8 blocker, reverses cerebellar deficits in a mouse model of multiple sclerosis. PLoS One *10*.

Shin, T., Ahn, M., and Matsumoto, Y. (2012). Mechanism of experimental autoimmune encephalomyelitis in Lewis rats: recent insights from macrophages. Anat. Cell Biol. *45*, 141.

Shindler, K.S., Ventura, E., Dutt, M., and Rostami, A. (2008). Inflammatory demyelination induces axonal injury and retinal ganglion cell apoptosis in experimental optic neuritis. Exp. Eye Res. *87*, 208–213.

Sloane, J.A., Batt, C., Ma, Y., Harris, Z.M., Trapp, B., and Vartanian, T. (2010). Hyaluronan blocks oligodendrocyte progenitor maturation and remyelination through TLR2. Proc. Natl. Acad. Sci. U. S. A. *107*, 11555–11560.

Smith, C.A., and Chauhan, B.C. (2015). Imaging retinal ganglion cells: Enabling experimental technology for clinical application. Prog. Retin. Eye Res. *44*, 1–14.

Smith, C.A., and Chauhan, B.C. (2018). In vivo imaging of adeno-associated viral vector labelled retinal ganglion cells. Sci. Rep. *8*.

Smith, K.J., and Lassmann, H. (2002). The role of nitric oxide in multiple sclerosis. Lancet Neurol. *1*, 232–241.

Soares, R.M.G., Dias, A.T., Castro, S.B.R. De, Alves, C.C.S., Evangelista, M.G., Silva, L.C. Da, Farias, R.E., Castanon, M.C.M.N., Juliano, M.A., and Ferreira, A.P. (2013). Optical neuritis induced by different concentrations of myelin oligodendrocyte glycoprotein presents different profiles of the inflammatory process. Autoimmunity *46*, 480–485.

Sriram, S., Solomon, D., Rouse, R. V., and Steinman, L. (1982). Identification of T cell subsets and B lymphocytes in mouse brain experimental allergic encephalitis lesions. J. Immunol. *129*, 1649–1651.

Stadelmann, C., Wegner, C., and Brück, W. (2011). Inflammation, demyelination, and degeneration - Recent insights from MS pathology. Biochim. Biophys. Acta - Mol. Basis Dis. *1812*, 275–282.

Stirling, D.P., and Stys, P.K. (2010). Mechanisms of axonal injury: internodal nanocomplexes and calcium deregulation. Trends Mol. Med. *16*, 160–170.

Stromnes, I.M., and Goverman, J.M. (2006a). Active induction of experimental allergic encephalomyelitis. Nat. Protoc.

Stromnes, I.M., and Goverman, J.M. (2006b). Passive induction of experimental allergic encephalomyelitis. Nat. Protoc. *1*, 1952–1960.

Stys, P.K., Waxman, S.G., and Ransom, B.R. (1991). Na+-Ca2+ exchanger mediates Ca2+ influx during anoxia in mammalian central nervous system white matter. Ann. Neurol. *30*, 375–380.

Stys, P.K., Waxman, S.G., and Ransom, B.R. (1992). Ionic mechanisms of anoxic injury in mammalian CNS white matter: role of Na+ channels and Na(+)-Ca2+ exchanger. J. Neurosci. *12*, 430–439.

Stys, P.K., Sontheimer, H., Ransom, B.R., and Waxman, S.G. (2006). Noninactivating, tetrodotoxin-sensitive Na+ conductance in rat optic nerve axons. Proc. Natl. Acad. Sci. *90*, 6976–6980.

Stys, P.K., Zamponi, G.W., Van Minnen, J., and Geurts, J.J.G. (2012). Will the real multiple sclerosis please stand up? Nat. Rev. Neurosci. *13*, 507–514.

Sugawara, T., Tsurubuchi, Y., Agarwala, K.L., Ito, M., Fukuma, G., Mazaki-Miyazaki, E., Nagafuji, H., Noda, M., Imoto, K., Wada, K., et al. (2001). A missense mutation of the Na+ channel αII subunit gene Nav1.2 in a patient with febrile and afebrile seizures causes channel dysfunction. Proc. Natl. Acad. Sci. U. S. A. *98*, 6384–6389.

Svensson, L., Abdul-Majid, K.B., Bauer, J., Lassmann, H., Harris, R.A., and Holmdahl, R. (2002). A comparative analysis of B cell-mediated myelin oligodendrocyte glycoprotein-experimental autoimmune encephalomyelitis pathogenesis in B cell-deficient mice reveals and effect on demyelination. Eur. J. Immunol. *32*, 1939–1946.

Takeda, K., and Akira, S. (2005). Toll-like receptors in innate immunity. Int. Immunol. *17*, 1–14.

Tang, S.C., Arumugam, T. V., Xu, X., Cheng, A., Mughal, M.R., Dong, G.J., Lathia, J.D., Siler, D.A., Chigurupati, S., Ouyang, X., et al. (2007). Pivotal role for neuronal Toll-like receptors in ischemic brain injury and functional deficits. Proc. Natl. Acad. Sci. U. S. A. *104*, 13798–13803.

Teramoto, N., and Yotsu-Yamashita, M. (2015). Selective blocking effects of 4,9-anhydrotetrodotoxin, purified from a crude mixture of tetrodotoxin analogues, on NaV1.6 channels and its chemical aspects. Mar. Drugs *13*, 984–995.

Tertian, G., Yung, Y.P., Guy-Grand, D., and Moore, M.A.S. (1981). Long-term in vitro culture of murine mast cells. I. Description of a growth factor-dependent culture technique. J. Immunol. *127*, 788–794.

The Lenercept Multiple Sclerosis Study Group and The University of British Columbia MS/MRI Analysis Group. (1999). TNF neutralization in MS: results of a randomized, placebo-controlled multicenter study. The Lenercept Multiple Sclerosis Study Group and The University of British Columbia MS/MRI Analysis Group. Neurology *53*, 457–465.

Trapp, B.D., and Kidd, G.J. (2003). Structure of the Myelinated Axon. In Myelin Biology and Disorders, pp. 3–27.

Trapp, B.D., Peterson, J., Ransohoff, R.M., Rudick, R., Mörk, S., and Bö, L. (1998a). Axonal transection in the lesions of multiple sclerosis. N. Engl. J. Med. *338*, 278–285.

Trapp, B.D., Peterson, J., Ransohoff, R.M., Rudick, R., Mörk, S., and Bö, L. (1998b). Axonal transection in the lesions of multiple sclerosis. N. Engl. J. Med. *338*, 278–285.

Tsan, M.-F., and Gao, B. (2004). Endogenous ligands of Toll-like receptors. J. Leukoc. Biol. *76*, 514–519.

Tumani, H., Hartung, H.P., Hemmer, B., Teunissen, C., Deisenhammer, F., Giovannoni, G., and Zettl, U.K. (2009). Cerebrospinal fluid biomarkers in multiple sclerosis. Neurobiol. Dis. *35*, 117–127.

Uzawa, A., Mori, M., Taniguchi, J., Masuda, S., Muto, M., and Kuwabara, S. (2013). Anti-high mobility group box 1 monoclonal antibody ameliorates experimental autoimmune encephalomyelitis. Clin. Exp. Immunol. *172*, 37–43.

Vanoye, C.G., Gurnett, C.A., Holland, K.D., George, A.L., and Kearney, J.A. (2014). Novel SCN3A variants associated with focal epilepsy in children. Neurobiol. Dis. *62*, 313–322.

Van Der Veen, R.C., Dietlin, T.A., Karapetian, A., Holland, S.M., and Hofman, F.M. (2004). Extra-cellular superoxide promotes T cell expansion through inactivation of nitric oxide. J. Neuroimmunol. *153*, 183–189.

Veeramah, K.R., O'Brien, J.E., Meisler, M.H., Cheng, X., Dib-Hajj, S.D., Waxman, S.G., Talwar, D., Girirajan, S., Eichler, E.E., Restifo, L.L., et al. (2012). De novo pathogenic SCN8A mutation identified by whole-genome sequencing of a family quartet affected by infantile epileptic encephalopathy and SUDEP. Am. J. Hum. Genet. *90*, 502–510.

Vega, A. V., Henry, D.L., and Matthews, G. (2008). Reduced expression of Nav1.6 sodium channels and compensation by Nav1.2 channels in mice heterozygous for a null mutation in Scn8a. Neurosci. Lett. *442*, 69–73.

Visser, L., Jan de Heer, H., Boven, L.A., van Riel, D., van Meurs, M., Melief, M.-J., Zähringer, U., van Strijp, J., Lambrecht, B.N., Nieuwenhuis, E.E., et al. (2005). Proinflammatory Bacterial Peptidoglycan as a Cofactor for the Development of Central Nervous System Autoimmune Disease. J. Immunol. *174*, 808–816.

Wade, B.J. (2014). Spatial Analysis of Global Prevalence of Multiple Sclerosis Suggests Need for an Updated Prevalence Scale. Mult. Scler. Int. *2014*, 1–7.

Wagnon, J.L., and Meisler, M.H. (2015). Recurrent and non-recurrent mutations of SCN8A in epileptic encephalopathy. Front. Neurol. *6*.

Walker, C.A., Huttner, A.J., and O'Connor, K.C. (2011). Cortical injury in multiple sclerosis; the role of the immune system. BMC Neurol. *11*.

Walsh, D., McCarthy, J., O'Driscoll, C., and Melgar, S. (2013). Pattern recognition receptors-Molecular orchestrators of inflammation in inflammatory bowel disease. Cytokine Growth Factor Rev. *24*, 91–104.

Van Wart, A., and Matthews, G. (2006). Impaired Firing and Cell-Specific Compensation in Neurons Lacking Nav1.6 Sodium Channels. J. Neurosci. *26*, 7172–7180.

Waxman, S.G. (2006). Axonal conduction and injury in multiple sclerosis: The role of sodium channels. Nat. Rev. Neurosci. *7*, 932–941.

Waxman, S.G. (2008). Mechanisms of Disease: Sodium channels and neuroprotection in multiple sclerosis - Current status. Nat. Clin. Pract. Neurol. *4*, 159–169.

Weiner, H.L. (2008). A shift from adaptive to innate immunity: A potential mechanism of disease progression in multiple sclerosis. In Journal of Neurology, pp. 3–11.

Werling, D., and Jungi, T.W. (2003). TOLL-like receptors linking innate and adaptive immune response. Vet. Immunol. Immunopathol. *91*, 1–12.

West, A.P., Brodsky, I.E., Rahner, C., Woo, D.K., Erdjument-Bromage, H., Tempst, P., Walsh, M.C., Choi, Y., Shadel, G.S., and Ghosh, S. (2011). TLR signalling augments macrophage bactericidal activity through mitochondrial ROS. Nature *472*, 476–480.

Williams, S.K., Maier, O., Fischer, R., Fairless, R., Hochmeister, S., Stojic, A., Pick, L., Haar, D., Musiol, S., Storch, M.K., et al. (2014). Antibody-mediated inhibition of TNFR1 attenuates disease in a mouse model of multiple sclerosis. PLoS One.

Willis, L.M., and Whitfield, C. (2013). Capsule and lipopolysaccharide. In Escherichia Coli: Pathotypes and Principles of Pathogenesis: Second Edition, pp. 533–556.

Wilmes, A.T., Reinehr, S., Kühn, S., Pedreiturria, X., Petrikowski, L., Faissner, S., Ayzenberg, I., Stute, G., Gold, R., Dick, H.B., et al. (2018). Laquinimod protects the optic nerve and retina in an experimental autoimmune encephalomyelitis model. J. Neuroinflammation *15*.

Wittmack, E.K., Rush, A.M., Hudmon, A., Waxman, S.G., and Dib-Hajj, S.D. (2005). Voltage-gated sodium channel Nav1.6 is modulated by p38 mitogen-activated protein kinase. J. Neurosci. *25*, 6621–6630.

Wojkowska, D.W., Szpakowski, P., Ksiazek-Winiarek, D., Leszczynski, M., and Glabinski, A. (2014). Interactions between Neutrophils, Th17 Cells, and Chemokines during the Initiation of Experimental Model of Multiple Sclerosis. Mediators Inflamm. *2014*, 1–8.

Xie, W., Strong, J.A., Ye, L., Mao, J.X., and Zhang, J.M. (2013). Knockdown of sodium channel NaV1.6 blocks mechanical pain and abnormal bursting activity of afferent neurons in inflamed sensory ganglia. Pain *154*, 1170–1180.

Yang, C., Zhang, L., Hao, Z., Zeng, L., and Wen, J. (2013a). Sodium channel blockers for neuroprotection in multiple sclerosis. In Cochrane Database of Systematic Reviews, p.

Yang, M., Rui, K., Wang, S., and Lu, L. (2013b). Regulatory B cells in autoimmune diseases. Cell. Mol. Immunol. *10*, 122–132.

Yang, Y., Wang, Y., Li, S., Xu, Z., Li, H., Ma, L., Fan, J., Bu, D., Liu, B., Fan, Z., et al. (2004). Mutations in SCN9A, encoding a sodium channel alpha subunit, in patients with primary erythermalgia. J. Med. Genet. *41*, 171–174.

Yi, H., Guo, C., Yu, X., Zuo, D., and Wang, X.-Y. (2012). Mouse CD11b + Gr-1 + Myeloid Cells Can Promote Th17 Cell Differentiation and Experimental Autoimmune Encephalomyelitis . J. Immunol. *189*, 4295–4304.

Zakon, H.H. (2012). Adaptive evolution of voltage-gated sodium channels: The first 800 million years. Proc. Natl. Acad. Sci. U. S. A.

Zanoni, I., Ostuni, R., Marek, L.R., Barresi, S., Barbalat, R., Barton, G.M., Granucci, F., and Kagan, J.C. (2011). CD14 controls the LPS-induced endocytosis of toll-like receptor 4. Cell *147*, 868–880.

Zawadzka, M., Rivers, L.E., Fancy, S.P.J., Zhao, C., Tripathi, R., Jamen, F., Young, K., Goncharevich, A., Pohl, H., Rizzi, M., et al. (2010). CNS-Resident Glial Progenitor/Stem Cells Produce Schwann Cells as well as Oligodendrocytes during Repair of CNS Demyelination. Cell Stem Cell.

Zekki, H., Feinstein, D.L., and Rivest, S. (2006). The Clinical Course of Experimental Autoimmune Encephalomyelitis is Associated with a Profound and Sustained Transcriptional Activation of the Genes Encoding Toll-like Receptor 2 and CD14 in the Mouse CNS. Brain Pathol. *12*, 308–319.

Zhang, L., Zhang, J., and You, Z. (2018). Switching of the microglial activation phenotype is a possible treatment for depression disorder. Front. Cell. Neurosci. *12*.

Zhang, M.Z., Wang, X., Wang, Y., Niu, A., Wang, S., Zou, C., and Harris, R.C. (2017). IL-4/IL-13–mediated polarization of renal macrophages/dendritic cells to an M2a phenotype is essential for recovery from acute kidney injury. Kidney Int. *91*, 375–386.

Zhang, X.Y., Wen, J., Yang, W., Wang, C., Gao, L., Zheng, L.H., Wang, T., Ran, K., Li, Y., Li, X., et al. (2013). Gain-of-Function mutations in SCN11A cause familial episodic pain. Am. J. Hum. Genet. *93*, 957–966.

Zhong, M.C., De Rosbo, N.K., and Ben-Nun, A. (2002). Multiantigen/multiepitope-directed immune-specific suppression of "complex autoimmune encephalomyelitis" by a novel protein product of a synthetic gene. J. Clin. Invest. *110*, 81–90.

Zhou, J., Stohlman, S.A., Hinton, D.R., and Marten, N.W. (2003). Neutrophils Promote Mononuclear Cell Infiltration During Viral-Induced Encephalitis. J. Immunol. *170*, 3331–3336.

Zhu, B., Bando, Y., Xiao, S., Yang, K., Anderson, A.C., Kuchroo, V.K., and Khoury, S.J. (2007). CD11b + Ly-6C hi Suppressive Monocytes in Experimental Autoimmune Encephalomyelitis . J. Immunol. *179*, 5228–5237.

Zonta, B., Tait, S., Melrose, S., Anderson, H., Harroch, S., Higginson, J., Sherman, D.L., and Brophy, P.J. (2008). Glial and neuronal isoforms of Neurofascin have distinct roles in the assembly of nodes of Ranvier in the central nervous system. J. Cell Biol. *181*, 1169–1177.